FLOOD MODELING USING GIS-BASED WATERSHED HYDROLOGICAL MODEL AND REMOTELY SENSED DATA

ABOLGHASEM AKBARI

THESIS SUBMITED IN FULFILMENT OF THE REQUIRMENTS FOR THE DEGREE OF DOCTOR OF PHILOSOPHY

FACULTY OF ENGINEERING
UNIVERSITY OF MALAYA
KUALA LUMPUR

2011

UNIVERSITY OF MALAYA

ORIGINAL LITERARY WORK DECLARATION

Name of Candidate: **ABOLGHASEM AKBARI**

Registration/Matric No: **KHA060029**

Name of Degree: **Doctor of Philosophy**

Title of Thesis: **FLOOD MODELING USING GIS-BASED WATERSHED HYDROLOGICAL MODEL AND REMOTELY SENSED DATA**

Field of Study: **Civil Engineering**

I do solemnly and sincerely declare that:

1) I am the sole author/writer of this Work;
2) This Work is original;
3) Any use of any work in which copyright exists was done by way of fair dealing and for permitted purposes and any excerpt or extract from, or reference to or reproduction of any copyright work has been disclosed expressly and sufficiently and the title of the Work and its authorship have been acknowledged in this Work;
4) I do not have any actual knowledge nor ought I reasonably to know that the making of this work constitutes an infringement of any copyright work;
5) I hereby assign all and every rights in the copyright to this Work to the University of Malaya (UM), who henceforth shall be owner of the copyright in this Work and that any reproduction or use in any form or by any means whatsoever is prohibited without the written consent of UM having been first had and obtained;
6) I am fully aware that if in the course of making this Work I have infringed any copyright whether intentionally or otherwise, I may be subject to legal action or any other action as may be determined by UM.

Candidate's Signature Date: …………………..

Subscribed and solemnly declared before,

Witness's Signature Date: …………………..

Name: ……………………..

Designation: ……………….

FLOOD MODELING USING GIS-BASED WATERSHED HYDROLOGICAL MODEL AND REMOTELY SENSED DATA

Abstract :

Due to land use and climate changes, more severe and frequent floods occur worldwide. Flood simulation as the first step in flood risk management can be robustly conducted with an integration of GIS, RS and flood modeling tools. The primary goal of this thesis is to examine the practical use of public domain satellite data and GIS-based hydrologic model. To achieve all objectives of this research, firstly the value and importance of data in water resources engineering specifically for rainfall runoff modeling is discussed. A review of the literatures is provided on modeling concept, watershed models and its classification; spatial data model and its application in hydrology are presented. In addition, common approaches that GIS integrates with hydrologic models are reviewed and basic concept of surface-runoff modeling and its equations that relates to this subject are presented. Secondly, database development using raw data collected from different sources is described. GIS tools and techniques were used in the light of relevant literature to achieve the appropriate database. Watershed delineation and parameterizations were carried out using cartographic DEM derived from digital topography at a scale of 1:25000 with 30 m cell size and SRTM elevation data at 90 m cell size that originally were acquired in 30 m resolution. The SRTM elevation dataset is evaluated and compared with cartographic DEM. Advanced and novel GIS techniques were used for DEM manipulation and watershed delineation. The research questions were answered with the assistance of statistical measures such as Correlation coefficient (*r*), Nash-Sutcliffe efficiency (NSE), Percent Bias (PBias) or Percent of Error (PE). The results are described in detail with the assistance of several tables and illustrations. Based on NSE index, SRTM-DEM can be used for watershed delineation and parameterization with 87% similarity with Topo-DEM in a complex and

underdeveloped terrains. Overall agreement is significantly achieved (95%) when only non-urbanized areas with rugged topography are considered. However NSE (33%) exhibits a high level of discrepancy between Topo and SRTM DEM-derivatives in urbanized areas with mild slope.

Spatio-temporal variations of rainfall events over Klang watershed are discussed to achieve the one of other objectives of this study. Primary investigation is made for eight floods resultant from rainfall events in 2002. Then four rainfall events were selected for further analysis. Kriging interpolation is used to define the areal distribution of rainfall over the study area. The same rainfall events acquired by TRMM (V6) were analyzed and compared with the gauge data. It is concluded that TRMM estimates do not give adequate information about the storms as it can be drawn from the rain gauges. A pure and novel GIS analysis and flood simulation model supported by two public domain satellite data was conducted. Event-based comparison is made for TRMM precipitation estimates with the rainfall catch at rain gauges. Then evaluation is followed by rainfall-runoff modeling using HEC-HMS. Several conclusions at the technological and application levels have been achieved with this research. At the technological level, GIS has proven to be a useful tool with the ability to extract multiple parameters from a DEM and create a hydrological database from it. At the application level, it was proved that SRTM elevation dataset has the ability to obviate the lack of terrain data for hydrologic modeling where appropriate data for terrain modeling and simulation of hydrological processes is unavailable. However TRMM precipitation estimates failed to explain the behavior of rainfall events and its resultant peak discharge and time of peak. However TRMM data could reasonably simulate the volume of outflow for investigated flood event.

PEMODELAN BANJIR MENGGUNAKAN MODEL HIDROLOGI KAWASAN TADAHAN AIR BERDASARKAN SISTEM MAKLUMAT GEOGRAFI DAN PENDERIAAN JAUH.

Abstrak:

Penukaran gunatanah dan perubahan iklim dan cuaca telah menyebabkan kejadian banjir lebih kerap dan teruk di merata dunia. Antara langkah pertama untuk menangani risiko banjir ialah dengan menggunakan kaedah integrasi Sistem Maklumat Geografi (SMS)(Geographical Information System (GIS)), Penderian Jauh (PJ) (Remote Sensing) dan kaedah-kaedah pemodelan banjir. Tujuan utama tesis ini ialah untuk mengkaji penggunaan praktikal data satelit di domain awam dan model hidrologi berdasarkan GIS untuk memodelkan discaj sungai. Pada peringkat awal perbincangan dibuat mengenai nilai dan kepentingan data dalam kejuruteraan sumber air khususnya untuk pemodelan air larian hujan. Perbincangan literatur diberikan mengenai konsep pemodelan, model-model kawasan tadahan air dan pengkelasannya; model data ruang dan aplikasinya di dalam bidang hidrologi. Disamping itu, pendekatan lazim yang mengintegrasikan SMS dengan model-model hidrologi dikaji semula dan konsep asas pemodelan air larian dan persamaan-persamaan yang berkait juga dibentangkan. Kemudianya pembangunan pangkalan data yang menggunakan data asas yang di ambil dari berbagai daripada pelbagai sumber dibentangkan. Peralatan dan teknik-teknik GIS yang berkait dan literatur yang relevan digunakan untuk mencapai pangkalan data yang sesuai. Persempadanan kawasan tadahan air dan pemparameteran telah dilakukan dengan menggunakan kaedah kartografi DEM yang dihasilkan daripada peta topografi digital berskala 1:25000 dengan saiz sel 30 m dan juga data elevasi SRTM dengan saiz sel 90 m yang berkait dengan resolusi imej dalam 30 m. DEM dari imej SRTM ini dinilai dan dibandingkan dengan DEM yang dihasilkan dari peta topografi digital. Teknik-teknik GIS yang termaju dan baru telah digunakan untuk pengolahan DEM dan persempadanan kawasan tadahan air di kawasan kajian. Soalan-soalan penyelidikan berkait dengan perbadingan DEM ini telah dilakukan dengan bantuan pengukuran statistik seperti 'Correlation coefficient (r), Nash-Sutcliffe efficiency (NSE), percent Bias (PBias) atau Peratus (PE)'. Keputusannya diterangkan dengan terperinci dengan bantuan beberapa jadual dan ilustrasi. Berdasarkan kepada indeks NSE, SRTM-DEM boleh digunakan untuk persempadanan kawasan tadahan air dan pemparameteran dengan 87% kesamaan dengan Topo-DEM untuk kawasan rupa bumi yang komplek dan “terrain” yang samar-samar. Persetujuan keseluruhan SRTM-DEM yang baik dicapai

(95%) di kawasan-kawasan luar bandar yang mempunyai “terrain” yang lebih curam. Di kawasan bandar yang mepunyai “terrain” yang landai perbezaan DEM-Topo dan DEM-SRTM adalah besar dengan nilai NSE sebanya 33%. Perubahan “spatial-temporal” taburan hujan dikawasan kajian juga diselidiki sebagai salah satu daripada satu objektif kajian. Terdapat lapan kes hujan lebat pada tahun 2002 yang mengakibatkan banjir di kawasan kajian. Empat kes hujan lebat telah dipilih untuk analisis selanjutnya. Interpolasi Kriging digunakan untuk menentukan taburan “spatial” hujan di kawasan kajian . Pencerapan kejadian hujan yang sama yang diperolehi dari satelit TRMM (V6) telah dianalisa dan dibandingkan dengan data tolok hujan. . Kedua analisis taburan “spatial” ini bandingkan dan boleh disimpulkan bahawa anggaran dari TRMM tidak dapat memberi maklumat yang mencukupi tentang taburan “spatial-temporal” kejadian hujan berbanding dengan tolok hujan. Percubaan analisis GIS yang digabungkan dengan model simulasi banjir dari dua pangkalan data satelit di domain awam telah dijalankan. Perbandingan pertama dibuat diantara anggaran hujan TRMM dengan hujan yang dicerap pada sistem tolok hujan. Ini kemudiannya disusuli pemodelan air larian dengan menggunakan HEC-HMS untuk anngaran TRMM dan juga anggaran dari sistem tolok hujan. Beberapa kesimpulan dapat dihasilkan dari kajian ini. Pertama pada tahap teknologi GIS telah dibuktikan sebagai satu kaedah yang berguna dengan keupayaan untuk mengekstrak pelbagai parameter dari DEM dan mewujudkan pangkalan data hidrologi daripadanya. Pada tahap aplikasi, kajian ini telah membukktikan bahawa data elevasi SRTM mempunyai keupayaan untuk mengatasi masalah kekurangan data rupa bumi untuk pemodelan hidrologi di mana data yang sesuai untuk pemodelan rupa bumi dan simulasi proses-proses hidrologi tidak didapati. Bagaimanapun anggaran hujan TRMM gagal mencerap “spatial-temporal” kejadian hujan dan itu perubahan aliran puncak dan masa puncak discaj sungai. Walaubagaimanpun, data TRMM dapat mensimulasikan jumlah isipadu discaj untuk kejadian banjir yang disiasat.

ACKNOWLEDGMENTS

Boundless thanks the GOD that gave me the ability to complete this project

I am grateful to my supervisors Associate Prof. Dr. Faridah Othman and Professor Azizan Abu Samah, who helped me and encouraged me in this research. I believe without them, this piece of thesis was impossible to complete. I would also like to thank Dr. Ramani Bai for help and support within the two years supervision of my research. I am also thankful to all people that remotely contributed to my research particularly Professor Richard H. Hawkins form University of Arizona, Professor Amin Alizade from Ferdowsi University of Mashhad and Matthew Fleming and Feldman from Hydrologic Engineering Center, US Army Corps of Engineers. Dr Feldman from HEC was very helpful in setting up a semi-distributed hydrologic model (HMS). I would like to express my indescribable thanks to staff members of Faculty of Engineering and Department of Civil Engineering. All DID staff members especially Mr. Abu Salim (hydrologic section) were friendly and generous in providing the stream flow and rainfall records and river cross-section for the Klang Watershed. I do greatly appreciate my family, brothers and sister for their help and moral supports during my study. My special thanks go to NASA for providing freely global satellite data specifically SRTM and TRMM dataset. I do appreciate ITC for providing powerful and free raster-GIS software of ILWIS and USACE for providing free hydrologic modeling system (HEC-HMS) and its GIS link GeoHMS. I would like to express my great thanks to Miss Nadia Mahmoudi for valuable help and cooperation in submission process. I would like to thank my relatives who have shared my joy and suffering together during my study. I would like greatly thank the University of Malaya for financial support of this research. It was impossible to finish this research without their help and support.

"I dedicate this work to Elham, my father and spirit of my late mother"

TABLE OF CONTENTS

ABSTRACT: III

ABSTRAK: V

ACKNOWLEDGMENTS VII

LIST OF FIGURES XIII

LIST OF TABLES XVIII

LIST OF ABBREVIATIONS XX

LIST OF SYMBOLS XXII

CHAPTER I: INTRODUCTION 1

1.1 Availability of data 3

1.2 Status of topography mapping in the world 4

1.3 Public domain hydrological software 5

1.4 Public domain datasets 5

1.5 Knowledge Gaps on Satellite-Based Flood Modeling 6

1.6 Objectives and scope 6

1.7 Key Assumptions 7

1.8 Thesis outline 8

CHAPTER II: LITERATURE REVIEW 9

2.1 Spatial Hydrology 10

2.1.1 Modeling concepts 10

2.1.2 Flood modeling 11

2.1.3 Watershed hydrological model 12

2.2 Classification of watershed hydrological models 12

2.2.1 Processing environment 13

2.2.2 Spatial variability 13

2.2.3 Time intervals 14

2.2.4 Spatial scales 14

2.2.5 Applications 15

2.2.6 Measured-parameter or fitted-parameter 15

2.2.7 Inventory of the WHMs 15

2.2.8 Deficiencies of models 17

2.3 Geospatial information systems (GIS) 17

2.3.1 Definition 17

2.3.2 Spatial data types 18
2.3.3 Spatial Data Models 19
2. 4 Remote sensing (RS) 22
2.4.1 Landsat 22
2.4.2 SRTM 24
2. 4.3 TRMM 24
2. 4.4 TRMM3B42 Characteristics 26
2.5 GIS-based watershed hydrological model 27
2.6 Current approaches to integrate GIS with WHMs 28
2.6.1 Loose coupling 30
2.6.2 Tight coupling 31
2.6.3 Embedding WHM in GIS 31
2.6.4 Embedding GIS in WHM 32
2.7 Geospatial Hydrologic Modeling 33
2.8 Rainfall-Runoff Modeling 35
2.8.1 Precipitation Component 35
2.8.2 Gauge rainfall data 36
2.8.3 TRMM 3B42 precipitation data 37
2.8.4 Spatial and temporal pattern 38
2.8.5 Areal storm patterns 39
2.8.6 Temporal storm patterns 40
2.8.7 Criteria for storm selection 40
2.9 Infiltration Component 41
2.9.1 SCS-CN method 42
2.9.2 Modified SCS-CN method 43
2.9.3 Advantage, disadvantages and limitations 44
2.10 Runoff Component 45
2.10.1 Basic Concepts of the Unit Hydrograph 46
2.10.2 Synthetic Unit Hydrograph 48
2.10.3 Snyder's Synthetic Unit Hydrograph 49
2.10.4 SCS Dimensionless Hydrograph 51
2.11 Routing Component 53
2.11.1 Kinematic Wave Flood Routing 54
2.11.2 Determination of **ac** and **mc** for Stream channels 55
2.11.3 The reservoir routing equation 56
2.12 Runoff models 57
2.13 Calibration of Runoff Models 58
2.14 DEM-based Watershed Modeling 58

2.14.1 Background of applications 59
2.14.2 DEM resolution 60
2.14.3 Topographic Maps 63
2.14.4 Satellite-based DEM 64
2.15 DEM optimization..66
2.15.1 DEM Smoothing 66
2.15.2 Filling sinks on DEM 67
2.15.3 DEM reconditioning..68
2.15.4 Watershed delineation algorithm..69
2.15.5 Flow direction..70
2.15.6 Flow accumulation 71
2.15.7 Watershed threshold..71
2.16 Basic evaluation measures 72
2.16.1 Correlation coefficient (r)..72
2.16.2 Coefficient of determination **r2 or R2**..73
2.16.3 Nash-Sutcliffe efficiency (NSE):..74
2.16.4 Percent Bias (PBias) 74
2.16.5 Scatter plot and line of best fit 75

CHAPTER III: METHODOLOGY AND STUDY AREA..76

3.1 Methodology..77
3.2 Description of study area and used materials..79
3.2.1 Location 79
3.2.2 Climate..80
3.2.3 Main drainage system..81
3.2.4 Flood history in Klang watershed 83
3.2.5 Forms of Flooding in Klang watershed 84
3.2.6 Flood magnitude..84
3.2.7 Evaporation 85
3.3 Data collection and database development..86
3.3.1 Topographic maps..86
3.3.2 Problems associated with the collected digital topo maps 89
3.3.3 Typical observed errors in digital topo maps..90
3.3.4 Land use (LU) 92
3.3.5 Checking LU with Landsat image 94
3.3.6 Hydrologic Soil Group (HSG) 96
3.3.7 SCS-CN map development..97
3.3.8 Generating of CN map..98

3.3.9 HYDROLOGIC CONDITION 99
3.3.10 ANTECEDENT MOISTURE CONDITION (AMC) 99
3.4 HYDROLOGIC TIME SERIES 102
3.4.1: RAINFALL EVENTS...102
3.4.2 STREAM FLOW RECORD 105
3.5 CHANNEL GEOMETRY 105
3.5.1 CHANNEL LENGTH...105
3.5.2 CHANNEL CROSS-SECTION 106
3.5.3 DRAINAGE DENSITY 107

CHAPTER IV: RESULTS AND DISCUSSIONS 109

4.1 WATERSHED MODELING 110
4.2 CREATING TOPO-DEM...110
4.2.1 TOPO-DEM SMOOTHING...111
4.2.2 FILLING DEPRESSIONS / SINKS 113
4.2.3 TOPO-DEM RECONDITIONING..113
4.3 WATERSHED SEGMENTATION AND PARAMETERIZATION 115
4.3.1 AUTOMATED DELINEATING WATERSHED BOUNDARIES 115
4.3.2 FLOW DIRECTION MAP 115
4.3.3 FLOW ACCUMULATION MAP..115
4.3.4 SELECTION OF THRESHOLD FOR THE STREAM INITIATION 116
4.3.5 WATERSHED POLYGON PROCESSING...117
4.3.6 WATERSHED PARAMETERIZATION WITH TOPO-DEM..120
4.3.7 AGGREGATING CURVE NUMBERS BY SUB-WATERSHEDS 121
4.3.7.1 URBAN IMPERVIOUS AREA 123
4.4 SRTM-DEM PROCESSING..125
4.4.1 WATERSHED DELINEATION AND PARAMETERIZATION WITH SRTM-DEM 128
4.4.2 EVALUATION OF DEMS AND DEM-DERIVATIVES 131
4.4.3 COMPARISON OF TOPO-DEM WITH SRTM-DEM..131
4.5 COMPARISON OF DEM-DERIVATIVES 134
4.5.1 COMPARISON OF DEM-DERIVATIVES FOR ENTIRE STUDY AREA 134
4.5.2 COMPARISON OF DEM-DERIVATIVES FOR LF1...138
4.5.3 COMPARISON OF DEM-DERIVATIVES FOR LF2...140
4.6 GENERAL DISCUSSION 142
4.8 SATELLITE-BASED FLOOD MODELING WITH HEC-HMS 164
4.9 CONSTRUCTING HEC-HMS COMPONENTS 164
4.9.3 SELECTED RAINFALL-RUNOFF EVENTS 167
4.9.4 UNIT HYDROGRAPH TRANSFORMATION 167
4.9.5 KINEMATIC WAVE ROUTING METHOD 167

4.9.6 Reservoir Flood routing method....169
4.10 Meteorological model 170
4.11 HEC-HMS output for flood event 6-May 171
4.11.1 Running for Topo-DEM derived parameters and rain gauges data (Run1) 171
4.11.2 Running for modified CN (Run2)....174
4.11.3 Running for SRTM-derived sub-watershed area (Run3) 177
4.11.4 Running for Topo-derived sub-watershed area and TRMM data (Run4)..179
4.11.5 Running for SRTM-derived sub-watershed area and TRMM data (Run5) 181
4.12 Overall assessment of the modeling results....183

CHAPTER V: SUMMARY AND CONCLUSION....184

5.1 Summary 185
5.2 Conclusion 189
5.3 Future plan 190

LIST OF REFERENCES:....192

LIST OF APPENDICES 207

Appendix A: Status of world mapping and List of used digital topo sheets....208
Appendix B: Types of Known Hydrological models....210
Appendix C: Time-series results of flood simulation by HEC-HMS....212
Appendix D: List of Publications from the Thesis 227

List of Figures

Figure 1.1: Conceptual representation of watershed as a hydrologic system 3
Figure 2.1: Presenting features in real world by means of raster and a vector model 19
Figure 2.2: Schematic representation of basic features in GIS 21
Figure 2.3: workflow of generating color composite..24
Figure 2.4: The TRMM instruments (Source: http://www.jaxa.jp/projects/sat/trmm/) 26
Figure 2.5: TRMM Online Visualization and Analysis System (TOVAS) 3-hourly TRMM Rainfall Estimate (3B42 V6)..27
Figure 2.6 Interrelationship between GIS disciplines 28
Figure 2.7: Integrating GIS with hydrological models 30
Figure 2.8 Conceptual modeling of rainfall-runoff process...48
Figure 2.9: Snyder's synthetic UH, a) Standard UH ($tlag\ = 5.5tr$), b) Required UH ($tlagR\ = 5.5tR$) 51
Figure 2.10: SCS synthetic UHs; a) Dimensionless hydrograph and b) Triangular UH..............52
Figure 2.11: Schematic diagram of inflow and outflow flood hydrographs 54
Figure 2.12: Typical trapezoidal section...55
Figure 2.13: Web interface of HydroSHEDS download site 65
Figure 2.14: Profile view of sink in DEM (left) and filled depression of DEM (right)...............68
Figure 2.15: DEM reconditioning using attributes table of stream network................................69
Figure 2.16: Schematic representation of DEM reconditioning 69
Figure 2.17: Illustration of flow direction matrix 70
Figure 2.18: Illustration of direction codes for determining flow direction.................................71
Figure 3.1: Work flow of watershed delineation and assessment of SRTM derivatives. 78
Figure 3.2: Conceptual representation of GIS-based hydrological simulation showing methodology followed in the research 79
Figure 3.3: Study area 80
Figure 3.4: Main drainage system and local names of Klang watershed. 82
Figure 3.5: Cumulative plot of annual floods for the Klang watershed at Sulaiman Bridge 85
Figure 3.6: Monthly distribution of Evap. at 3511301 Tanjung Karang at Selangor 85
Figure 3.7: Watershed-layout in map index of topo sheets at scale of 1:25000 87
Figure 3.8: Filling void areas at sheet number 3757b (scale 1:25000) with topo sheets at scale 1:10000 88
Figure 3.9: Final merged topo maps used for generating DEM..89
Figure 3.10 Illustration of code consistency (a) and false coding errors on digital topo maps....91
Figure 3.11 Illustration of edge matching error in digital topo maps 92
Figure 3.12: Land use map of study area 93
Figure 3.13: Histogram of land use classes for the study area 93

Figure 3.14: Illustrations of NDVI mapping....................94
Figure 3.15: Land use classification based on NDVI....................95
Figure 3.16:....................95
a) Color composite image showing the cloud masses over the study area....................95
b) Cloud cover and its shadow....................95
c) Showing the affect of cloud cover in NDVI classification and represent the weakness of NDVI in detection of cloud cover....................95
Figure 3.17: Hydrologic Soil Group for the study area....................97
Figure 3.18: Histogram of HSG for Klang watershed.....................97
Figure 3.19: Work flow of generating CN map of study area.....................101
Figure 3.20: Generating subbasins CN map (left) from the gridded-CN map (right)....................102
Figure 3.21: Layout of the rainfall stations in and near to the Klang watershed....................104
Figure 3.22: Difference between the design and the existing cross-section at water level telemetric station (Code: 3116535) on the Batu River on 15 Feb 2002....................106
Figure 3.23: Typical cross-section of main channel system at the Klang watershed....................107
Figure 3.24: Illustration of Strahler order and hierarchical structure of Klang watershed....................108
Figure 4.1: Illustration of Topo-DEM processing from topo maps and spot heights....................111
Figure 4.2: Topo-DEM Smoothing and its effect on the elevation of watershed. (a) Original DEM before smoothing, (b) Smoothed DEM, (c) Zooming box....................112
Figure 4.3: Smoothing effect on elevation magnitude of DEM.....................112
Figure 4.4: Smoothing effect on number of elevation classes of DEM.....................113
Figure 4.5: Planimetric view of sink in Topo-DEM (left) and sink-free Topo-DEM (right)....................113
Figure 4.6:....................114
(a) Topo-DEM before reconditioning.....................114
(b) Topo-DEM after reconditioning.....................114
(c) Zooming area....................114
Figure 4.8: Drainage network derived from Topo-DEM defined by 8 km^2 threshold.....................116
Figure 4.7:....................116
(a) Cell elevations of Topo-DEM....................116
(b) Flow direction in each cell....................116
(c) Flow accumulation value in each cell....................116
(d) Zooming box....................116
Figure 4.9: Selecting sub-watershed (left) and merging result (right)....................117
Figure 4.10: Zooming on point of interest to subdivide (left) and splitting result (right)....................117
Figure 4.11: Selecting sub-watershed to split at confluence (left) and splitting result of watershed at confluence (right)....................117
Figure 4.12: Primary delineated subbasins boundary before batch point processing (left) and after batch point processing and merging and splitting subbasins (right)....................119

Figure 4.13: Sub-watershed boundaries derived from Topo-DEM 120
Figure 4.14: Generating sub watershed CN map (left) from the gridded-CN map (right).........121
Figure 4.16: Pixels with negative values 127
Figure 4.17: Spatial representation of resampling SRTM90 to SRTM30................................128
Figure 4.18: Sub-watershed boundaries derived from Topo-DEM 129
Figure 4.19: Visual comparison of Topo-DEM (left) and SRTM-DEM (right) with the same elevation classes..132
Figure 4.20: Comparing accumulation of watershed area vs. elevation derived from Topo-DEM and SRTM-DEM...132
Figure 4.21: Comparison of slope derived from Topo-DEM and SRTM-DEM.......................133
Figure 4.22: Overlying two watershed boundaries delineated from Topo and SRTM DEMs on Land sat true color composite. 133
Figure 4.23: Scatter plots of Topo-derived parameters against SRTM-derived parameters in whole study area; (1) perimeter, (2) Mean elevation, (3) river slope, (4) longest flow length, (5) curve number, (6) lag time, (7) watershed slope and (8) watershed area. 135
Figure 4.24: Sub-watershed located in LF2 highlighted by yellow color for both DEM- derived watershed boundaries. Topo-DEM (left) and SRTM-DEM (right) 138
Figure 4.25: Scatter plots of Topo-derived parameters against SRTM-derived parameters in LF1; (1) Mean elevation, (2) river slope, (3) longest flow length, (4) curve number, (5) watershed slope and (6) lag time, (7) watershed area. (8) Perimeter. 139
Figure 4.26: Scatter plots of Topo-derived parameters against SRTM-derived parameters in LF2; (1) Mean elevation, (2) river slope, (3) longest flow length, (4) curve number, (5) watershed slope and (6) lag time, (7) watershed area. (8) Perimeter. 141
Figure 4.27: Distribution of total rainfall recorded at stations for storm Jun. 2, 2002..............147
Figure 4.28: Distribution of total rainfall recorded at stations for storm Apr 29, 2002 147
Figure 4.29: Distribution of total rainfall recorded at stations for storm May 6, 2002 148
Figure 4.30: Distribution of total rainfall recorded at stations for storm Jun 11, 2002.............148
Figure 4.31: Distribution of total rainfall recorded at stations for storm Sep. 6, 2002 148
Figure 4.32: Distribution of total rainfall recorded at stations for storm Oct.8, 2002 149
Figure 4.33: Distribution of total rainfall recorded at stations for storm Nov.8, 2002 149
Figure 4.34: Distribution of total rainfall recorded at stations for storm Dec. 21, 2002............149
Figure 4.35: Spatial distribution of rainfall events over Klang watershed using Kriging interpolation with Gaussian Semi-variogram model; a) rainfall event 6-May2002, b) rainfall event 29-Apr2002, c) rainfall event 11-jun2002 d) rainfall event 21-Dec2002........................150
Figure 4.36: Observed flood hydrograph resultant from storm event of 29-Apr 2002 151
Figure 2.37: Observed flood hydrograph resultant from storm event of 21-Dec 2002.............152
Figure 4.38: Observed flood hydrograph resultant from storm event of 6-May 2002 153
Figure 4.39: Observed flood hydrograph resultant from storm event of 11-Jun 2002..............153

Figure 4.40: Graphical representation of storm pattern (6-May) at 18 rain gauges. 154
Figure 4.41: TRMM grid map overlaid on Klang watershed..155
Figure 4.42: Accumulated 3-horly rainfall (mm) estimates of TRMM 3B42 (v6) for flood event 6-May 2002. 156
Figure 4.43: Accumulated 3-horly rainfall (mm) estimates of TRMM 3B42 (v6) for flood event 29-Apr 2002. 157
Figure 4.44: Accumulated 3-horly rainfall (mm) estimates of TRMM 3B42 (v6) for flood event 11-June 2002. 158
Figure 4.45: Accumulated 3-horly rainfall (mm) produced by TRMM 3B42 (v6) for rainfall event 21Dec2002. 159
Figure 4.46: Spatial distribution of total rain depth over 6 TRMM cells..................................161
a) Comparison of TRMM estimates with observed storm depth of 6-May 2002 161
b) Comparison of TRMM estimates with observed storm depth of 29-Apr 2002 161
c) Comparison of TRMM estimates with observed storm depth of 11-June 2002 161
c) Comparison of TRMM estimates with observed storm depth of 21-Dec 2002 161
Figure 4.47: Subbasins wiz estimation of accumulated TRMM rainfall (event 6-May) over Klang watershed. Crossing sub-watersheds with TRMM estimates result from events 6-May 2002 (left). Groping the TRMM cell values based on sub-watersheds using ILWIS (right).....162
Figure 4.48: HEC-HMS model for Klang watershed...165
Figure 4.49: Component of kinematic wave routing method for the reach RSW11.................168
Figure 4.50: Cross section of Klang Gate Dam. Taken from Gibson and Dodge (1983) 169
Figure 4.51: Cross section of Batu Dam. Taken from DID 169
Figure 4.52: Storage-discharge relationship of Klang Gate dam...170
Figure 4.53: Storage-discharge relationship of Batu dam...170
Figure 4.54: Illustration of rain gauge 3116003 and its hyetograph for event 6-May 171
Figure 4.55: Flood hydrograph resultant from event 6-May in sub-watershed SW13 172
Figure 4.56: Schematic illustration flood diversion channels of Klang watershed...................173
Figure 4.57: Observed and simulated flood hydrograph resultant from event 6-May at Sulaiman Bridge...174
Figure 4.58: Computed flood hydrograph resultant from run1 at watershed outlet...................174
Figure 4.59: Flood hydrograph resultant from Modified CN in sub-watershed SW13 175
Figure 4.60: Observed and simulated flood hydrograph resultant from modified-CN for event 6-May at Sulaiman Bridge. 176
Figure 4.61: Computed flood hydrograph resultant from modified CN in sub-watershed SW13 176
Figure 4.62: computed flow hydrograph at sub basin SW13...178
Figure 4.63: observed and computed flood hydrograph at Sulaiman Bridge based on SRTM-derived sub-watershed areas. 178

Figure 4.64: Computed flood hydrograph resultant from Run3 in sub-watershed SW13 178
Figure 4.65: TRMM hyetograph at gauge Cell4 179
Figure 4.66: Computed flood hydrograph resultant from Run4 in sub-watershed SW13 180
Figure 4.67: Computed flood hydrograph for Run4 at Sulaiman Bridge 180
Figure 4.68: Computed flow hydrograph resultant from Run4 at the watershed outlet.............181
Figure 4.69: Computed flood hydrograph resultant from Run5 in sub-watershed SW13 181
Figure 4.70: Observed and computed flood hydrograph for Run5 at Sulaiman Bridge 182
Figure 4.71: Computed flow hydrograph resultant from Run5 at the watershed outlet.............182
Figure C.1: Scatter plots for Summary results of investigated scenarios in all hydrologic elements: 226

List of Tables

Table 2.1: Spectral and spatial resolution of Landsat7 23
Table 2.2: TRMM 3B42 Characteristics....................26
Table 2.3: Symbology used in HEC-HMS for watershed elements....................34
Table 2.4: Recommended DEM cell sizes and their typical range of applications....................63
Table 3.1: SCS soil groups and corresponding loss rates 99
Table 3.2: Total 5-day antecedent rainfall (mm) 100
Table 3.3: General characteristics of rainfall stations located in and near to the Klang watershed. 103
Table 3.4: General characteristics of stream flow stations 105
Table 3.5: Drainage density and drainage orders....................108
Table 4.1: The RSO coordinates for selected control points in Klang watershed 118
Table 4.2: Sub-watershed parameters derived from Topo-DEM....................122
Table 4.3: Impervious area of sub-watershed derived from Topo-DEM and SRTM-DEM......125
Table 4.4: Sub-watershed parameters derived from SRTM-DEM 130
Table 4.5: Evaluation of two DEM-derived parameters by statistical measures 136
Table 4.6: Differentiating DEM-derived parameters based on land form and slope of investigated sub-watersheds....................137
Table 4.7: Results of statistical measures for evaluation of two DEM-derived parameters in LF1 140
Table 4.8: Results of statistical measures for evaluation of two DEM-derived parameters inFL2 140
Table 4.9: Investigated storms for selecting suitable rainfall-runoff event for modeling..........146
Table 4.10: Observed time-to-peak and peak runoff for selected flood events 151
Table 4.11: Temporal variations of selected storm events....................152
Table 4.12: Observed temporal pattern of storm event (6-May) at 18 rain gauges. 154
Table 4.13: Cell-base comparison of observed rainfall with TRMM estimates 160
Table 4.14: Comparison of total rain depth estimated by TRMM and measured in rain gauges for investigated flood events 161
Table 4.15: Caparison the amount of rain that falling to the sub-watershed from gauge rainfall and TRMM rainfall estimates. 163
Table 4.16: Loss estimation parameters based on SCS method....................166
Table 4.17: Routing parameters based on kinematic wave method....................168
Table 4.18: Summary results of for flood event of 6 May 2002 at Sulaiman bridge station 176
Table 4.20: Statistical measures different Runs for eighty hydrologic elements....................183
Table A.1 Status of world mapping in1990 (Source: Konecny, 2003)....................208
Table A.2: Update rates of world mapping (Source: Konecny, 2003)....................208

Table A.3: List of used digital topo sheets at scale of 1:10000 208
Table A.4: List of used digital topo sheets at scale of 1:25000 209
Table B.1: Popular hydrological models..210
Table B.2: Known Hydrological model, types of data mode and their interface level 211
Table C.1: Time-series results flood simulation at Sulaiman Bridge for event 6-May2002 (Run1) 212
Table C.2: Time-series results flood simulation at Sulaiman Bridge for event 6-May2002 (Run2) 214
Table C.3: Summary results of flow simulation for eighty hydrologic elements resultant from rainfall event 6-May 2002 over Klang watershed (Run1). 216
Table C.4: Summary results of flow simulation for eighty hydrologic elements resultant from rainfall event 6-May 2002 over Klang watershed (Run2). 218
Table C.5: Summary results of flow simulation for eighty hydrologic elements resultant from rainfall event 6-May 2002 over Klang watershed (Run3). 220
Table C.6: Summary results of flow simulation for eighty hydrologic elements resultant from rainfall event 6-May 2002 over Klang watershed (Run4). 222
Table C.7: Summary results of flow simulation for eighty hydrologic elements resultant from rainfall event 6-May 2002 over Klang watershed (Run5). 224

List of abbreviations

AGNPS	Agricultural Non-Point Source pollution
ALS	Airborne Laser Scanning
AMC	Antecedent Moisture Condition
ASA	Average Size Area
ASM	Antecedent Soil Moisture
C.V	Coefficient of Variation
CERES	Clouds and the Earth's Radiant Energy System
CN	Curve Number
D8	Deterministic 8
DBMS	Database Management Systems
DEM	Digital Elevation Model
DGM	Digital Ground Models
DHM	Digital Height Models
DID	Department of Irrigation and Drainage
DMA	Defense Mapping Agency
DOA	Department of Agriculture
DSM	Digital Surface Model
DTEM	Digital Terrain Elevation Model
DTM	Digital Terrain Model
DXF	Drawing Exchange File
EOS	Earth Observation Satellite
ESRI	Environmental Systems Research Institute
ETM+	Enhanced Thematic Mapper Plus
FDA	Flood Damage Analysis
GeoHMS	GIS processor
GES DISC	Goddard Earth Sciences Data and Information Services Center
GIS	Geospatial Information Systems
GPM	Global Precipitation Measurement
GPM	Global Precipitation Measurement
GWHM	GIS-based Watershed Hydrological Model
HEC	Hydrologic Engineering Center
HEC-GeoHMS	Geospatial Hydrologic Modeling System
HEC-HMS	Hydrologic Modeling System
HSG	Hydrologic Soli Group
HydroSHEDS	Hydrological data and maps based on SHuttle Elevation Derivatives at multiple Scales
ILWIS	Integrated Land and Water Information System
IA	Impervious Area
KL	Kuala Lumpur
LiDAR	Light Detection And Ranging
LIS	Lightning Imaging Sensor

LU	Land Use
MACRES	Malaysian Centre for Remote Sensing
MAF	Mean Annual Flood
MLA	Maximum Location Accuracy
MLD	Minimum Legible Delineation
MSE	Mean Square Error
NDVI	Normalized Difference Vegetation Index
NSE	Nash-Sutcliffe Efficiency
PBias	Percent Bias
PE	Percent of Error
R2	coefficient of determination
Radar	Radio Detecting And Ranging
RAS	River Analysis System
RGB	Red, Green and Blue
RMSE	Root Mean Square Error
RS	Remote Sensing
RSO	Rectified Skew Orthomorphic
Run1	Running for Topo-DEM derived parameters and rain gauges data
Run2	Running for modified CN
Run3	Running for SRTM-derived sub-watershed area
Run4	Running for Topo-derived sub-watershed area and TRMM data
Run5	Running for SRTM-derived sub-watershed area and TRMM data
SCS	Soil Conservation Service
SFS	Stream Flow Stations
SMART	Stormwater Management and Road Tunnel
SN	Scale Number
SRTM	Shuttle Radar Topography Mission
SWAT	Soil and Water Assessment Tools
TMI	TRMM Microwave Imager
TMPA	TRMM Multi-Satellite Precipitation Analysis
TOVAS	TRMM Online Visualization and Analysis System
TRM.R	TRMM Rainfall
TRMM	Tropical Rainfall Measuring Mission
TSDIS	TRMM Science Data and Information System
UH	Unit Hydrograph
USACE	US Army Corps of Engineers
USACE	US Armey Corps of Engineers
USDA	US Department of Agriculture
UTC	Coordinated Universal Time
VIRS	Visible and Infrared Scanner
WHM	Watershed Hydrological Model

List of symbols

P	Precipitation
I	Infiltration
ET	Evapotranspiration
D	Deep percolation
ΔS	Soil moisture storage change
N_g	Number of gauges
Q	Direct runoff
S	The potential maximum soil storage
I_a	Initial abstraction/loss
λ	Ratio of initial abstraction to maximum potential retention
Q_n	Direct runoff
P_m	Excess rainfall
m	Pulses of excess rainfall
n	Pulses of direct runoff
t_{lag}	Lag time
t_r	Effective rainfall duration
C_1	Constant value (0.75)
C_t	Coefficient derived from gauged watersheds in the same region
L	Length of the main stream from the outlet to the upstream divide
L_c	Distance from the outlet to a point on the stream nearest the centroid of the watershed area
C_2	Constant value (2.7)
C_p	Coefficient derived from gauged watersheds in the same region
t_R	Effective duration
t_r	Effective rainfall duration
q_{pR}	Required peak discharge per unit drainage area
t_b	base time of unit hydrograph
C_3	Constant value (5.56)
W	The width of a UH at a discharge equal to a certain percent of the peak discharge
C_w	1.22 for the 75-percent width and 2.14 for the 50-percent width of UH
q_p	Standard peak discharge per unit drainage area
C	Constant value (2.08)
A	Watershed area
T_c	Time of concentration of the watershed
T_p	Time to peak
I	The inflow
dt	Incremental time
A_c	Cross sectional area of flow
Q_c	Discharge
q_0	Lateral inflow per unit length

x	Distance along the stream
a_c	Kinematic wave parameters for a particular cross sectional shape, slope and roughness
v	volume
d	Known interval
P_{size}	Recommended DEM cell size
P	Pixel size
Δh	The change in elevation
r	Correlation coefficient
Y_{TD}	Parameter derived from the Topo-DEM
Y_{SD}	Parameter derived from the SRTM-DEM
R^2	Coefficient of determination
$\overline{Y_{TD}}$	Mean values of Parameter derived from the Topo-DEM
$\overline{Y_{SD}}$	Mean values of Parameter derived from the SRTM-DEM
CN_s	weighted average CN for sub-watershed
CN_i	CN value of sub-basin i
A_i	Drainage area of sub-basin i
$I_{a\ 0.2}$	Initial abstraction based on λ=0.2
$I_{a\ 0.05}$	Initial abstraction based on λ=0.05
$S_{0.2}$	The potential maximum storage based on λ=0.2
$S_{0.05}$	The potential maximum storage based on λ=0.05
I_2	Inflow at time t2
I_1	Inflow at time t1
Q_2	Outflow at time t2
Q_1	Outflow at time t1
S_1	Storage at time t1
S_2	Storage at time t2
A_1	Surface area of reservoir at level 1
A_2	Surface area of reservoir at level 2
A_m	Average surface area of reservoir between level 1 and level 2
V	volume

Chapter I:

Introduction

Hydrology is an applied science that deals with all aspects of water circulation in the environment. According to McCuen (1998) hydrology is the scientific study of water and its properties, distribution, and effects on the earth's surface, soil, and atmosphere. The most common spatial unit of consideration in hydrologic studies is a watershed (Davie, 2008). A watershed is a dynamic system that involves several natural processes (see Figure 1.1). It is believed that the rainfall-runoff relationship is one of the complicated hydrologic processes in a watershed. It is due to the spatial variation of terrain characteristics that can significantly affect spatial and temporal precipitation patterns, and the number of variables involved in the physical processes. In addition, prediction of hydrological process such as flood simulation and inundation mapping is very important to water resources engineers. The increasing number of extreme flood events (Varley and Marr, 2004) is an important subject among the present and the past hydrologists. In particular, consideration of flood characteristics is one of the main issues in construction activities and watershed management projects. Since 1961 (by the invention of Stanford Watershed Model), computer technology has significantly assisted water resource engineers in developing hydrologic models to study hydrological processes (Crawford and Burges, 2004). In recent years, GIS-based hydrologic models have increasingly developed and deficiencies related to lack of appropriate data for hydrological analysis have been reduced. The current research is an attempt to introduce some of remote sensing data and its application in GIS-based hydrologic models with emphasis on flood-runoff modeling. This is the most active area of research in GIS and RS related to hydrology. The goal is to determine the parameters needed for hydrologic modeling by analysis of the satellite-based terrain data and precipitation estimates by using GIS tools and techniques.

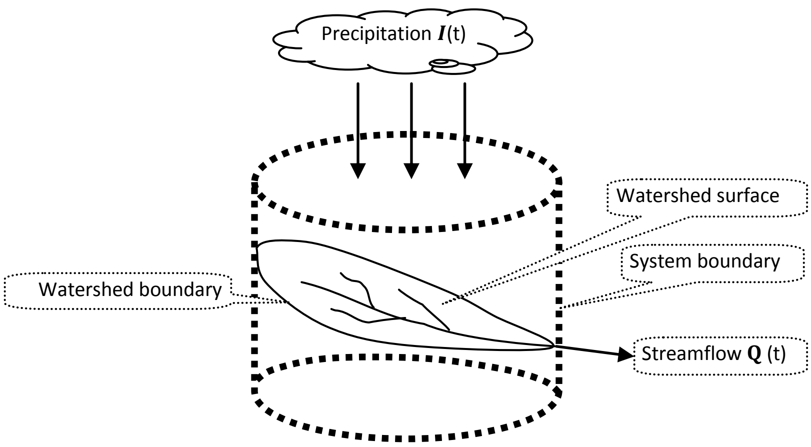

Figure 1.1: Conceptual representation of watershed as a hydrologic system (Chow et al., 1988)

1.1 Availability of data

Regardless of the hydrologic model, algorithms and type of processes, input datasets can significantly influence the model outputs. Hydrological data, including associated hydraulic data, are the vital raw materials in water resource planning and flood modeling (ASCE, 1996). In particular hydrologic data include watershed and sub-watershed boundaries, areas, channel length and slope, watershed slope and aspects, land use, soil type, runoff coefficient, precipitation and stream flow records and so forth. The quantity and quality of the raw hydrologic data highly depends on the investment made to map and monitor an area. Data collection is an expensive process and therefore it needs strong financial support. On the other hand, It is evident that inadequate and uncoordinated hydrologic data resulting from budget shortages has long-term adverse effects on the efficiency and certainty of planning and design thus creating uncertainty and significant risk to public safety (ASCE, 1996). The above statements enhance the value and importance of hydrologic data and its role in rainfall-runoff modeling. Unavailability and sparseness of those data becomes a great barrier in using hydrologic models in many regions. These barriers and advances in computational methods motivate probing on flood modeling and prediction using new spatial analysis tools and available data known as Geospatial Information Systems (GIS) and Remote Sensing (RS) data. GIS is a computerized information system allowing quick access and retrieval of spatial data. GIS tools provide a set of spatial operators that calculate new datasets from existing data. For instance, flow direction, flow accumulation, drainage networks, and watershed boundaries can be generated from a digital elevation model (DEM).

1.2 Status of topography mapping in the world

The UN Secretariat has tried to monitor existing base maps for different countries and continents at different scale. According to Konecny (2003) a near global coverage only exists at the scale of 1:200000 or 1:25000. About 65% of the world has the topography at scale of 1:50000 and about one-third of the land area is covered at scale of 1:25000 (See Appendix A, Table A.1 and A.2). The coverage at these scales is in analogue form and need to be digitized.

The conclusion of these surveys is that the update rate for the 1:50000 maps are only 4% in Asia. This means the average existing 1:50000 maps of the Asian countries are about 37 years old, and the average existing 1:25000 map is 25 years old. Additionally, aerial photogrammetry applied in the 20th century was able to provide mapping coverage in other continents, at least in prominent areas. But technological, financial or organizational limitations have stymied efforts to provide an updated basic mapping coverage needed for sustainable development. Inadequate topography map has also been reported in European countries such as Romania and the Ukraine (Haase and Frotscher, 2005a). Iran as a developing country is another example that still suffers from lack of adequate topographic maps at the scale of 1:25000. According to the Iranian National Cartographic organization, 80% of the country is covered by maps at scale 1:25000 until 2005 (Yegane and Payvandi, 2005). In many more countries, these data sources may have poor quality or inadequate topographic map coverage (Zerger, 1999, Haase and Frotscher, 2005b). Therefore, utilizing new geo-information technologies is required to achieve the new sources of data (Konecny, 2003). In addition, against the background of an inadequate data situation in developing countries and associated actual and future challenges for water management activities, there is a great demand for solutions for the low cost and public domain datasets and software.

1.3 Public domain hydrological software

The first step towards computer modeling was made by Crawford and Linsley in 1962 by introducing the Stanford Watershed Model. It was one of the notably successful efforts in introducing a complex rainfall-runoff model accounting for the dynamics of hydrologic processes in a watershed (Sorooshian et al., 2008). Since then, numerous hydrological models have been developed. It is believed that the reliability and applicability of a hydrological model increase with the integration of GIS and RS. Hydrologic Modeling System (HEC-HMS) is a watershed scale model widely used as public domain software with the capability to link with GIS environment through the Geospatial Hydrologic Modeling System (HEC-GeoHMS). Soil and Water Assessment Tools (SWAT) is another public domain model actively supported by the US Department of Agriculture (USDA). SWAT is a watershed scale model developed to quantify the impact of land management practices in large complex watersheds.

1.4 Public domain datasets

Remote sensing can provide earth's surface and atmosphere information of a large area in temporal periods with different scales. Recent advances in RS technology have provided valuable information related to the terrain characteristics, soil moisture, radiations, precipitation, cloud cover, land use and so forth. Ravenous computation also exists between the satellite industries and software vendors. This competition has great effect on data markets and make it low cost and therefore, easy to access by many communities through the web. Consequently, it is needed to investigate and assess the potential applications for the new RS data. This research has been designed to address the methodology for flood modeling using public domain hydrologic model and global free satellite datasets with emphasize on Shuttle Radar Topography Mission (SRTM) and Tropical Rainfall Measuring Mission (TRMM) datasets. The primary focus of this work is not the accuracy of the elevation data themselves, but the attributes derived from them.

1.5 Knowledge Gaps on Satellite-Based Flood Modeling

Understanding the current knowledge gaps in satellite based flood modeling is critical for successful application of satellite-based rainfall and terrain data over regions that have no access to a conventional rainfall and terrain data sources. The central theme on the current knowledge gap deals with the hydrologic implications of uncertainty of the satellite data in different regions. Thus, critical assessment of satellite rainfall and terrain data provides the opportunities for flood modeling in un-gauged watersheds. According to Cai and Yeh (2008) satellite- based data can prevent humankind from flood hazard. Although previous researches had contributed to use of remotely sensed data specifically SRTM (Hendricks et al., 2003b, Jarvis et al., 2004a, Rodriguez et al., 2005, Kiel et al., 2006, Pryde et al., 2007) and TRMM (Feidas et al., 2006, Harris et al., 2007, Su et al., 2007), researches for enhancing practical applications of these data for flood study are still rare specifically in Asia.

1.6 Objectives and scope

Considering the above discussion the main objectives of this research are:

1. To expand the ability of GIS tools and techniques for establishment of hydrological database using digital elevation model (DEM) for Klang watershed.

2. To probe on the ability of SRTM elevation data for watershed delineation and parameterization.

3. To assess the ability of TRMM estimates for explaining the spatial and temporal pattern of storms responsible for flood events in Klang watershed.

4. To extend the practical use of two public domain satellite data (SRTM and TRMM) for flood simulation using public domain hydrological model (HEC-HMS and HEC-GeoHMS).

5. To assess the SCS loss method with the new initial abstraction ratio (0.05) in tropic region.

In other words, this research has been designed to answer the following questions:

1- How well can GIS tools and techniques and RS database are used for the purpose of watershed delineation and parameterization?

2- How well SRTM-DEM can delineate watershed boundaries and investigated parameters compared to Topo-DEM and how significant can new sources obviate the lack of topographic data?

3- How well TRMM data can explain the spatial and temporal pattern of storms responsible for flood events in Klang watershed and what is the effective influence range of rain gauges and what is the optimal method and cell size for interpolating gauge data in order to determine the spatial variation of storm events over Klang watershed?

4- How well public domain satellite data (SRTM and TRMM) and public domain software can be used to simulate flood hydrograph for a flood event?

5- How is the performance of modified SCS initial abstraction ratio in flood simulation?

1.7 Key Assumptions

There were several key assumptions made in this research as follows:

1- Gauge rainfall data (collected from DID Malaysia) from a very dense gauge network is assumed as the most reliable source of rainfall data in the study area.

2- Digital topo sheet at scale of 1:25000 and 1:5000 obtained from the authorized organization (JUPEM Malaysia) represents the most reliable existing terrain characteristics of study area.

3- Land use and soil maps obtained from the DOA Malaysia truly represent the spatial variation of land types and topsoil properties of the watershed for the year 2002.

4- Under the conditions of floods for the selected events errors associated with measurements in stream flow and rainfall gauges are negligible.

1.8 Thesis outline

The thesis is organized in 5 chapters including the following materials:

- Chapter 1 is a gateway to the subject and the objectives of research.
- Chapter 2 contains a broad range of literatures regarding to different aspects of this research. It includes some basic theories related to the subjects and previous studies related to this research. Literatures mainly selected from specialized books and journals.
- Chapter 3 explains the methodology of the research then the study area and materials used for this research were organized and described. Data collection processing and database development are also explained in this chapter.
- Chapter 4 includes result and discussion which organized in three parts. At first watershed delineation and parameterization are performed based on Top-DEM and SRTM. Then Spatial and temporal characteristic of rainfall events based on gauge data and TRMM were investigated. Finally flood simulation is perfumed based on ground data (Topo-DEM, gauge data) and satellite data (SRTM-DEM and TRMM) by using HEC-HMS.
- Chapter 5 outlines the main outcomes of this research and feature plan for further development.

Chapter II:

Literature Review

2.1 Spatial Hydrology

The literatures on this section contain three major parts. In the first part, literature related to modeling concepts and flood modeling is reviewed. It also review works being done to refine the network and watershed delineation methods which utilize DEM data for hydrological processes. In second part, GIS-based hydrological models and related issues including GIS, spatial data models and remote sensing technology are reviewed. Finally, literature relevant to rainfall runoff modeling component and utilization of DEM data in hydrologic modeling are presented. It is noted that the issues are separated here for better organization. However, from a modeling point of view they are strongly related to each other and thus some overlap between topics may be apparent.

2.1.1 Modeling concepts

Meyer (1985) defined the model as an object or a concept which is used to represent something else. A more comprehensive definition is found in the Oxford dictionary of science (2005) in which a model is defined as a simplified description of a physical system intended to capture the essential aspects of the system in a sufficiently simple form to enable the mathematics to be solved. According to Li et al. (2005a) models are classified into three categories known as conceptual, physical and mathematical models. Also, a problem may be either deterministic or subject to changes and therefore probabilistic (Li et al., 2005a). Thus, in this aspect mathematical models are classified into functional models, which are those intended to solve deterministic problems and stochastic models, which are those used to solve probabilistic problems. There are several reasons for using mathematical models. Saaty and Alexander (1981) express some of them as follows:

i. Models permit abstraction based on logical formation using a convenient language expressed in a shorthand notation, thus enabling one to better visualize the main elements of a problem while at the same time satisfying communication, decreasing ambiguity, and improving the chance of agreement on the results.

ii. They allow one to keep track of the important parts of the problem.

iii. They help to generalize and apply the results to the other areas.

iv. They provide an opportunity to consider all the possibilities, to evaluate alternatives, and to eliminate the impossible ones.

v. They are tools for understanding the real world and discovering natural laws.

A mathematical model is used based on the problem and the goodness of representing the real situation.

2.1.2 Flood modeling

It is believed that flood (as hydrologic phenomena) is a watershed response to an intense rainfall event which can cause serious undesirable effects on people and the Environment. Chow et al. (1988) define the flood as a relatively high flow, which overtaxes the natural channel provided for the runoff. Flood can be occurring in different forms. Smith et al. (1998) classified floods into two types, which are river floods and coastal floods with different characteristics. According to the DID (2000) types of river flood in Malaysia are: monsoon flood, urban flash flood, debris flow and dam release. Major flood studies have concentrated on urban watershed. This is because urban development extends the impermeable surfaces that increase runoff, and construction of drainage systems that accelerate the flood mechanism (Gruntfest and Huber, 1991, Smith et al., 2002). To mitigate the potential flood impacts on the watershed properties and protect manmade and natural infrastructure, flood prevention activities are involved by means of flood simulation. Recently, many hydrologic models with rainfall-runoff components have been developed. Some of the newly developed models are capable of utilize the GIS tools and remotely sensed data.

2.1.3 Watershed hydrological model

The terms watershed models (Ogden et al., 2001, Singh and Woolhiser, 2002, Singh and Frevert, 2006), hydrologic models (Maidment and Djokic, 2000, Singh and Woolhiser, 2002, Singh and Frevert, 2006, Sorooshian et al., 2008), watershed hydrology models (Singh and Woolhiser, 2002), watershed hydrological models (Fried, 1991, Chen et al., 2001, Cau and Paniconi, 2007, Huang and Chen, 2008) have been used for almost the same meaning. The term watershed hydrological model (WHM) is used for development of this thesis instead of all other terms. It is because the world *hydrological* emphasizes the hydrological process and the word *watershed* indicates the system. WHMs simulate natural processes of the flow of water, sediment, chemicals, nutrients, and microbial organisms within watersheds, as well as quantify the impact of human activities on these processes (Singh and Frevert, 2006).WHMs is a main tool for study of a wide range of environmental and water resources problems such as floods . Flood modeling is one of the most important subjects in tropic regions due to high amounts of rainfall. It has high effects on water resources planning, development, design, operation, and management. Hydrologic models are developed to utilize flood modeling in a systematic approach. Many researchers have studied on comparison of different aspects of WHMs. Each model concerns the specific issues and situation. This is the main reason for classification of WHMs into several domains. However, some WHMs are able to consider more than one aspect. In other word they are multipurpose models.

2.2 Classification of watershed hydrological models

Many different schemes for classification of WHMs have been introduced in the literatures over the past and recent decades. Often models have been classified according to distinguishable properties like lumped versus distributed, deterministic versus stochastic, steady state versus time variable and so forth (Anderson, 2005). A former classification by Chow et al. (1988) introduces WHMs into two categories known as deterministic and stochastic models. Deterministic physical equation is often referred to as white box models. The stochastic models can be grouped into grey box models and black box models (Jonsdottir, 2006). The grey box models are described by physical equations and a noise factor. Stochastic models are not the focus of this research, therefore no more detail is provided.

2.2.1 Processing environment

Maidment (1993b) classified the hydrologic models based on the flow environment and the major variables for which hydrologic models are constructed. In this aspect hydrologic models are classified into surface water or groundwater flow model and surface water quality or ground water transport models. In addition, Feng (2004) classified hydrologic models in two categories known as physically-based or empirical-based hydrologic models.

2.2.2 Spatial variability

According to Cunderlik et al. (2003), deterministic WHMs are classified into three main categories:

1- Lumped models: Parameters of lumped WHMs do not vary spatially within the watershed and thus, watershed response is evaluated only at the outlet, without explicitly accounting for the response of individual sub-basins. Parameters of lumped models often do not represent physical features of hydrologic processes and usually use empirical equations. The effect of spatial variability of model parameters is assessed by using averaged values for the entire basin. The most commonly employed procedure is an area-weighted average (Haan et al., 1982). If the interest is primarily in the discharge prediction only, then these models can provide just as good simulations as complex physically based models (Beven, 2001).

2- Semi-distributed models: Parameters of semi-distributed models are partially allowed to vary in space by dividing the watershed into a number of smaller sub-watersheds. There are two main types of semi-distributed models known as kinematic wave theory models such as HEC-HMS and Probability distributed models such as TOPMODEL (Cunderlik et al., 2003).

3- Distributed models: Parameters of distributed models are fully allowed to vary in space at an appropriate resolution usually chosen by the user. Distributed modeling approach attempts to incorporate data concerning the spatial distribution of parameter variations together with computational algorithms to evaluate the influence of this distribution on simulated rainfall-runoff behavior (Cunderlik et al., 2003). Distributed models generally require large amounts of (often unavailable) data for parameterization in each grid cell. Inaccessibility of data in such detail is a big challenge for this type of models. However, the governing physical processes are modeled in detail, and if properly applied, they can provide the highest degree of accuracy.

2.2.3 Time intervals

According to Diskin and Simon (1979), watershed models can be classified based on time intervals as: a) continuous-time or event-based, b) daily, c) monthly, or d) yearly models. This classification discriminates a model based on the watershed-runoff processes so that the event model simulates a single storm. The duration of the storm may range from a few hours to a few days. A continuous model simulates a longer period, predicting watershed response both during and between precipitation events.

2.2.4 Spatial scales

The models can also be classified by spatial scale. In this aspect Singh (1995) classified watershed models into three classes based on size of watershed. Those are small scale models (area ≤ 100 km^2), medium scale models (area between 100 and 1000 km^2), and large scale models (area >1000 km^2). This classification is arbitrary, although it is related to the concept of homogeneity and the validity of averaging of hydrological processes over a particular area.

2.2.5 Applications

Wurbs (1998) has divided watershed models based on types of application into seven categories as: (i) Runoff models, (ii) River hydraulic models, (iii) Water quality models, (iv) Reservoir/river operation models, (v) Groundwater models, (vi) Water distribution models and, (vii) Demand forecasting models.

2.2.6 Measured-parameter or fitted-parameter

This classification is critical in selecting models for application when observations of input and output are unavailable. Variables in measured-parameter model are determined from system properties, either by direct or indirect methods. A fitted-parameter model, on the other hand, includes parameters that cannot be measured. Instead, the parameters must be found by fitting the model with observed values of the input and the output. HEC-HMS includes both measured-parameter models and fitted-parameter models. For example, the baseflow model is empirical, so its parameters cannot be measured. Instead, for a selected watershed, the baseflow-model parameters can be found by calibration. On the other hand, the soil characteristics in the Green and Ampt loss model can be determined by sampling.

2.2.7 Inventory of the WHMs

Since July 1962 when the Stanford Watershed Model was published as Crawford's PhD thesis, Linsley recognized the high potential for computer based modeling (Crawford and Burges, 2004). Thereafter, many WHMs have been developed during the past several eras. Model development has been made based on wide range of demand for water resource issues. In 1991 the Bureau of Reclamation, prepared an inventory of 64 WHMs classified into 4 categories, and the inventory has been updated over the past several years. As result of shared work between Texas A&M University and the Bureau of Reclamation essential information is provided for a wide spectrum of WHMs to the academic, administrative and private users. In 1999 the Hydrologic Modeling Inventory Website was established as a joint project between Louisiana State University and the Bureau of Reclamation. Developers of famous models are asked to complete an inquiry form providing basic information including the capabilities of their model, input requirements, output information, assumptions, hardware requirements and author information. Dr. Vijay P. Singh, Dr. Donald K. Frevert and several other Bureau of Reclamation staff members catalog the models in the Hydrologic Modeling Inventory Website based on characteristic of the models. (See: http://hydrologicmodels.tamu.edu). Singh (1995) edited a book that summarized 26 most popular models presented by 53 prominent hydrologists around the globe. Preliminary remarks on watershed modeling, model calibration and reliability estimation are also provided in this book. The First Federal Interagency Hydrologic Modeling Conference proceeding introduced many popular WHMs developed by federal agencies in the US (Singh and Frevert, 2006). In another evaluation Singh and Woolhiser (2002) introduced 68 popular WHMs. From the comparison of WHMs Singh and Woolhiser (2002) point out the following conclusions:

1. Many of the current WHMs are comprehensive, distributed, and physically based. They possess the capability to accurately simulate watershed hydrology and can be applied to address a wide range of environmental and water-resources problems.

2. The scope of mathematical models is growing, and the models are capable of simulating not only water quantity but also quality.

3. The technology of model calibration is much improved, although not all models have taken full advantage of it.

4. The models are becoming embedded in modeling systems whose mission is much larger, encompassing several disciplinary areas.

5. The technology of data collection, storage, retrieval, processing, and management has improved by leaps and bounds. In conjunction with literally limitless computing prowess, this technology has significantly contributed to the development of comprehensive distributed watershed models.

2.2.8 Deficiencies of models

There is multitude of WHMs with diverse application so that one can easily find more than one WHM for a particular problem. Although WHMs have become increasingly more complex, there is a long way to go before they become “household” tools (Singh and Frevert, 2006). According to Singh and Frevert (2006) the most universal deficiencies of the WHMs are as follows:

a) Lack of user-friendliness. b) Large data requirements. c) Lack of quantitative measures of their reliability e) unclear statement of their limitations f) unclear guidance for their applicability. g) Some of the models cannot be embedded with social, political, and environmental systems.

2.3 Geospatial information systems (GIS)

2.3.1 Definition

The term GIS has been defined in several ways. To some GIS means only the software used to analyze geo-referenced data. But to some this term includes the hardware utilized by the system. However, academic definitions presented for the GIS convey almost common concepts, but from different views. Aronoff (1989) defined GIS as a computer based system that provides four sets of capabilities to handle geo-referenced data. Those are data input, data storage and retrieval, data manipulation and analysis, and data output. Goodchild (1993) defined GIS as a general-purpose technology for handling geographic data in digital form with following capabilities: (i) the ability to preprocess data from large stores into a form suitable for analysis such as map projection, resample and generalization, (ii) direct support for analysis and modeling, and (iii) post processing of results such as reformatting, tabulation, report generation and mapping. Burrough and McDonnell (1998) defined GIS as a set of tools for collecting, storing, retrieving, transforming and displaying geo-spatial data from the real world for a particular set of purposes. According to Goodchild (2003) and Johnson (2009) a high proportion of the data needed for hydrological analysis are inherently geographic. With the development of computer science and evolution of geospatial information tools, WHMs have received much support from GIS technology. GIS framework allows taking into account the spatial variations of hydrologic phenomena over the watersheds effectively. The use of WHMs in the GIS environment would allow hydrologists to model hydrologic phenomena more quickly and efficiently, and provide planners whit a better tool for evaluating different scenarios (Goodchild et al., 1993). Considering these benefits have motivated the usage of GIS and WHMs among researchers and developers. In recent years several prominent researchers have been attempted to employ GIS tools for hydrologic modeling (Goodchild et al., 1993, Maidment and Djokic, 2000, Maidment, 2002, Lyon, 2003 , Shamsi, 2005, Singh and Frevert, 2006, Bedient et al., 2008, Sorooshian et al., 2008, Johnson, 2009). The integration of GIS and HM have formed a new generation of WHM known as GIS-based Watershed Hydrological Model (GWHM) (An, 2007).

2.3.2 Spatial data types

GIS technology employs two basic types of data known as spatial data and attribute data. Spatial data describes the absolute and relative location of geographic features and attribute data describes characteristics of the spatial features. Attribute data is often referred to as tabular data. According to Longley et al.(2005) all geographic features in the real world can be characterized and defined as one of three basic feature types known points, lines and polygons. Point data exists when a feature is associated with a single location in space. Examples of point features include a rainfall and stream flow stations, dam site and so on. Linear data exists when a feature's location is described by a string of spatial coordinates. Drainage network and watershed boundaries are examples of linear features. Polygons or areal data exists when a feature is described by a closed string of spatial coordinates. Examples of polygon data include land use classes, hydrologic soil group, and so on. Most polygon data is considered to be homogeneous in nature and thus the quality or quantity remains constant in certain zone.

2.3.3 Spatial Data Models

Spatial data has been traditionally stored and presented in the form of a paper map. Two basic types of spatial data models have developed for storing geospatial data digitally. These are known as Vector and Raster models (see Figure 2.1). These methods are used to reduce geographic phenomena to forms that can be coded in computer databases (Longley et al., 2005).

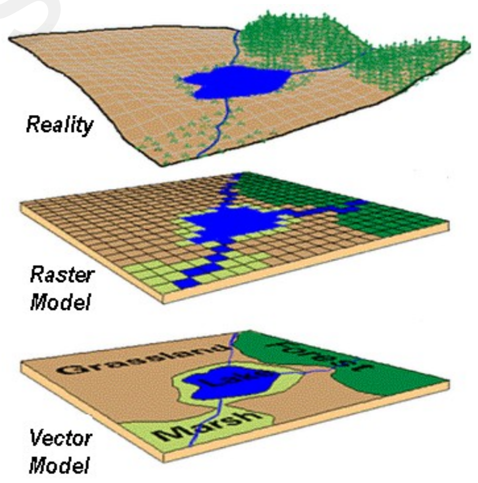

Figure 2.1: Presenting features in real world by means of raster and a vector model (Taken from Bio diversity GIS web page: http://bgis.sanbi.org/gis-primer/page_15.htm)

- Raster data model

Many types of data are often measured and stored in raster format. In a raster representation space is divided into an array of rectangular cells. All spatial variation is then expressed by assigning an attribute to each cell. The cell is sometimes called pixel. A pixel in raster model represents the generalized characteristics of an area of specific size on or near the surface of the Earth (Fazal, 2008). When information is represented in raster form, all details within a cell are lost, and instead the cell is given a single value (Longley et al., 2005). The raster data structure is perhaps one of the more familiar data structures in hydrology (Vieux, 2004b). Johnson (2009) has been stated that raster model is often used to represent hydrological variables such as temperature, rainfall, and elevation. One of the most common forms of raster data is produced by remote-sensing satellites. The actual ground size depicted by a pixel is dependent on the desired resolution of data and satellite sensor technology, which may range from less than one meter (e.g., 41 cm, GeoEye-1, launched on September 6 2008) to several meters (e.g., 90 m, SRTM launched on February 11, 2000) or several kilometers (e.g., ~4.4 km, TRMM, launched on November 28, 1997). In a raster model, a point is given by a point identifier, its coordinates, and the attribute value. A line is given by a line identifier, a series of coordinates forming the line, and the attributes. A polygon segment is given by an area identifier, a group of coordinates forming the polygon, and the attributes.

- Vector data model

According to Longley (2005) Vector storage implies the use of vectors (directional lines) to represent a geographic feature. Vector data is characterized by the use of sequential points or vertices to define a linear segment. Each vertex consists of an X coordinate and a Y coordinate (Buckley, 1997). While in a raster representation space is divided into an array of rectangular cells or pixels. All geographic variation is then expressed by assigning properties or attributes to these cells (Longley, 2005). As illustrated in Figure 2.2, all environmental objects can be represented in three basic forms. The image format is an encoding technique. Image data utilizes techniques very similar to raster data, however typically omits the internal formats required for analysis and modeling of the data (Buckley, 1997). The connection between raster and vector data is critical in spatial hydrology, compared to other applications of GIS. According to Maidment (1998) a well-constructed geospatial database for hydrology incorporates both vector and raster data in a tightly connected raster-vector data model.

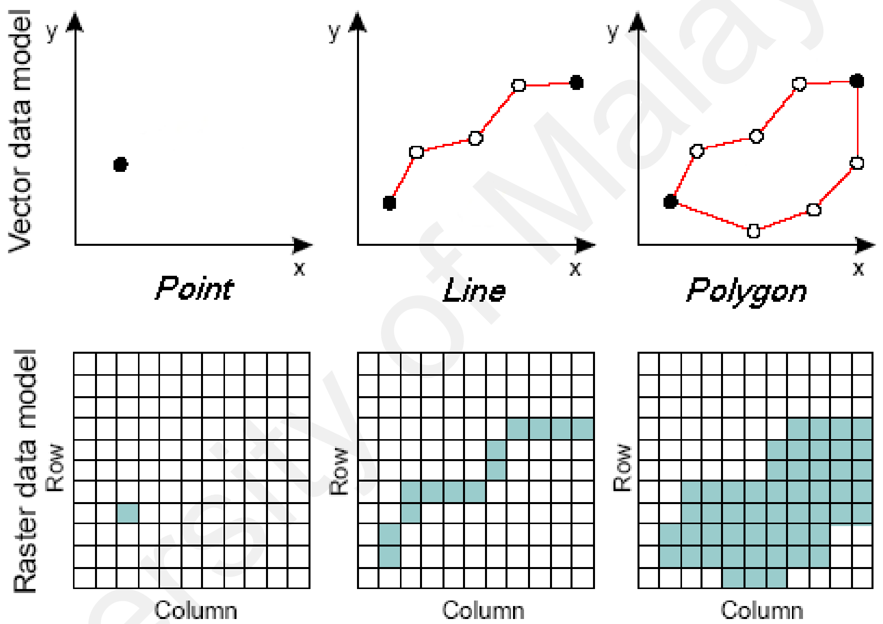

Figure 2.2: Schematic representation of basic features in GIS (Taken from: http://library.oceanteacher.org/OTMediawiki/index.php/Geographic_Information_System_Data_Models)

The raster and vector data model is currently used in a wide range of GIS applications and many of them are strongly associated with water resources. Numerous scientific sources are available regarding GIS components, spatial data models, spatial analysis, tools and techniques and applications. Those are available in specialized proceedings, journals, books and authorized web pages (For more in-depth information see: Aronoff, 1989, Goodchild et al., 1993, Singh et al., 1996b, Buckley, 1997, Burrough and McDonnell, 1998, Maidment, 2002, Shamsi, 2002, Goodchild, 2003, Lyon, 2003 , Li et al., 2005a, Longley et al., 2005, Shamsi, 2005, Zhou et al., 2008, Johnson, 2009, Brimicombe, 2009).

2. 4 Remote sensing (RS)

Generally, remote sensing includes the activities of recording, observing, perceiving (sensing) objects or events at far away (remote) places. It is believed that without RS imagery, GIS could not be attractive for many water resources applications. GIS tools and techniques have had significant influence in the development of hydrologic models over the past decades. Hydrological applications of satellite imagery have been discussed by several researchers. Meijerink (1996), Wong et al. (2001) and Koudmani (2004) have addressed a wide range of RS applications in the field of hydrology. It has been specifically used for flood modeling and management (Hossain, 2004, Sanyal and Lu, 2004, Harris et al., 2007a), snow mapping (Faria et al., 2000a) and watershed delineation (Alarcon and O'Hara, 2006) precipitation estimation (Sorooshian et al., 2000b, Feidas et al., 2006a), etc. This research utilizes three types of remote sensing products.

2.4.1 Landsat

Land sat provide one of the most accurate means of measuring the extent and pattern of changes in landscape conditions over time (DeFries and Belward, 2000).
Landsat-1 was the world's first earth observation satellite (EOS), launched by the United States in 1972 (NAS, 2008). Its excellent set of capabilities emphasized the importance of state-of-the-art remote sensing. Landsat7 ETM+ is currently operated as a primary satellite. Landsat 7 was launched on 15 April 1999 at Vandenberg Air Force Base in California. It collects data in accordance with the World Wide Reference System, which has catalogued the world's land mass into 57,784 scenes, each 183 km wide and 170 km long (NAS, 2008). It collects data in eight spectral bands (See table 2.1).

Table 2.1: Spectral and spatial resolution of Landsat7

Band	Wave length	Resolution m
1	0.45-0.515	30
2	0.525-0.605	30
3	0.63-0.69	30
4	0.75-0.90	30
5	1.55-1.75	30
6	10.4-12.5	60
7	2.09-2.35	30
8	0.52-0.9	15

Source: official web site of Landsat7 (http://landsat.gsfc.nasa.gov/about/etm+.html)

Landsat imagery can use to make natural or false color composites with the color composite operation (Koolhoven et al., 2007). Nijmeijer (2001) states that color composites are created and displayed on the screen, by combining the spectral values of three individual bands (see Figure 2.3). Each band is displayed using one of the primary colors which are Red, Green and Blue (RGB). Color composite could represent natural or false representation of land colors. In a false color composite, the red color is assigned to the near infrared band, the green color to the red visible band and the blue color to the green visible band. The green vegetation will appear reddish, the water bluish and the bare soil in shades of brown and gray (Nijmeijer, 2001). Satellite images contain boundaries between surfaces with different frequency responses. Boundaries can be crop types, urban-rural fringe, vegetation, soil type, or rock type. Boundaries are known as edges and they rapidly change in value across a small area (Nijmeijer, 2001). The edges enhancement techniques such as stretching and filtering are used to achieve the sharper boundaries on images. That could assist visual interpretation of the images.

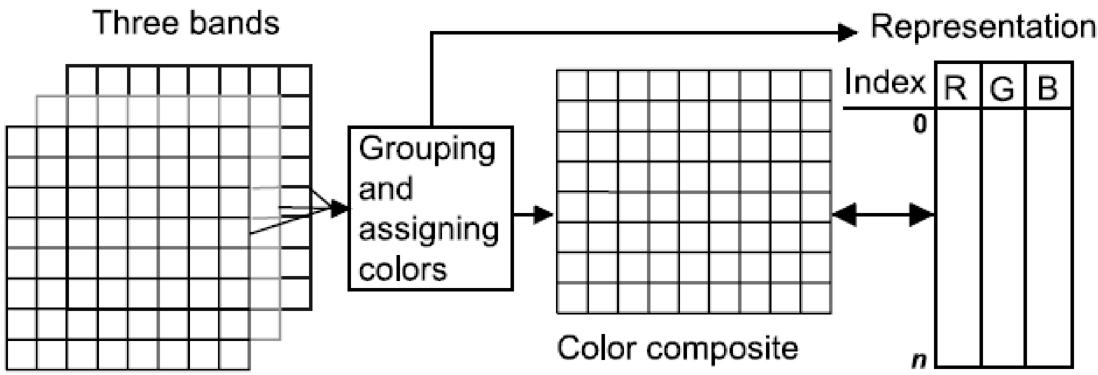

Figure 2.3: workflow of generating color composite
(Taken from ILWIS application guide)

2.4.2 SRTM

According to Jarvis et al. (2004b) the Shuttle Radar Topography Mission (SRTM) elevation data have been produced using radar images gathered from the National Aeronautics and Space Administration's shuttle. Two antennae received the reflected radar pulses at the same time, one antenna located in the shuttle's cargo bay, the other at the tip of a 60-m-long mast. This configuration allowed single-pass radar interferometry, and consequently the generation of a highly accurate global elevation model with a vertical accuracy of 6 m and a horizontal pixel spacing of 30 m (Jarvis et al., 2004b). NASA released the SRTM dataset in 2003.

2. 4.3 TRMM

TRMM is a joint NASA/Japan satellite designed specifically to monitor rainfall and its associated latent heating in the tropics and subtropics (King et al., 2004). The total rainfall and its distribution are important, because the atmosphere gets three-fourths of its heat energy from the release of latent heat in the process of precipitation. The horizontal and vertical location at which this energy is released affects the weather around the world. Despite its fundamental importance to global climate, the total rainfall in the tropics is not well known, and the vertical distribution of latent heating can only be estimated imprecisely. Although the sensors on TRMM have utility beyond the primary rainfall parameters, the TRMM science team has defined and developed a set of “standard products” that are critical to monitoring rainfall and its vertical structure. These standard products are processed by the TRMM Science Data and Information System (TSDIS).The algorithms are coded by members of the TRMM science team who have the responsibility to develop these products. As an example, the passive microwave (TMI) team has the responsibility for generating code to produce TMI calibrated brightness temperatures (1B-11), TMI rainfall structure products (2A-12), and TMI monthly surface rainfall maps (3A-11). Japan supplied the launch vehicle and precipitation radar for TRMM, and NASA provided a TMI, a Visible and Infrared Scanner (VIRS), a Clouds and the Earth’s Radiant Energy System (CERES), a Lightning Imaging Sensor (LIS), and the TRMM spacecraft. TRMM was launched on a Japanese H-II launch vehicle in November 1997 (NASA, 2006). TRMM instruments are shown in Figure 2.4. The TRMM mission has identified four main ground validation sites, which include ground based radars and their associated rain gauge networks. Radar sites located on Southern Florida, Australia (Darwin), Southeastern Texas, and the Marshall Islands (NASA, 2006). Ground validation data are processed at Goddard Space Flight Center in cooperation with the TRMM ground validation team. According to Serafin et al. (2007) TRMM technology is now under development to operate in near future (2013) operate as a Global Precipitation Measurement (GPM) with the capability to measure rainfall depth from 2.5 to 250 mm.

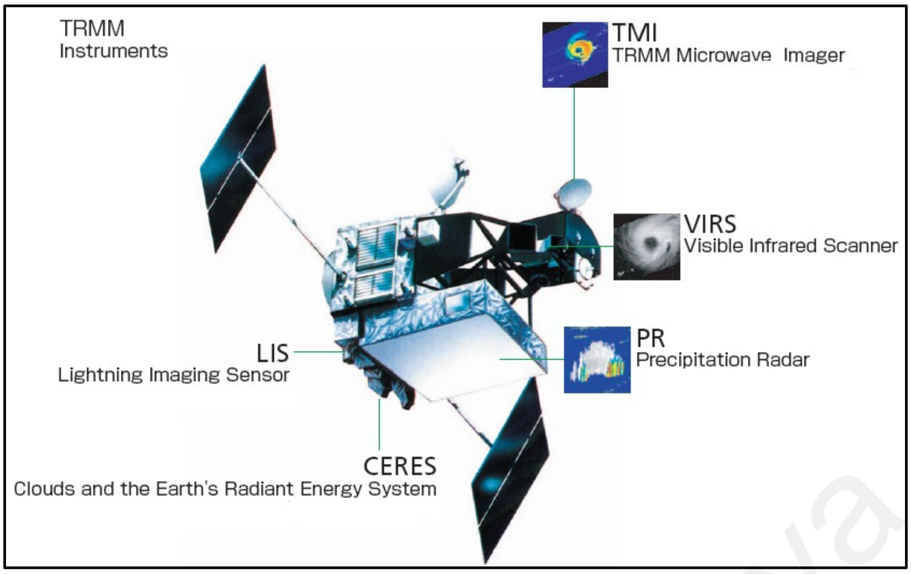

Figure 2.4: The TRMM instruments (Source: http://www.jaxa.jp/projects/sat/trmm/)

2. 4.4 TRMM3B42 Characteristics

According to NASA (2009) the combined instrument rain calibration algorithm (3B-42) uses an optimal combination of 2B-31, 2A-12, SSMI, AMSR and AMSU precipitation estimates, to adjust IR estimates from geostationary IR observations. Specifications of TRMM3B42 data are presented in Table 2.2.

Table 2.2: TRMM 3B42 Characteristics

Temporal Coverage Start Date	1998-01-01; Stop Date: -
Geographic Coverage Latitude	50°S - 50°N; Longitude:180°W - 180°E
Horizontal Resolution	0.25° x 0.25°
Temporal Resolution	3-Hour
Average File Size	Compressed: ~285 KB; Original: ~4.5 MB
File Type	HDF, NetCDF, KMZ, ASCII
Product	Precipitation, range 0.0-100.00 mm

As shown in Figure 2.5 TRMM Online Visualization and Analysis System (TOVAS) provide 3-hourly TRMM Rainfall Estimate for every geographic coverage between latitude :50°S - 50°N; and longitude:180°W - 180°E.

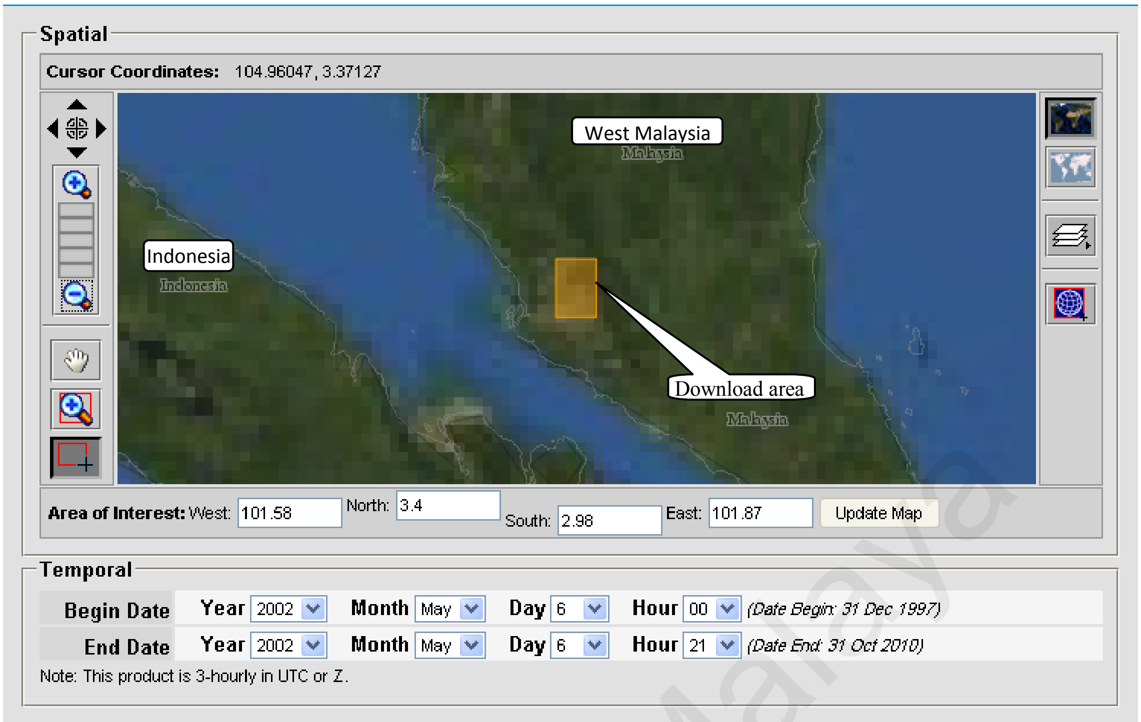

Figure 2.5: TRMM Online Visualization and Analysis System (TOVAS) 3-hourly TRMM Rainfall Estimate (3B42 V6). (Source: http://gdata1.sci.gsfc.nasa.gov)

According to TRMM web site (http://earth.nasa.gov/trmm/index.html) the mission time for TRMM is Coordinated Universal Time (abbreviated to UTC). Malaysia Time (MYT) in Kuala Lumpur is equal to GMT +8 hours. Therefore time adjustment has to be made for rainfall events. However due to coarse temporal resolution of TRMM (3 hours) compare to gauge rainfall (15 minutes), significant uncertainty influences identifying the starting and ending of storm event and consequently their resultant time of peak flow which is extremely important in flood forecasting systems.

2.5 GIS-based watershed hydrological model

GIS and database management systems (DBMS), graphic and visual design tools are employed for processing of large quantities of data (Singh et al., 1996). In fact, DBMS and graphic are two important companion parts of GIS as subsystem; thus we consider both GIS and DBMS as unique systems. In addition as shown in Figure 2.6, Remotely Sensed (RS) technology has significant contribution to promote GIS by providing a wide range of environmental datasets.

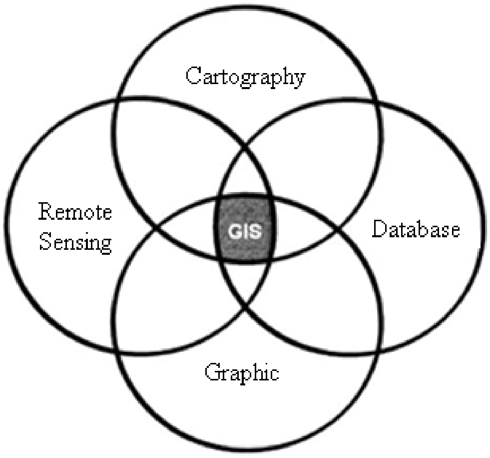

Figure 2.6 Interrelationship between GIS disciplines
Adapted from: Konecny, 2003

As mentioned before, the first computerized WHM (Stanford Watershed Model) has been developed in 1962 (Crawford and Burges, 2004). But twenty years later (in 1982) the first version of ARC/INFO (as widely used GIS software) was launched by Environmental Systems Research Institute (ESRI). Several years later ESRI added a number of functions that were useful to hydrologists in addition to a large number of geospatial data processing and coordinate conversion routines. In terms of history, a significant gap is clearly seen between these two computing technologies. In other worlds they have been originally developed separately but, in recent years, due to highly increasing demands in analytical solutions of water resource problems, developers have been attempting to integrate GIS into hydrologic models in several ways.

2.6 Current approaches to integrate GIS with WHMs

The use of GIS in environmental modeling has increased over the past decades. However, to date, no generalized GIS system has the data representation flexibility for space and time together with algorithmic capability needed to construct process-based models internally. In addition, it has been stated that GIS is still limited in its ability to perform any kind of engineering modeling (Yang and Tsai, 2000) and can only provide for data storage, management, inventory, general spatial analysis and cartographic functionalities. Maidment (1993b) also emphasizes that until GIS has explicit time variation in its data structures, its role will largely be limited to an input data provider, output display, and mapping device. Thus, environmental models and GIS must be coupled. In particular, coupling methods for integrating GIS and hydrologic engineering models have been explored since the late 1980s as part of the GIS community's efforts to improve the analytical capabilities of GIS (Sui and Maggio, 1999). Moreover, it has been believed that GIS can contribute to WHMs by sharing its capabilities for handling and storing massive spatially distributed data which is then given a format for the input of a given model or imported after a model simulation is executed for visualization and spatial analysis (Sui and Maggio, 1999). The rapid transmission of GIS in society has the potential to make various WHMs more clear and enable the communication of their operations and results to a large group of users. Discussions around coupling method for sharing benefits have grown in the literature over the past decades (Maidment, 1993b, Singh, 1995, Maidment, 1996, Sui and Maggio, 1999, Loague and Corwin, 2000, Shamsi, 2002, Feng, 2004, Martin et al., 2005b). Several researches have focused on the improvement of spatial analytical and modeling capabilities of GIS technology during the past (Goodchild et al., 1992). So far, different approaches have been employed to integrate GIS with WHMs. Although overlapping with many other GIS modeling efforts in terms of the general methodology (Sui, 1998), the coupling of GIS with hydrological modeling has a set of different issues from other kinds of GIS-based environmental modeling (Goodchild et al., 1993). Generally, four of the most common strategies have been widely used for linking a GIS to WHMs. Those are known as: (a) loose coupling, (b) tight coupling, (c) embedding WHMs in GIS, (d) embedding GIS in WHMs. Coupling approach is conceptually shown in Figure 2.7.

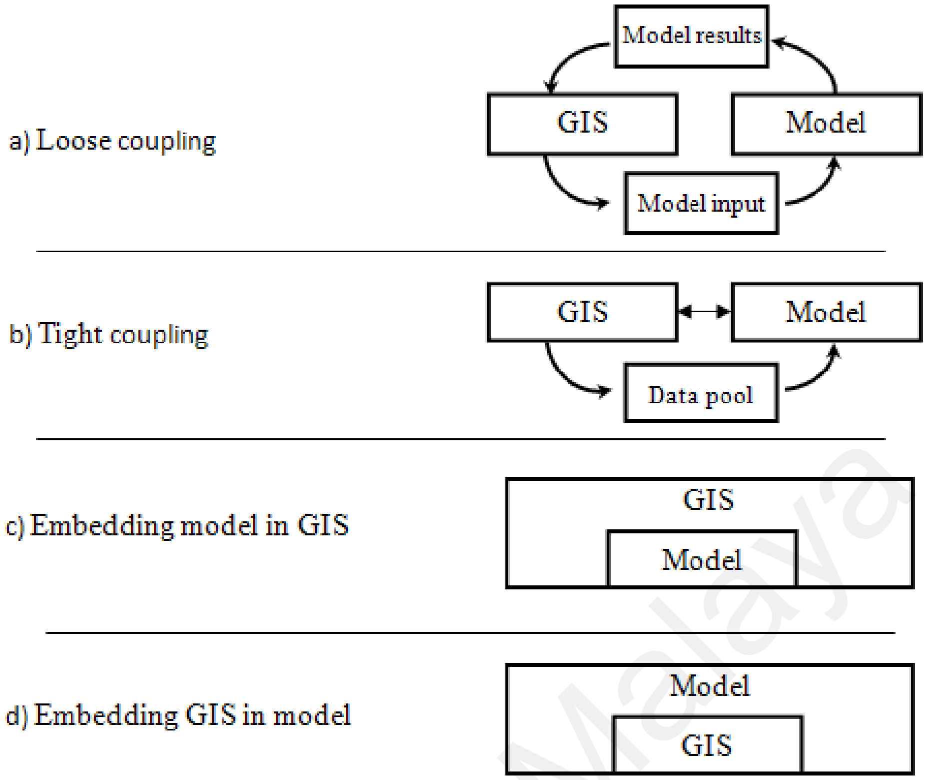

Figure 2.7: Integrating GIS with hydrological models
(Adapted from Sui and Maggio (1999))

2.6.1 Loose coupling

A loose coupling (Figure 2.7a) involves data transfer from one to another by storage of data in one system and subsequent reading of data by another. The important characteristic of loose coupling is separate functionality of the programs that implement the GIS and those that implement the model. This approach usually involves a standard GIS package (e.g., ArcGIS) and hydrological/hydraulic modeling programs (e.g., HEC-HMS 2.1). Hydrological modeling and GIS are integrated, via data exchange using either ASCII or binary data format, among several different software packages without a common user interface. The advantage of this approach is that repetitive programming is avoided, but always data conversion between different packages can be boring or associated with error and the conversion outputs are imperfect. Because computer programming is minimal, this approach may be the most realistic method for most GIS users and hydrological/hydraulic engineers to conduct modeling work (Sui and Maggio, 1999).

2.6.2 Tight coupling

A tight coupling (Figure 2.7b) provides a common user interface for both the GIS and the model. A tightly coupled model and the GIS must share the same database. This approach embeds certain WHMs within a commercial GIS software package via either GIS macro or conventional programming. With the recognition of the users' need to develop customized applications, more and more GIS software vendors are providing macro and script programming capabilities (e.g., ESRI's AML, ILWIS's scripts) so that users can lump a series of individual tools in a batch mode or develop a user defined interface for appropriate applications. But such languages have some limitations and may not be powerful enough to implement advanced models.

2.6.3 Embedding WHM in GIS

As the degree of coupling between GIS and the model increases, to the point where the model's functions are essentially part of the built-in functionality of the GIS, the model becomes embedded (Robayo, 2005) (see Figure 2.7c). A few leading GIS software vendors in recent years have made extra efforts to improve the analytical and modeling capabilities of their products. Pioneered by HEC-SAS developed by the Army Corps of Engineers (Davis, 1978), several commercial software vendors have developed stand-alone GIS modules with functions that can be used for a variety of hydrological modeling needs. Certain hydrological modeling functions have been embedded in leading generic GIS software packages such as ESRI's ArcStorm and ArcGrid, and so on. This approach builds on top of a commercial GIS software package and takes full advantage of built-in GIS functionalities, but the modeling capabilities are usually simplistic and calibrations must take place outside of the package.

2.6.4 Embedding GIS in WHM

This approach aims to embedding GIS functionalities in hydrological modeling packages, and has been adopted primarily by hydrological modelers who think of GIS essentially as a mapping tool and conceptually irrelevant to the fundamentals of hydrological modeling (see Figure 2.7d). This approach usually gives system developer maximum freedom for system design. Implementation is not constrained by any existing GIS data structures, and usually this approach is capable of incorporating the latest development in hydrological modeling. The developers of the latest version of RiverCAD, HEC-HMS and MODFLOW have basically taken this approach. This new generation of WHMs is still in the elementary development steps. Adding map overlay capabilities and supporting grid cell parameters in the latest version of HEC-HMS 3.4 may be considered as an example of embedding GIS in WHMs.

The above mentioned approaches in integration of GIS with WHSs have resulted in numerous studies in various regions in the world, most of which rely on a combination of loose/tight coupling (Sui and Maggio, 1999). The studies reported in the literature range from simple data preprocessing and hydrological parameter estimation (Bhaskar et al., 1992, Doan, 2003, Miller et al., 2007, Melesse, 2004, Ogden et al., 2001); to testing the validity of distributed hydrological models (Beven, 2001, Melesse, 2004, Moreda et al., 2006, Efstratiadis et al., 2007, Bahremand and De Smedt, 2008), from using GIS merely as mapping and visualization tools (Shamsi, 2002, Robayo, 2005, Shamsi, 2005) to comprehensive hydrological storm water modeling and management (Maidment and Djokic, 2000, Feldman, 2000b, Yongbo, 2004, Bedient et al., 2008). The study areas range from the world's most densely populated cities in Asia (Shrestha, 2003, Lai et al., March 2008) to rural areas in Africa (Corbett & Carter, 1997). In terms of geographical scales they includes from a local watershed (Haan et al., 1982, Gosain and Rao, 2004) to regional water resource planning (Hiscock and Hilburn, 1998, Loague and Corwin, 2000, Knebla et al., 2005). Although ESRI's Arc/Info and the US Army Corps of Engineer's HEC series dominated these modeling works, a variety of other GIS and modeling software tools have also been used, such as INTEGRAPH's InRoads, GRASS and TOPMODEL, SWAT, (Miller et al., 2007).

2.7 Geospatial Hydrologic Modeling

The Hydrologic Engineering Center (HEC) within the US Armey Corps of Engineers (USACE) is one the pioneer institutions that provided a numerical model with capability to simulate the surface runoff response of a watershed to precipitation by representing the dendrite drainage with interconnected hydrologic and hydraulic components (Feldman et al., 1981). It began with develop of a flood hydrograph package named HEC-1by Beard and other staff members of HEC in 1961(Feldman et al., 1981). Later, Feldman et al. (1981) made major revision on HEC-1. Final version of HEC-1 was released in 1998. The new generation of HEC-1 was released in three specialized version called RAS (River Analysis System), HMS (Hydrologic Modeling System) and FDA (Flood Damage Analysis). The first version of HEC-HMS released in April 1998 and the current version is HEC-HMS 3.4. The HEC-HMS is a numerical model that provides a large set of methods to simulate watershed runoff, infiltration losses, river flood routing, and water-control structure behavior, thus predicting flow and timing (Ford et al., 2008). According to Scharffenberg and Fleming (2008) HEC-HMS contains wide range of methods suitable for both event and continuous simulation.

Three main components are recognized in HMS model. Those are basin model, meteorological model and control specifications manger. Watershed elements characteristics, loss methods, transformation methods and baseflow method are provided in the basin model. Table 2.3 shows the symbology used in HEC-HMS for watershed elements. Precipitation, evaporation and snowmelt and their spatial patterns are defined in meteorological model. Starting and ending date/ time and time interval for observed/calculated hyetograph and hydrograph ordinates are set in control specifications manger. The methods employed in each part are the most common used and recommended methods of rainfall-runoff simulation.

Table 2.3: Symbology used in HEC-HMS for watershed elements

Symbol	Description
	Sub-watershed
	Reach
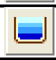	Reservoir
	Junction
	Diversion
	Source
	Sink

The theory and algorithm of the used methods are well documented in the HEC-HMS's Technical Reference Manual (Feldman, 2000b), Application Guide (Ford et al., 2008) and User's manual (Scharffenberg and Fleming, 2008). HEC-HMS is free and can be downloaded from http://www.hec.usace.army.mil/software/hec-hms/download.html. Most of the models included in HEC-HMS are event-based models.

A GIS companion product has been developed to assist in the design of watershed models. It is called the Geospatial Hydrologic Modeling Extension (HEC-GeoHMS) and can be used to create basin and meteorological models for use with the program. It is a joint project between HEC and ESRI and university of Texas headed by professor Maidment. HEC-GeoHMS allows visualizing spatial information, documenting watershed characteristics, performing spatial analysis, and delineating sub-basins and streams. Working with HEC-GeoHMS through its interfaces, menus, tools, buttons allows the user to create hydrologic inputs for HEC-HMS.

The HEC-HMS which is considered as a standard model in the private sector and government organizations is suggested to use for rainfall-runoff modeling in this research. It has been used in many research projects (Akbari, 1998, Cunderlik and Simonovic, 2004, Redfearn, 2005, Knebla et al., 2005, Robayo, 2005, Lowrey, 2006, Verdi, 2007, Ahn, 2007). The model has been widely used for design of drainage systems and quantifying the effect of land use change on floods in the US (Bekoe, 2005).

2.8 Rainfall-Runoff Modeling

Rainfall-runoff relationship is one of the most complicated hydrologic phenomena and prediction of hydrological process such as flood simulation is extremely important to water resources engineering (An, 2007). A significant aspect of flood modeling is the estimation of the magnitude of streamflow at various locations in a watershed resulting from a given precipitation input and hydrological characteristics of watershed (USACE, 1994). Basically, all rainfall-runoff models tend to satisfy Eq. 2.1 that is known as water balance equation.

$$P = I + D + ET \pm \Delta S \qquad \text{Eq. 2.1}$$

Where:

P: precipitation (mm) I: infiltration (mm) ET: evapotranspiration (mm)

D: Deep percolation (mm) ΔS: soil moisture storage change (mm)

The basic components of a rainfall-runoff model include precipitation, losses and runoff module. In this section different component of rainfall-runoff models are reviewed.

2.8.1 Precipitation Component

The precipitation component serves as the driving force in a hydrologic model and therefore accurate precipitation inputs are essential for reliable hydrologic prediction (Osborn and Lane, 1982, Su et al., 2007). Several investigators have discussed the importance of precipitation and its spatial and temporal pattern and its impacts on the surface runoff (Niemczynowicz, 1984, Abrahams et al., 1988, Patrick and Stephenson, 1990, Watts and Calver, 1991, Obled et al., 1994, Dirks et al., 1998, Bell and Moore, 2000, Goovaerts, 2000, Faures et al., 2006, Thavorntam et al., 2007). In particular, some of the researches have been focused on the spatio-temporal variability of rainfall over Klang watershed (Desa and Niemczynowicz, 1996a, Desa and Niemczynowicz, 1996b, Desa and Niemczynowicz, 1997, Dirks et al., 1998). Depending on the technology used the measurement can based on the ground rain gauges or by means of remote sensing technology. The role of a snow component could be of special importance in models that are explicitly used in cold regions where the snowpack defines the subsurface and surface hydrology (Faria et al., 2000b). However, due to tropical climate condition of Malaysia (Tick and Samah, 2004), snowing record has not observed in Klang watershed. Therefore, snow and snowmelt does not contribute to rainfall-runoff process in this area. The temporal resolution of rainfall can be expressed in minutes, hourly, daily or monthly. Spatial pattern of rainfall can vary depending on the rain gauge density or used remote sensing technology.

2.8.2 Gauge rainfall data

Rainfall measured at a rain gauge is called point rainfall. Event-base flood-runoff analysis requires recording rain gauges. According to Raghunath (2006b) three types of recording rain gauges are more frequently used. Those are tipping bucket gauge, weighing gauge and float gauge. There are some problem associates with rain gauges that can affect the rainfall data. Wind speed, exposure, and height of gauge have been addressed by USACE (1994). In addition, to provide a consistent record adjustment of the measured data is necessary when the catch at rain gauges is inconsistent over a period of time (McCuen, 1998). A consistent record is one where the characteristics of the recording gauges have not changed with time. To analyze actual storm events in flood modeling it is necessary to extend the gauging rainfall data to areal estimates. Three types of extending point estimates to areal averages have been introduced by McCuen (1998). Those are station-average, Thiessen polygon and Isohyetal method. According to Kobold (2007) the number of rain gauges in the watershed should be densely enough to give proper areal precipitation. The US Army Corps of Engineers (USACE) related the gauge density for hydrologic modeling to watershed area (Vieux, 2004b). The number of gauges, *Ng*, can be estimated from Eq. 2.2 purposed by the USACE (1996):

$$\mathrm{N_g} = 0.73 \times \mathrm{A}^{0.33} \qquad \text{Eq. 2.2}$$

Where A is the watershed area in km^2 and $\mathrm{N_g}$ is the number of gauges required for hydrologic modeling.

2.8.3 TRMM 3B42 precipitation data

Rain gauges measure rainfall at specific points, whereas radar, satellites, and other remote sensing techniques typically average a surrogate measure over a volume or area (Vieux, 2004b). A better estimate of rainfall may be achieved by a dense gauge network, but such a network is very expensive. The TRMM Multi-Satellite Precipitation Analysis (TMPA) products (version 3B42) are available with a spatial resolution of $0.25^\circ \times 0.25^\circ$ and a temporal resolution of 3 hours. The TMPA provides a calibration-based sequential scheme for combining rainfall estimates from various satellites. According to AghaKouchak et al. (2009) at fine scales TRMM precipitation estimates, provide high resolution information that has the potential to improve hydrologic predictions and global climate studies. However, satellite estimates are subject to significant uncertainties from various sources. As stated by AghaKouchak (2009) the uncertainties remain even after calibration of satellite estimates with ground references data. These uncertainties are to be quantified and characterized before using satellite estimates in hydrologic applications.

TRMM data are distributed via the FTP and web sites. According to Huffman and Bolvin (2009) there are numerous similar data sets, although no other matches all the attributes of being routinely produced, publicly available, fine-scale in space and time, quasi-global, available from January 1998 onwards. These data sets are inter-calibrated, and formed by combining multiple data sources including precipitation gauges (Huffman and Bolvin, 2009). As an example, PERSIANN system developed by Sorooshian et al. (2000a) applies the PERSIANN neural network to calibrate IR with microwave. CMORPH system, developed by Joyce et al.(2004) applies the CMORPH morphing scheme to time-interpolate microwave patterns with IR-based motion vectors. The TRMM Online Visualization and Analysis System (TOVAS) have created and supported by the Goddard Earth Sciences Data and Information Services Center (GES DISC). It provides a web-based resource for accessing 3B42RT, 3B42, 3B43, and other data, performing basic sub-setting, time and space-averaging and outputting results are produced in plots, ASCII text, HDF, Netted and KMZ. The TOVAS URL is http://disc2.nascom.nasa.gov/Giovanni/tovas/.

2.8.4 Spatial and temporal pattern

Rainfall measured at a rain gauge is called point rainfall (USACE, 1994). Rainfall gauge can be recording or non-recording. Spatial and temporal distribution of rainfall, play an important role in rainfall-runoff process.

As stated by Earls and Dixon (2007), interpolated rainfall data and its accuracy is controlled by the spatial distribution of the rainfall gauges and the interpolation methods used which may or may not reflect reality. Several studies have shown that the spatial variability of rainfall is a major factor influencing flood formation in urban areas (Niemczynowicz, 1984, Watts and Calver, 1991, Obled et al., 1994, Bell and Moore, 2000, Faures et al., 2006). A number of studies specifically related to characterizing short-term rainfall properties have been carried out in Klang watershed

(Niemczynowicz, 1987, Bacchi and Kottegoda, 1995, Desa and Niemczynowicz, 1996b). Effects of meteorological, orographic, and space-time aggregation scales and a discussion on network design, areal mean calculations and storm velocities on spatial correlation functions have explained by Bacchi and Kottegoda (1995). The results indicate that the spatial correlation of rainfall generally decreases with distance, and different correlation structures are observed during different rainfall events. The areal extension of thunderstorms in Klang watershed, which create most floods, is limited and there are no routines to account for this in design (Desa and Niemczynowicz, 1996b). There are also errors attached to such estimated areal rainfall due to the effects of inadequate temporal resolution, inadequate spatial coverage or network configuration, and instrument error (Peters-Lidard and Wood, 1994). Moreover, storm velocity enlarges the uncertainty of the point data at the stations. The importance of these issues has been discussed by Desa and Niemczynowicz (1996a), in a small-urbanized sub-basin (23 km^2) of Klang watershed equipped with sixteen rain gauges. They had estimated the mean storm velocity about 2.63 m/s (Desa and Niemczynowicz, 1997, Desa and Niemczynowicz, 1996a). They have also reported that there is no clearly preferred direction for the storm movement and propagation is chaotic in direction.

2.8.5 Areal storm patterns

The interpolation technique is used to gives values for the points where there are no direct measurements. Estimating a smooth spatial distribution from noisy observations and constructing smoothed maps and predicting at locations for which no data are available have been the focus of researchers. Currently GIS in the light of geostatistics theories provide several types of interpolation technique. Geostatistics studies the spatial variability of regionalized variables (Gomez, 2007). Regionalized variables are variables that have an attribute value and a location in two or three dimensional space. A number of methods have been proposed for the interpolation of rainfall data. According to Goovaerts (2000), geostatistics which is based on the theory of regionalized variable is increasingly preferred because it allows the capitalization of the spatial correlation between neighboring observations to predict attribute values at un-sampled locations. Phillips et al.(1992), Haberlandt (2006), Paciorek and Schervish (2006) and Gomez (2007) have been shown that the Kriging technique for the interpolation process provides more reliable results than any other methods. For this purpose, GIS software have equipped with geo-statistical tools. Specifically, ILWIS 3.4 employ standard GIS-base geo-statistical functions in a raster environment for analyzing point data. Kriging method has been used in several regions to predict spatial distribution of rainfall. Goovaerts (2000) employed simple Kriging for rainfall interpolation in Portugal and found that ordinary Kriging yields more accurate prediction. Karamouz and Araghinejad (2005) applied the Kriging method to evaluate monthly regional rainfall in the central part of Iran. Thavorntam et al (2007) indicated ordinary Kriging with spherical model performed better for interpolation of rainfall within the Thailand region.

2.8.6 Temporal storm patterns

According to Ball (1994) temporal storm pattern has a significant influence on watershed response. The influence is evident in the different time-to-peak of the resultant runoff hydrographs and in its hydrograph shape (Ball, 1994). As a result, it is concluded that the time of concentration is not fixed parameters for a watershed.

2.8.7 Criteria for storm selection

Straub et al. (2000) stated that storm events for determining parameters for synthetic unit hydrographs should be selected to conform as closely as possible to the definition and assumptions of a unit hydrograph. According to Viessman et al. (1989) and

Feldman (2000b) the following criteria were applied for selecting individual rainfall events suitable for the calibration of the runoff model:

1- Rainfall-runoff events generated by the same rainfall event.
2- Streamflow peaks representing all runoff due to the selected rainfall event.
3- Adequate spatial coverage of rainfall-runoff events, preferably covering the whole watershed.
4- The duration of rainfall events exceeding the time of concentration of the watershed.

6- The magnitude of rainfall events selected for calibration approximately equal the magnitude of rainfall events the model is intended to analysis.

7- A simple-storm structure, resulting in well-defined hydrographs with distinct peaks.

8- Uniform rainfall distribution throughout the period of effective precipitation.

9- Uniform spatial distribution over the entire watershed.

10- The direct runoff for the selected storm should range from 12.7 to 44.5 mm.

2.9 Infiltration Component

Determining the amount of effective rainfall is highly dependent on the infiltration model. In this aspect complexities and nonlinearities of flow generation processes are much greater than the routing processes (Beven, 2001). High level of complexity arises from the nonlinearity of infiltration process. The rate of infiltration is influenced by the physical characteristics of the soil, land use, water content of the soil, soil temperature, and rainfall intensity or rate of snowmelt (Jutla, 2006).

Several infiltration models have been formulated in the form of mathematical equations to account for the losses from rainfall events. Most of them can be classified into two categories which are empirical and physical equations. Empirical infiltration equations are the result of curve fitting exercises of observed infiltration rate with time-dependent functions or water storage characteristics of the soil (Jutla, 2006), whereas, physically-based infiltration equations have been developed by solving the governing equations for basic soil water movement (Jutla, 2006). The principle core of these equations is Darcy's law and the mass conservation equation (Smith, 1981). Infiltration equations developed by Horton (1940), Holtan (1932), Huggins and Monke (1966), Smith (1972) and Mockus (1965) are known as empirical infiltration models, whereas infiltration equations developed by Green and Ampt (1911), Philip (1957) and Richards (1931) are known as physical-based infiltration models. Basic concept and formulation of the mentioned models have described by McCuen (1998) in detail. Herein, further details about the SCS-CN infiltration method purposed by Mockus (1965) is provided.

2.9.1 SCS-CN method

According to McCuen (1982) the SCS-CN is a purely empirical method that was based upon the assumption that the ratio of actual runoff and potential runoff could be related to the ratio of actual retention to potential retention. In fact SCS-CN is a method for calculating direct runoff from the given storm. However, it includes the infiltration component. In this approach infiltration capacity is quantified in a parameter derived by the SCS called Curve Number (CN). The CN is determined from land use, soil and land cover type, and hydrologic soil group (USDA, 1986). Soil groups are determined based on type and infiltrability of the soil. The infiltration loss method is derived from a set of empirical equations developed by SCS (1972b) that define the partitioning of rainfall into infiltration and direct runoff. General form of SCS-CN model defines with Eq. 2.3, Eq. 2.4 and Eq. 2.5:

$$Q=\frac{(P-I_a)^2}{(P-I_a+S)} \quad for\ P>I_a$$
$$Q=0 \quad for\ P\leq I_a \qquad \text{Eq.2.3}$$

$$I_{a=\lambda*S} \qquad \text{Eq.2.4}$$

And $$s=\frac{25400}{CN}-254 \qquad \text{Eq.2.5}$$

Where:

Q: Direct runoff (mm)
P: Rainfall (mm)
S: The potential maximum soil storage (mm)
I_a: Initial abstraction/loss (mm)
λ: Ratio of initial abstraction (I_a) to maximum potential retention

Initial abstraction is a variable parameter that takes into account losses prior to the start of runoff such as interception and depression storage. Evapotranspiration losses are considered negligible for the preliminary model due to several factors: the intensity of the storm being modeled, the continuous saturation of the air, and the resulting assumption that ET volume is negligible compared to runoff volume (USDA, 1986). The ratio of initial abstraction (I_a) to maximum potential retention (S) was assumed in its original development to be equal to 0.2 in the SCS-CN method (SCS, 1972b).

2.9.2 Modified SCS-CN method

Investigation on experimental data by different researchers have shown that λ value is sensitive to the hydrologic and climate conditions. Singh et al. (1996a) and Chandramohan et al. (2007) reported that most of the studies taken up in India suggest that the appropriate λ for Indian conditions vary between 0.01 to 0.3. Recent study in the US have shown that the term I_a is not linearly proportional to S as reported by USDA (Hawkins, 1998, Mishra and Singh, 1999, Hawkins et al., 2002b, Woodward et al., 2002, Baltas et al., 2007). Probing into 307 case studies in the US showed that the λ is not a constant from storm to storm, or watershed to watershed, and that the assumption of λ =0.20 is unusually high (Hawkins et al., 2002b). The study determined that λ of 0.05 fits observed rainfall-runoff data much better than does the handbook (NEH-4) value of 0.20. Similar results have been reported by other investigators outside the US. A case study in Greece showed that the average λ values of the entire watershed was equal to 0.014 and corresponding values at a sub-watershed was 0.037(Baltas et al., 2007). Another case study in china showed that the λ values, using event rainfall-runoff data, varied from 0.010 to 0.154, with a median of 0.048 (Shi et al., 2009). Therefore, new CN tables must be constructed for λ =0.05 (Hawkins, 2009 : personal communication). Since the CN table has not been modified, the standard CN values are used.

$$S_{0.05} = 1.33 * (S_{0.20})^{1.15} \qquad \text{Eq. 2.6}$$

There is little experience with CNs for tropical forests. Hawkins (2009) suggested low CNs for large storms, and a general "Standard" behavior for tropic forest That is, a declining CN with increasingly large storms, but CN approaching a constant value asymptotically. It is noted, when the method was developed in the USA there were no tropical forest watersheds in their data set (Hawkins, 2009: personal communication).

Preserving the basic definition of CN = 1000/ (10+S), the Eq.2.6 permits conversion from the 0.20-based CNs to 0.05-based CNs. Making the substitutions and simplifying gives new CN that can be calculated with Eq.2.7:

$$CN_{0.05} = \frac{100}{1.879*\left[\frac{100}{CN_{0.02}}-1\right]^{1.15}+1} \qquad \text{Eq. 2.7}$$

2.9.3 Advantage, disadvantages and limitations

The SCS-CN method has some advantages and disadvantages. According to Ponce and Hawkins (1996) advantages of the method are its simplicity, its predictability, its stability, its reliance on only one parameter and its responsiveness to major runoff-producing watershed properties (soil type, land use/treatment, surface condition, and antecedent condition). According to Ponce and Hawkins (1996) disadvantages are: its marked sensitivity to curve number, varying accuracy for different biomes, no clear guidance on how to vary antecedent condition, the absence of an explicit provision for spatial scale effects and the fixing of the initial abstraction ratio at 0.2, preempting a regionalization based on geologic and climatic setting.

According to the USDA (1986) there are some limitations for SCS-CN applications which are: 1) The modeling accuracy decreases with historical storm, 2) Runoff curve number equation is used with caution when re-creating specific features of an actual storm. The equation does not take into account the time, therefore, it does not account for rainfall duration or intensity. 3) The assumption that reflected in the initial abstraction term (I_a) derived from the agriculture watershed and should be used with caution elsewhere. Especially in an urban harvest a significant initial loss that may not take place, 4) Runoff from snowmelt or rain on frozen ground cannot be estimated using these procedures, 5) It does not recognize subsurface flow from the surface runoff, 6) It is less accurate when runoff is less than 13 mm.

2.10 Runoff Component

According to Horton (1933) runoff is generated when the rainfall rate exceeds the infiltration rate. The excess water after satisfying the soil moisture dynamics can be routed as overland flow. In lumped or semi-distributed models, overland flow volume is generally dependent on the accuracy and boundary conditions of the infiltration equations. Most lumped models are based on storage concepts (Jutla, 2006). Water in each storage zone is dynamically linked with other storage zones using various empirical or physical equations. In such models, overland flow is generally simulated using the threshold principle. For instance, when the soil layer gets saturated then the excess water should be routed as overland flow (Ye et al., 1997). The SCS method is another important runoff model and widely used for computing the runoff depth from a rainfall event(Feldman, 2000b). Numerous literatures have been reported regarding the SCS runoff model theory and applications. The SCS-CN method is one of the most popular methods for computing the volume of direct surface runoff for a given rainfall event (Mishra et al., 2008). With a number of applications worldwide, it forms part of several standard software packages dealing with physically based, distributed rainfall-runoff modeling, such as Hydrologic Engineering Center (HEC-HMS) (Feldman, 2000b), Agricultural Non-Point Source pollution (AGNPS) model (Young et al., 1987), Soil and Water Assessment Tool (SWAT) (Neitsch et al., 2002), to cite a few among many others. It is frequently employed in most remote sensing and geomorphologic information system (GIS)-coupled packages (Jacobs et al., 2003, Kim et al., 2002). Besides being fairly accurate in runoff prediction, the adaptability of SCS-CN applications lies in the fact that the method is simple, easy to understand and apply, stable, and capable of incorporating several watershed runoff producing characteristics (Mishra et al., 2008).

2.10.1 Basic Concepts of the Unit Hydrograph

Chow (1988) defined the unit hydrograph (UH) as unit pulse response function of a linear hydrologic system. As originally purposed by Sherman (1932), it is the watershed outflow resulting from one unit (usually 1 cm) of direct runoff generated uniformly over the watershed at a uniform rainfall rate during a specified period of rainfall. Based on UH theory, the runoff process is linear, therefore the runoff from greater or less than one unit is simply a multiple of the unit runoff hydrograph (Feldman, 2000b). Sherman (1932) classified runoff into surface runoff and groundwater runoff and defined the UH for use only with surface runoff. According to Chow (1988) the following basic assumptions are inherent in the UH model:

1) rainfall intensity is constant within the effective duration, 2) No spatial variation of rainfall distribution is considered, 3) The base time of the direct runoff hydrograph resulting from an excess rainfall is constant in a given duration, 4) The ordinates of all direct runoff hydrographs of a common base time are directly proportional to the total amount of direct runoff represented by each hydrograph and 5) For a given watershed,

the hydrograph resulting from a given excess rainfall reflects the unchanging characteristics of the watershed. Those assumptions limit the applications of UH in some aspects. Inapplicability to large watershed or runoff originating from snow or ice are clear examples of such limitations reported by Chow et al. (1988).

Moreover, the above assumptions cannot be perfectly satisfied in the real conditions. Hence, to meet the assumptions the selection of hydrologic data should be made with care (Chow et al., 1988). The rainfall events selected for analysis should have short duration, because that is more susceptible to produce an intense and nearly constant excess rainfall rate, yielding a well-defined single-peaked hydrograph of short time base. In addition the UH have to be used with caution in a large watershed. The UH has been found applicable to small watersheds from less than 0.5 hectares to 25 km^2 (Chow et al., 1988). Based on the theory of UH the direct runoff from given excess rainfall is computed with convolution Eq. 2.8:

$$Q_n = \sum_{m=1}^{n \leq M} P_m U_{n-m+1} \qquad \text{Eq. 2.8}$$

Q_n : Direct runoff P_m: excess rainfall

m : Pulses of excess rainfall n : pulses of direct runoff in the rainfall event.

Once the unit hydrograph has been determined, it may be applied to find the direct runoff and stream-flow hydrographs.

According to McCuen (1998) the runoff hydrograph is conceptually separated into direct runoff and baseflow (See Figure 2.8).The direct runoff results from excess rainfall thus, the volumes of excess rainfall and direct runoff must be equal (McCuen, 1998). The UH is a transfer function that transforms the excess rainfall into the direct runoff. The baseflow is the runoff that has resulted from an accumulation of water in the watershed from the past events.

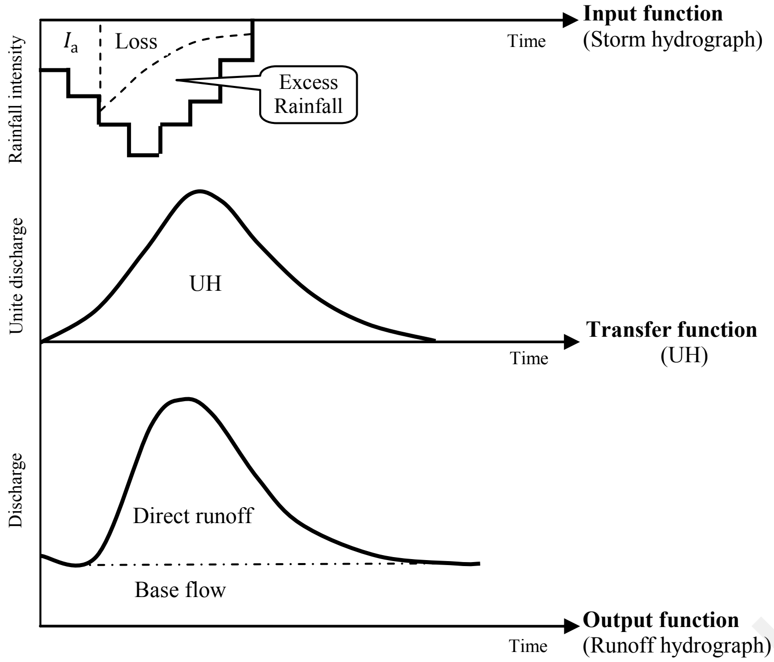

Figure 2.8 Conceptual modeling of rainfall-runoff process
(Adapted from McCuen(1998))

2.10.2 Synthetic Unit Hydrograph

The UH developed from rainfall and streamflow data on a watershed represent the rainfall-runoff process on the corresponding watershed where the streamflow data were measured (Chow et al., 1988). Synthetic UH approach are used to develop UHs for other locations on the stream in the same watershed or for nearby watersheds with similar character. According to Chow et al. (1988) three types of synthetic UHs are recognized: 1) UHs that relate watershed characteristics together (Snyder, 1938, Gray, 1961), 2) Dimensionless UH (SCS, 1972a), and 3) Watershed storage-based UH (Clark, 1943). Some important method that is found in hydrologic models is reviewed. Further reading is referred to popular text books (Chow et al., 1988, McCuen, 1998, Dingman, 2002, Viessman and Lewis, 2003b, Karamouz and Araghinejad, 2005, Reddy, 2005, Raghunath, 2006b, Bedient et al., 2008)

2.10.3 Snyder's Synthetic Unit Hydrograph

Snyder (1938) purposed synthetic relations for some characteristics of a standard UH. The case studies located mainly in the Appalachian highlands in US with varying in size from about 30 to 30,000 km^2. According to Chow et al. (1988) a standard UH is associated with specific effective rainfall duration and watershed lag time defined with Eq. 2.9.

$$t_{lag} = 5.5\, t_r \qquad \text{Eq. 2.9}$$

Where t_{lag} lag time of is watershed and t_r is effective rainfall duration.

Watershed lag time is defined with Eq. 2.10:

$$t_{lag} = C_1 C_t (L\, L_c)^{0.3} \qquad \text{Eq. 2.10}$$

where t_{lag} is in (hr), L is the length of the main stream in (km) from the outlet to the upstream divide, L_c is the distance in (km) from the outlet to a point on the stream nearest the centroid of the watershed area, C_1 = 0.75 and C_t is a coefficient derived from gauged watersheds in the same region. The peak discharge per unit drainage area in m^3/s-km^2 of the standard UH is calculated with Eq. 2.11:

$$q_p = \frac{C_2 C_p}{t_{lag}} \qquad \text{Eq. 2.11}$$

Where C_2= 2.75 and C_p is a coefficient derived from gauged watersheds in the same region. To compute C_t and Cp for a gauged watershed, the values of L and L_c are measured from the watershed map. Effective duration t_R in hours, watershed lag t_{lagR} in hours, and peak discharge per unit drainage area, q_{pR} in $(m^3/(s.km^2.cm))$ are obtained from derived UH of the watershed. If t_{lagR} = 5.5t_R, then t_R = t_r and t_{lagR} =t_{lag}, q_{pR}=q_p, and C_t and C_p are computed with Eq. 2.9 and 2.10. If t_{lagR} is quite different from 5.5t_R, the standard basin lag is calculated with Eq. 2.12:

$$t_{lag} = t_{lagR} + \frac{t_r - t_R}{4} \qquad \text{Eq. 2.12}$$

Now Eq. 3.8 and 3.11 are solved simultaneously for t_r and t_{lag}. Then, the values of C_t and C_p are obtained from Eq. 2.10 and Eq. 2.11 with q_{pR} =q_p and t_{lagR} = t_{lag}.

When an un-gauged watershed appears to be similar to a gauged watershed, the coefficients $C_t$and C_p for the gauged watershed can be used in the above equations to derive the required synthetic UH for the un-gauged watershed. The relationship between q_{pR} and q_{pR} of the required UH is calculated with Eq. 2.13:

$$q_{pR} = \frac{q_p t_{lag}}{t_{lagR}} \qquad \text{Eq.2.13}$$

The base time t_b (hr) of the UH can be determined using the fact that the area under the UH is equivalent to a direct runoff of 1 cm. Assuming a triangular shape for the UH, the base time may be estimated with Eq. 2.14:

$$t_b = \frac{C_3}{q_{pR}} \qquad \text{Eq. 2.14}$$

Where C_3 = 5.56

As shown in Figure 2.9 all characteristics of a required UH for a given excess rainfall duration may be calculated from the Eq. 2.8 to 2.13. The width (hr) of a UH at a discharge equal to a certain percent of the peak discharge q_{pR} is given with Eq. 2.15:

$$W = C_w\left(q_{pR}\right)^{-1.08} \qquad \text{Eq. 2.15}$$

Where C_w = 1.22 for the 75-percent width and 2.14 for the 50-percent width. Usually one-third of this width is distributed before the UH peak time and two-thirds after the peak.

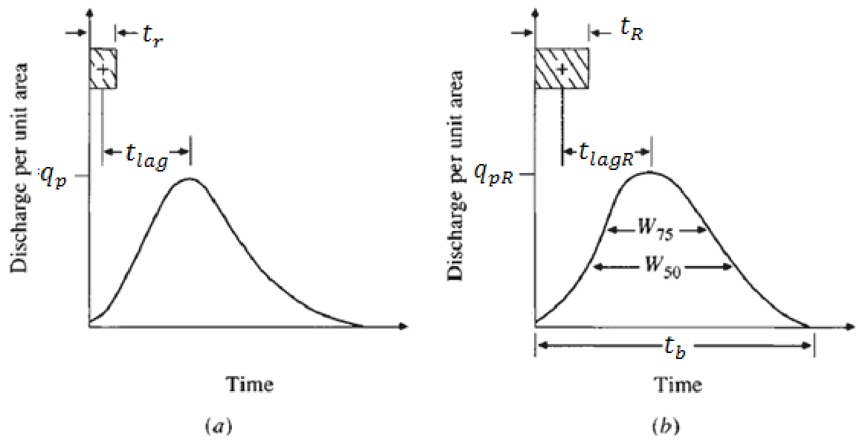

Figure 2.9: Snyder's synthetic UH, a) Standard UH ($t_{lag} = 5.5t_r$), b) Required UH ($t_{lagR} = 5.5t_R$) (Adapted from Chow et al.(1988)).

2.10.4 SCS Dimensionless Hydrograph

The SCS dimensionless hydrograph is a synthetic UH in which the discharge is expressed by the ratio of discharge to peak discharge (q/q_p) and the time by the ratio of time t to the time to peak of the UH (t/T_p). Given the peak discharge and lag time for the duration of excess rainfall, the UH can be estimated from the synthetic dimensionless hydrograph for the given watershed. Figure 2.10a shows such a dimensionless hydrograph, prepared from the UHs of a variety of watersheds.

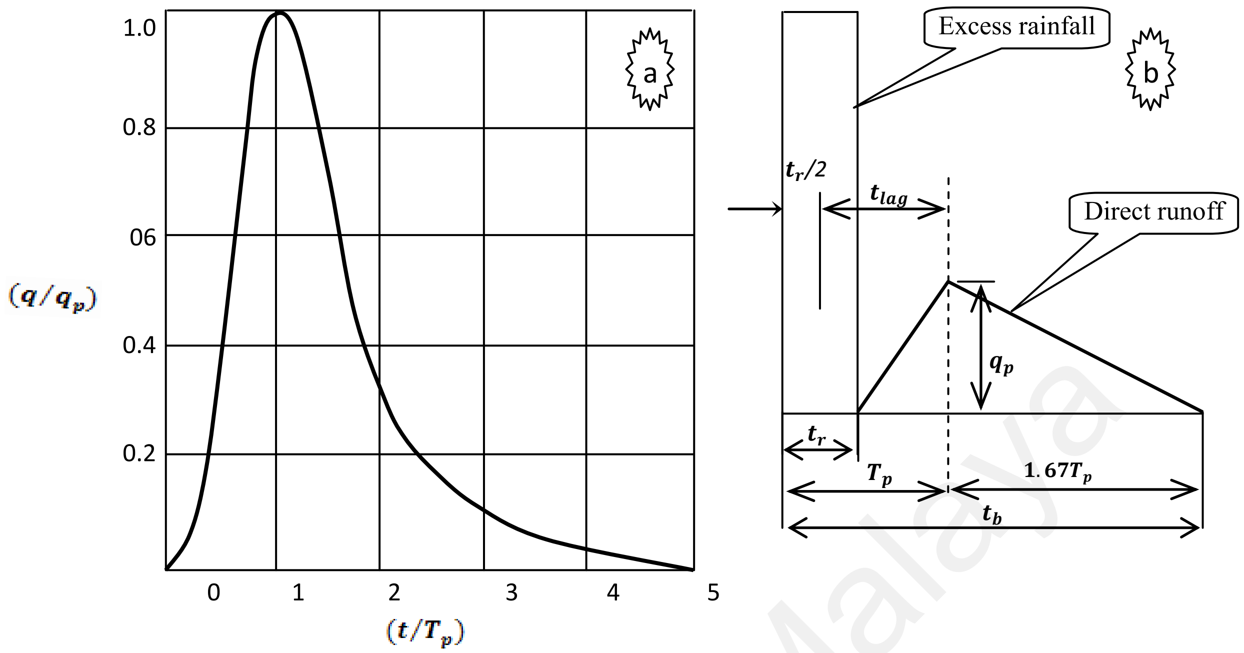

Figure 2.10: SCS synthetic UHs; a) Dimensionless hydrograph and b) Triangular UH.
(Source: Chow et al., 1988)

According to SCS (1972a), q_p and T_p may be estimated using a simplified model of a triangular UH shown in Figure 2.10b, where the time is in hours and the discharge (in m^3/s.cm). From a review of a large number of UHs, the SCS suggests the time of recession may be approximated as $1.67T_p$. As the area under the UH should be equal to a direct runoff of 1 cm, it is shown thatq_p is calculated with Eq. 2.16:

$$q_p = \frac{CA}{T_p} \qquad \text{Eq. 2.16}$$

Where C = 2.08 (in the SI system) and A is the watershed area in km^2. Further, a study of UHs of many large and small rural watersheds indicates that the watershed lag $t_{lag} \cong 0.6T_c$ where T_c is the time of concentration of the watershed. As shown in Fig. 3.4b, time to peak T_p can be expressed in terms of lag time t_{lag} and the duration of effective rainfall t_r with Eq. 2.17:

$$T_p = \frac{t_r}{2} + t_{lag} \qquad \text{Eq.2.17}$$

2.11 Routing Component

According to Chow et al. (1988) flow routing is a procedure to determine the time and magnitude of flow at a point on a river from known or assumed hydrographs at one or more points upstream. The procedure is specifically called flood routing when the flow is a flood. Chow (1988) identified two types of routing which are lumped and distributed routing method. In a lumped model, the flow is calculated once in a certain location, while in a distributed routing the flow is calculated as a function of space and time in the system. Lumped routing methods are called hydrologic routing and distributed routing methods is sometimes referred to as hydraulic routing (Chow et al., 1988). In addition, if routing techniques are applied to movement of flow through the river, it is called river routing and if applied to movement of flow through the reservoirs, it is called reservoirs routing. In this section, hydrologic routing method is applied to movement of flow through reservoirs and river reaches.

A reach element conceptually represents a segment of stream or river; the actual calculations are performed by a routing method selected for the reach. Six different routing methods are provided in HEC-HMS. Each of the methods implements a hydrologic routing methodology as compared to a hydraulic approach that implements the full unsteady flow equations (Ford et al., 2008). Each method included in the program provides a different level of detail and not all methods are equally adept at representing a particular stream. According to McCuen (1998) for the purpose of developing an equation for routing through either stream channels or reservoirs, the continuity of mass can be expressed with Eq. 2.18:

$$I - Q = \frac{dS}{dt} \approx \frac{\Delta S}{\Delta t} \qquad \text{Eq. 2.18}$$

Where: I and Q are the inflow and outflow, respectively, dt is incremental time, and S is the storage. For channel flow routing, I and Q are the upstream and downstream discharge hydrographs. For the hydrographs shown in Figure 2.11, the continuity equation can be expressed in terms of the inflow and outflow at two times t_1, and t_2. By averaging inflow and outflow at times t_1 and t_2 the numerical form of routing equation is shown with Eq. 2.19:

$$\frac{1}{2}(I_2 - I_1) - \frac{1}{2}(Q_2 - Q_1) = (S_2 - S_1)/\Delta t \qquad \text{Eq. 2.19}$$

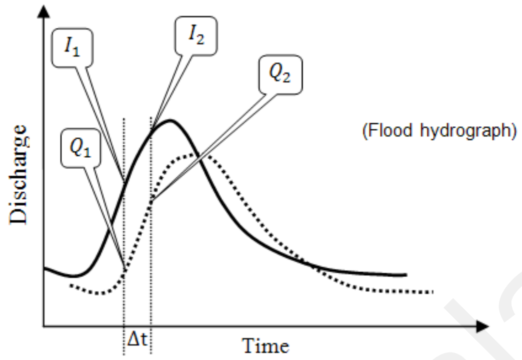

Figure 2.11: Schematic diagram of inflow and outflow flood hydrographs

2.11.1 Kinematic Wave Flood Routing

According to Scharffenberg and Smith (2004) and Fleming (2008) The kinematic wave routing method approximates the full unsteady flow equations by ignoring inertial and pressure forces. The energy line and the bed slope are assumed to be equal in this method. It is a best method in urban areas where natural channels have been modified to have regular shapes and slopes and yields results of very acceptable accuracy in the storm drainage systems (Smith, 2004).

For stream channel segments, simple cross section shapes have been used to simulate prototype channels. Flows entering the collectors and the stream channels can consist of both flows from upstream sections and lateral inflows from adjacent watershed surfaces. Their slope, length, cross sectional dimensions, shape, and Manning's 'n' value, describes these representative channels. The standard Manning's ‘n’ is used because stream channel segments behave as normal open channel flows. According to MacArthur and DeVries (1993) the kinematic wave equations for flood routing through the channels are expressed with Eq. 2.20 and Eq. 2.21:

$$\frac{\partial Q_c}{\partial x} + \frac{\partial A_c}{\partial t} = q_0 \qquad \text{Eq. 2.20}$$

$$Q_c = a_c A_c^{m_c} \qquad \text{Eq. 2.21}$$

Where:

$\boldsymbol{A_c}$ is cross sectional area of flow in m^2; Q_c is discharge in cms; q_0 is lateral inflow per unit length in cms/m from overland flow strips; t is time in seconds; x = distance along the stream in meter; a_c and m_c are kinematic wave parameters for a particular cross sectional shape, slope and roughness. The subscript c denotes the subscripted variables used in Eq. 2.20 and Eq. 2.21 for a typical channel.

2.11.2 Determination of a_c and m_c for Stream channels

Depends on the shape of cross section a_c and m_c will be different for each reach elements and will vary with effective Manning's 'n' and channel slope as well (MacArthur and DeVries, 1993). Based on the field observation and relevant reports (DID, 1994, DID, 2003b), rectangular and trapezoidal channel shapes are more frequently observed in Klang watershed that makes it possible to model with HEC-HMS.

- **Rectangular Section**

A rectangular shape is obtained by $z = 0$ in Figure 2.12. This produces a channel with wide (W (m)) and with vertical walls. This shape may represent man-made channels and rectangular concrete drain sections.

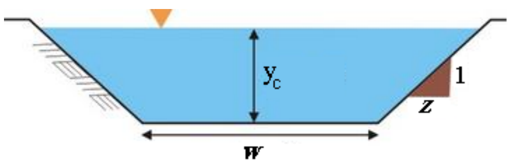

Figure 2.12: Typical trapezoidal section

For the wide shallow channel case:

$$a_c = \frac{S_c^{1/2}}{n} * w^{-2/3} \qquad \text{Eq.2.22; and} \qquad m_c = \frac{5}{3} \qquad \text{Eq. 2.23}$$

For the rectangular channel where $w \approx y_c$:

$$a_c = \frac{0.63 * S_c^{1/2}}{n} \quad \text{Eq.2.24; and} \quad m_c = \frac{4}{3} \quad \text{Eq. 2.25}$$

- **Trapezoidal Section**

The trapezoidal section is one of the two basic sections considered HEC-HMS. As showed in Figure 2.12 when describing a trapezoidal section the side slopes z and the channel bottom widths w should be accurately defined. According to (MacArthur and DeVries (1993) it is not possible to derive a simple relationship for a_c and m_c from the geometric properties . Therefore it becomes necessary to fit a_c and m_c to the Manning equation at two or more depths y_c and use numerical techniques of fitting the kinematic equation to these values to obtain values for a_c and m_c for various flow conditions. Details for numerical solution of the Kinematic Wave Equations can be found in several sources specifically by MacArthur and DeVries (1993).

2.11.3 The reservoir routing equation

According to Raghunath (2006a) reservoir routing is the process of determining the reservoir stage, storage volume of the outflow hydrograph corresponding to a known hydrograph of inflow into the reservoir. The same as channel routing, the equation for reservoir routing is derived from the mass conservation equation (See Eq. 2.18).

With approximating $\frac{ds}{dt}$ by $\frac{\Delta s}{\Delta t}$ Eq. 2.17 can be expressed with Eq. 2.26:

$$I\Delta t - O\Delta t = \Delta s \quad \text{Eq. 2.26}$$

If the subscripts 1 and 2 are used for inflow and outflow to the reservoir at times t and (t +Δt) respectively, then Eq. 2.26 can be written with Eq. 2.27:

$$\frac{1}{2}(I_1 + I_2)\Delta t - \frac{1}{2}(Q_1 + Q_2)\Delta t = S_2 - S_1 \quad \text{Eq. 2.27}$$

While,I_1, I_1 , Q_1 and s, are known at any time t, values for , Q_2 and S_2 are unknown. Eq. 3.26 can be rearranged with Eq. 2.28 for the known values on the left side of the equal sign and the unknowns on the right side:

$$\frac{1}{2}(I_1 + I_2)\Delta t + (S_1 + \frac{1}{2}Q_1\Delta t) = (S_2 + \frac{1}{2}Q_2\Delta t) \quad \text{Eq. 2.28}$$

The capacity curve of the reservoir, i.e., 'storage vs. pool elevation', and 'outflow rate vs. pool elevation', are required for reservoir routing. Storage volumes for different pool elevations are determined from DEM of the reservoir site by using GIS tools. For example, the volume of water stored V, between two successive levels having areas A_1 and A_2 with the known interval(d), is given with Eq.2.29 and Eq.2.30:

Cone formula $\quad V = \frac{d}{3}(A_1 + A_2 + \sqrt{A_1A_2} \quad$ Eq. 2.29

Prismoidal formula $\quad V = \frac{d}{6}(A_1 + A_2 + 4A_m) \quad$ Eq. 2.30

2.12 Runoff models

According to Huggins (1982) there are two approaches to compute runoff from the watersheds. Those are known as *transfer functions* and *phenomenological relationships*. The first approach develops an empirical equation using available historical data. In this method the needs for modeling all hydrological processes in the watershed are eliminated. However, long record of rainfall-runoff data is required to build a transfer function. In phenomenological functions individual components of the physical rainfall-runoff process that occur in the watershed are employed (Huggins, 1982). This approach relies on observed data for calibration of the parameters. The phenomenological relationships yield a range of simple to very complex watershed models (Jutla, 2006). Simple models may make use of the SCS model, whereas, complex watershed models may require solution of the Saint-Venant equations (Explained by Chow et al., 1988) which use the mass conservation and momentum equations to simulate overland flow.

Numerous models have been cited in the literature for rainfall-runoff modeling. According to Woolhiser and Brakensiek (1982), selection of watershed models for the particular problem are based on four criteria: simplicity, accuracy of prediction, consistency of parameter estimates and sensitivity of the results to changes in the parameter values. In addition, as stated Woolhiser and Brakensiek (1982), selection of model is usually made based on the time-frame available for development, input data resources and experience of the modeler. According to Jutla (2006) some popular watershed models and their characteristics are introduced in Appendix B (Table B.1 and Table B.2).

2.13 Calibration of Runoff Models

According to Viessman and Lewis (2003a) calibration is defined as the process of improving algorithms, determining parameter values and sequencing hydrological processes so that model represents the real world phenomena. It is evident that some physically-based or empirical equations representing various hydrological processes require tuning of the input parameters or constants so as to provide reliable estimates of the desired outputs. Nash and Sutcliffe (1970) concluded that although runoff models uphold the requirement for mass balance, the mechanisms describing the relationships among the watershed processes are defined by mathematical transfer functions. Thus, physically-based equations, which describe the system, demonstrate a hidden empirical behavior. Sorooshian (1983) discussed the importance of calibration in watershed modeling and summarized that the purpose of calibration is to get a realistic and unique parameter value set that should help in understanding the watershed processes, and to obtain parameter values so that the observed watershed response matches the simulated results. Calibration of watershed models is generally done by comparing and analyzing observed and simulated streamflow data (Singh, 1988, Ambroise et al., 1995).

2.14 DEM-based Watershed Modeling

Increasing complexity of environmental and water-resource problems require the use of modeling approaches that can incorporate knowledge from a broad range of scientific disciplines. Watershed characterization and parameterization is an important step in environmental modeling. Digital terrain data is main tool for watershed modeling that provides a capability to derive watershed boundaries and associated parameters. The Digital Terrain Model (DTM) has defined as a numerical representation of the terrain. Since Miller and Laflamme (1958) who coined the original term, other expressions such as digital elevation model (DEM), digital height models (DHM), digital surface model (DSM), digital ground models (DGM) and digital terrain elevation model (DTEM) have been used by Maidment (1993a), Djokic and Ye (2000), Vieux (2004a) and Li et al. (2005b). These terms originated from different countries. According to Li et al. (2005b) DEM is widely used in US; DHM in Germany; DGM is used in the United Kingdom; and DTEM was introduced and used by USGS and the Defense Mapping Agency (DMA). Although, there are some differences between the above mentioned terms, in practice, these are often assumed to be synonymous (Li et al., 2005a). In this thesis DEM is used as a more popular term. In the field of hydrology and water resources, applications of DEM have mainly focused on automate watershed segmentation, definition of drainage divides, and identification of river networks. This automatic extraction of network and sub-watershed properties from the DEM represents a convenient and rapid way to parameterize a watershed (Garbrecht and Campbell, 1997).

2.14.1 Background of applications

Several studies have been conducted to use the elevation dataset to extract the physical watershed parameters (Yu, 1997). The technique is based on the raster or rarely vector terrain data model. With the advent of satellite-based DEMs in fine resolution, this possibility has been provided to delineate watershed boundaries and associated parameters effectively. Several types of satellite-based DEM are available. SRTM data is one of the best available free alternatives for watershed modeling. Numerous researchers have investigated the potential application of SRTM elevation data. Hendricks et al.(2003a) used SRTM for estimation of channel slope in Amazon watershed. An comprehensive study conducted by Jarvis et al. (2004b) to evaluate the SRTM data against the cartographic DEM derived from topo maps at scale 1:50000 for Honduras areas. Tulu (2005) assessed the suitability of SRTM-DEM for runoff studies and compared with ASTER-DEM. He observed that daily runoff output of SWAT model when ASTER-DEM is used is higher than when the SRTM-DEM is used. Hancock et al. (2006) used 90 meter SRTM elevation data for drainage network and hydrologic modeling. They have found that 90 m SRTM data results in incorrect drainage network patterns and different runoff properties compare to DEM with high resolution of 10 m. Osorio et al. (2007) compared ASTER and SRTM DEMs with DEM derived from topo map at scale 1:50000 for watershed delineation.

2.14.2 DEM resolution

One of the most important characteristics of DEM is its cell size. A coarse spatial resolution may provide an inaccurate representation of surface, yet be desirable because of cost, efficiency and data storage considerations. Also vertical accuracy may be limited or inaccurate due to instrument or operational limitations. According to Giles and Franklin (1996) sharp ridges, peaks and deep valleys are smoothed during creation of the DEM, and accurate recreation of these areas is not possible. Several researches have been conducted to investigate the impact of DEM resolution on the behavior of hydrological models. Syed (1999) in a comprehensive study assessed the DEM cell size range from 2.5 to 40 meter and its impact on kinematic model simulations over a range of watershed scales. This study indicated that high resolution DEM data does not necessarily result in a better geometric definition of the small watershed but it can significantly change the results when the watershed becomes larger. Finally, Syed proposed Eq. 2.31 that relates watershed area with DEM resolution:

$$P_{size} = 0.023A - 3.65 \times 10^{-6}A^2 + 1.63 \times 10^{-10}A^3 + 14.4 \qquad \text{Eq. 2.31}$$

Where A is watershed area (he), P_{size} is recommended DEM cell size (m) and $5 \leq A \leq 15000\ he$.

Another research conducted by Zhang and Montgomery (1994) to examine the effect of DEM cell size on the portrayal of land surface and results of hydrologic simulations in two small watersheds in Western US. The DEM resolutions of 2 to 90 m was examined and concluded that DEM cell size of 10 m would adequate for many DEM-based hydrologic modeling in moderately to steep gradient topography.

Seybert (1996) used land use, soil and DEM datasets to examine the effect of spatial data resolution degradation on the output of event-based surface runoff model. The study was performed on a small agriculture watershed in central Pennsylvania. The cell dimensions ranging from 5 to 500 m were investigated. Results indicated that the peak flow estimates are more sensitive to spatial resolution change than runoff volume estimates. Also increasing number of sub-watershed caused the model to increase estimates of peak flow and runoff volume. Finally the ratio of mean sub-watershed area to the grid cell area was used as an indicator of spatial resolution. Overall ratio about 102 was found to be acceptable threshold of spatial resolution for reasonable modeling results. This ratio can be expressed for pixel size with Eq. 2.32:

$$P_{size} = \sqrt[2]{\frac{A}{102}} \qquad \text{Eq. 2.32}$$

Where, A is average sub-watershed area (m^2) and P_{size} is cell size (m). According to Quattrochi and Goodchild (1997) and Goodchild (2001), spatial resolution and extent are still strongly related with the traditional cartographic concepts. For example, in traditional soil cartography the scale of an existing map is commonly assessed by estimating either the maximum location accuracy (MLA) or average size area (ASA) of the polygons on the ground (Rossiter, 2003). These cartographic definitions can also be used to estimate the suitable grid resolution for a given mapping scale (Hengl, 2006). Rossiter (2003) suggests that four grid cells can be considered equivalent to the minimum legible delineation (MLD), which is the smallest size area that we map and Vink (1975) has defined the MLD as 0.25 cm^2 on the map. Hengl (2006) has combined this tow definitions and purposed the Eq. 2.33 and Eq. 2.34 to estimate the suitable grid resolution based on the scale number (SN):

$$P \leq \sqrt{\frac{MLD}{4}} = \frac{\sqrt{SN^2 \times 0.000025}}{2} = SN \times 0.0025 \qquad \text{Eq. 2.33}$$

Or $MLD = SN^2 \times 0.000025$ Eq. 2.34

Where *P* is the pixel size and *MLD* (m^2) is the minimum legible delineation area on the ground. For map at scale of 1:25000, *MLD* is 1.56 ha and suitable grid resolution is 62.5 m, which seems fairly coarse. Valenzuela and Baumgardner (1990) have been also recommended somewhat larger grid resolutions from 0.5 to 3mm on the map. If we consider grid resolution based on the MLA as stated by Vink (1975) which commonly ranges from 0.25mm to maximum of 0.1mm on the map, then the smallest legible resolutions is estimated with Eq. 2.35 (Hengl, 2006).

$$P_{size} \geq \mathrm{SN} \times 0.00025 \text{ or } \mathrm{P} \geq \mathrm{SN} \times 0.0001 \qquad \text{Eq. 2.35}$$

For map at scale of 1:25000, suitable grid resolution is estimated about 6.25 m. Some researchers have related the grid resolution with the size of area and computer processing power (Lagacherie and McBratney, 2005) and (Akbari et al., 2009). Maidment (1996) have proposed a tabular relation for DEM cell size, size of watershed and their typical range of applications. (See Table 2.4)

Table 2.4: Recommended DEM cell sizes and their typical range of applications

Geographic Cell Size	Linear Cell Size	Watershed Area (km^2)	Region Area (km^2)	Typical Application
1"	30 m	5	1000	Urban watersheds
3"	90 m	40	8000	Rural watersheds
15"	460 m	1000	200,000	River basins
30"	930 m	4000	900,000	Nations
3'	5.6 km	150,000	30,000,000	Continents
5'	9.3 km	400,000	90,000,000	Global

Yu (1997) used a distributed watershed model with a series of DEM that had resolutions of 36 through 1097m to examine the effect of DEM grid size on the land surface representation and hydrologic simulation. The study showed that overall a 366 m grid size provides basic estimations in both surface-water and ground-water simulations.

The above literature survey provides some indications for adequate DEM resolution for specific applications. But it is seen that no definite guidelines for DEM cell size for general applications exist. In theory, the DEM resolution should be selected as a function of the land surface features, scale of the process that are modeled, and numerical model used to model process (Maidment and Djokic, 2000). But in practice the selection of DEM is often driven by data availability, judgment, test applications, experience and, last but not least, cost (Garbrecht and Martz, 2000). Two source of DEM are utilized in this research which include Topo-DEM and SRTM-DEM.

2.14.3 Topographic Maps

Topography defines the pathways of surface water movement across a watershed, and thus is a major factor affecting watershed hydrologic response to rainfall inputs (Wua et al., 2008). The DEMs have been widely applied to efficiently derive topographic attributes used in hydrologic modeling such as slope and upslope watershed area and mean elevation. Any uncertainties in the topographic models are propagated into the output of hydrologic model prediction, causing inaccuracies (Wua et al., 2008). One of such uncertainties arises from the choice of DEM grid size. Every country has topographic maps and these data are used as the main source for DEM. In most developed countries and even some developing countries like China, most of the terrain is covered by good-quality topographic maps containing contours (Liu et al., 2005). But in many developing countries, topographic maps at appropriate scale are rare or contain the poor quality of the height and contour information contained in the maps. Iran is an example that still suffering from lack of coverage of topography. According to National Cartographic organization of Iran, 80% of country covered by maps at scale 1:25000 until 2005 (Yegane and Payvandi, 2005).

2.14.4 Satellite-based DEM

SRTM provides a worldwide DEM between 60° N and S latitudes with a consistent datum. For areas outside of the conterminous United States, the original 1 arc-second data (SRTM-1; cell size approximately 30 meters at the equator) have resample into 3 arc-second data (SRTM-3) by averaging (JPL/NASA, 2006).The 3-arc-second (approx. 90 meters at the equator) SRTM dataset version 2 (known as finished data) that provided by HydroSHEDS (**Hydro**logical data and maps based on **SH**uttle **E**levation **D**erivatives at multiple **S**cales) was used for delineation of Klang watershed boundaries. HydroSHEDS data are free for non-commercial use (Lehner et al., 2006a). Raw data were downloaded from the from HydroSHEDS website made by U.S. Geological Survey (2008) (see http://hydrosheds.cr.usgs.gov/). The HydroSHEDS is an internet-based data center that provides pre-processed SRTM elevation data and other products. As shown in Figure 2.13, the web page has well organized and provides useful download tools. Refer to Lehner et al. (2006a) the quality of HydroSHEDS data has much improved compare to version 1 by major editing efforts and exhibits well-defined water bodies and coastlines.

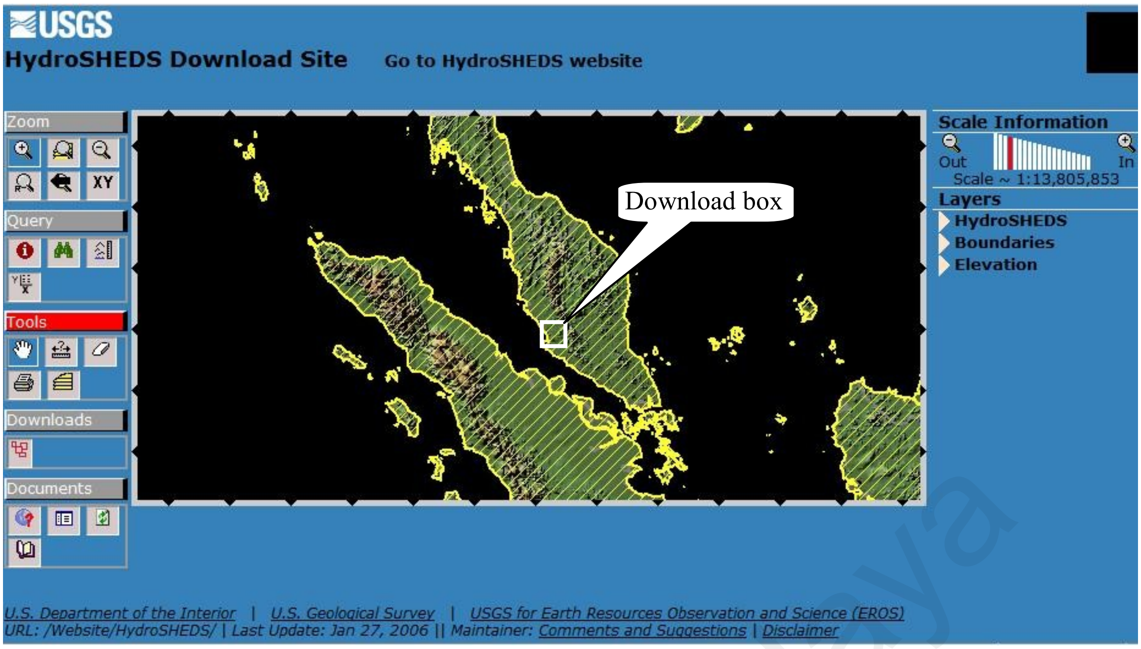

Figure 2.13: Interface of HydroSHEDS Web site and downloaded area

Vertical accuracy of SRTM elevation data has been the focus of several researches. Research done one the accuracy of SRTM implies that the accuracy may change place by place and highly depends on the type of land use and landforms. A comprehensive research conducted by Jarvis et al. (2004b) in five case studies provided a broad range of analyses on the quality, accuracy, and usability of SRTM data. According to Falorni et al. (2005) relief has a strong effect on the vertical accuracy of the SRTM-DEM. So that in the high-relief terrain, large errors and data voids are frequent, and their location is strongly influenced by topography, while in the low- to medium-relief site, errors are smaller. Pryde et al. (2007) reported that the accuracy of SRTM is dependent upon the terrain vegetation as a radar cannot penetrate it. Several applications have been reported for STRM elevation dataset. Rasemann et al. (2004) have been used STRM –DEM for recognition and quantification of landforms. Alsdorf et al. (2007) used SRTM data to measure water surface elevations directly, which contributes to the improvement of flood forecasting. Simultaneously with this research, Chebud and Melesse (2008) delineated sub-watershed boundary using 90-m SRTM-DEM using ArcHydro tools. Wale et al.(2008) derived a total of 23 physical watershed characteristics from SRTM

DEM analysis. Lastly Miliaresis (2008) used SRTM-DEM to capture Aeolian processes on the basis of the morphology of linear mega-dunes in desert regions.

Raw SRTM elevation data includes void or holes ranging from one pixel to regions of 500 km^2 (Reuter et al., 2007). The existence of no-data in the SRTM-DEM can causes significant problems for deriving hydrological products, which require continuous flow surfaces (Lehner et al., 2006b). Therefore DEM should be free from void or holes. Several algorithms have been developed for filling void by using various spatial analysis techniques (Reuter et al., 2007). Most of void areas of SRTM elevation data have been edited and filled in HydroSHEDS version. However, for some areas voids are still present (JPL/NASA, 2006). The existence of no-data in the DEM causes significant problems for deriving hydrological products, which require continuous flow surfaces (Lehner et al., 2006).

2.15 DEM optimization

Before utilizing DEM in watershed modeling some optimization techniques are applied. Optimization can be performed in several ways. Widely used optimization techniques include filling sinks, reconditioning (Hellweger and Maidment, 1997) and smoothing (Vieux, 2004b). Optimization operations have been well adapted with some GIS software including ArcHydro and HEC-GeoHMS and DEM hydro-processing in ILWIS 3.4 (Koolhoven et al., 2007) that are based on AGREE-DEM algorithm developed by Hellweger and Maidment (1999).

2.15.1 DEM Smoothing

Sharp ridges, peaks and deep valleys are smoothed during creation of the DEM. Level of smoothing directly depends on the selected cell size for generating of DEM. extra smoothing of DEM can change significantly hydrologic simulation results depending on DEM resolution. However as stated by Vieux (2004b), DEM smoothing is often necessary before automatic delineation of the watershed and stream network to reduce the number of spurious high or low points, referred to as pits and spikes. Moreover, smoothing can also adjust artifact ridges and peaks resulting from none matching of the two adjacent topo sheets. It is believed that there is no clear indication for the level of DEM smoothing for semi-distributed hydrologic modeling. But clearly too much smoothing eliminates spatial variability, leading to a smooth surface that is visually pleasing, but many terrain features are eliminated (Vieux, 2004b). Filtering is the common method to smooth the DEM. Filtering is a process in which each pixel value in a raster map is replaced with a new value. The new value is obtained by applying a certain function to each input pixel and its direct neighbors. These neighbors are usually the 8 adjacent pixels (in a 3 x 3 filter) (Koolhoven et al., 2007). Simple averaging is the simplest and perhaps most efficient filter, and is thus most commonly used for smoothing DEM (Zhou et al., 2008). However, the low-pass filter, the median filter and the Kalman filter, have also been used (Zhou et al., 2008).

2.15.2 Filling sinks on DEM

The sinks are often considered as errors in the DEM due to re-sampling and interpolating the grid. For example, in a window size of 3×3, if the center cell has the lowest elevation compared to its eight neighboring cells, then the center cell's elevation will be increased equaling the next lowest cell. In the past, several algorithms have been proposed for filling depressions of DEMs. O'Callaghan and Mark (1984), Jenson (1987) and Skidmore (1990) have developed the algorithms to produce depressionless DEMs from regularly spaced grid elevation data. Numerical filling of depressions, whether from artifacts or natural depressions, facilitates the automatic delineation of watersheds. Filling the depressions allows water to flow across the landscape. This assumption is generally valid when a large storm event fills up the small depressions and any incremental amount of water that flows into the depression will displace the same amount of water from the depression (Fleming and Doan, 2009). Representation of sink and filled sink is schematically demonstrated in Figure 2.14.

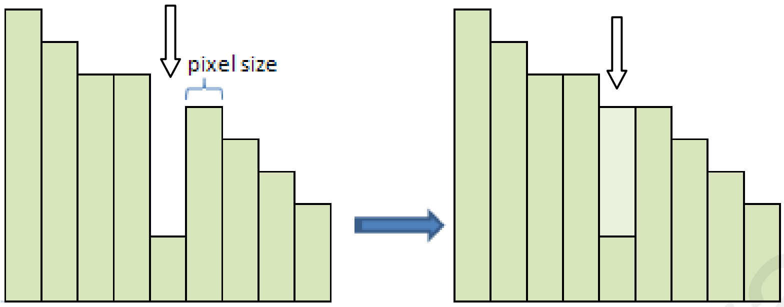

Figure 2.14: Profile view of sink in DEM (left) and filled depression of DEM (right)

2.15.3 DEM reconditioning

Recondition is an optimization method utilized in widely GIS software such as ArcGIS and ILWIS. One method for enforcing flow direction is to use an ancillary map to restrict drainage direction where a mapped stream channel exists. In this case, a river or stream vector map may be used to burn in the elevations, forcing the stream network to coincide with the vector map depicting the desired stream network (Vieux, 2004b). The algorithm is known as AGREE DEM introduced by Hellweger and Maidment (1999). The DEM optimization operation enables us to 'burn' existing drainage features into a DEM, so that a subsequent Flow direction operation on the output DEM will better follow the existing drainage pattern (Koolhoven et al., 2007). As shown in Figure 2.15 the DEM reconditioning operation in ILWIS 3.4 offers the following possibilities :

1- Smooth drop of drainages in the output DEM over a certain distance to the drainages.
2- Additional sharp drop or raise of segments on top of the smooth drop or raise.

Optionally it is possible to select the attribute table belonging to drainage map in case that different buffer distances, smooth drop values, and/or sharp drop values for individual segment classes are performed (see Figure 2.16). Buffer distance(s) should be larger than zero. Smooth drop value(s) indicate the height with which segments should be dropped or raised in the output DEM. The drop or raise value(s) will be reached gradually on either side of the segments, using the buffer distance(s). Smooth drop value(s) > 0 represent a drop; smooth drop value(s) < 0 represent a raise; smooth drop value(s) of 0 represent no drop and no raise . Sharp drop value(s) indicate the height with which segments should additionally be dropped or be raised in the output DEM on top of the Smooth drop value (s). Sharp drop value(s) > 0 represent an additional drop; sharp drop value(s) < 0 represent an additional raise; sharp drop value(s) of 0 represent no additional drop and no additional raise .

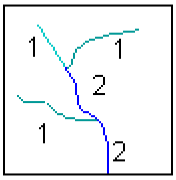

	Buffer_dist	Smooth_drop	Sharp_drop
2	40	2.0	2.0
1	20	1.0	1.0

Figure 2.15: DEM reconditioning using attributes table of stream network

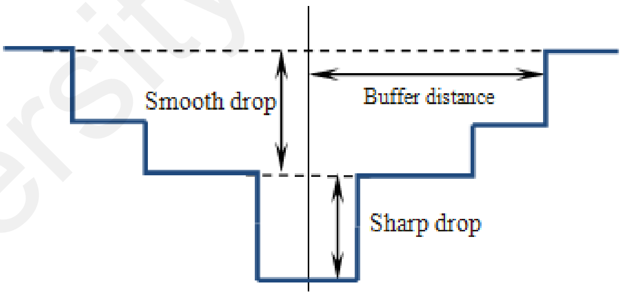

Figure 2.16: Schematic representation of DEM reconditioning

2.15.4 Watershed delineation algorithm

Peucker and Douglas (1975) are the first investigators who attempted to determine surface area and drainage networks from DEMs. Delineating watershed boundary is a primary and basic step in hydrological analysis. Topo-based DEMs are most common source of watershed delineation. In previous decades, several new algorithms have been introduced by researchers. Most of these algorithms are based on

DEM applications (Fairfield and Leymarie, 1991, Freeman, 1991, Lea and 1992, Costa-Cabral and Burges, 1994, Tarboton, 1997). However, some other algorithms have been developed based on TIN and contour-line models (Jones et al., 1990, Moore and Grayson, 1991, Nelson et al., 1994). These algorithms have not become popular because of their complexity or problematic results. According to Kiss (2004) the most commonly used method is Deterministic 8 (D8) introduced by O'Callaghan and Mark (1984). The procedure is based on determining flow direction from DEM.

2.15.5 Flow direction

The flow direction concept has been originally employed by O' Callaghan and Mark (1984) and later Jenson and Domingue (1988) outlined a grid scheme for delineating watershed boundaries and stream networks. According to Jenson and Domingue (1988) Values in the drainage direction matrix were defined with Eq. 2.36:

$$\begin{aligned} DDIRN(i,j) &= 2^{d-1} \;\; for \;\; d = 1,2,\ldots,8 \\ &= 0 \;\; \text{for an undefined direction} \end{aligned} \qquad \text{Eq.2.36}$$

Flow direction values derived from Eq. 2.36 are related to eight standard geographic directions as shown in Figure 2.17.

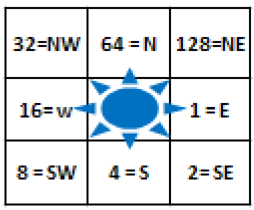

Figure 2.17: Illustration of flow direction matrix

Figure 2.18 illustrate the D8 algorithm for encoding the flow direction applied on depressionless Topo-DEM. The HEC-GeoHMS is used the direction of maximum drop from each DEM cells to determine the direction of flow with Eq. 2.37 (Fleming and Doan, 2009):

$$Maximum\ drop = \frac{\Delta h}{d} \qquad \text{Eq.2.37}$$

Where *Δh* is the change in elevation and *d* is the distance between two cells center. Therefore if considering the DEM cell-size is 1m, the distance between two orthogonal cells is 1m and the distance between two diagonal cells is 1.414 m. If the maximum drop to several cells is the same, the neighborhood is enlarged until the steepest descent is found. When a direction of steepest descent is found, the output cell is coded with the value representing that direction.

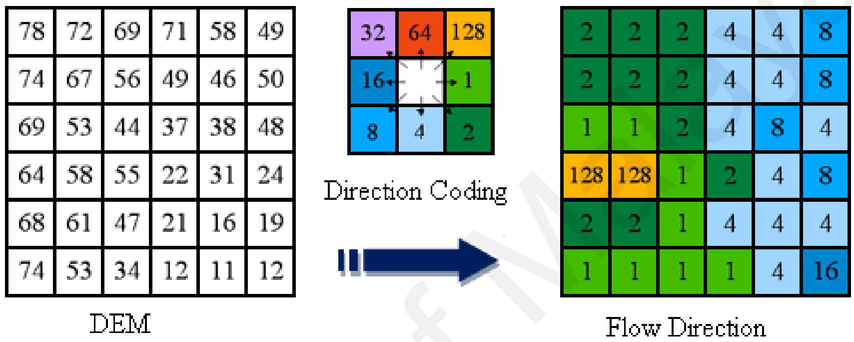

Figure 2.18: Illustration of direction codes for determining flow direction

2.15.6 Flow accumulation

The accumulated flow value for each pixel is calculated using a recursive function. When a pixel has neighboring pixels pointing to it, the values of these neighbors are accumulated, including the value of the pixel itself. Flow accumulation is calculated based on the flow direction grids.

2.15.7 Watershed threshold

The flow accumulation for a particular cell must exceed the user-defined threshold for a stream to be initiated. Threshold is defined based on the number of cells or appropriate size of sub-watershed area. The threshold values leading to maintain the number of sub-watersheds. Choosing the small threshold delineate the greater number of sub-watersheds. Initial value for the threshold can be the default value purposed by Geo-HMS. Thereafter, sub-watersheds may need to be split or aggregated depending on the location of stream flow stations, dams and land homogeneity etc. According to Djokic and Ye (1999) a good threshold starting value can be 1/500 the number of cells in the DEM. The HEC-GeoHMS use one percent (1%) of the largest drainage area in the entire DEM as default (Fleming and Doan, 2009). Recently, Chen et al. (2010) suggested that the optimum accumulation area threshold is 7.2 km^2

2.16 Basic evaluation measures

Several correlation coefficients and error indices are commonly used in model evaluation. These include sample correlation coefficient (*r*), coefficient of determination R^2, mean square error (MSE), and root mean square error (RMSE). These indices are valuable because they indicate correlation and error in the units of the constituent of interest, which aids in analysis of the results. Correlation coefficient and coefficient of determination values of 1 indicate perfect correlation. RMSE, MAE, and MSE values of 0 indicate a perfect fit. Singh et al. (2004) state that RMSE and MAE values less than half the standard deviation of the measured data may be considered low and that either is appropriate for model evaluation.

2.16.1 Correlation coefficient (r)

The quantity *r*, called the linear correlation coefficient, measures the strength and the direction of a linear relationship between two variables. it is sometimes referred to as the Pearson product moment correlation coefficient in honor of its developer Karl Pearsonr (Roberts and Roberts, 1998). The *r* values range from -1 to +1. Positive values imply positive correlation and negative values implies negative correlation. If there is a strong positive linear correlation, *r* is close to +1. A perfect correlation of ± 1 occurs only when the data points all lie exactly on a straight line.

This statistical measure used to evaluate the goodness of fit between SRTM-DEM derived and Topo-DEM derived parameters. The *r* is calculated with Eq.2.38:

$$r = \frac{n\sum_{i=1}^{n} Y_{TD}\, Y_{SD} - (\sum_{i=1}^{n} Y_{TD})(\sum_{i=1}^{n} Y_{SD})}{\sqrt{n(\sum_{i=1}^{n}(Y_{TD})^2) - (\sum_{i=1}^{n} Y_{TD})^2}\ \sqrt{n(\sum_{i=1}^{n} Y_{SD}) - (\sum_{i=1}^{n} Y_{SD})^2}} \qquad \text{Eq.2.38}$$

Where:

Y_{TD}: Parameter derived from the Topo-DEM
Y_{SD}: Parameter derived from the SRTM-DEM
n: Number of sub-watersheds

A correlation greater than 0.8 is generally described as strong, whereas a correlation less than 0.5 **is** generally described as weak (Roberts and Roberts, 1998).

2.16.2 Coefficient of determination r^2 or R^2

The coefficient of determination is useful because it gives the proportion of the variance (fluctuation) of one variable that is predictable from the other variable (Roberts and Roberts, 1998). It is a measure that allows us to determine how certain one can be in making predictions from a certain model/graph. The R^2 values range from .0 to 1.0 ($0 \leq R \leq 1$), and denotes the strength of the linear association between Y_{TD} and Y_{SD}. The coefficient of determination is a measure of how well the regression line represents the data. If the regression line passes exactly through every point on the scatter plot, it would be able to explain all of the variation. The further the line is away from the points, the less it is able to explain (Roberts and Roberts, 1998). R^2, calculate with Eq. 2.39:

$$R^2 = \frac{\sum_{i=1}^{n}((Y_{TD})_i - \overline{Y_{TD}})\,((Y_{SD})_i - \overline{Y_{SD}})}{\sqrt{\sum_{i=1}^{n}((Y_{TD})_i - \overline{Y_{TD}})^2\ \sum_{i=1}^{n}((Y_{SD})_i - \overline{Y_{SD}})^2}} \qquad \text{Eq. 2.39}$$

Where:

Y_{TD}: Parameter derived from the Topo-DEM
Y_{SD}: Parameter derived from the SRTM-DEM
$\overline{Y_{TD}}$: Mean values of Parameter derived from the Topo-DEM
$\overline{Y_{SD}}$: Mean values of Parameter derived from the SRTM-DEM
n: Number of sub-watersheds

2.16.3 Nash-Sutcliffe efficiency (NSE):

The Nash-Sutcliffe efficiency (NSE) is a normalized statistic that determines the relative magnitude of the residual variance ("noise") compared to the measured data variance ("information") (Nash and Sutcliffe, 1970). NSE can be used for all the components of concern and it is accurately computing the statistic values (Moriasi, 2009 ; personal communication). NSE ranges between -∞ and 1.0, with NSE = 1 being the optimal value. Values between 0.0 and 1.0 are generally viewed as acceptable levels of performance, whereas values < 0.0 indicates that the mean base value is a better predictor than the simulated value, which indicates unacceptable performance (Moriasi et al., 2007). Nash-Sutcliffe efficiencies can also be used to quantitatively describe the accuracy of model outputs other than discharge. This method can be used to describe the predicative accuracy of other models as long as there is reference data to compare the model results. Nash-Sutcliffe efficiencies have been reported in scientific literature for model simulations of discharge, and water quality constituents such as sediment. NSE is computed as shown in Eq. 2.40:

$$NSE = 1 - \left(\frac{\sum_{i=1}^{n}((Y_{TD})_i - (Y_{SD})_i)^2}{\sum_{i=1}^{n}((Y_{TD})_i - \overline{Y_{TD}})^2}\right) \qquad \text{Eq. 2.40}$$

Where:

Y_{TD} : Parameter derived from Topo-DEM
Y_{SD} : Parameter derived from SRTM-DEM
$\overline{Y_{TD}}$: Mean values of parameter derived from Topo-DEM
n: Number of sub-watersheds

The NSE values implicate that overall the SRTM-DEM derivatives (slope, area, perimeter and mean, etc) is as good as the Topo-DEM derivatives.

2.16.4 Percent Bias (PBias)

Percent bias (PBias) measures the average tendency of the estimated parameters to be larger or smaller than their reference counterparts (Gupta et al., 1999). The optimal value of PBias is 0.0, with low-magnitude values indicating accurate model simulation (Moriasi et al., 2007). Positive values indicate model underestimation bias, and negative values indicate model overestimation bias (Gupta et al., 1999). PBias is calculated with Eq. 2.39:

$$PBias = \left[\frac{\sum_{i=1}^{n}((Y_{TD})_i - (Y_{SD})_i) * 100}{\sum_{i=1}^{n}(Y_{TD})_i}\right] \quad \text{Eq. 2.41}$$

Where:

Y_{TD}: Parameter derived from Topo-DEM
Y_{SD} : Parameter derived from SRTM-DEM
n: Number of sub-watersheds

2.16.5 Scatter plot and line of best fit

A scatter plot is a type of mathematical diagram using Cartesian coordinates to display values for two variables for a set of data (Utts, 2004). The data is displayed as a collection of points, each having the value of one variable determining the position on the horizontal axis and the value of the other variable determining the position on the vertical axis (Utts, 2004). The DEM-derived parameters were plotted to see how two comparable datasets agree with each other.

Chapter III:

Methodology and Study area

3.1 Methodology

The methodology used in this research includes DEM generation, watershed delineation and parameterization and database development using GIS and RS tools and techniques and rainfall-runoff simulation. To achieve the all objective of this research several GIS analysis and hydrological process was performed. The methodology can describe in three steps.

In the first step Klang watershed boundaries and hydrologic parameters are determined using Topo-DEM and SRTM-DEM by means of HEC-GeoHMS. Then statistical measures are used to assess the performance of SRTM-DEM for watershed modeling. Several preprocessing is implemented on raw data with assistant of GIS Tools and techniques. Workflow for watershed delineation and parameterization is shown in Figure 3.1. Spatial and temporal pattern of rainfall over Klang watershed are determined by using rain gauges data and TRMM precipitation data. Kriging interpolation techniques are used by means of geostatistical analysis tools available in ILWIS 3.4.

The HEC-HMS as an event-base flood model supporting with satellite data is conducted because most of the floods in Klang watershed are as result of severe storms in short time which cause flash floods. Two dataset that generated from previous stages are used for flood simulation. Flood event of 6 May 2002 is used for calibration of HEC-HMS. The performance of SRTM and TRMM data for flood modeling is assessed by the assistant of basic statistical measures. Workflow for flood modeling showed in Figure 3.2.

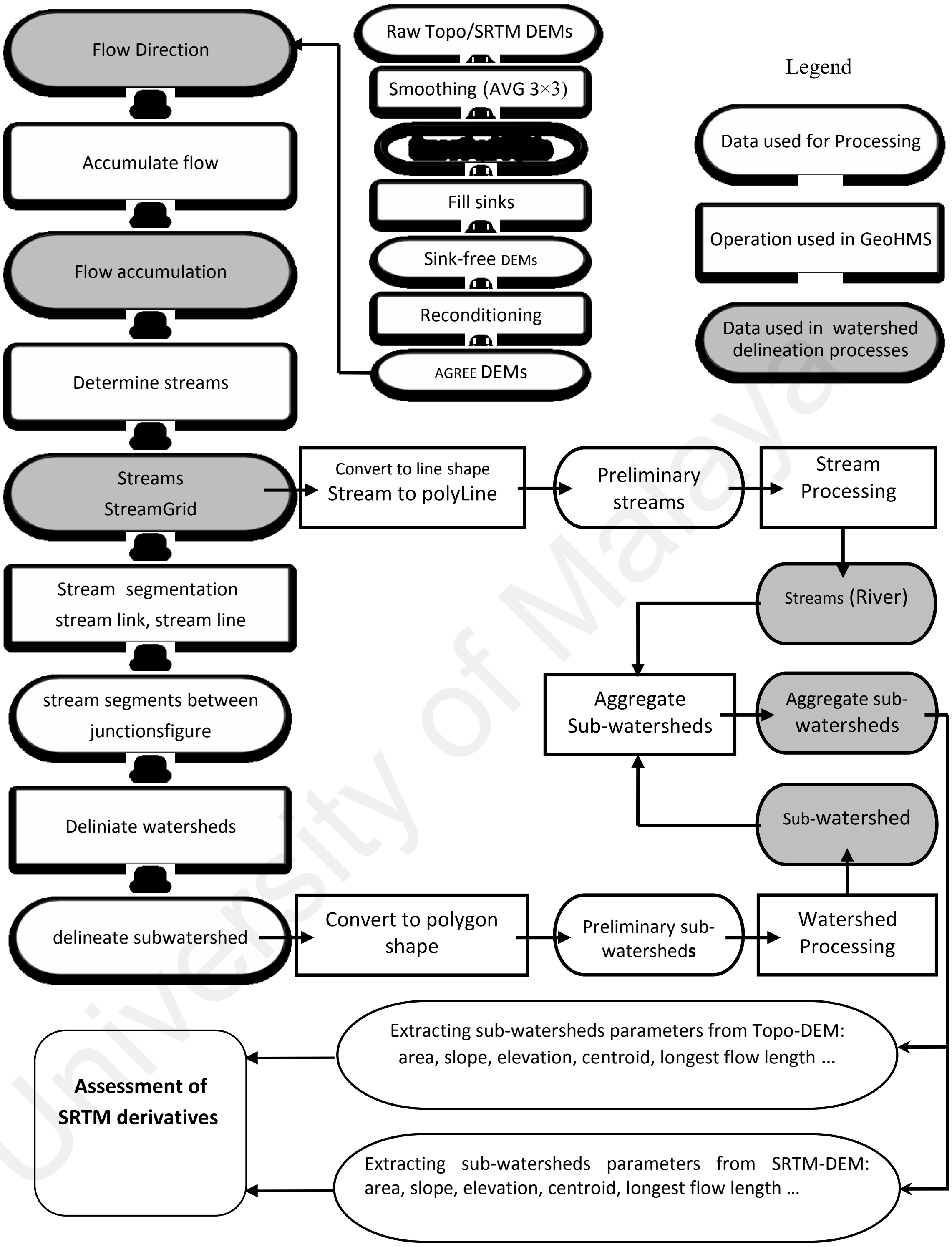

Figure 3.1: Work flow of watershed delineation and assessment of SRTM derivatives.

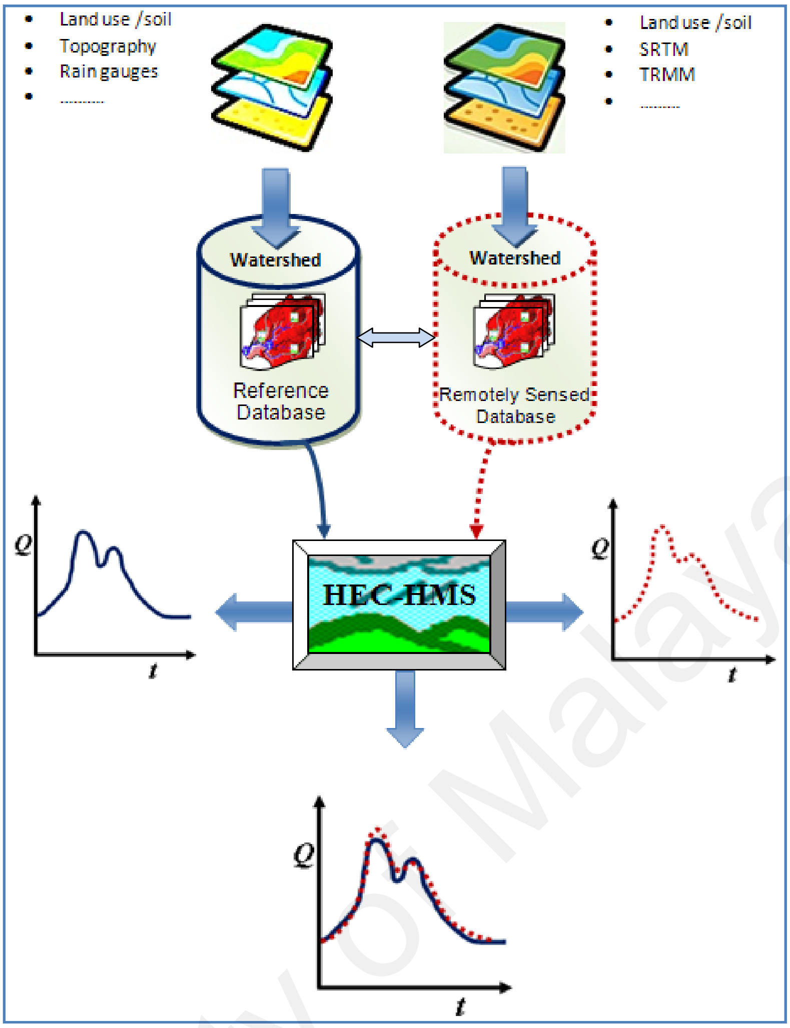

Figure 3.2: Conceptual representation of GIS-based hydrological simulation showing methodology followed in the research

3.2 Description of study area and used materials

At this section Klang watershed characteristics that related to the runoff modeling and primary analysis for database development are provided.

3.2.1 Location

The study area is the upper part of Klang watershed (hereafter Klang watershed) located on the west coast of Peninsular Malaysia; it encompasses the Federal Territory of Kuala Lumpur (KL) and parts of the State of Selangor. It is situated at 101° 30′- 101° 55′ longitude and 3°- 3° 30′, latitude (See Figure 3.3). The Klang watershed at the outlet where shown in Figure 4.2 has an area of about 675 sq km. The elevation ranged from 20 m at the outlet to 1420 m at the upstream.

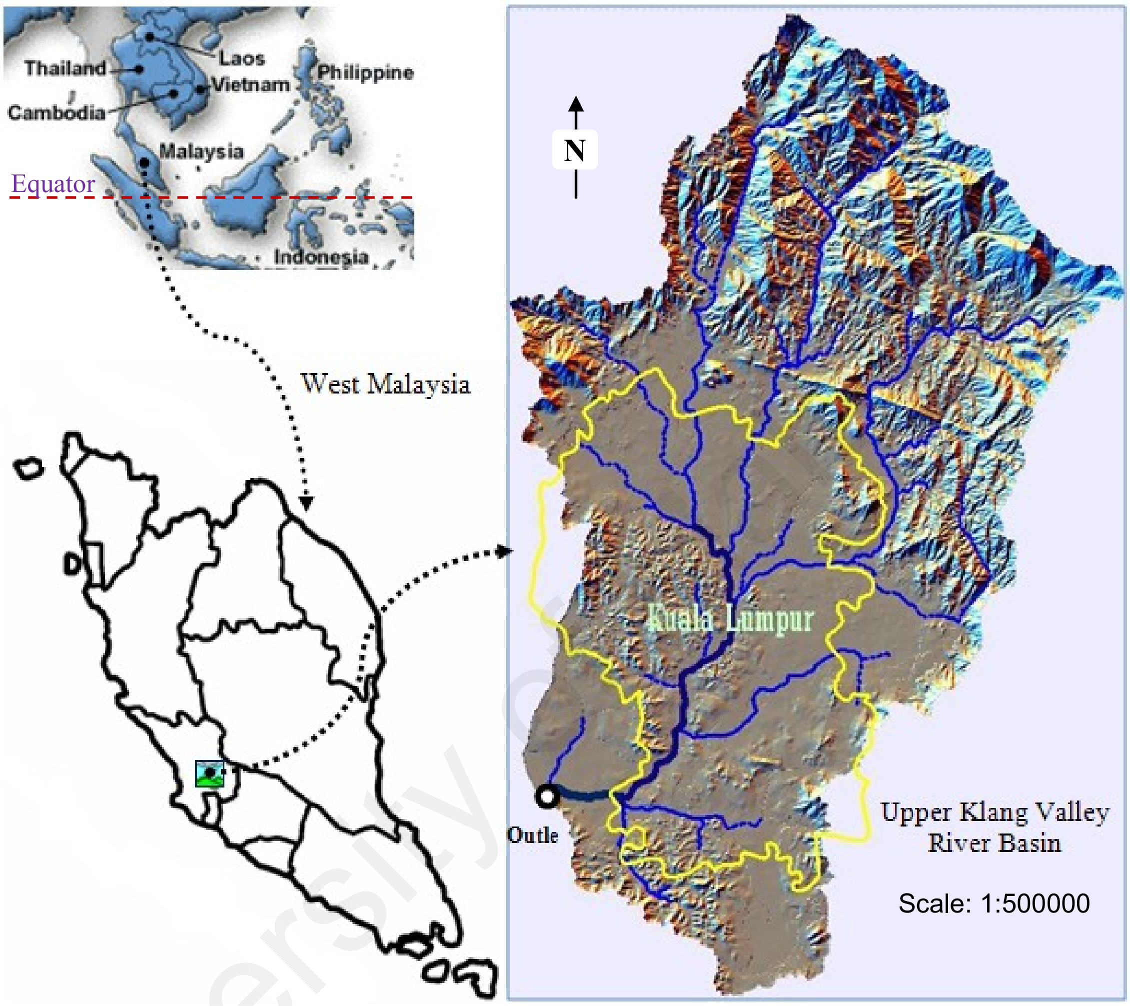

Figure 3.3: Study area

3.2.2 Climate

The climate condition is the typical tropic condition with high amount of rain and humidity. Previous studies have shown that mean annual rainfall is about 2400 mm and mean monthly rainfall ranges from 200 to 400 mm (Tick and Samah, 2004). The highest rainfall occurs in the months of April and November and the lowest rainfall occurs in June. Climate can be loosely defined by the following seasons :The north-east monsoon from December to March, a transitional period from April to May, the south-west monsoon from June to September and a transitional period from October to November.

It is also characterized by uniform high temperature, high relative humidity, heavy rainfall and little wind. The wet seasons occur in the transitional periods between the monsoons, from March to April and from October to November.

The temperature throughout the year is quite constant with a mean of 27ºC. The highest temperature increased at 1pm with an average of 32ºC and the lowest temperature decreased at 7am with an average of 23ºC (Hoong, 2004). As the relative humidity is very closely related to the surrounding temperature, its variation throughout the year is also with minimum an average value of 82%. The evaporation depth for open water is measured to be around 1500 mm per annum or monthly mean of around 125mm/month (Hoong, 2004).

3.2.3 Main drainage system

The main tributary system at the upper reach of the Klang watershed includes Batu, Gombak and upper Klang (see Figure 3.4). The confluences of Batu with Gombak and Gombak with Klang just downstream are at the heart of KL city, thus giving rise to the latter's name of 'muddy confluence'. At this point, the valley slope turns milder from that of about 1:300 to nearly 1:1000 as it flows through the city at its middle reach (DID, 2003c). Since 2007 a Stormwater Management and Road Tunnel (SMART) has operated, diverting the excess flood water from upstream of Ampang and Klang rivers in a certain conditions.

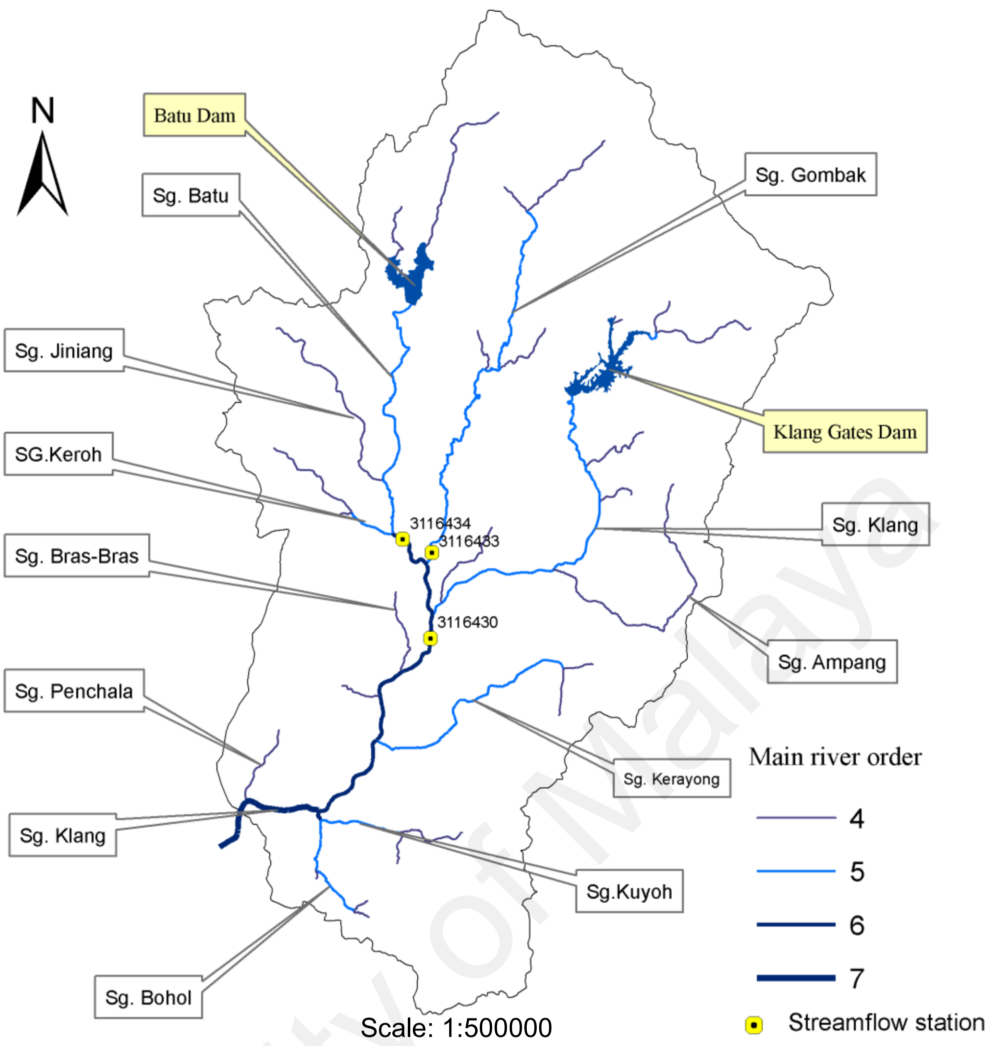

Figure 3.4: Main drainage system and local names of Klang watershed.

Under the SMART project, 280 m^3/s of flood discharge is diverted into the Kg. Berembang holding pond with an area of 8 hectare and having a capacity of 600,000 m^3. The water flows into a by-pass tunnel 9.8 km long and with an internal diameter measuring 11.8 meters. The total storage provided by the tunnel during diversion is 1 million m3 and discharge into a storage reservoir of 23 ha at Taman Desa having a capacity of 1.4 million m3 (Abdullah, 2006). The other major tributaries of Klang include Jinjang, Keroh, Kemunsing, Ampang, Kerayong, Kuyoh and Penchala. Jinjang and Keroh are significant tributaries of Batu, which flows in from the Northwestern region of the watershed through the relatively dense urban township of Kepong. Keroh confluences with Batu near the Jalan Duta-Segambut round about outside the center of

KL. The confluence of Batu and Gombak is located near the Putra World Trade Centre (PWTC) building about 2.8 km downstream of the Batu-Keroh confluence. The last of the three main streams that confluence at the heart of KL is the Klang itself flowing in from the North Eastern region of the watershed. As it skirts around the eastern boundary of KL, it picks up most of its runoff contribution from its right bank, where the KL boundary is, and hence the dense urban development areas. The left bank is still predominantly virgin forest where Kemensah Heights and the National Zoo are currently located.

The Klang picks up the runoff from its tributary of Ampang upstream of the eastern boundary of DBKL at Jelatek Street. At this point onwards, the contributing watersheds are the dense urbanized of Ampang Town and the eastern portion of KL, right up to the city center passing the Golden Triangle area. The confluence of Gombak and Klang is only about 2.5 km downstream of the confluence of Batu and Gombak and is at the heart of KL city center, namely at Masjid Jamek. Just upstream of the confluence is the bridge of Tun Perak Street on Klang River, which is a significant flood monitoring location as a flood gauging station is located here. The other significant flood gauging station is downstream of this confluence at the Jalan Sultan Sulaiman Bridge over Klang River.

3.2.4 Flood history in Klang watershed

Klang watershed has a long history of flooding. According to DID (2004) major flood in Klang watershed have occurred in the years 1926, 1971, 1982, 1986, 1988, 1993, 1995, 1996, 1997, 30 April 2000, 20 June, 26 April and 29 October 2001, 29 April, 6 May, 2 June, 11 June, 6 Sep, 8 Oct., 8 Nov. and 21 Dec. 2002, 6 April 2003 15 April and 16 July 2004. From the observed stream flow, we found significant floods that have recorded in 20 June 2005, 10 June 2006 and 9 April 2007 at the Sulaiman Bridge station.

3.2.5 Forms of Flooding in Klang watershed

Previous studies have identified two types of flooding that affected the Klang watershed (Jamaluddin, 1985, Hoong, 2004, Abdullah, 2006, Shaaban et al., 2008). The first is monsoonal type flooding caused by long duration of low intensity rainfall, precipitating over a large area. Rainfall duration ranges from 3 to 10 days with intensity about 20 mm/hr. The localized rainfall with very high intensities and short durations are the specifications of second type of flood termed as flash flood. It is occurred by rainfall duration from 2 to 5 hr with intensity bigger than 150 mm/hr. This causes what is termed as flash flooding. As the name would suggest, flash floods are quick to manifest after a storm and equally swift thereafter to subside. The flooding rather than being spread is confined to specific locations and is gone within a few hours.

3.2.6 Flood magnitude

The mean annual flood (MAF) provides useful preliminary information concerning the flood regime of a watershed because it indicates the general magnitude of flood flows (Mlmikou and Gordios, 1989). The MAF is usually needed in hydrological design, especially for small projects. Mlmikou and Gordios (1989) defined that the MAF is determined as the mean of the annual maximum flow series of a watershed. Varley and Marr (2004) have already shown that due to urbanization growth in Klang watershed the MAF at Sulaiman Bridge has increased from148 m^3/s (during the 1910-1986) to 440 m^3/s (during the 1986-1996). We investigated the annual peak discharge trend from 1996 to 2007 at the same station and found out that the MAF has reached to 519 m^3 /s (see Figure 3.5). This means that MAF have increased by 85% just during the 10 years.

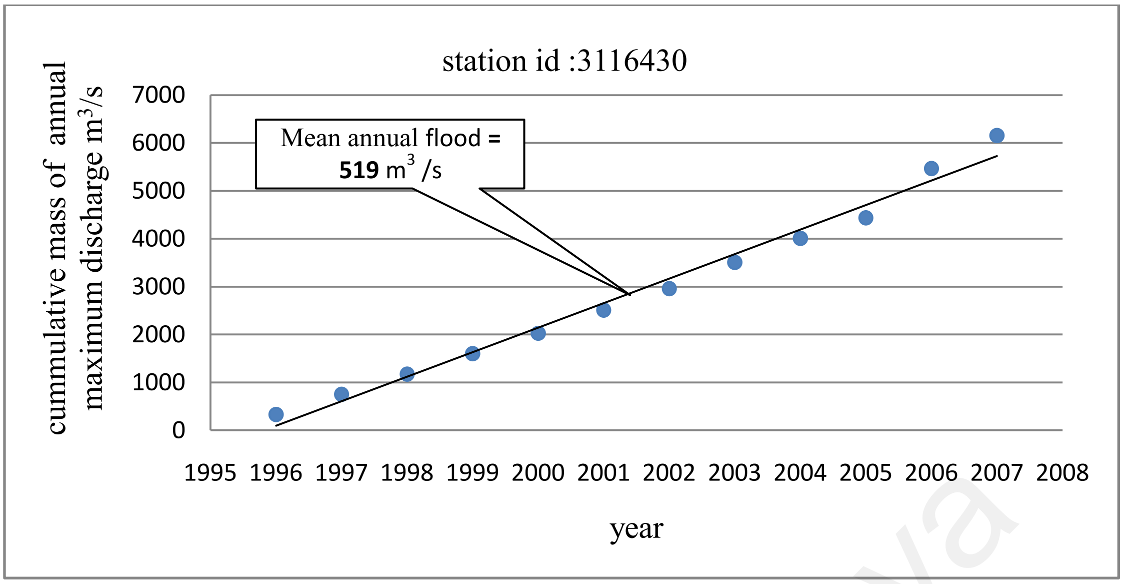

Figure 3.5: Cumulative plot of annual floods for the Klang watershed at Sulaiman Bridge

3.2.7 Evaporation

The Tanjung Karang at Selangor is only pan evaporation station near to Klang watershed. Monthly records for this station were collected from DID for the time period of 1981-2008. As illustrated in Figure 3.6 evaporation has no significant changes through the year. Evaporation ranges from minimum 47 mm for December to maximum 54 mm for March. In the event-based modeling, only the first process is usually considered since Evapotranspiration can be often negligible in the simulation of short rainfall-runoff events (Cunderlik and Simonovic, 2004).

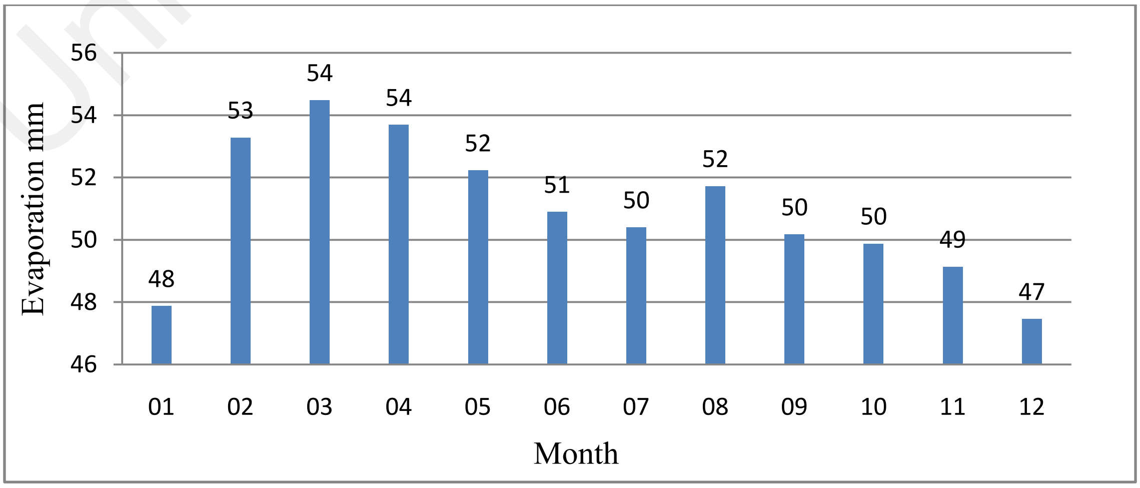

Figure 3.6: Monthly distribution of Evap. at 3511301 Tanjung Karang at Selangor

3.3 Data collection and database development

There were no data readily available; therefore the data were collected from a variety of sources.

3.3.1 Topographic maps

It is essential to use good topographic maps for most hydrologic studies. It is because the maps contain contours of terrain surface elevation; so that watershed boundaries can be delineated and important parameters such as area, slope, and stream patterns can be determined.

These maps show not only the contours, but also any significant streams or other bodies of water, forest cover, built-up areas or individual buildings and other features. According to USACE (1997) topographic maps at scale 1:25,000 are usually necessary for satisfactory hydrologic studies. Existing topographic survey maps form the basis for much derived topographic work. For instance, DEM have often been created from existing paper topographic maps. Digital topo maps for this research were obtained from the Department of Survey and Mapping Malaysia (known as JUPEM in Malaysia). According to the map index for digital topo sheets at the scale of 1:25,000 (series L8028) shown in Figure 3.7, the study area is covered with nine topo sheets.

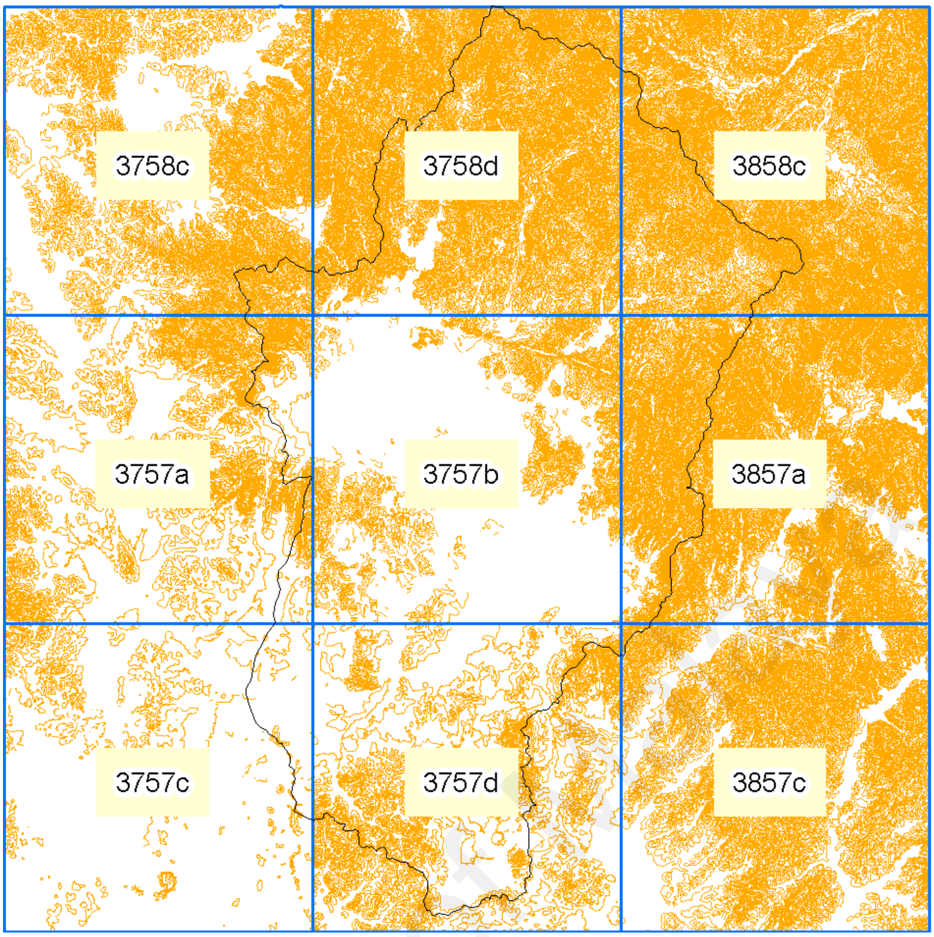

Figure 3.7: Watershed-layout in map index of topo sheets at scale of 1:25000

As it is seen in Figure 3.7, many contour lines have missed in sheet 3757b (Kuala Lumpur's sheet). This indicates that existing topo sheets at scale 1:25000 cannot capture the watershed relief in the urban areas. Therefore, void area was filled with twenty-four digital topo sheets at the scale of 1:10,000 from series of L808 (see Figure 3.8). Topo sheets were obtained from the Malaysian department of surveying and mapping (JUPEM) through the research grant funded by the University of Malaya. The relief is shown by contour lines with 20 and 5 meters interval for 1:25000 and 1:10000 respectively. Top of hills and ridges are shown in the form of spot heights. The Digital topo sheet is the cartographic production of aerial photographs taken in different years and thus, they are not uniform products.

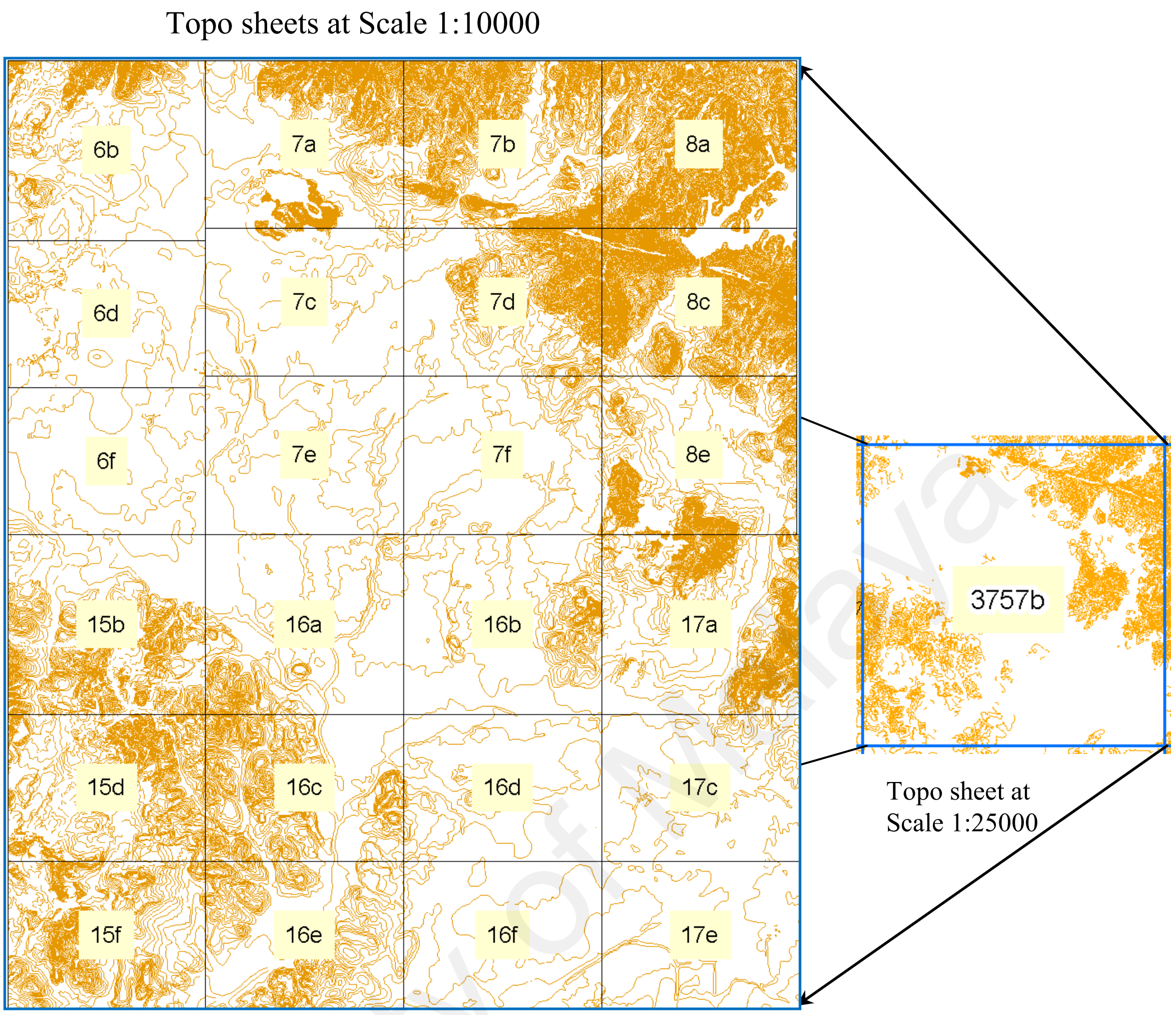

Figure 3.8: Filling void areas at sheet number 3757b (scale 1:25000) with topo sheets at scale 1:10000

Merging topo sheets at scale 1: 10000 to the topo map at 1:25000 adds more detail to the terrain in the urban areas of Klang watershed. As Doan (2003) has stated, in theory, combining GIS data sets of different resolutions is generally not recommended because of the difficulty in assessing the accuracy and the precision of the resulting data set and outputs. In practice, however, combining data set of various resolutions is necessary due to lack of uniform data and data coverage. In addition, when the map source has multiple contour intervals, the largest interval is used for a conservative estimate (GIAJ, 1998). Final topo map used for generating Topo-DEM presented in Figure 3.9.

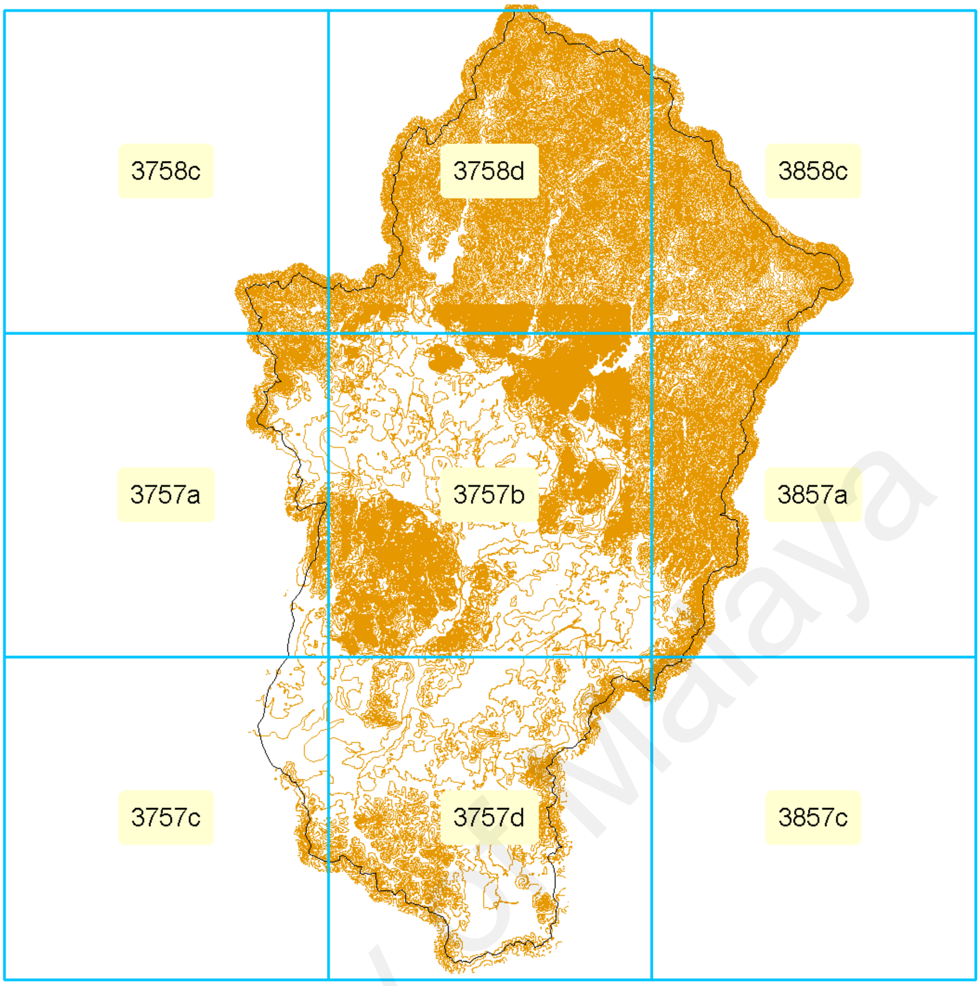

Figure 3.9: Final merged topo maps used for generating DEM

3.3.2 Problems associated with the collected digital topo maps

- **Reference system**

There is only one origin and projection system that should be used for the whole database. That is the Rectified Skew Orthomorphic system (RSO) (JUPEM, 2006). Thus, geo-referencing is required to transform the datasets so as to be in the same datum and projection system if they have projected in a different projection system.

- **Data format and software issues**

The discrepancy of data structure between datasets is not possible when employing the GIS environment for further analyses. Existing spatial data are not in a GIS ready format and data conversion and transformation has to be performed. Digital topo sheets have been stored in the CAD drawing format file to fulfill hard copy map production.

CAD format is a vector format file, which is good for presenting the geometry of spatial data. Autodesk's Drawing Exchange File (DXF) format is also utilized, considering that it is one of the most widely used vector data transfer format, and because it offers some very strong advantages. Among others it contains very complete display information and almost every graphic program can read it. However this format is not suitable for GIS analysis. CAD stores all the feature types such as point, line, polygon, multipath, or annotation in one file. Moreover there is no attribute database associated with the feature types in DXF/DWG formats. CAD has poor handling of object attribute, limited and slow database links and elementary spatial analysis and cartographic capabilities. Resolution of this dilemma lies in taking a best of breed approach and building better linkages between CAD and GIS software packages (Panda, 2006).

3.3.3 Typical observed errors in digital topo maps

Raw vector data might have several factual and topological errors. The following are commonly observed errors in the topo sheets:

- Self-overlap: some segments overlap themselves .
- Dead ends: segments have dead ends which appears in over-shot and under-shot
- Intersections - different segments cross each other. Contour lines with different height values are not supposed to cross each other.
- Code consistency: segments, which are connected to each other by a node, have the same value. It should be check whether a contour line, which consists of multiple consecutive segments, has one height value .
- Closed segments: Check whether each segment has only 1 node serving both as the begin node and as the end node .
- Edge matching: contour lines in two adjacent sheets should match together.

Purchase processing including licensing and payment and map editing was the most difficult part of this project. It almost took about one year to finish the editing preprocessing. The work completed by spending much time to edit digital topo and stream network maps. Figure 3.10 illustrates the typical errors observed in digital topo maps and its effects on DEM processing. Figure 3.10.a shows a contour line with different elevation which could generate pits or peaks in DEM. Figure 3.10.b shows a set of contour lines that wrongly have the same elevations. This type of error produce a flat area on DEM. Figure 3.11 shows another example of errors that emphasizes edge matching problem in two adjacent topo sheets. In addition, detecting such errors in a large area requires long time experience in GIS and data management. Detecting those types of error from the source data is quite difficult, time consuming and has no systematic approaches.

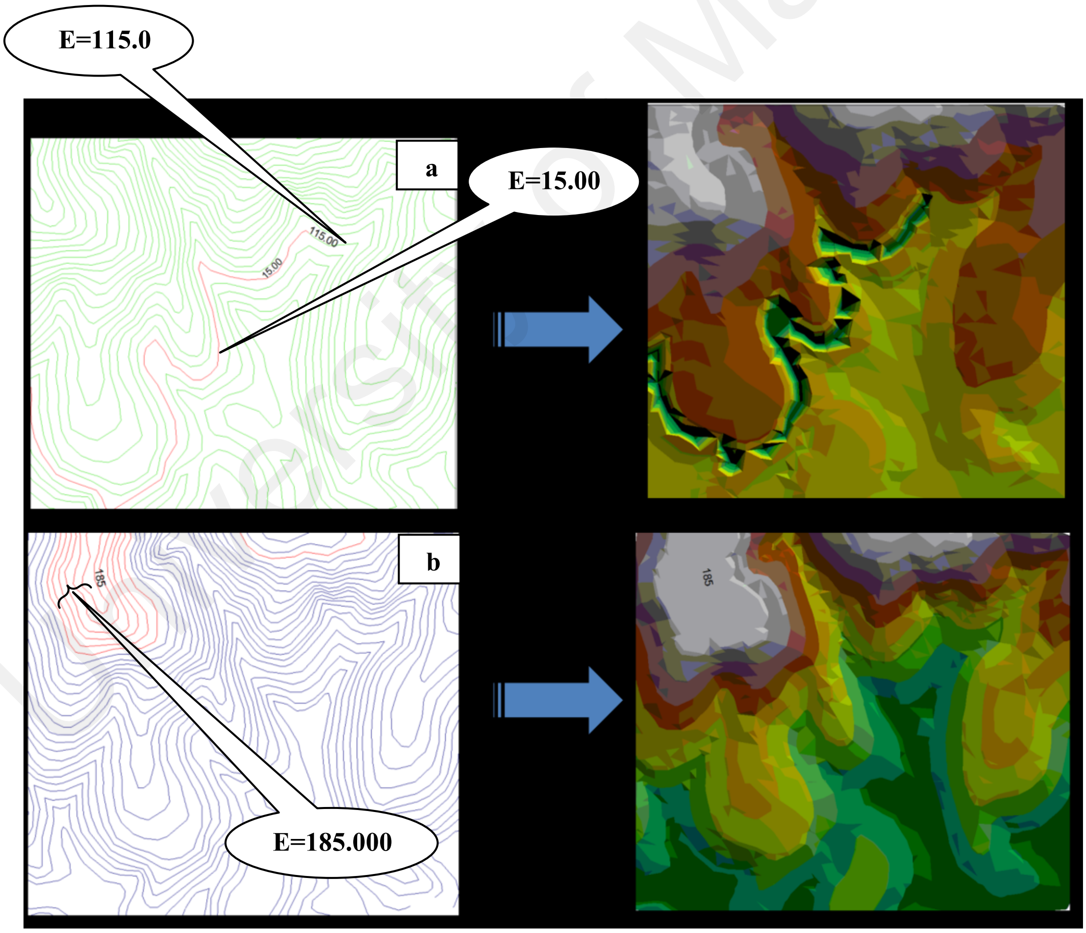

Figure 3.10 Illustration of code consistency (a) and false coding errors on digital topo maps

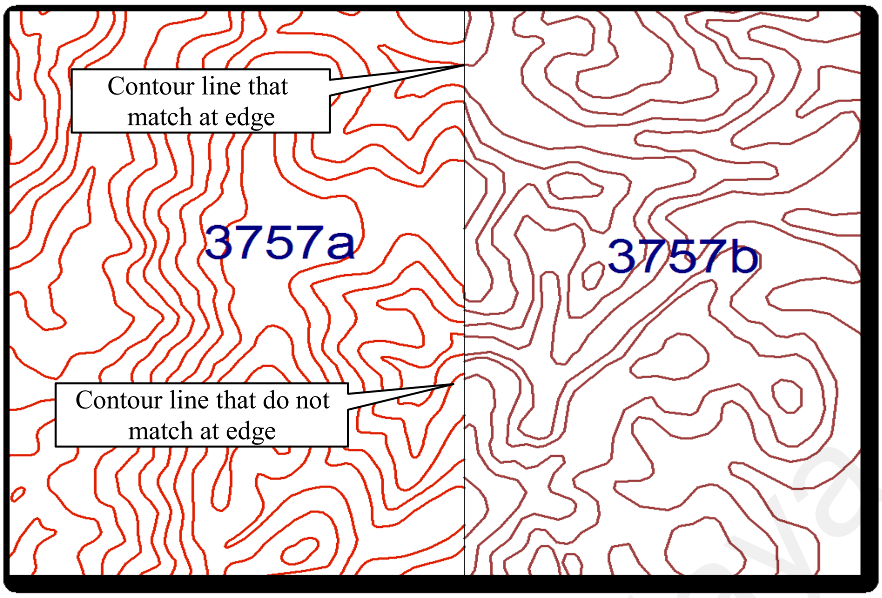

Figure 3.11 Illustration of edge matching error in digital topo maps

3.3.4 Land use (LU)

It is well known that land use can significantly affect the runoff characteristics of the land surface (Vieux, 2004b). The LU is sometimes available as geospatial data derived from aerial photography or satellite imagery. To be useful, this LU must be reclassified into parameters that reflect the hydrologic processes. Examples of reclassification from a LU map into hydrologic parameter include impervious areas that limit soil infiltration capacity. The level of detail in the LU map determines the spatial variability of the derived hydrologic model parameter. LU map for this study was collected from The Malaysian Department of Agriculture (DOA). It was derived from the land sat images acquired on 20 September 2001 and distributed in ESRI shape file format. According to DOA spatial detail of LU map is equivalent to the scale of 1:65000. As shown in Figure 3.12 land use in Klang watershed can be classify under several major classes which are forest, agriculture, mining, newly cleared land, grass land, swamp, urban areas and water bodies. According to Figure 3.13 dominant classes are forest and urban areas with 36.6% and 49.5% respectively. Further attempt was made to achieve the better visualization of the Klang watershed by assistant of Landsat 7 Satellite image from the study area.

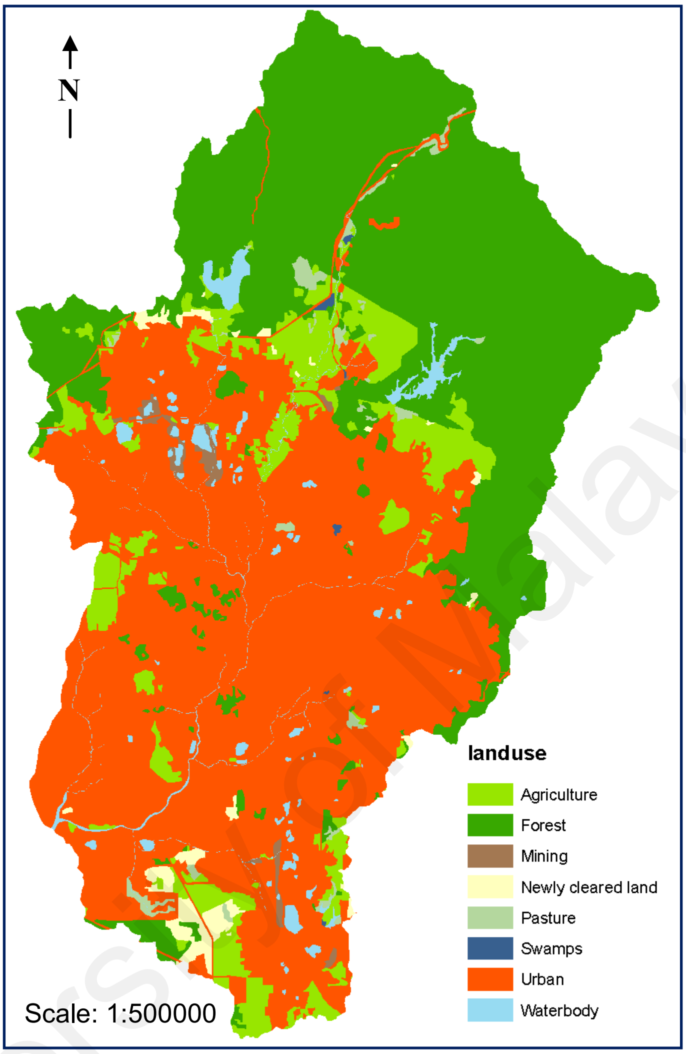

Figure 3.12: Land use map of study area

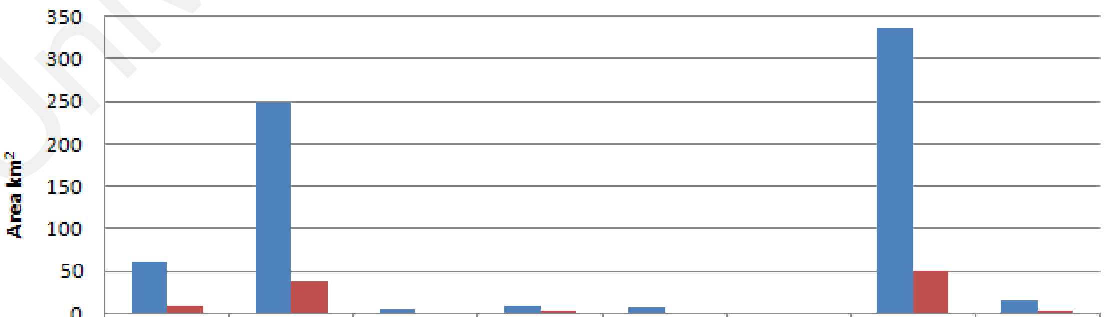

	Agriculture	Forest	Mining	Newly cleared land	Pasture	Swamps	Urban	Waterbody
Area km2	59.95	249.19	4.10	8.69	6.23	0.64	336.57	14.82
Area %	8.82	36.64	0.60	1.28	0.92	0.09	49.49	2.18

Figure 3.13: Histogram of land use classes for the study area

3.3.5 Checking LU with Landsat image

LU map were assessed by means of Normalized difference vegetation index (NDVI) image interpreter. For this purpose raw Landsat images (ETM+) for the year 2002 were obtained from Malaysian Centre for Remote Sensing (MACRES) through the research grant funded by University of Malaya. 3NDVI capitalizes on the strong energy absorbed by the chlorophyll in the red portion of the electromagnetic spectrum (RED), and on th*e* energy scattered by the internal structure of leaves in the near-infrared (NIR), and uses this contrast as an estimate of vegetation greenness, by the formula: NDVI=(NIR–RED)/(NIR+RED) (Rouse et al., 1974). For Landsat 7 this formula is written as follow: NDVI= (band3–band4)/ (bans3+bands4). The result is an image with pixel values that range from –1 to 1 (see Figures 3.14 and 3.15). Privies study by (Martinuzzi et al., 2008) have shown that in the coastal lowlands, the NDVI is segmented into three major classes: a) forest, including semi-deciduous and plantations (NDVI ≥0.70), b) woodland and shrub land (0.60≤ NDVI <0.70), and c) grasses (NDVI <0.60). (4), now abandoned, from the semi-deciduous forest (Martinuzzi et al., 2008). Zero for rock and bare soil differential for water bodies such as rivers and dams have the opposite trend to vegetation and the index is negative.

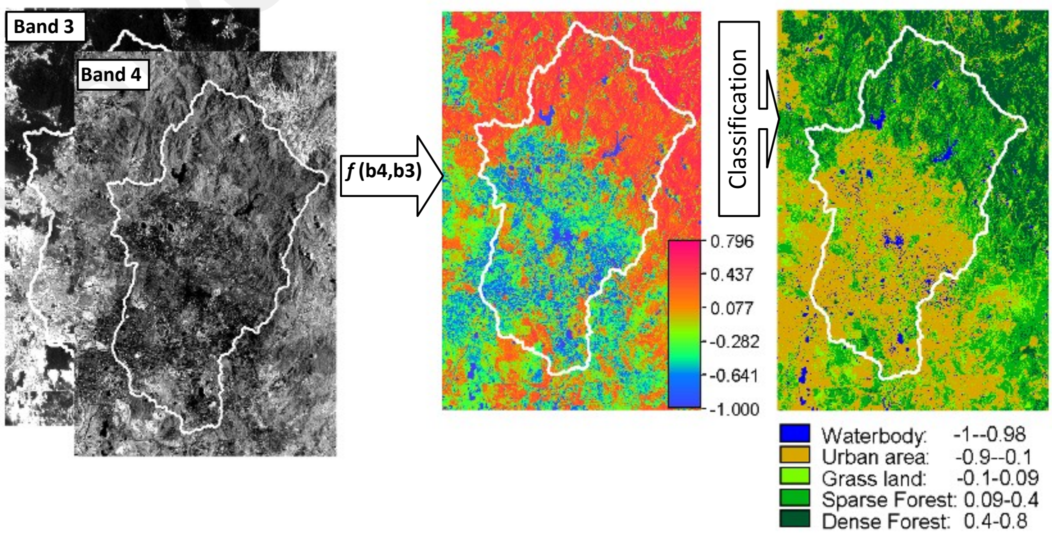

Figure 3.14: Illustrations of NDVI mapping

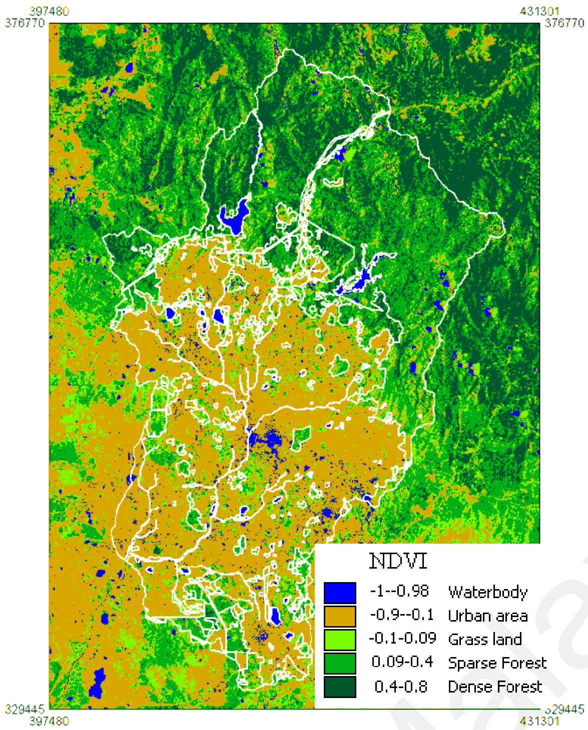

Figure 3.15: Land use classification based on NDVI

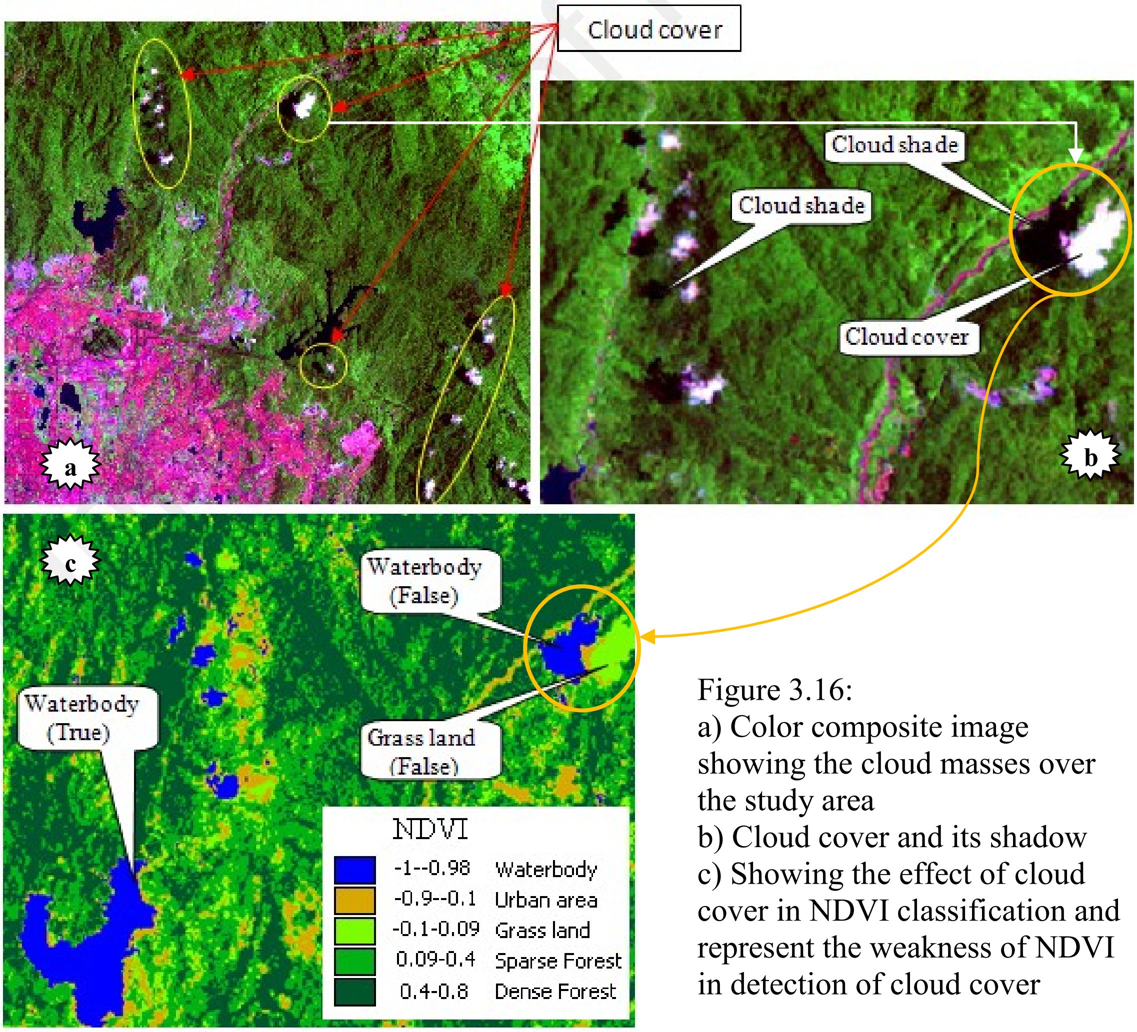

Figure 3.16:
a) Color composite image showing the cloud masses over the study area
b) Cloud cover and its shadow
c) Showing the effect of cloud cover in NDVI classification and represent the weakness of NDVI in detection of cloud cover

NDVI is an excellent tool for land use classification. However, as illustrated in Figure 3.16.c cloud mass and its shadow can cause problem in image classification. In such cases cloud shadows are wrongly classified as water bodies.

3.3.6 Hydrologic Soil Group (HSG)

Soil properties play an important role in determining the runoff generation behavior (Abrahams et al., 1988, Martınez-Mena et al., 1998). Infiltration capacity is an important characteristic of soils in hydrological processes. Thus, as result of spatial variability of soil infiltration capacities runoff generation has no uniform pattern over the watershed. HSG reflects the runoff potential of soils over the study area. In humid areas this variability is mainly attributed to spatial differences in soil moisture (Troendle, 1985). The HSG map was derived from the digital soil map obtained from DOA (ESRI shape file format at scale of 1:500000). No larger scale was available for Klang watershed. However, Asnita (2007) informed that the soil map of Peninsular Malaysia at scale of 1:25000 is currently under development by DOA. But the project has not been completed and no data have been published yet. According to JPS (2003) the textural classification of topsoil is coarse sandy clay loam in the center of watershed. Figure 3.17 shows the HSG map and Figure 3.18 shows the histogram of soil groups for Klang watershed. As shown in this two figures the dominant classes are A and D with 35.76 % and 48.64% respectively.

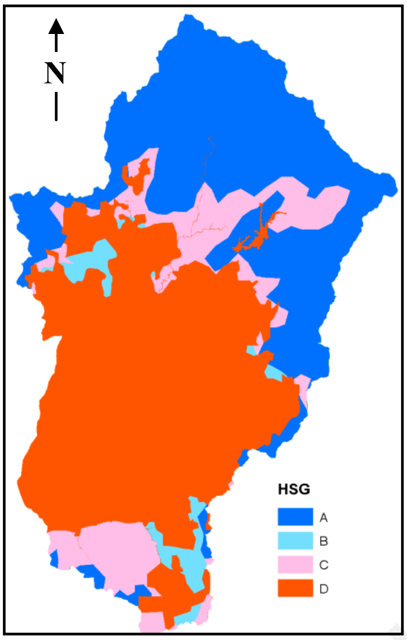

Scale: 1:1000000

Figure 3.17: Hydrologic Soil Group for the study area

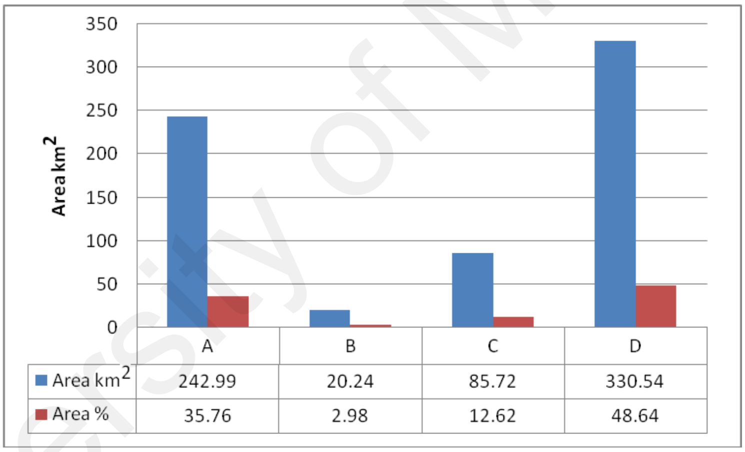

Figure 3.18: Histogram of HSG for Klang watershed.

3.3.7 SCS-CN map development

The Soil Conservation Service (now Natural Research Center) curve number (SCS-CN) method is one of the most popular methods for computing the volume of surface runoff for a given rainfall event from small agricultural watersheds. The CN method, developed by the USDA-Soil Conservation Service (SCS, 1972b), for predicting surface runoff from rainfall, is widely accepted in the world (Huang et al., 2006). It is used extensively in various hydrologic, erosion, and water-quality models. The method has been widely used in continuous modeling schemes. Referring to

Mockus (1965) the CN is derived from the tables given in the National Engineering Handbook section 4 (NEH-4) for watershed characteristics, such as soil type, land use, hydrologic condition, and initial soil moisture condition. CN may vary from 0 to 100, though most CNs is in the 55-95 range (Hawkins, 1998). Lack of information for soils in or near the Klang watershed specifically for alluvium areas of the KL metropolis have been reported by DID (2003a). According to DID (2003a) some important soil characteristics relating to infiltration are described as:

The forested residual soils in the sloping upper Klang watershed are all highly permeable with 3-hour infiltrations well above 130 (mm) which is about 43 (mm/hr). However, tin-mine spoil materials, beneath 2/3 of KL, show moderate to low infiltration rates. The remaining permeable areas under trees or grass have an infiltration rate of only 25mm in the first hour, and infiltration rates after 1 hour fall to 12mm/hour. They have also found that, building on forested residual soils would increase run-off very much more than building on tin-mine spoil materials.

3.3.8 Generating of CN map

The SCS runoff cure number was developed as an index that represents the combination of a hydrologic soil group and a land use and treatment class. Empirical analyses suggested that the CN was a function of three factors: soil group, the cover complex, and antecedent moisture conditions (McCuen, 1998). The soil scientists of the U.S. Soil Conservation Service (SCS) classified soils on the basis of their runoff potential and grouped them into four hydrologic soil groups that are identified by the letters A, B, C, and D. The soil characteristics associated with each group adapted from McCuen (1998 : page 155) and given in Table 3.1.

Table 3.1: SCS soil groups and corresponding loss rates

Group	Characteristics of Soils	Minimum infiltration rate (mm/hr)
A	Deep sand; deep loess; aggregated silts	7.62-11.43
B	Shallow loess; sandy loam	3.81-7.62
C	Clay loams; shallow sandy loam; soils low in organic content; soils usually high in clay	1.27-3.81
D	Soils that swell significantly when wet; heavy plastic clays; certain saline soils	0-1.27

3.3.9 Hydrologic Condition

The hydrologic condition reflects the level of land management. It is separated into three classes: poor, fair, and good. Not all of the land uses are separated by treatment or condition. The type of vegetation or ground cover on a watershed, and the quality or density of that cover, has a major impact on the infiltration capacity of a given soil. Further refinement in the cover type is provided by the definition of cover quality as follows: the hydrologic condition is Poor when the areas are heavily grazed or regularly burned. In this condition less than 50 percent of the ground surface is protected by plant cover or brush and tree canopy. The hydrologic condition is fair when 50 to 75 percent of the ground surface protected by vegetation. If more than 75 percent of the ground surface protected by dense vegetation, hydrologic condition is called good. In most cases, the cover type and quality of a watershed in existing conditions can be readily determined by a field review of a watershed. According to climate condition of Klang watershed, hydrologic condition is considered as good condition.

3.3.10 Antecedent Moisture Condition (AMC)

According to McCuen (1998) antecedent soil moisture is known to have a significant effect on both the volume and rate of runoff. Recognizing that it is a significant factor, SCS developed three antecedent AMCs, which were labeled I, II, and III. The soil condition for each is as follows:

AMC I: Soils are dry but not to wilting point; satisfactory cultivation has taken place
AMC II: Average conditions
AMC III: Heavy rainfall, or light rainfall and low temperatures have occurred within the last five days; saturated soil

Refer to McCuen (1998) CN values obtained from TR-55 represent condition II. AMC are classified base on the amount of rain fall in 5-days prior as presented in Table 3.2.

Table 3.2: Total 5-day antecedent rainfall (mm)

SMC	Dormant Season	Growing Season
I	< 13	< 36
II	13-28	36-53
III	>28	>53

ILWIS version 3.4 was used to introduce GIS-based approach for generating CN map of Klang watershed. ILWIS is raster based-GIS software and have good functionality in raster operations. According to USDA (1986) SCS-CN is determined based on the LU, HSG, hydrologic condition and antecedent soil moisture (ASM) conditions (see Figure 3.19) . Antecedent soil moisture condition is determined based on 5-days antecedent rainfall is derived from crossing land use (LU) map and Hydrologic Soli Group (HSG). In addition, the new values are assigned for the pixels from the two-dimensional table. The general form of this operation is shown with Eq. 3.1.

$$OutMap = TwoDim\ [InMap1,\ InMap2] \qquad \text{Eq. 3.1}$$

Where; *OutMap* is the output map, *TwoDim* is a two-dimensional table, *InMap1*and *InMap2* are two input map with the same cell size and the same projection.

A two-dimensional table is used to combine two raster maps with a Class, Group or identifier domain (Koolhoven et al., 2007). It defines a new class or a value for each possible combination of input classes or groups. To generate CN map, the above operation is set for CN table, LU and HSG maps with Eq. 3.2:

CNmap=CN [LU, HSG] Eq. 3.2

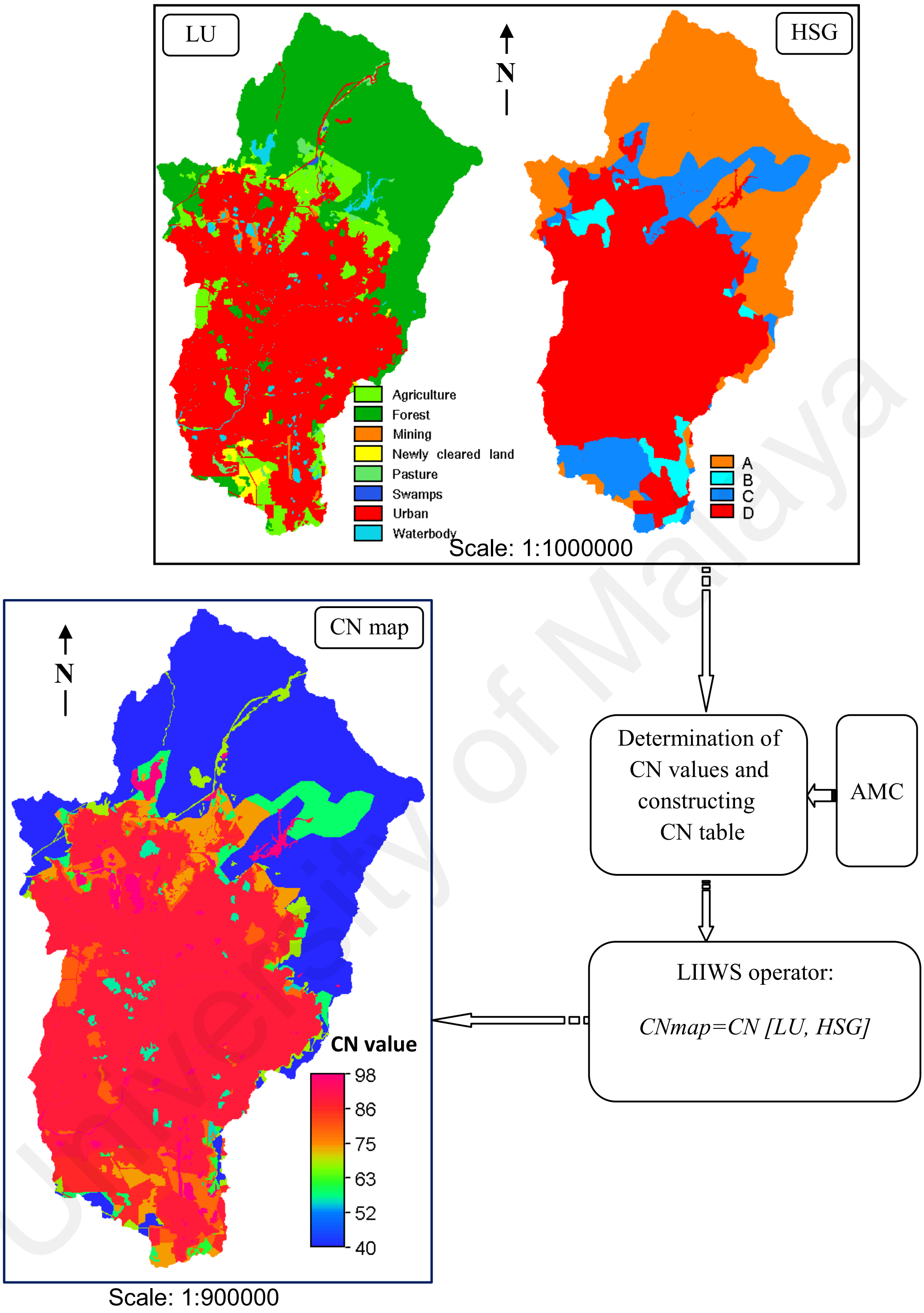

Figure 3.19: Work flow of generating CN map of study area.

A two-dimensional table view consists of rows representing one domain, and columns representing another domain. In the two-dimensional table, you have to assign a value, class name or ID to each possible combination of your input domains.

Then two-dimensional table was formed based on the soil and land use maps and SCS rules and regulations. Figure 4.20 demonstrates the algorithm developed for generating CN map. Final CN map was sliced under 12 classes (See Figure 3.20; CN map). CN values in the maps represent the normal condition labeled as CN-II.

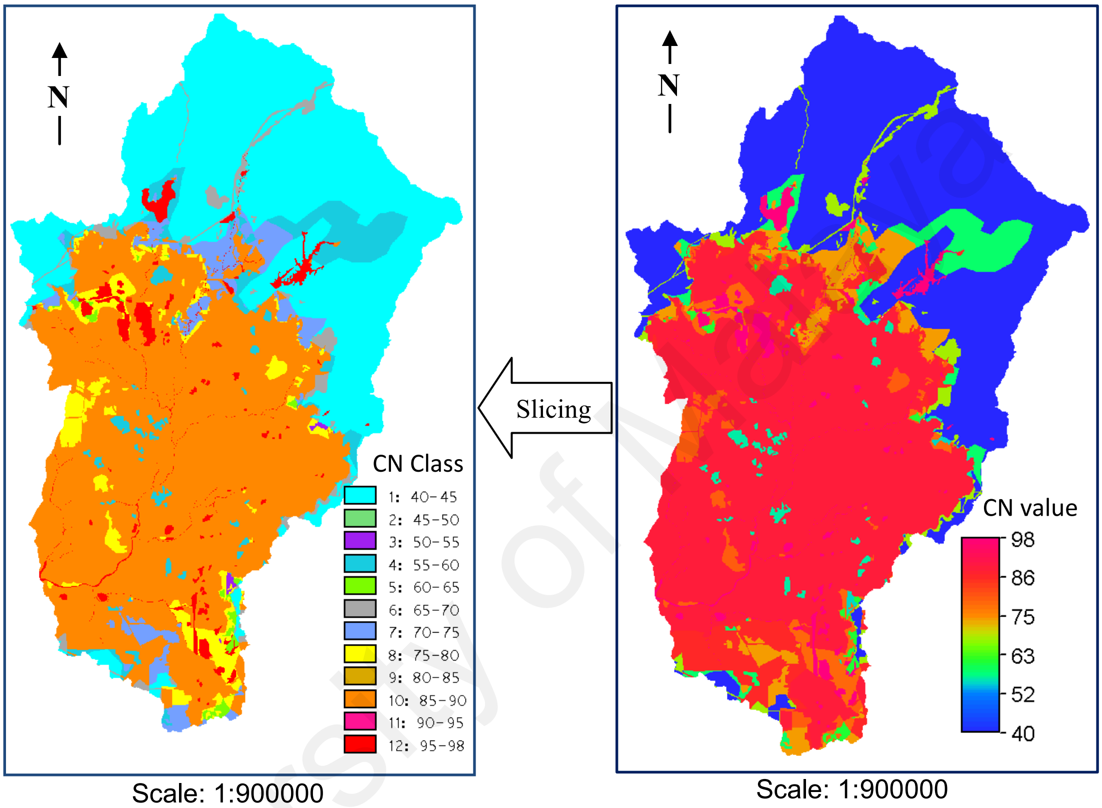

Figure 3.20: Classifying CN map (left) from the gridded-CN map (right)

3.4 Hydrologic time series

3.4.1: Rainfall events

Rainfall data for 29 stations located at the upper Klang watershed (see Figure 3.21) were collected form Department of Irrigation and Drainage (DID) of Malaysia. General characteristics of the rainfall stations are provided in Table 3.3.

Table 3.3: General characteristics of rainfall stations located in and near to the Klang watershed. (Longitude and Latitude are in Degree, Minute and Second)

No.	Station id	Local Name	State	Longitude	Latitude
1	3216005	Bate Dam	Kuala Lumpur	101 40 48	03 15 36
2	3117080	Bukit Antarabangsa	Selangor	101 46 12	03 10 48
3	3016077	Jalan 222	Selangor	101 37 48	03 05 24
4	3015001	Jambatan Petaling	Kuala Lumpur	101 39 36	03 04 48
5	3217102	Jinjang	Kuala Lumpur	101 39 36	03 13 48
6	3117070	JPS Ampang	Kuala Lumpur	101 45 00	030 9 00
7	3116004	JPS Wilayah	Kuala Lumpur	101 42 00	03 09 36
8	3217002	Klang Gates Dam	Kuala Lumpur	101 45 00	03 13 48
9	3217004	Kuala Seleh	Kuala Lumpur	101 46 12	03 15 36
10	3116006	Ldg Edinburgh	Kuala Lumpur	101 37 48	03 10 48
11	3116074	Leboh Pasar	Kuala Lumpur	101 42 00	03 09 00
12	3117104	Pandan Indah	Kuala Lumpur	101 45 00	03 07 48
13	3016001	Puchong Drop	Selangor	101 36 00	03 01 12
14	3017105	Seri Kembangan	Selangor	101 43 12	03 00 36
15	3317001	Sg.Batu Waterfall	Kuala Lumpur	101 42 00	03 19 48
16	3117002	Simpang Tiga	Kuala Lumpur	101 43 12	03 15 00
17	3218101	Stn. Jenaletrik Lln. Ponsoon	Selangor	101 52 48	03 13 12
18	3217005	Gombak Damsite	Kuala Lumpur	101 42 00	03 13 48
19	3216001	Kg. Sg. Tua	Kuala Lumpur	101 40 48	03 16 12
20	3216004	SMJK Kepong	Kuala Lumpur	101 37 48	03 13 12
21	3317004	Genting Sempah	Kuala Lumpur	101 46 12	03 22 12
22	3016103	Taman Desa	Kuala Lumpur	101 40 48	03 6 00
23	3114114	Kg. Berembang at Keramat	Kuala Lumpur	101 44 24	03 10 12
24	3116003	Pejabat JPS Malaysia	Kuala Lumpur	101 40 48	03 09 00
25	3116005	Sek. Ren. Taman Maluri	Kuala Lumpur	101 38 24	03 12 00
26	3117101	Kerayongvat Cheras Baru	Kuala Lumpur	101 42 00	03 06 00
27	3117102	Taman Miharja	Kuala Lumpur	101 43 48	03 07 12
28	3217003	Ibu Bekalan KM.11 at Gombak	Kuala Lumpur	101 42 00	03 14 24
29	3016102	Taman Sg. Besi	Kuala Lumpur	101 41 24	03 06 00

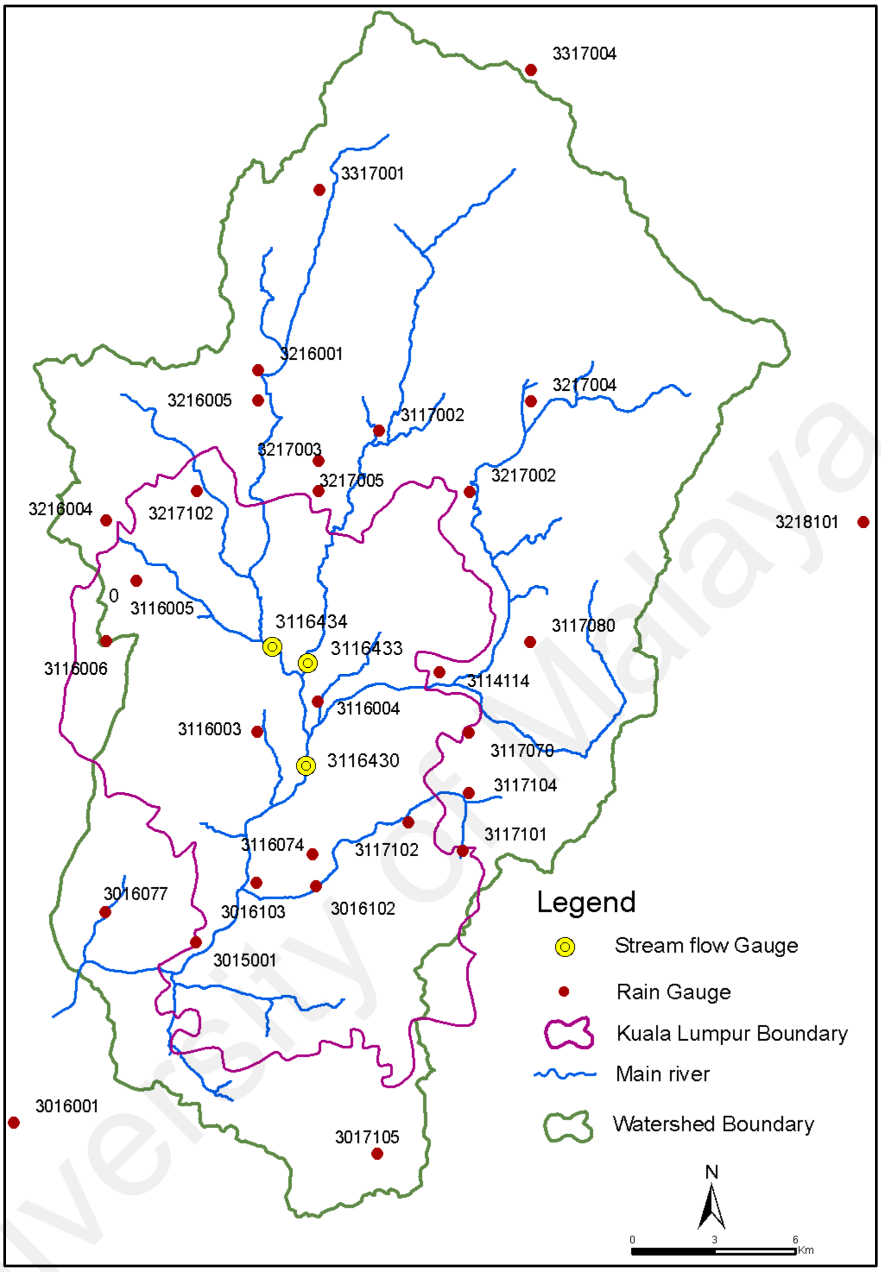

Figure 3.21: Layout of the rainfall stations in and near to the Klang watershed

According to Eq. 2.2 the number of rain-gauges required for hydrologic modeling in Klang watershed is about 6 rain-gauges. It is seen that gauge density in Klang watershed (one gauge per 24 km^2) is much more than gauge density derived from Eq. 2.2 (one gauge per 113 km^2). However gauge density is still less than the typical rain gauge density in urban watershed recommended by Vieux (2004) which can exceed one gauge per 10 to 20 km^2. All rainfall/stream flow stations and instruments visited within

3 days field survey and the rain gauge's locations were picked and mapped using Garman GPS*map* 76CSx. We found some shift between the geographic coordinates collected from DID and those obtained by GPS. Although the difference is negligible, but we used the GPS coordinates in the subsequent analysis.

3.4.2 Stream flow record

The streamflow data are important in calibrating the hydrologic model. There are three DID gauges inside the Klang. Figure 3.21 show the location of three active stream flow stations inside the study area. General characteristics of stream flow stations are provided below in Table 3.4

Table 3.4: General characteristics of stream flow stations

Station ID	Local name	River	Watershed area (km^2)	Lat	Lon
3116430	Jambatan. Sulaiman	Sg. Klang	468	101.70	3.14
3116433	Jln. Tun Razak	Sg. Gombak	122	101.70	3.17
3116434	Sentul	Sg. Batu	145	101.69	3.18

Observed stream flow discharge in hourly, daily and 15 minute time interval were collected from DID. Observed flood hydrograph can derive from the stream flow records. To ensure the position of rain gauges and stream flow station we identified to resurvey all the stations using handhold GPS CS76.

3.5 Channel geometry

3.5.1 Channel length

The channel length is used frequently in hydrologic computations. McCuen (1998) has identified two computational schemes for computing the channel length as follows: The distance measured along the main channel from the watershed outlet to the end of the channel which is denoted as L_C. The second is the distance measured along the main channel between two points located 10 and 85% of the distance along the channel from the outlet, which is denoted as $L_{10\text{-}85}$

3.5.2 Channel cross-section

In urban areas of Klang watershed, natural drainage system is rarely observed. Most of channels have uniform geometric cross section made by concrete. However, natural river system still is observed in newly developed areas. Specifically in Jinjang river and upper limits of Batu, Gombak and Klang rivers.

Unfortunately, there is no as-built cross section information available. DID (2003b) has reported that as-built cross-sections can differ significantly from design cross-sections and that there is heavy siltation or collapsing of concrete channels along many of these rivers. For example field cross section validation survey on 15 February, 2002 have been carried out at water level telemetric station (Code: 3116535) on the Batu River. As shown in Figure 3.22, it has observed a significant difference between the design and the existing cross-section. However, according to MacArthur and DeVries (1993) the kinematic wave model is not especially sensitive to channel cross-sectional shape in the simulation of discharge, and therefore, the complex channel shapes were simplified. The shapes that used in HEC-HMS are trapezoidal and rectangular. River cross-sections for this research were collected from river division of DID Kuala Lumpur as well as DID (1994). Typical observed cross-sections of main channel system of Klang watershed is demonstrated in Figure 3.23.

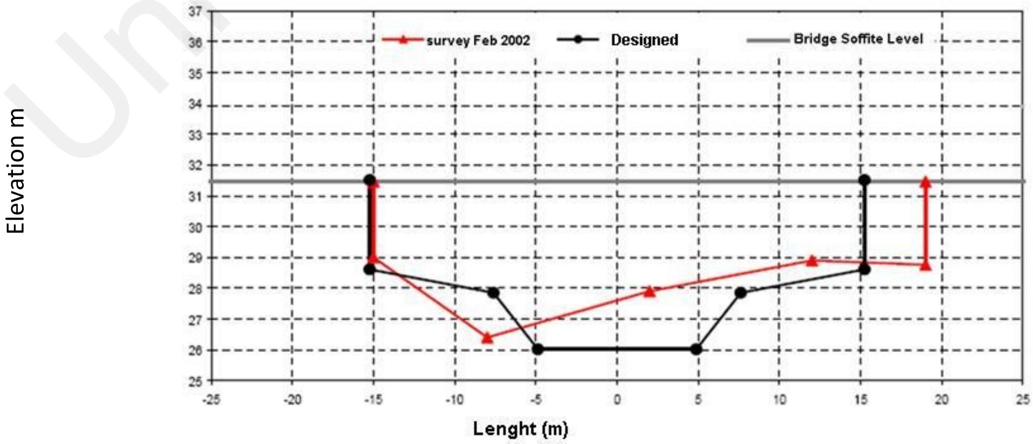

Figure 3.22: Difference between the design and the existing cross-section at water level telemetric station (Code: 3116535) on the Batu River on 15 Feb 2002.

Taken from (DID, 2003b)

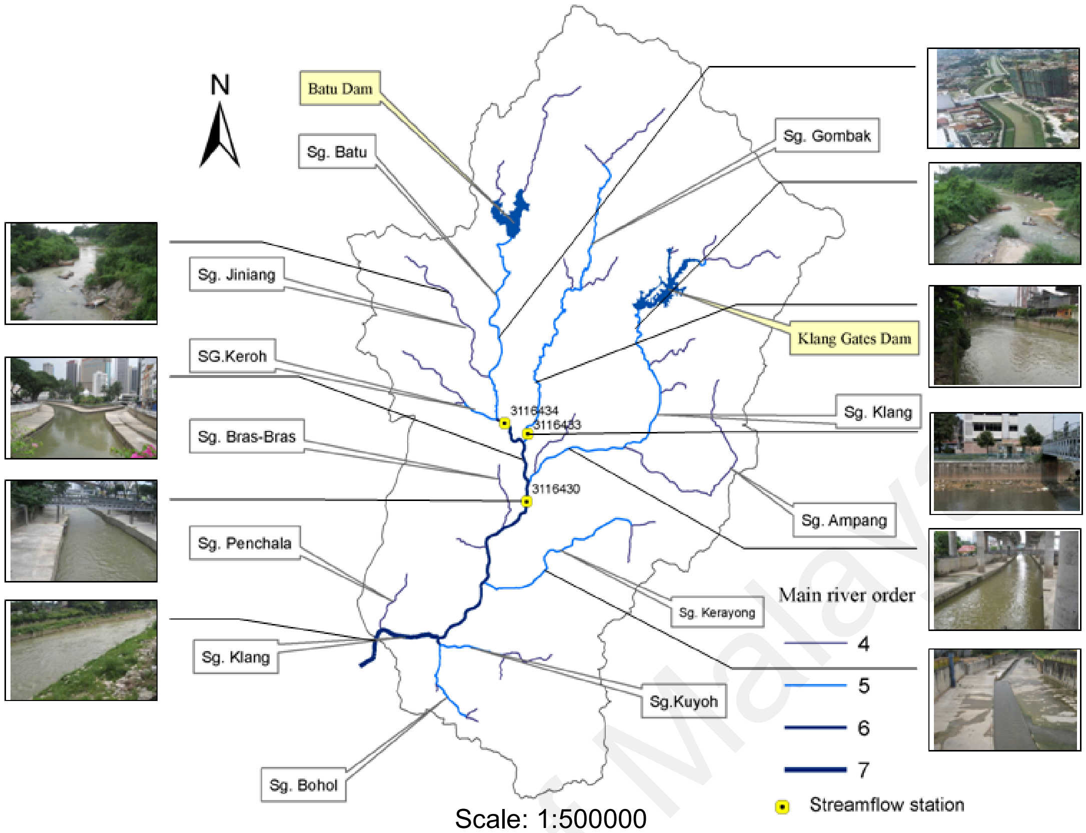

Figure 3.23: Typical cross-section of main channel system at the Klang watershed

3.5.3 Drainage Density

The drainage density (*D*) is the ratio of the total length of streams within a watershed to the total area of the watershed. Values typically range from 1 to 3.5 km/km^2 (McCuen, 1998). Table 3.5 shows drainage ordering of Klang watershed. It was calculated based on the drainage network derived from topo map at scale 1:25000 and according to Strahler method. Drainage density was calculated about 2.5 km/km^2 which represent the high drainage density and therefore, a high value of the drainage density would indicate a relatively high density of streams and thus a rapid storm response and high peak discharge (McCuen, 1998).

Table 3.5: Drainage density and drainage orders

Drainage order		Number segment	Length (km)
1		2975	996.03
2		1394	327.12
3		689	181.89
4		347	105.51
5		166	65.99
6		14	16.61
7		15	5.86
Total length	km		1699
watershed area	km^2		675
Drainage density			2.5

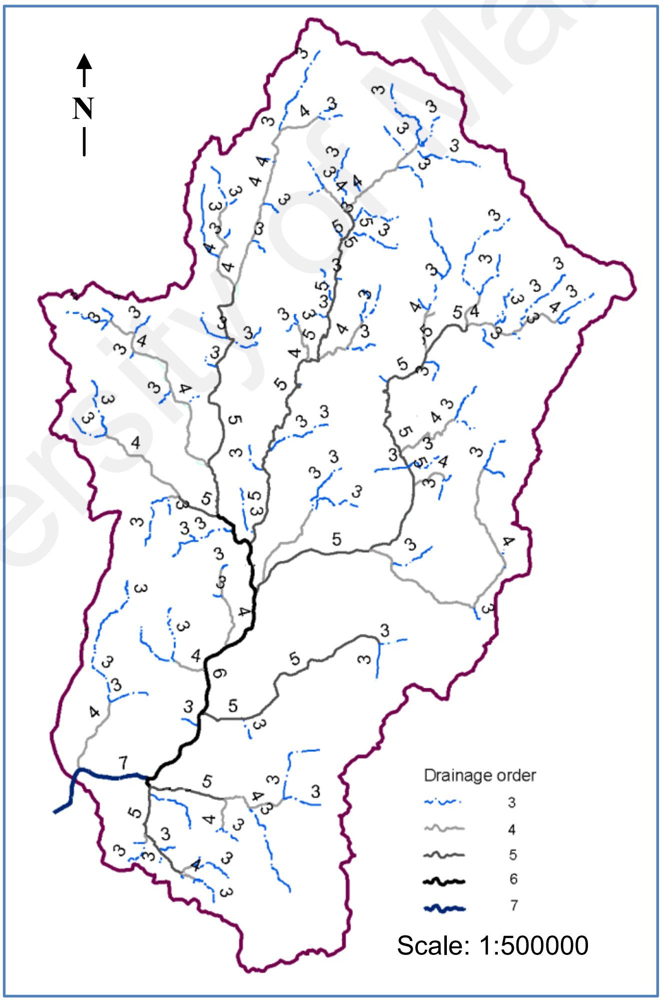

Figure 3.24: Illustration of Strahler order and hierarchical structure of Klang watershed

Chapter IV:

Results and Discussions

4.1 Watershed Modeling

This section focuses on the first and the second objective of the research. The pre-processing and DEM optimization techniques are performed using commonly used algorithm. Watershed boundaries and associated parameters are derived from both Topo-DEM and SRTM-DEM using GIS tools and Techniques. Finally the result of SRTM-derived parameters is compared and evaluated with the reference DEM using statistical measures.

4.2 Creating Topo-DEM

As shown in Figure 4.1 Topo-DEM was obtained by combining contour segments and spot heights, converting to raster map and then performing raster interpolating which gives a digital elevation grid using open source raster-GIS ILWIS 3.4. Considering the contours interval of topography at scale of 1:25000, a cell size of 30 m was chosen for the Topo-DEM. To avoid the interpolation error in watershed boundaries, topo map and spot heights was clipped using 500 m buffer on watershed boundary.

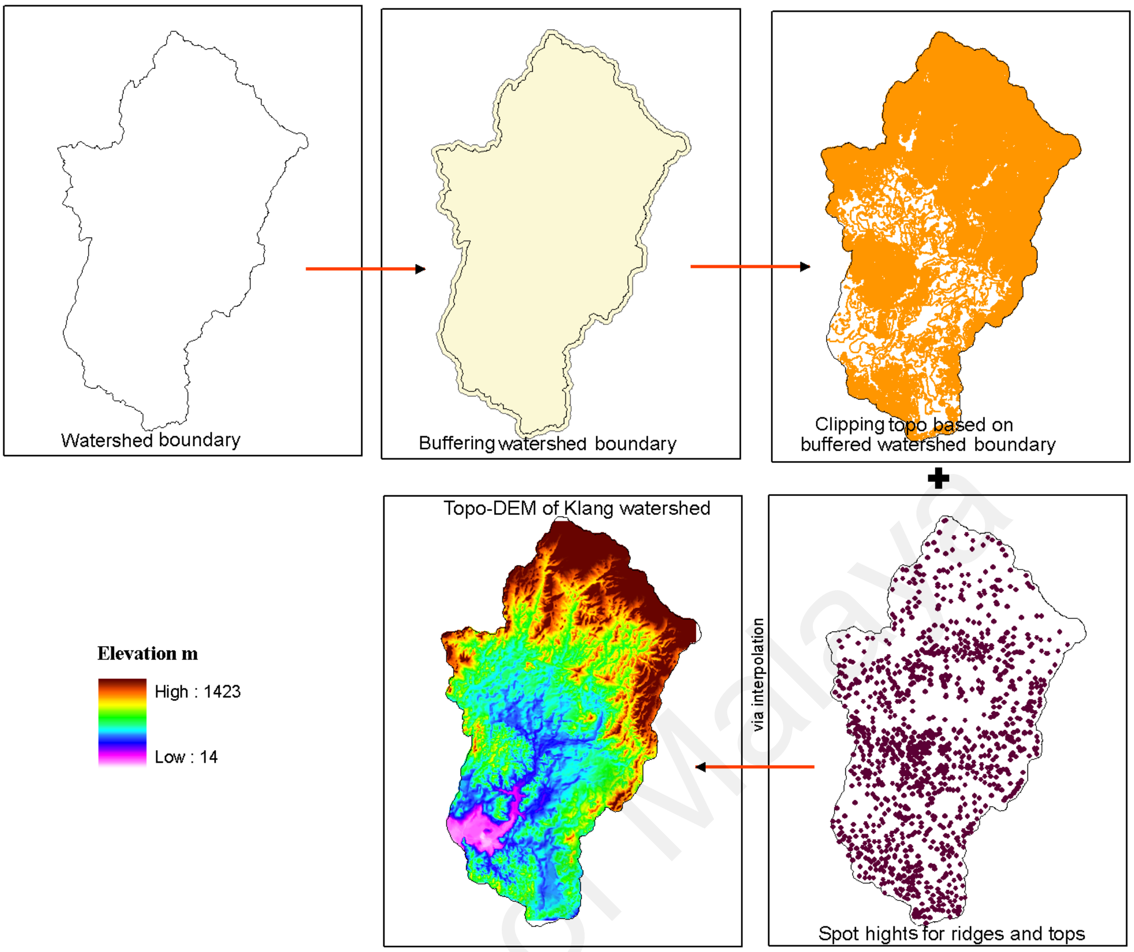

Figure 4.1: Illustration of Topo-DEM processing from topo maps and spot heights

4.2.1 Topo-DEM Smoothing

Smoothing is investigated on original 30 m Topo-DEM, by Appling 3×3 roving window that replace the center cell with arithmetic average of all cells in the roving window using ILWIS 3.4. As shown in Figure 4.2, by performing average filter, elevation at the bottom of valleys (blue area) is increased whereas; elevation is decreased in ridges (red areas). It is also observed that changes in pixel values are uniformly arranged in smoothed DEM and jagged cumulative curve is converted to the smooth and starched curve. Moreover, in this particular area, mean elevation reduces from 662 m to 661m; standard deviation reduces from 46 to 41; minimum elevation increases from 580 to 590 and maximum elevation reduces from 750 m to 749 m.

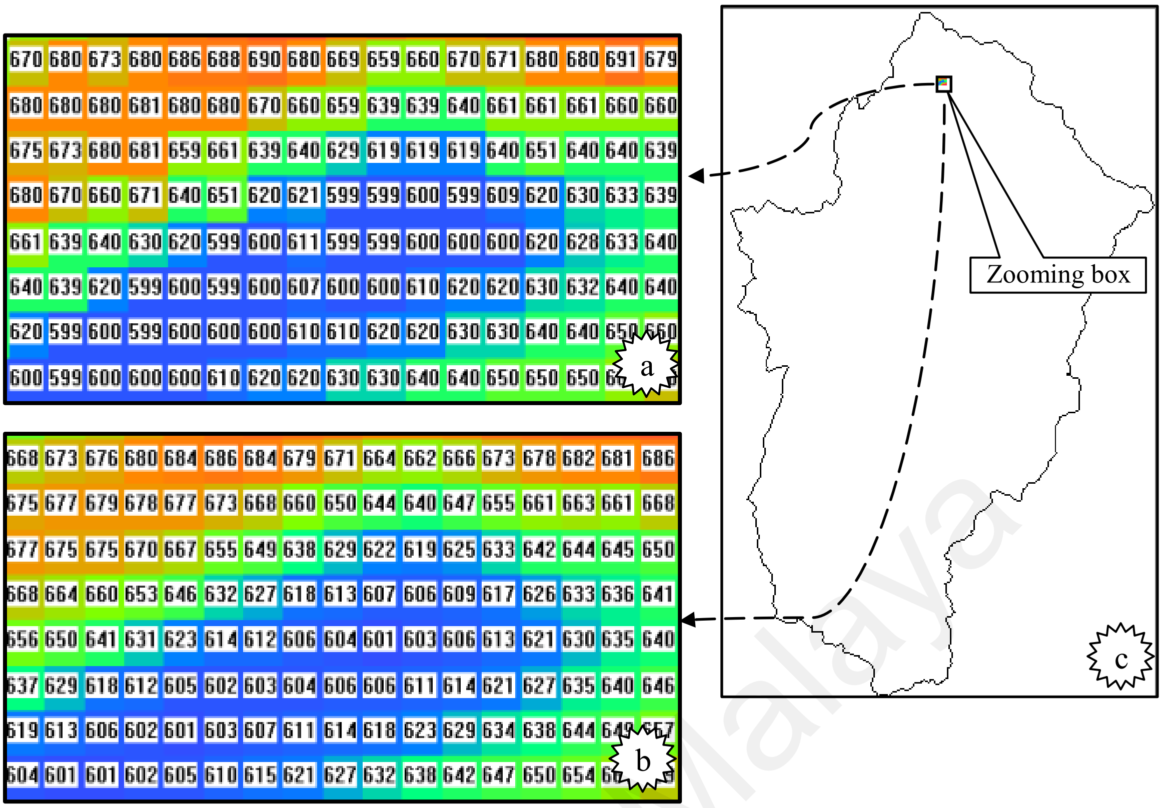

Figure 4.2: Topo-DEM Smoothing and its effect on the elevation of watershed. (a) Original DEM before smoothing, (b) Smoothed DEM, (c) Zooming box

As shown in Figure 4.3 and 4.4, smoothing operation can recondition the undulated terrain surfaces. By smoothing elevation values are expanded internally and therefore the numbers of elevation classes are increased.

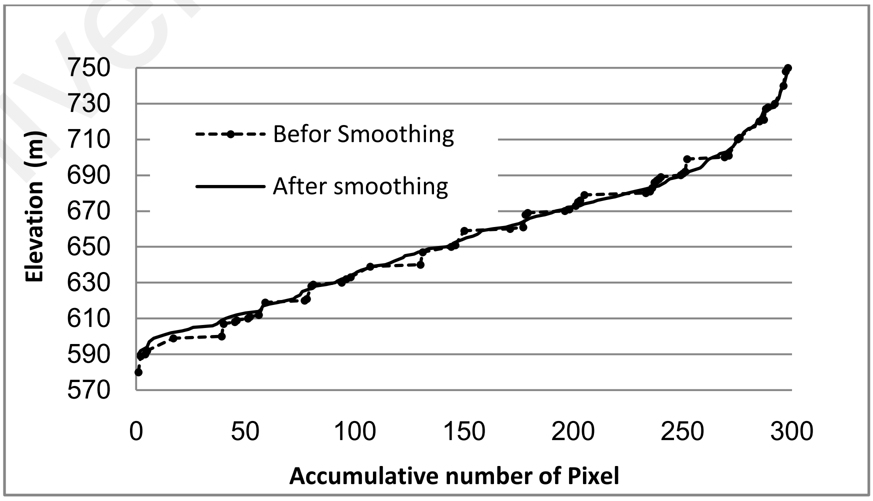

Figure 4.3: Smoothing effect on elevation magnitude of DEM.

As evident in Figure 4.4, before smoothing Topo-DEM, elevation values over the investigated box (see Figure 4.2) fall in 59 classes. But after smoothing elevation are stretched in 120 classes.

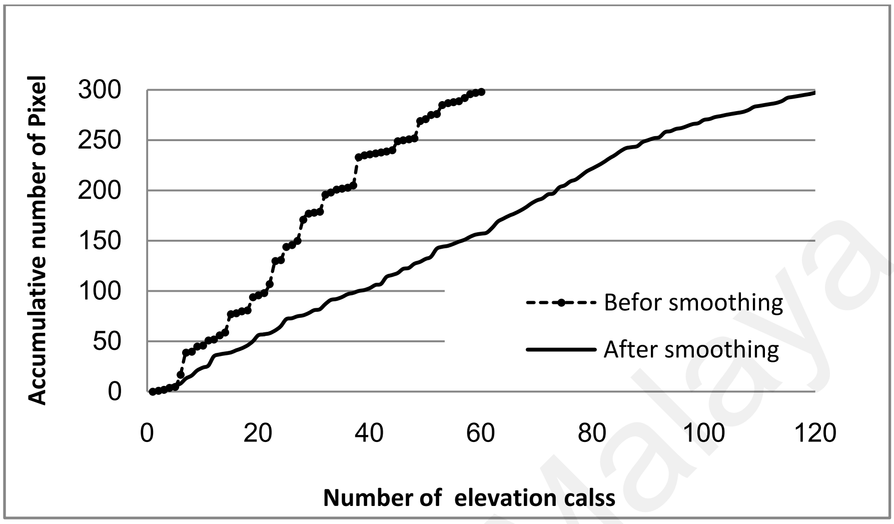

Figure 4.4: Smoothing effect on number of elevation classes of DEM.

4.2.2 Filling depressions / sinks

The depressionless DEM was created by filling the depressions and pits by using LIWIS3.4. The operation has shown for small window of study area in Figure 4.5.

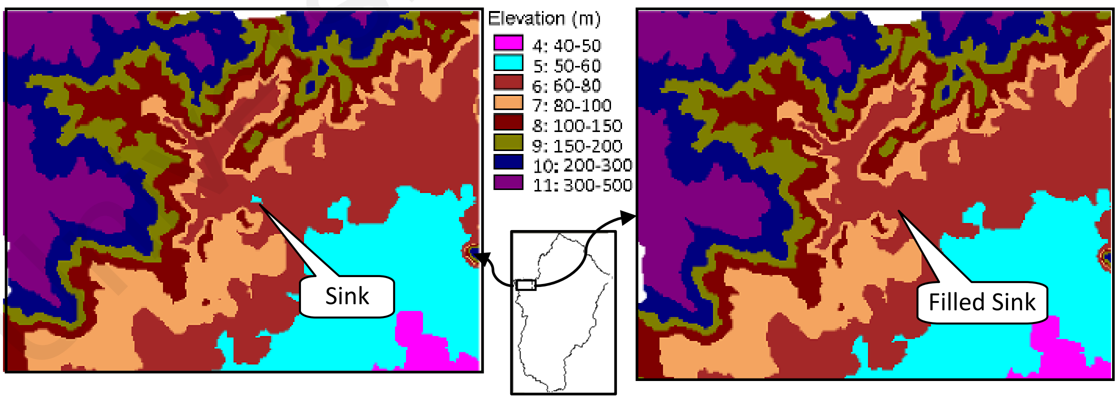

Figure 4.5: Planimetric view of sink in Topo-DEM (left) and sink-free Topo-DEM (right)

4.2.3 Topo-DEM reconditioning

DEM reconditioning was performed using AGREE DEM algorithm by using LIWIS3.4 as illustrated for small window of study area in Figure 4.6.

Buffer distance for each segment of drainage network was estimated by Google earth imagery and smooth drop and sharp drop were estimated based on the field observation. It is noted that the same tools that we employed in ILWIS 3.4; are available in GeoHMS.

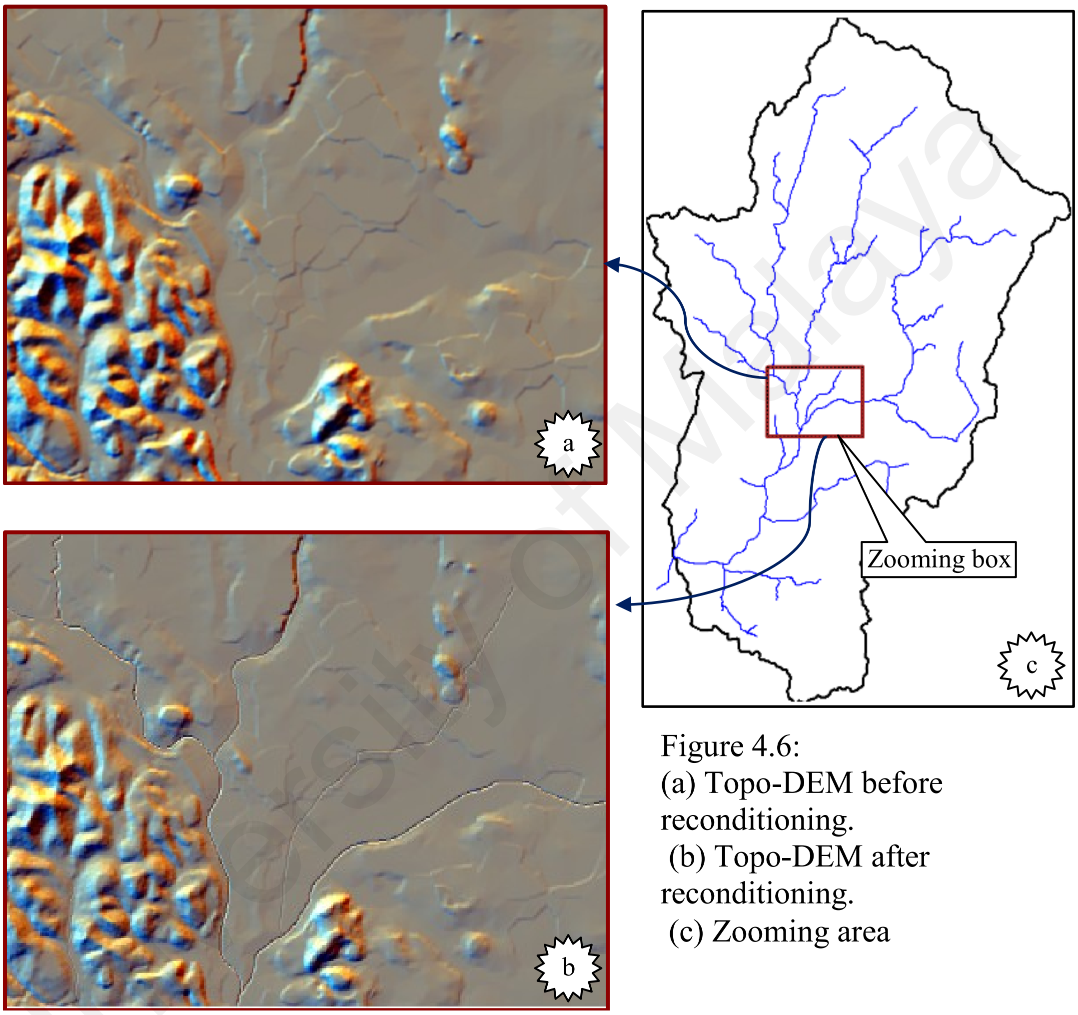

Figure 4.6:
(a) Topo-DEM before reconditioning.
(b) Topo-DEM after reconditioning.
(c) Zooming area

However DEM reconditioning operation does not allow application of the AGREE algorithm by attribute table of stream network. The optimized DEM is called AGREE DEM or HydroDEM. Based on my experience and considering the behavior of DEM optimization operations, it is better to perform smoothing, filling sinks and reconditioning respectively.

4.3 Watershed segmentation and parameterization

Watershed segmentation and parameterization includes several steps using HEC-GeoHMS.

4.3.1 Automated delineating watershed boundaries

Watershed boundaries were delineated based on flow direction and flow accumulation map derived from DEM. ILWIS 3.4 was used to demonstrate the implementation of D8 algorithm for generating flow direction/accumulation map of Klang watershed as illustrated in Figure 4.7. However GeoHMS is used as main tools in watershed delineation.

4.3.2 Flow direction map

Flow direction of Klang watershed was created based on D8 algorithm using GeoHMS. Flow direction map have demonstrated for small window in Figure 4.7b.

4.3.3 Flow accumulation map

Flow accumulation map of Klang watershed was derived from flow direction map as showed for small window in Figure 4.7c.

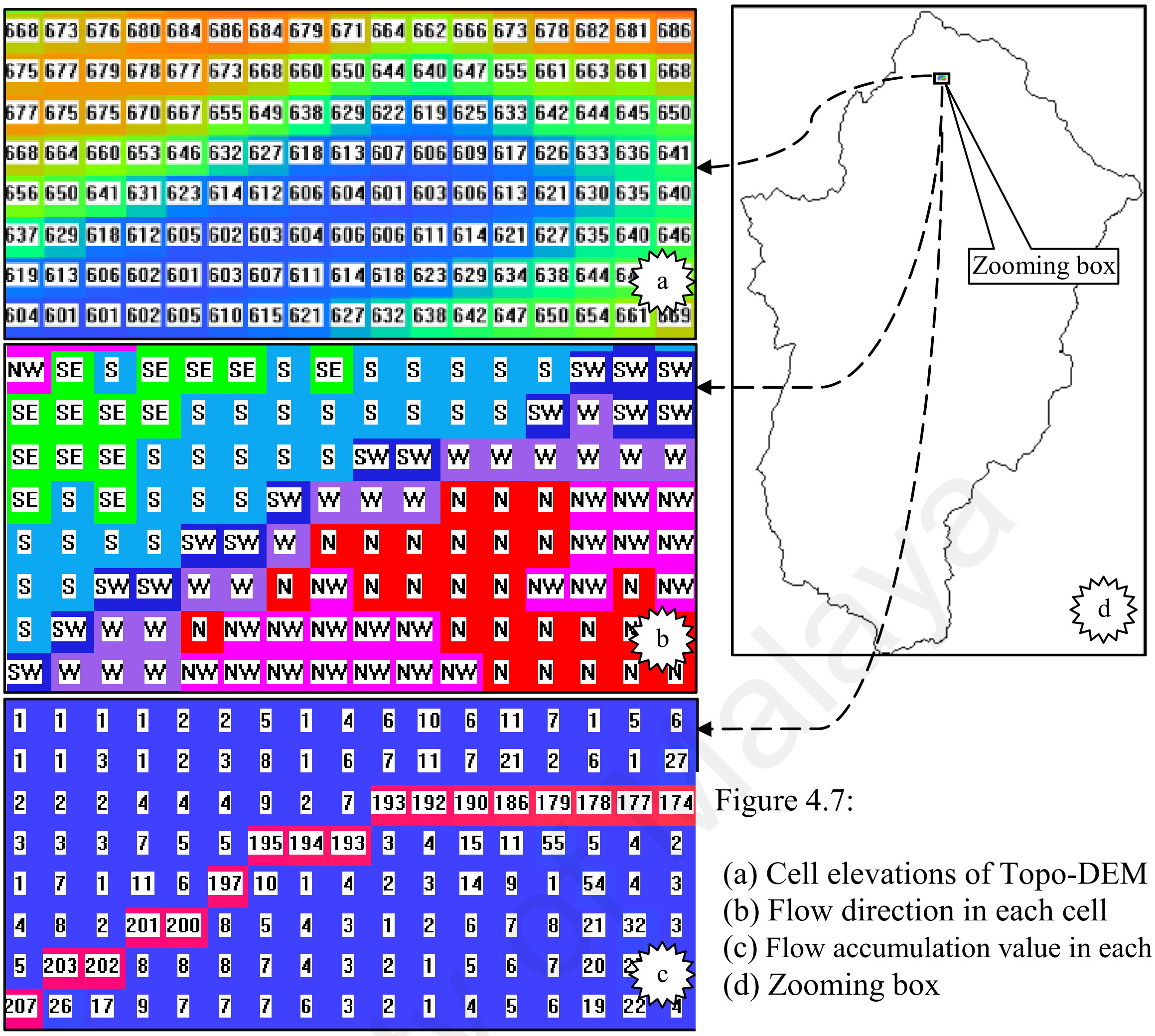

Figure 4.7:

(a) Cell elevations of Topo-DEM
(b) Flow direction in each cell
(c) Flow accumulation value in each cell
(d) Zooming box

4.3.4 Selection of threshold for the stream initiation

Based on previous experiences the GeoHMS model was set for the 8 km^2 (about 1% of entire watershed area) in the first run. Grid cells showing the stream network defined by 8 km^2 threshold value, is presented in Figure 4.8.

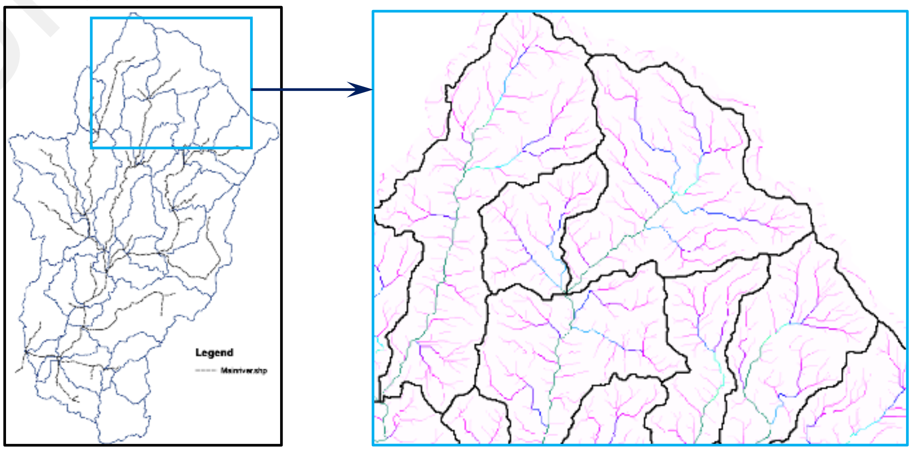

Figure 4.8: Drainage network derived from Topo-DEM defined by 8 km^2 threshold.

4.3.5 Watershed polygon processing

Sub-watersheds were delineated for every stream segment. Watershed delineator in GeoHMS generated 43 sub-watersheds. There are some stream flow stations (SFS) and dams in Klang watershed that were considered as control points for watershed delineation. In addition, some delineated sub-watersheds are too small and some of them are too big. Therefore sub-watersheds modification is performed to adjust the size of watershed.

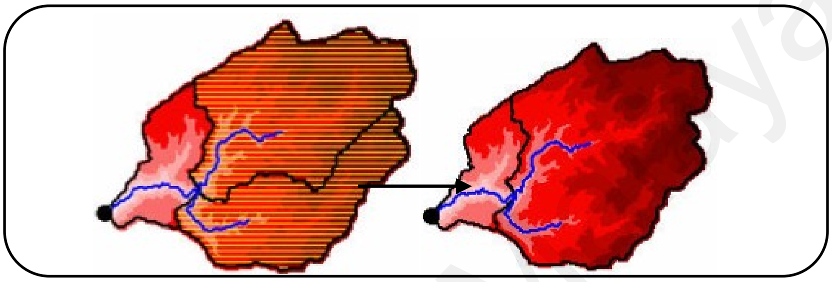

Figure 4.9: Selecting sub-watershed (left) and merging result (right)

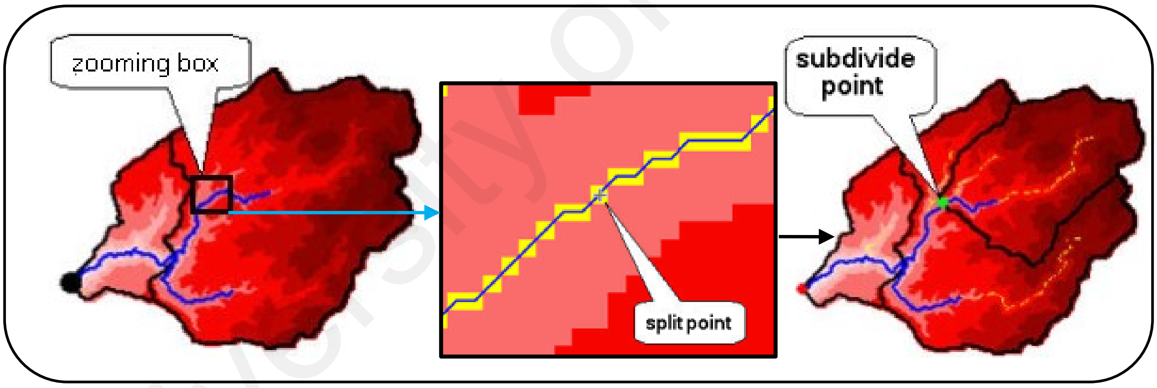

Figure 4.10: Zooming on point of interest to subdivide (left) and splitting result (right)

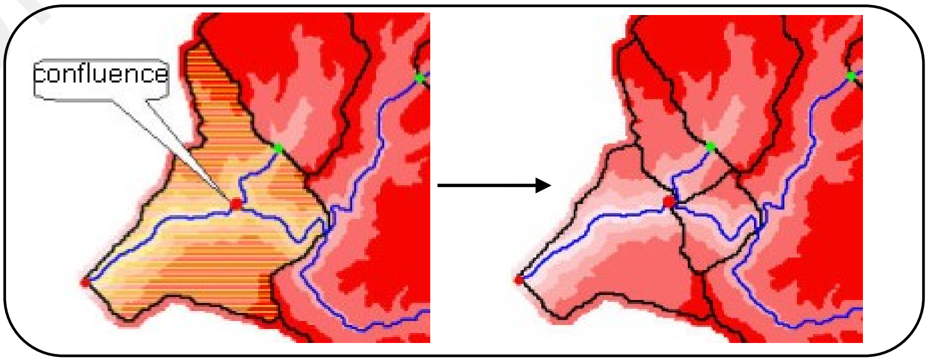

Figure 4.11: Selecting sub-watershed to split at confluence (left) and splitting result of watershed at confluence (right)

Modification of watershed delineations is typically subjected to the land use, location of existing hydraulic structures etc. As results, small sub-basins are merged or larger sub-basins are split. Typical watershed processing that utilized in GeoHMS is illustrated in Figure 4.9, 4.10 and 4.11. Sub-watershed delineation may also be accomplished through batch processing; this requires a point layer that contains the desired outlet locations. Fourteen points including stream flow stations and reservoirs employed in batch processing (See Table 4.1). Some points were generated by GeoHMS and some others were imported from existing point layers (such as stream flow stations). Figure 4.12 illustrate sub-watershed boundaries before and after modifications.

Table 4.1: The RSO coordinates for selected control points in Klang watershed

Location	X	Y	Location	X	Y
Batu Dam	410178	362092	Kwang seng WLS	413398	350274
Gombak (1)	415052	363557	Sentul SFS	409892	351671
Gombak (2)	413326	359084	TunRazak WLS	411396	348747
Klang Gate Dam	417347	357973	Suliman SFS	411161	347314
Gombak inlet Diversion	412740	356976	Sg.Midah	410929	338405
Gombak outlet Diversion	409555	356566	Kerayung	414430	345271
Jinjjan SFS	407288	357872	Ampang	421780	348306

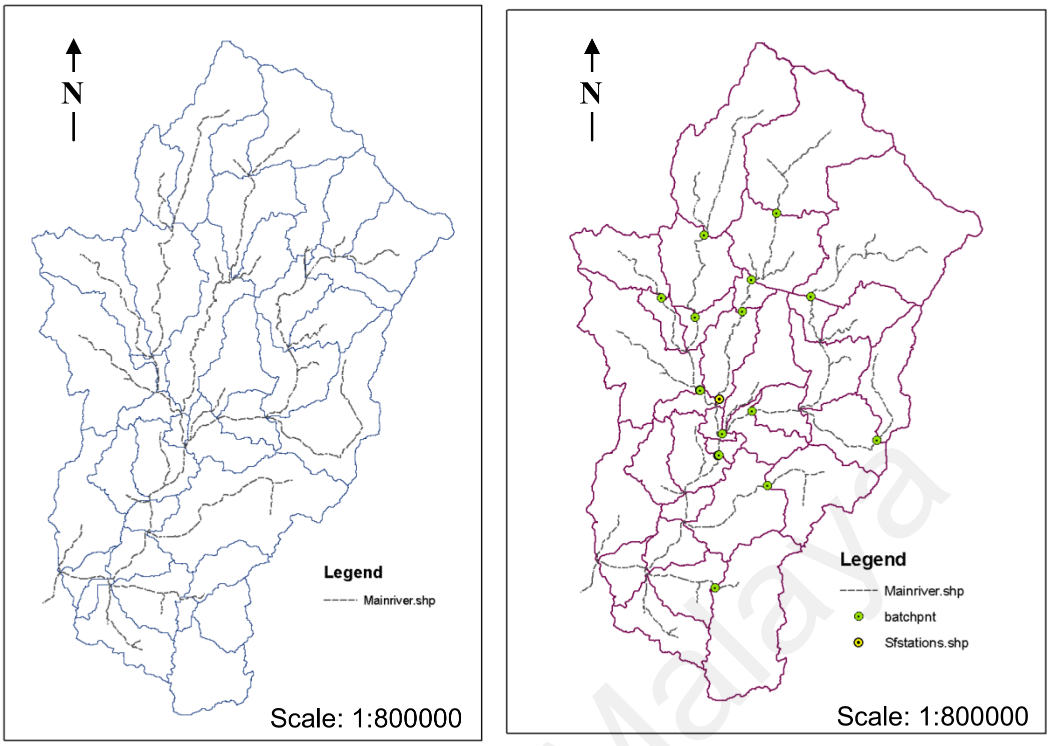

Figure 4.12: Primary delineated sub-basins boundary before batch point processing (left) and after batch point processing and merging and splitting sub-basins (right)

Final modifications on sub-watersheds that delineated by Topo-DEM reduces to 33 sub-watersheds (see Figure 4.13).

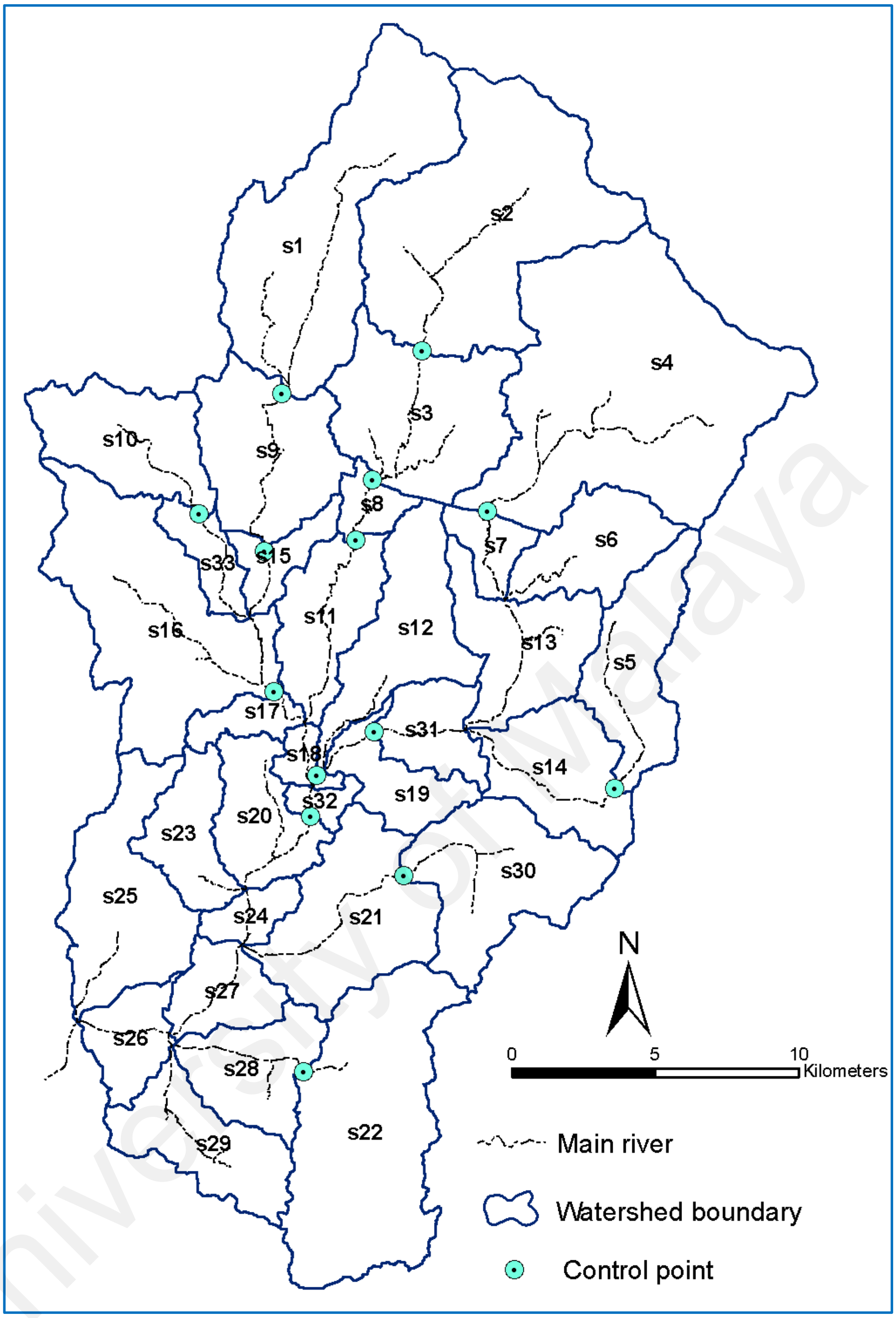

Figure 4.13: Sub-watershed boundaries derived from Topo-DEM

4.3.6 Watershed parameterization with Topo-DEM

A database was compiled within a GIS context for the Klang watershed. Several physiographic parameters systematically were derived for each sub-watershed by using GIS processor of GeoHMS. Investigated DEM-derived parameters are listed in Table 4.2.

4.3.7 Aggregating Curve Numbers by sub-watersheds

Once the watersheds were delineated, the different model parameters needed to be grouped and averaged based on the sub-watersheds. SCS-CN map of Klang watershed have been already generated. Distributed CN map were averaged based on sub-watershed boundaries. The ILWIS's Cross operation was employed to generate sub-watershed CN map. The Cross operation performs an overlay of sub-watershed map with CN map. These combinations give an output cross map and a cross table. As shown in Figure 4.14, by aggregating the CN values into sub-watersheds, a composite CN are calculated for sub-watersheds using Eq. 4.1:

$$\boldsymbol{CN_{sub}} = \frac{\sum \boldsymbol{A_i CN_i}}{\sum \boldsymbol{A_i}} \qquad \text{Eq. 4.1}$$

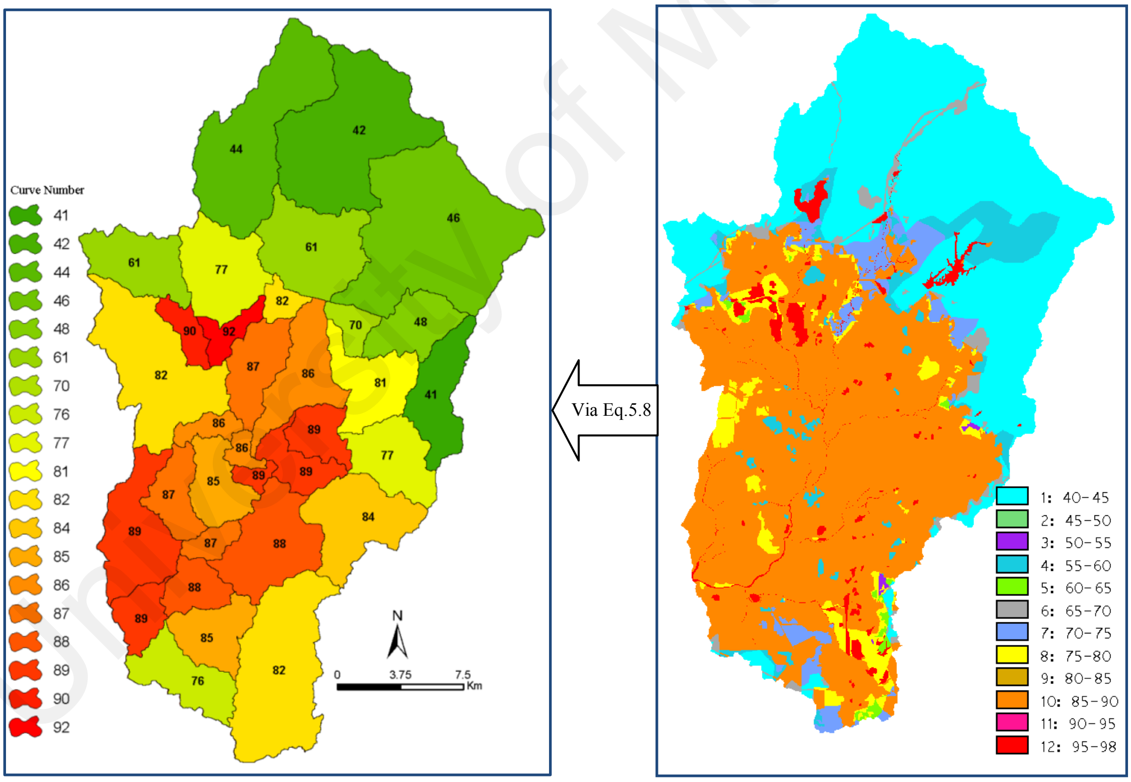

Figure 4.14: Generating sub watershed CN map (left) from the gridded-CN map (right)

Where: CN_{sub} is weighted average CN for sub-watershed; CN_i denotes the CN value and corresponding area A_i inside the specified sub-watershed.

Table 4.2: Sub-watershed parameters derived from Topo-DEM

SUB	P	WS	RS	LFL	LT	WA	ME	CN
	km	%	m:m	km	hr	Km^2	m	
s1	51.28	37.15	0.043	16.02	3.23	50.47	442.4	44
s2	50.88	41.78	0.076	14.96	3.04	56.74	509.7	42
s3	35.06	27.39	0.041	10.23	1.70	29.26	181.2	61
s4	59.26	33.96	0.037	15.65	3.15	75.65	368.3	46
s5	32.90	40.14	0.037	12.44	2.75	19.46	313.6	41
s6	26.60	31.66	0.041	10.11	2.18	15.20	212.3	48
s7	14.40	26.05	0.032	5.09	0.79	5.85	122.9	70
s8	13.18	14.71	0.018	4.16	0.63	4.56	80.5	82
s9	30.14	17.20	0.008	10.06	1.38	24.18	105.1	77
s10	29.66	27.55	0.020	9.37	1.58	19.69	180.6	61
s11	27.28	2.14	0.002	9.70	2.73	16.34	47.0	87
s12	36.44	9.32	0.004	12.70	1.68	21.23	70.3	86
s13	32.24	22.32	0.003	10.21	1.08	19.32	110.4	81
s14	28.30	18.04	0.007	8.67	1.19	18.91	105.2	77
s15	20.48	2.35	0.005	6.92	1.62	6.38	50.8	92
s16	51.82	10.61	0.016	13.74	1.93	43.29	86.9	82
s17	17.06	16.06	0.008	6.62	0.76	5.06	68.2	86
s18	12.42	11.71	0.006	2.98	0.47	3.25	50.7	86
s19	27.42	2.11	0.003	6.78	1.91	10.33	43.6	89
s20	26.26	13.02	0.005	7.77	1.00	14.12	58.8	85
s21	35.04	4.58	0.004	11.23	2.02	27.40	50.2	87
s22	48.46	7.51	0.004	10.98	1.91	47.49	65.0	87
s23	24.36	14.70	0.010	7.63	0.86	11.94	68.5	88
s24	13.60	8.60	0.010	4.13	0.69	5.11	46.6	89
s25	38.76	5.39	0.005	12.32	1.93	25.97	48.3	89
s26	20.68	3.66	0.008	6.03	1.32	9.52	29.0	88
s27	19.02	7.53	0.005	7.08	1.09	10.02	39.8	82
s28	25.48	9.24	0.006	7.65	1.17	15.29	52.3	85
s29	31.22	18.66	0.006	9.48	1.30	17.62	67.0	76
s30	35.48	9.61	0.010	9.75	1.44	26.57	88.8	84
s31	21.42	4.08	0.004	6.16	1.27	10.17	49.5	89
s32	11.46	7.57	0.008	3.45	0.59	2.84	48.9	89
s33	18.72	2.51	0.005	6.70	1.67	6.42	54.8	90
Min	11.46	2.11	0.002	2.98	0.47	2.84	28.95	41
Max	59.26	41.78	0.076	16.02	3.23	75.65	509.7	92
Mean	29.30	15.42	0.015	8.99	1.58	20.47	118.7	77
Std	12.46	11.75	0.017	3.44	0.75	17.05	120.17	16
Sum						675.65		

P : Perimeter
WS : Watershed slope
RS : Slope of main channel
LFL : Longest flow length
LT : Lag time
WA : Watershed area
ME : Mean elevation
CN : SCS curve number

It is noted that CN values are not the direct derivatives of Topo- DEM. However, they can be considered as indirect products of DEMs. Because watershed boundaries effects on CN values when it is weighted by area. The Delineated sub-watersheds from Topo-DEM were used to lump the CN for each sub-basins.

4.3.7.1 Urban impervious area

An impervious area is considered connected if runoff from it flows directly into the drainage system. It is also considered connected if runoff from it occurs as concentrated shallow flow that runs over a pervious area and then into the drainage system. Urban CN's taken from references, were developed for typical land use relationships based on specific assumed percentages of impervious area. One of the best choices for estimation of impervious areas is aggregation of building blocks that mapped on digital topo at scale 1:25000 (see Figure 4.15). Aggregation tool combines building blocks within a specified distance to each other into new polygons. Aggregation is necessary because building blocks are usually surrounded by access roads, streets and parking areas which are impervious. To calculate the percentage of impervious areas in each sub-watershed, new polygon map (Figure 4.15b) was crossed with the watershed boundaries derived from Topo/SRTM by using GIS tools. The Cross operation performs an overlay of two raster maps. Pixels on the same positions in both maps are compared and the occurring combinations are stored in a cross table. Table 4.3 demonstrates impervious area (IA) in each sub-watershed resultant from aggregation and cross operations. It is noted that, building blocks derived from topo maps at scale 1:25000. According to JUPEM, Topo sheets at scale of 1:25000 have been upgraded during the 1984-1998. Thus, due to rapid development of Klang watershed, some uncertainty is expected in representing the hydrologic conditions of urban area for 2002 which is the target year for selected rainfall events.

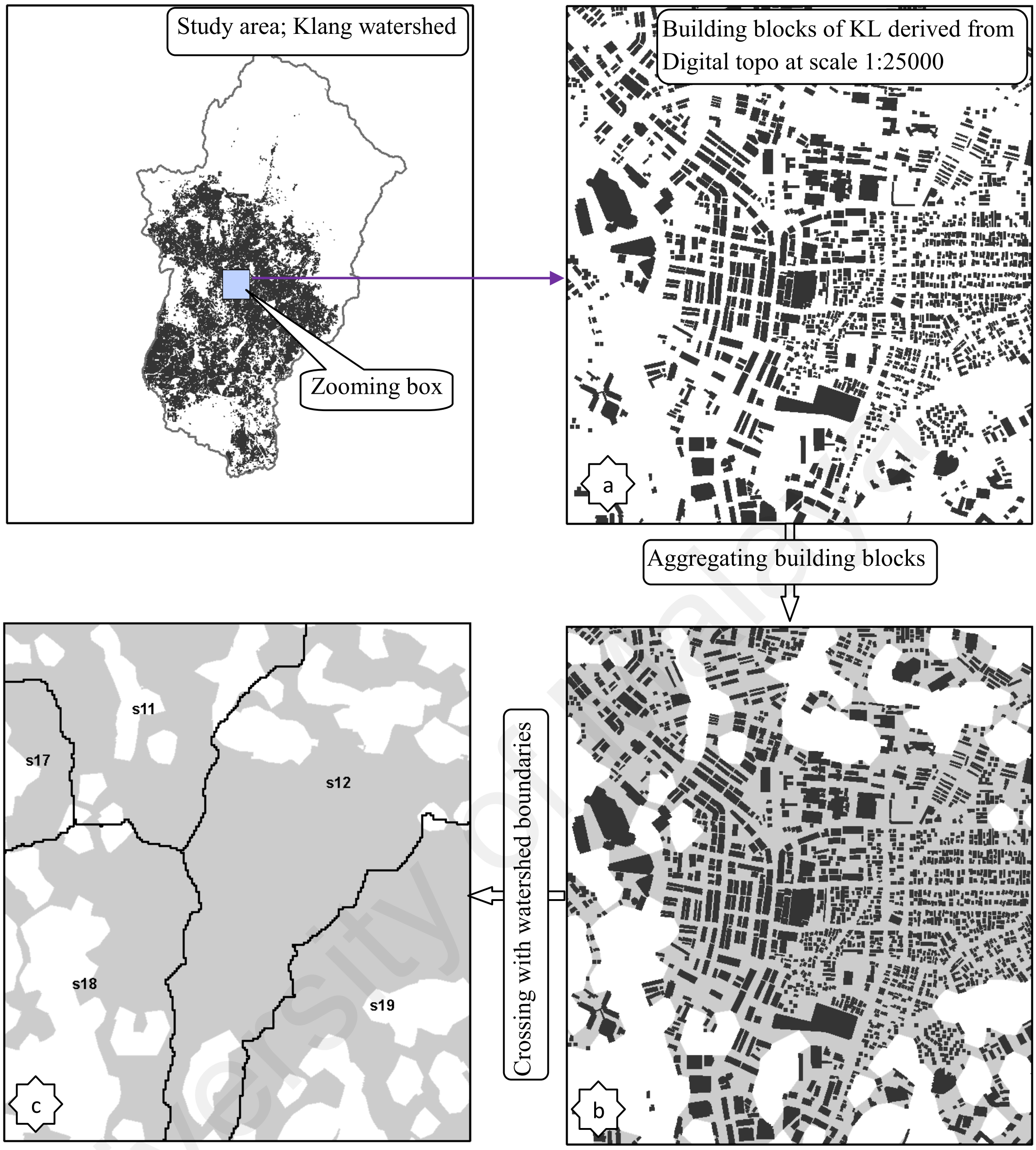

Figure 4.15: Workflow of calculating impervious area for Klang watershed. (a) Building blocks located in zooming box (b) Aggregated building blocks into new polygons and overlying non-aggregated building blocks on it. (c) Crossing aggregated building blocks with the watershed boundaries.

Table 4.3: Impervious area of sub-watershed derived from Topo-DEM and SRTM-DEM

SUB	Area	Impervious Area $_{TD}$		Impervious Area $_{SD}$	
	km^2	km^2	%	km^2	%
s1	50.47	0.01	0.03	0.01	0.03
s2	56.74	0.15	0.27	0.15	0.27
s3	29.26	0.88	3.02	0.89	2.89
s4	75.65	0.00	0.00	0.00	0.00
s5	19.46	0.00	0.00	0.00	0.02
s6	15.20	0.48	3.16	0.46	2.87
s7	5.85	1.03	17.67	1.00	18.18
s8	4.56	1.77	38.77	1.37	35.71
s9	24.18	8.53	35.27	5.37	31.65
s10	19.69	2.39	12.12	2.20	11.10
s11	16.34	11.16	68.33	15.30	57.56
s12	21.23	9.72	45.80	6.31	54.15
s13	19.32	6.05	31.33	6.20	30.92
s14	18.91	7.55	39.93	5.79	33.73
s15	6.38	1.85	28.97	1.86	27.65
s16	43.29	17.88	41.29	17.16	41.17
s17	5.06	1.75	34.52	1.97	35.91
s18	3.25	1.48	45.54	1.95	54.00
s19	10.33	6.56	63.56	5.66	67.60
s20	14.12	5.91	41.87	6.05	42.07
s21	27.40	13.47	49.15	19.33	54.23
s22	47.49	13.44	28.30	13.72	28.67
s23	11.94	4.29	35.93	3.87	35.18
s24	5.11	2.40	46.96	2.49	46.79
s25	25.97	16.33	62.87	14.66	56.45
s26	9.52	5.00	52.51	8.86	62.31
s27	10.02	6.50	64.86	5.69	63.59
s28	15.29	2.78	18.20	2.92	19.16
s29	17.62	0.84	4.76	0.92	5.25
s30	26.57	14.97	56.33	15.07	54.22
s31	10.17	7.91	77.75	6.13	69.48
s32	2.84	1.73	60.91	*	*
s33	6.42	2.79	43.41	5.38	44.08

TD: Topo-DEM, SD: SRTM-DEM

4.4 SRTM-DEM processing

Step1- projection conversion

SRTM elevation data is provided in geographic projection (latitude/longitude) referenced to WGS84 horizontal datum. Therefore, SRTM elevation data transformed from geographic projection into RSO projection by using GIS conversion tools.

Step2: Inspecting void and pits areas

To identify the void areas we used undefined-majority filter (MAJUNDEF) which is an image processing filter in ILWIS 3.4. The MAJUNDEF works in a 3x3 window. It considers 8 neighbors around an unclassified pixel and assigns the predominant class name of the neighbors to the unclassified pixel in the output map. This filter applied to fill the undefined pixel in SRTM elevation data. But, it is noted that this filter can only be applied when void areas contains few pixels. This approach dose not advises for the large void areas. To identify the void areas of SRTM elevation data, two steps were performed. First, undefined-majority filter was applied to the raw SRTM elevation data. If void pixels are exist in the raw data, then, new values are added to the output map. In step 2, new added values to the raw data were identified by simple map calculation as follows:

VFSRTM90= Map Filter (SRTM90, MAJUNDEF.fil, Color)
Undefinedpix=SRTM90- VFSRTM90

The second operation assigned pixel values of zero for *Undefinedpix* map which means no void areas are exist on the raw SRTM elevation dataset of Klang watershed. The SRTM processing was followed by filling pits and holes on SRTM-DEM. Raw SRTM elevation data contain values range from -22 to 1410 meters. From the Topo-DEM, it is already known that elevation values are bigger than 0.0 in Klang watersheds. Thus, pixels with negative values must be modified. ILWIS map calculation was used to find the negative values representing holes or pits by employing the following spatial operator on raw SRTM90:

SRTM90-ziro=iff (SRTM90<0.0, 0.0, SRTM90)

This operation on raw SRTM90 substitutes all pixels having negative values with 0.0. Seven pixels found with negative value which assigned by 0.0 (see Figure 4.16).

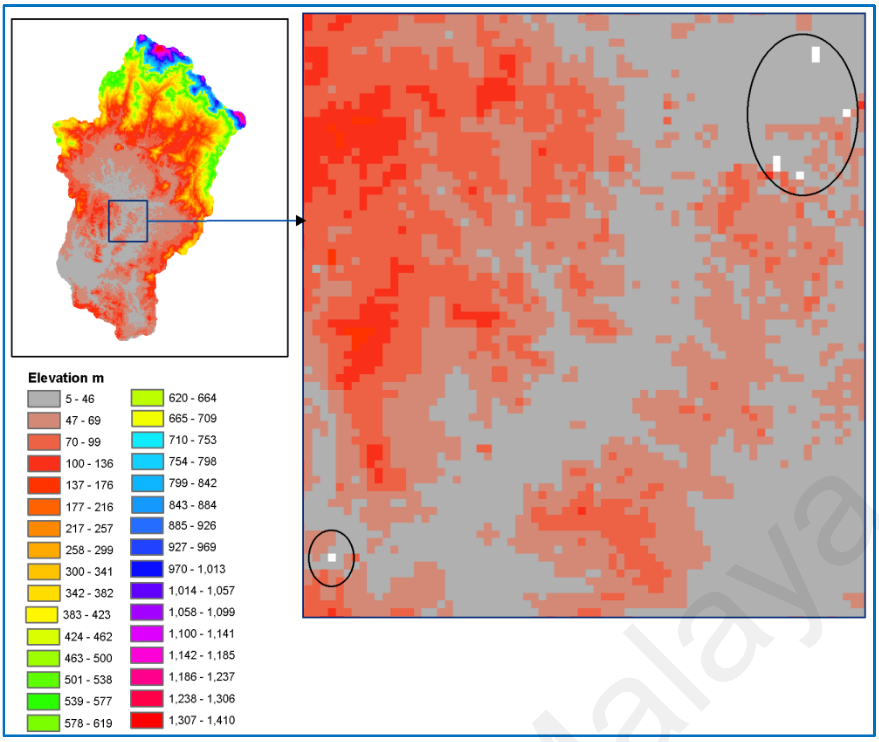

Figure 4.16: Pixels with negative values

Then, identified zero values were filled with majority of its neighborhoods by zero-majority filter (MAJZERO) using ILWIS 3.4.

SRTM90-modified = Map Filter (SRTM90-ziro, MAJUNDEF.fil, Color)

The MAJZERO filter only assigns the predominant value when the central pixel has value 0.0. If the central pixel in the input map does not have value 0.0, the value remains the same in the output map. This is a good advantage of MAJZERO filter that does not affect the value of other cells and reserve the original SRTM data.

Step 3: SRTM resampling

The Topo-DEM has 30 meters resolution; therefore, 90 meters SRTM-DEM was resample to 30 meters resolution. That is made possible to assess the efficiency of the SRTM-DEM derivatives against the Topo-DEM derivatives. To generate SRTM-DEM with 30 meter resolution, the *SRTM90-modified* converted to a points map. Then Spline estimation method was employed to interpolate the SRTM point data into the 30 meter grids. This interpolation did not add any new detail to the original data, but as

Grohmann and Steiner (2008) mentioned, that made it possible to generate coherent surface properties in neighboring pixels.

Step 4: SRTM-DEM optimization

The same optimization techniques that applied to Topo-DEM were employed to optimize the SRTM-DEM. There is one exception that we ignored DEM smoothing for SRTM-DEM. It is because that smoothing operation has already been done by NASA by resampling original SRTM data from 30 meters to 90 meters. Therefore no further smoothing is required. Schematic representation of SRTM-DEM processing is shown in Figure 4.17.

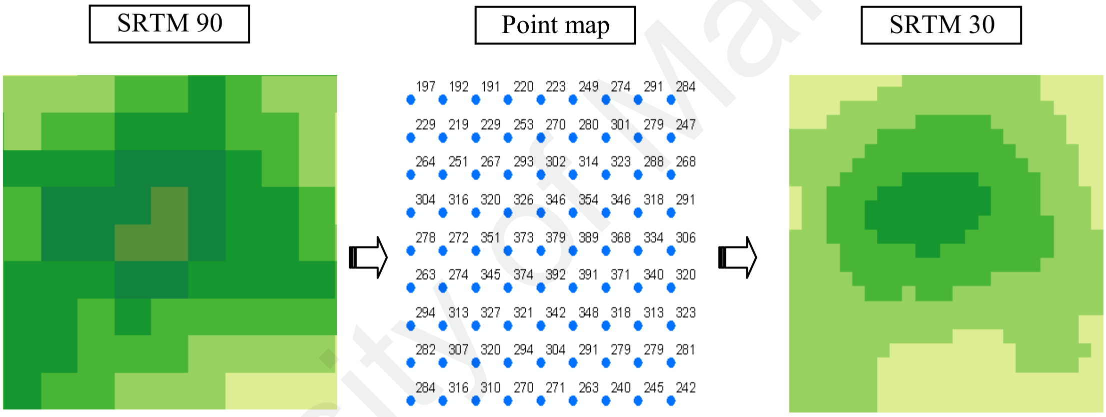

Figure 4.17: Spatial representation of resampling SRTM90 to SRTM30

4.4.1 Watershed delineation and parameterization with SRTM-DEM

Watershed delineation processes were performed to delineate the watershed boundaries from SRTM-DEM by using HEC-GeoHMS. The procedure was similar to one that applied to the Topo-DEM. Sub-watershed delineation was then accomplished through batch processing. The same reference points listened in Table 4.1 employed in batch processing in HEC-GeoHMS.

It is noted that threshold for the stream initiation and the number of control point in batch processing was remained the same as used for Topo-DEM. In this case 45 sub-watersheds were identified. This numbers reduced to 32 when batch processing was performed. Watershed boundaries derived from SRTM-DEM is shown in Figure 4.18 and corresponding sub-watershed parameters are listed in Table 4.4.

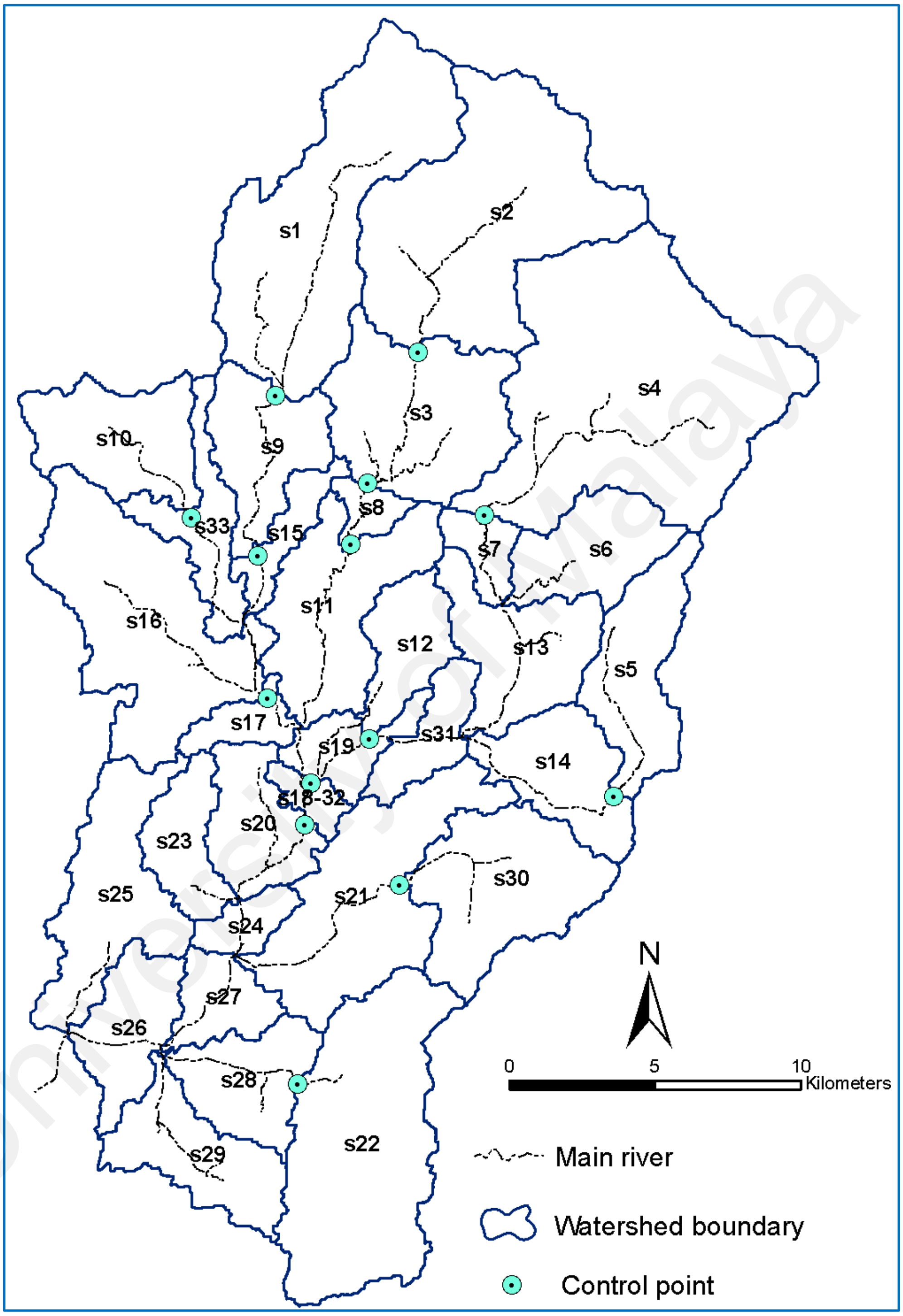

Figure 4.18: Sub-watershed boundaries derived from Topo-DEM

Table 4.4: Sub-watershed parameters derived from SRTM-DEM

SUB	P	WS	RS	LFL	LT	WA	ME	CN
	km	%	m:m	km	hr	Km^2	m	
s1	52.45	31.33	0.048	16.37	3.58	51.82	445.7	44
s2	51.46	33.56	0.078	14.98	3.40	55.74	510.0	42
s3	35.10	20.29	0.046	9.98	1.99	30.65	176.7	60
s4	58.74	27.32	0.040	15.26	3.44	76.13	374.3	46
s5	32.50	28.12	0.038	12.31	3.26	19.46	310.2	41
s6	27.36	23.83	0.046	9.82	2.52	15.88	208.2	47
s7	14.36	20.48	0.032	5.07	0.86	5.51	115.1	71
s8	13.38	12.00	0.026	3.60	0.62	3.83	74.4	82
s9	29.48	14.68	0.013	9.94	1.57	16.97	100.0	75
s10	31.36	23.39	0.024	9.53	1.74	19.77	184.2	61
s11	44.44	5.86	0.005	10.76	1.93	26.58	57.1	85
s12	23.70	5.50	0.004	7.28	1.25	11.65	55.3	89
s13	33.22	17.15	0.004	10.37	1.29	20.06	108.4	80
s14	29.38	17.46	0.010	8.91	1.32	17.17	105.1	75
s15	25.78	8.57	0.008	7.96	1.04	6.72	62.4	90
s16	53.79	10.21	0.006	14.38	2.04	41.69	84.2	82
s17	18.70	9.65	0.010	5.74	0.88	5.50	63.3	86
s18-32	14.48	10.24	0.014	3.36	0.51	3.62	46.8	86
s19	23.69	7.62	0.003	6.36	0.99	8.38	40.6	88
s20	26.48	11.10	0.008	8.18	1.08	14.37	55.3	86
s21	53.26	5.83	0.002	15.29	2.21	35.64	47.0	86
s22	47.13	8.04	0.003	12.85	2.03	47.88	61.9	87
s23	23.88	12.32	0.010	7.28	0.94	10.99	66.7	89
s24	14.70	9.62	0.011	4.22	0.66	5.32	47.2	88
s25	48.06	7.22	0.006	12.86	1.79	25.96	49.6	89
s26	28.96	5.14	0.006	7.54	1.33	14.21	28.6	88
s27	20.68	8.50	0.004	6.23	0.93	8.95	38.9	83
s28	26.10	8.94	0.007	7.72	1.20	15.21	49.4	85
s29	32.48	13.55	0.007	9.43	1.47	17.51	64.5	77
s30	36.30	10.50	0.008	9.67	1.37	27.80	90.9	84
s31	22.46	6.67	0.017	5.70	0.94	8.82	55.1	89
s33	41.78	6.12	0.014	10.51	1.79	12.22	68.6	86
Min	13.38	5.14	0.002	3.36	0.51	3.62	28.6	41
Max	58.74	33.56	0.078	16.37	3.58	76.13	510.0	90
Mean	32.36	13.78	0.017	9.36	1.62	21.31	120.2	76
Std	12.97	8.13	0.018	3.56	0.85	17.22	122.0	16
Sum						681.95		

P : Perimeter
WS : Watershed mean slope
RS : Slope of main channel
LFL : Longest flow length
LT : Lag time
WA : Watershed area
ME : Mean elevation
CN : SCS curve number

4.4.2 Evaluation of DEMs and DEM-derivatives

As mentioned in chapter 1 this research does not focus on the DEM accuracy but it evaluated DEM-derived parameters. Two watershed databases were developed. The first one derived from Topo-DEM and the second one derived from SRTM-DEM. Both databases contain DEM-derived sub-watershed parameters such as perimeter, area, mean elevation, slope, etc. these are the primary data required for flood modeling. Effectiveness of SRTM-DEM in hydrologic modeling can be evaluated in two ways. One way by ignoring the inter comparison of DEM-derived parameters just by running the rainfall-runoff model and see how well observed-flood-runoff is simulated by the model. There are significant uncertainties for rainfall and stream flow measurements that may affect the model prediction which may not be possible to relate it to the DEM-derived parameters. Thus, this approach may not be adequate procedure. The second approach is evaluation of the DEM-derived parameters based on the reference dataset (Topo-DEM derived dataset) and then employing the rainfall-runoff model. The second approach is followed for evaluation of SRTM-DEM and its derived parameters by using commonly used statistical measures.

4.4.3 Comparison of Topo-DEM with SRTM-DEM

The Topo-DEM (left) and SRTM-DEM (right) classified in the same classes as demonstrated in Figure 4.19. It is evident that both DEMs represent almost the same relief for Klang watershed. That is proved by comparing accumulation of watershed area and elevation in Figure 4.20. Visually, there is no significant difference between two DEMs. In terms of slope, there is a significant difference between two DEMs, specifically in low and high slope classes. It is seen that Topo-DEM depicts 13% of watershed with slope less than 5%, but SRTM-DEM cannot depict any area with slope less than 5%.

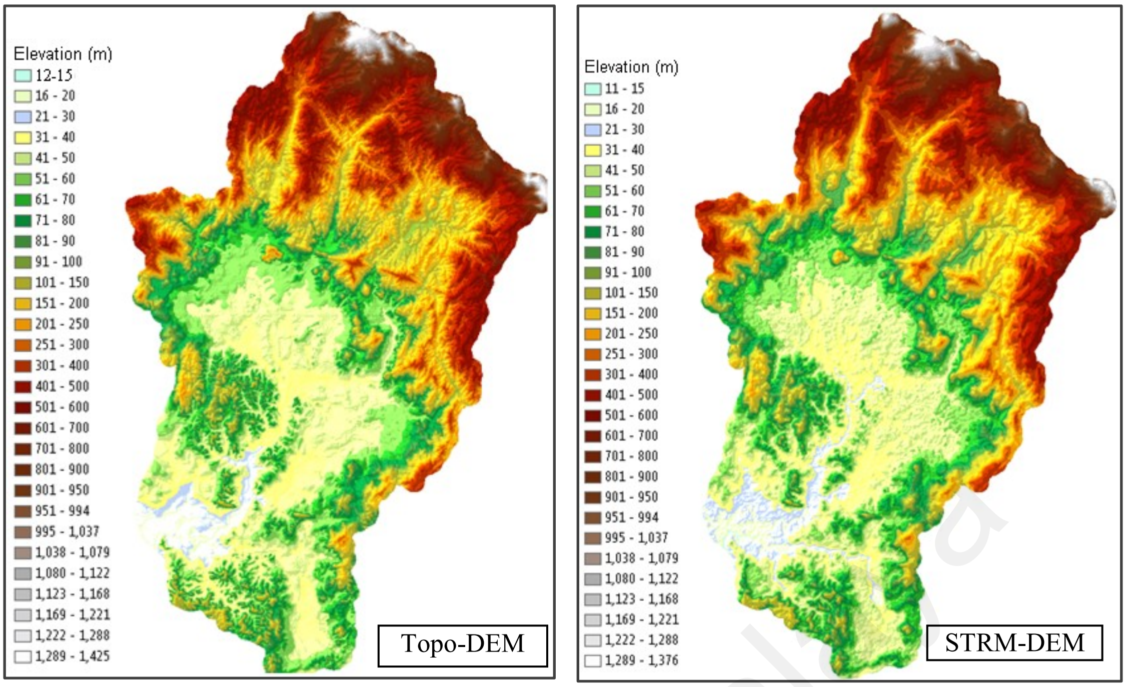

Figure 4.19: Visual comparison of Topo-DEM (left) and SRTM-DEM (right) with the same elevation classes.

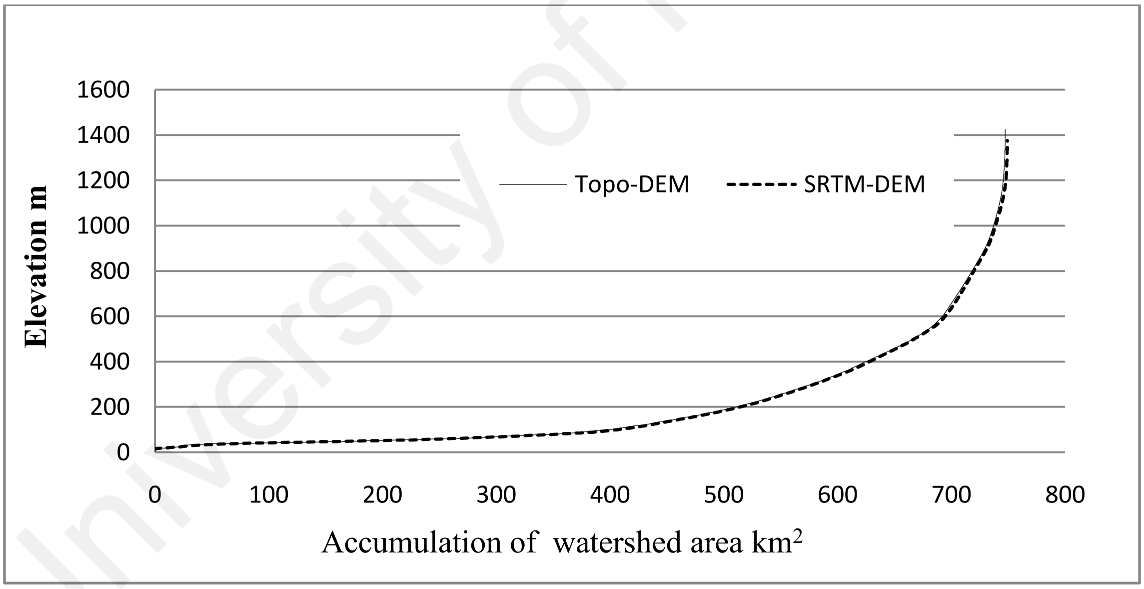

Figure 4.20: Comparing accumulation of watershed area vs. elevation derived from Topo-DEM and SRTM-DEM.

The same case is observed for the slope range from 40 to 42%. However, as shown in Figure 4.21, there are some similarities between two DEMs in the middle classes.

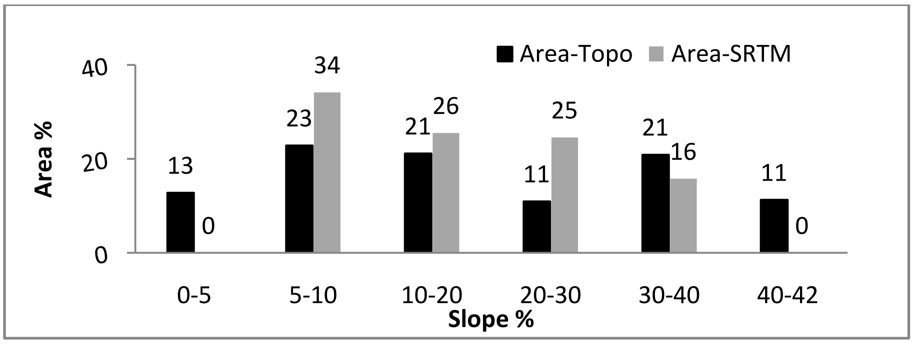

Figure 4.21: Comparison of slope derived from Topo-DEM and SRTM-DEM

As illustrated in Figure 4.22, visually there is no significant discrepancy between to DEM-derived boundaries in non-urbanized areas. However significant miss match is observed in highly urbanized areas.

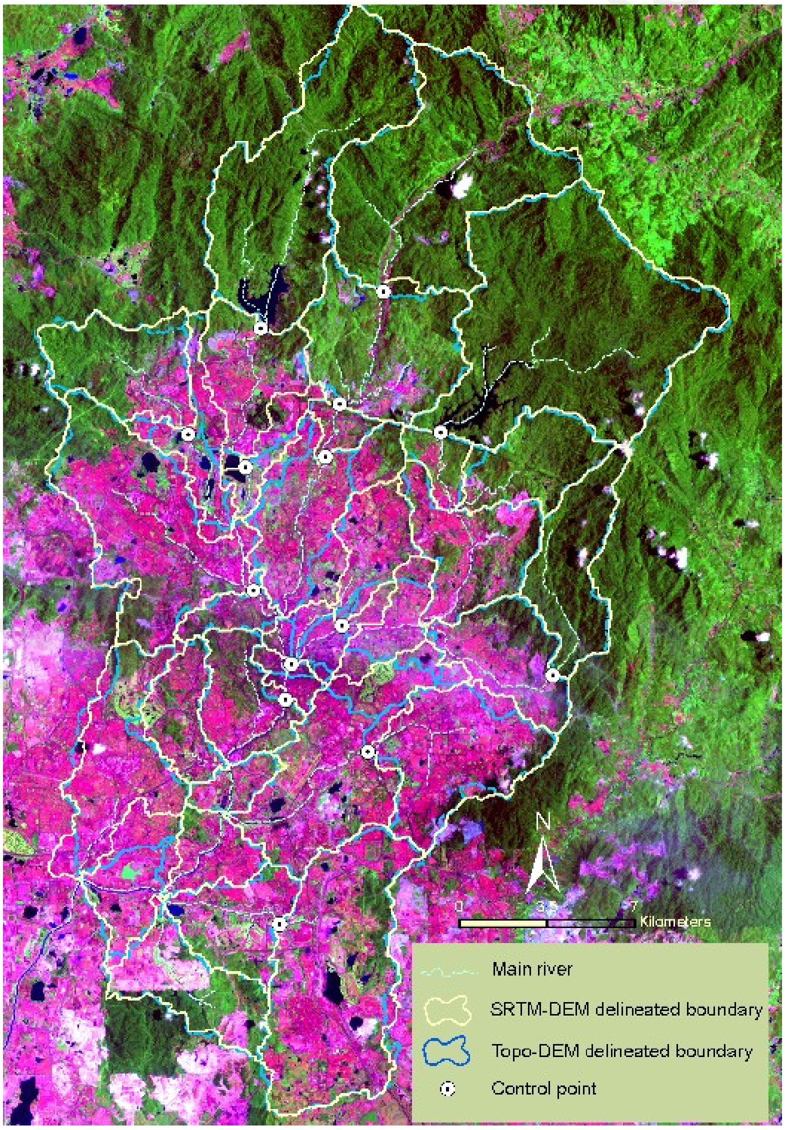

Figure 4.22: Overlying two watershed boundaries delineated from Topo and SRTM DEMs on Land sat true color composite.

4.5 Comparison of DEM-derivatives

Results of assessment analysis are presented in three scenarios. In the first stage the entire study area is assumed as one unit of consideration. Under this condition SRTM-derivatives of 31 sub-watersheds are evaluated by reference DEM-derivatives. It is noted that the number of sub-watershed are not equal it two DEM-derived watersheds due to high discrepancy ratio in the flat and highly urbanized areas. Two small sub-watersheds "s18" and "s32" are laid in one SRTM-derived sub-watershed denoted by "s18-32". Therefore, these two sub-watersheds did not consider and comparison was made based on remained 31 sub-watersheds. In addition, according to the terrain properties of Klang watershed, it is possible to differentiate sub-watersheds in two classes. The first class contains sub-watersheds located in highly urbanized area with mild slope and the second class contains sub-watersheds located in low or non-urbanized areas with gentle to steep slope.

4.5.1 Comparison of DEM-derivatives for entire study area

Scatter charts of investigated parameters are presented in Figures 4.23. Identity lines are often drawn as a reference.

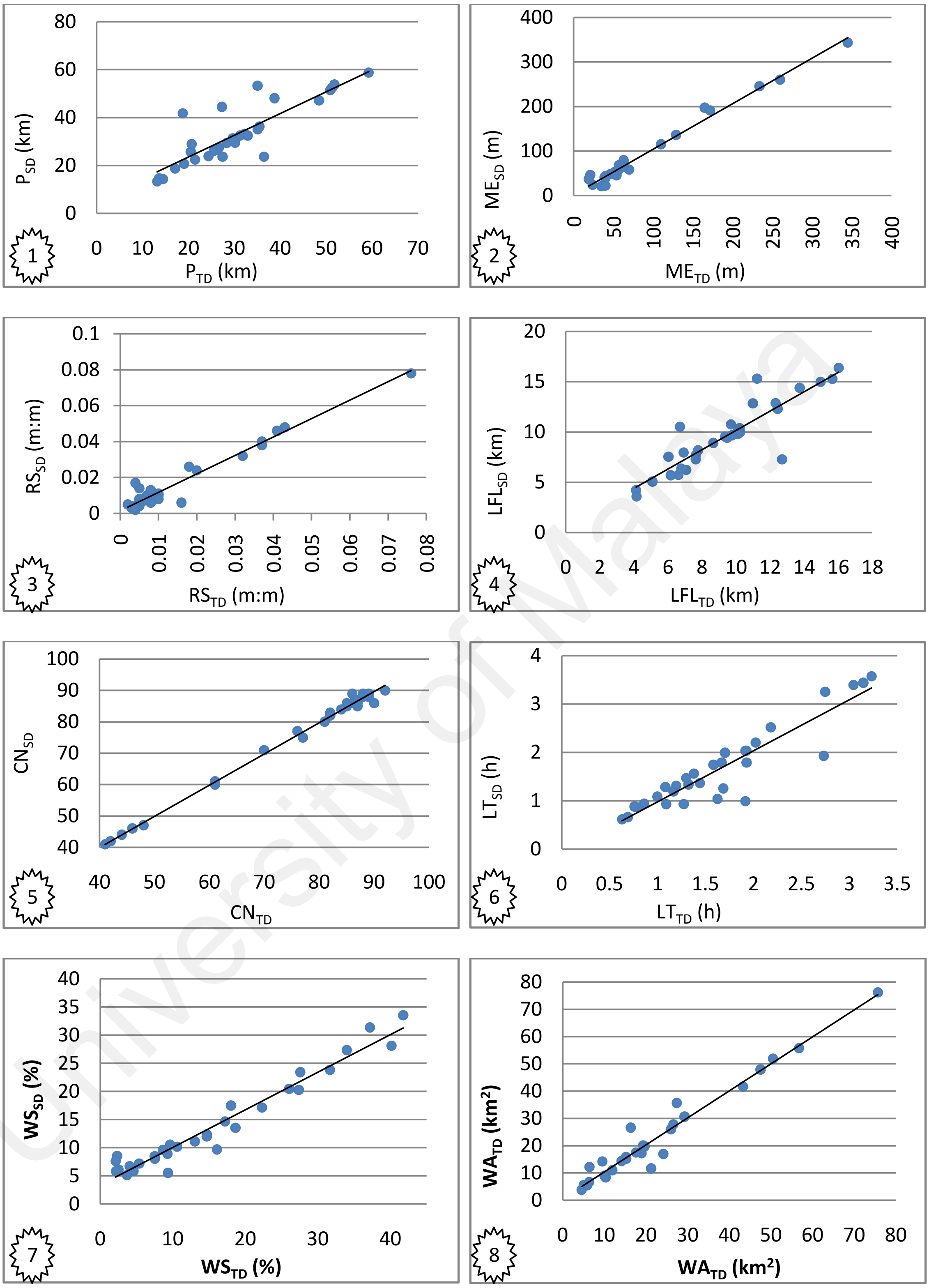

Figure 4.23: Scatter plots of Topo-derived parameters against SRTM-derived parameters in whole study area; (1) perimeter, (2) Mean elevation, (3) river slope, (4) longest flow length, (5) curve number, (6) lag time, (7) watershed slope and (8) watershed area.

Close concentration of two DEM-derived datasets in the vicinity of the identity lines, imply on relatively high similarity of two dataset when comparison is made based on the 31 sub-watershed. Statistical measures listed in Table 4.5 for 31 sub-watersheds. As it evident in scatter graphs, a good agreement is found between two DEM-derivatives. Overall agreement between DEM-derivatives of Topo and SRTM DEMs is about 0.90, 0.95 and 87 percent for R^2, r and NSE respectively which is acceptable level of agreement.

Table 4.5: Evaluation of two DEM-derived parameters by statistical measures

DEM derivatives	RMSE	R^2	r	NSE	Bias
Perimeters	7053	0.732	0.856	0.644	-8.30
Mean elevation	5.73	0.997	0.998	0.998	0.49
River Slope	0.004	0.952	0.976	0.933	-12.63
Longest flow length	1525	0.801	0.895	0.766	-1.99
SCS Curve Number	1.30	0.994	0.997	0.993	0.42
Lag time	0.32	0.950	0.975	0.797	-0.82
Watershed slope	4.73	0.848	0.921	0.840	12.06
Watershed area	3.57	0.956	0.978	0.954	-1.31
Overall agreement		0.90	0.95	0.87	

Comparatively high discrepancy is observed in some sub-watersheds between two DEM-derivatives (see Figure 4.8). Refer to the Land use map and DEM of Klang watershed indicate that those sub-watersheds are located in highly urbanized and flat areas. Those sub-watersheds are shown in Figure 4.24 and corresponding DEM-derived parameters highlighted in Table 4.6. Then, statistical measures calculated for those two classes, separately. Twenty sub-watersheds (77% of total study area) characterized with mild to steep slope and non to moderate urbanized areas denoted by land form 1 (LF1). The other eleven sub-watersheds (22% of total study area) are characterized by flat to gentle slope and highly developed urban areas denoted by land form 2 (LF2). The remained 1 % of study area does not contribute to this assessment.

Table 4.6: Differentiating DEM-derived parameters based on land form and slope of investigated sub-watersheds.

SUB	Topo-DEM derivatives							SRTM-DEM derivatives						
	P	WS	RS	LFL	LT	WA	ME	P	WS	RS	LFL	LT	WA	ME
	km	%	m:m	km	hr	Km^2	m	km	%	m:m	km	hr	Km^2	m
s1	51.28	37.15	0.043	16.02	3.2	50.47	442.4	52.45	31.33	0.048	16.37	3.6	51.82	445.71
s2	50.88	41.78	0.076	14.96	3.0	56.74	509.7	51.46	33.56	0.078	14.98	3.4	55.74	510.03
s3	35.06	27.39	0.041	10.23	1.7	29.26	181.2	35.10	20.29	0.046	9.98	2.0	30.65	176.65
s4	59.26	33.96	0.037	15.65	3.1	75.65	368.3	58.74	27.32	0.040	15.26	3.4	76.13	374.27
s5	32.90	40.14	0.037	12.44	2.7	19.46	313.6	32.50	28.12	0.038	12.31	3.3	19.46	310.25
s6	26.60	31.66	0.041	10.11	2.2	15.20	212.3	27.36	23.83	0.046	9.82	2.5	15.88	208.23
s7	14.40	26.05	0.032	5.09	0.8	5.85	122.9	14.36	20.48	0.032	5.07	0.9	5.51	115.07
s8	13.18	14.71	0.018	4.16	0.6	4.56	80.5	13.38	12.00	0.026	3.60	0.6	3.83	74.36
s9	30.14	17.20	0.008	10.06	1.4	24.18	105.1	29.48	14.68	0.013	9.94	1.6	16.97	100.01
s10	29.66	27.55	0.02	9.37	1.6	19.69	180.6	31.36	23.39	0.024	9.53	1.7	19.77	184.18
s11	27.28	2.14	0.002	9.70	2.7	16.34	47.0	44.44	5.86	0.005	10.76	1.9	26.58	57.06
s12	36.44	9.32	0.004	12.70	1.7	21.23	70.3	23.70	5.50	0.004	7.28	1.3	11.65	55.29
s13	32.24	22.32	0.003	10.21	1.1	19.32	110.4	33.22	17.15	0.004	10.37	1.3	20.06	108.36
s14	28.30	18.04	0.007	8.67	1.2	18.91	105.2	29.38	17.46	0.010	8.91	1.3	17.17	105.06
s15	20.48	2.35	0.005	6.92	1.6	6.38	50.8	25.78	8.57	0.008	7.96	1.0	6.72	62.37
s16	51.82	10.61	0.016	13.74	1.9	43.29	86.9	53.79	10.21	0.006	14.38	2.0	41.69	84.23
s17	17.06	16.06	0.008	6.62	0.8	5.06	68.2	18.70	9.65	0.010	5.74	0.9	5.50	63.29
s19	27.42	2.11	0.003	6.78	1.9	10.33	43.6	23.69	7.62	0.003	6.36	1.0	8.38	40.61
s20	26.26	13.02	0.005	7.77	1.0	14.12	58.8	26.48	11.10	0.008	8.18	1.1	14.37	55.27
s21	35.04	4.58	0.004	11.23	2.0	27.40	50.2	53.26	5.83	0.002	15.29	2.2	35.64	47.00
s22	48.46	7.51	0.004	10.98	1.9	47.49	65.0	47.13	8.04	0.003	12.85	2.0	47.88	61.92
s23	24.36	14.70	0.010	7.63	0.9	11.94	68.5	23.88	12.32	0.010	7.28	0.9	10.99	66.65
s24	13.60	8.60	0.010	4.13	0.7	5.11	46.6	14.70	9.62	0.011	4.22	0.7	5.32	47.25
s25	38.76	5.39	0.005	12.32	1.9	25.97	48.3	48.06	7.22	0.006	12.86	1.8	25.96	49.64
s26	20.68	3.66	0.008	6.03	1.3	9.52	29.0	28.96	5.14	0.006	7.54	1.3	14.21	28.62
s27	19.02	7.53	0.005	7.08	1.1	10.02	39.8	20.68	8.50	0.004	6.23	0.9	8.95	38.89
s28	25.48	9.24	0.006	7.65	1.2	15.29	52.3	26.10	8.94	0.007	7.72	1.2	15.21	49.40
s29	31.22	18.66	0.006	9.48	1.3	17.62	67.0	32.48	13.55	0.007	9.43	1.5	17.51	64.49
s30	35.48	9.61	0.010	9.75	1.4	26.57	88.8	36.30	10.50	0.008	9.67	1.4	27.80	90.94
s31	21.42	4.08	0.004	6.16	1.3	10.17	49.5	22.46	6.67	0.017	5.70	0.9	8.82	55.15
s33	18.72	2.51	0.005	6.70	1.7	6.42	54.8	41.78	6.12	0.014	10.51	1.8	12.22	68.63
Min	11.46	2.11	0.002	2.98	0.5	2.84	29.0	13.38	5.14	0.002	3.36	0.5	3.62	28.62
Max	59.26	41.78	0.076	16.02	3.2	75.65	509.7	58.74	33.56	0.078	16.37	3.6	76.13	510.03
Mean	29.30	15.42	0.015	8.99	1.6	20.47	118.7	32.36	13.78	0.017	9.36	1.6	21.31	120.18
Std	12.46	11.75	0.017	3.44	0.8	17.05	120.2	12.97	8.13	0.018	3.56	0.8	17.22	121.99

P : Perimeter
WS : Mean slope
RS : Slope of main channel
LFL : Longest flow length
LT : Lag time
WA : Watershed area
ME : Mean elevation

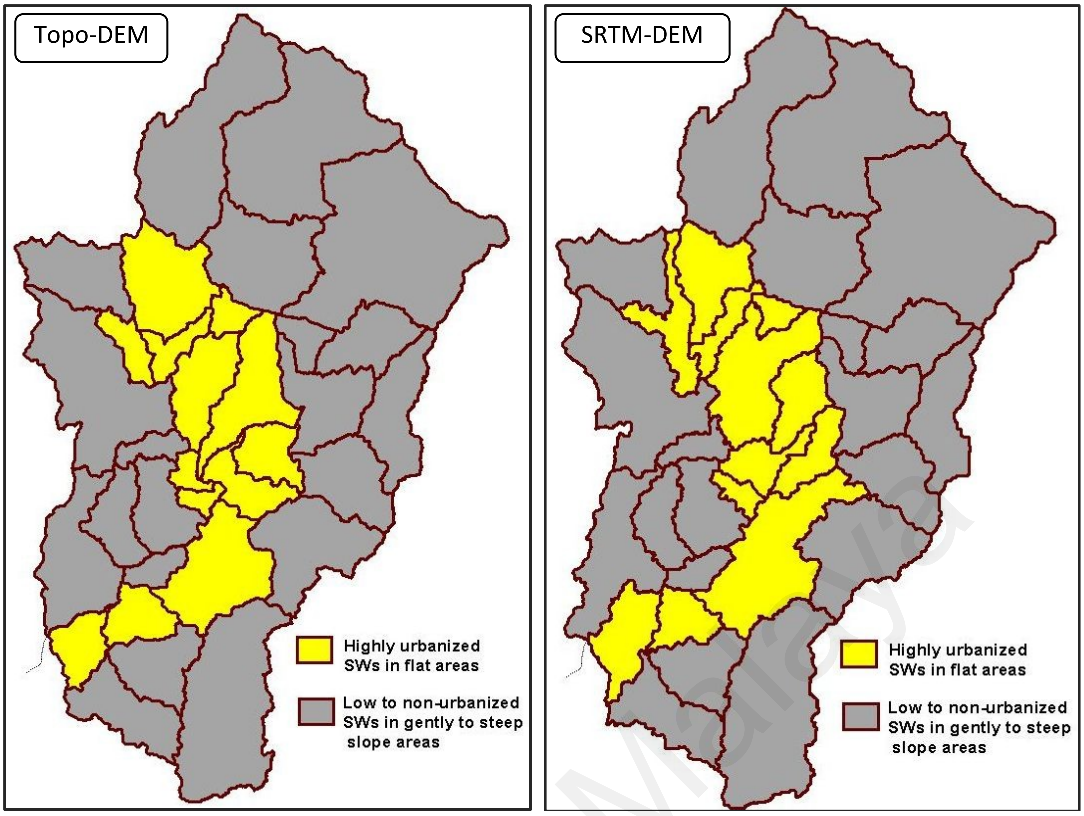

Figure 4.24: Sub-watershed located in LF2 highlighted by yellow color for both DEM-derived watershed boundaries. Topo-DEM (left) and SRTM-DEM (right)

4.5.2 Comparison of DEM-derivatives for LF1

Scatter charts and statistical measures for DEM-derived are presented in Figure 4.25 and statistical measures are provided in Table 4.7. As it evident in scatter graphs, a very good agreement is found between two DEM-derivatives in LF1. Overall agreement between DEM-derivatives of Topo and SRTM DEMs is about 0.99, 0.98 and 95 percent based on R2, r and NSE respectively that demonstrate perfectly acceptable level of agreement between Topo and SRTM DEM-derivatives.

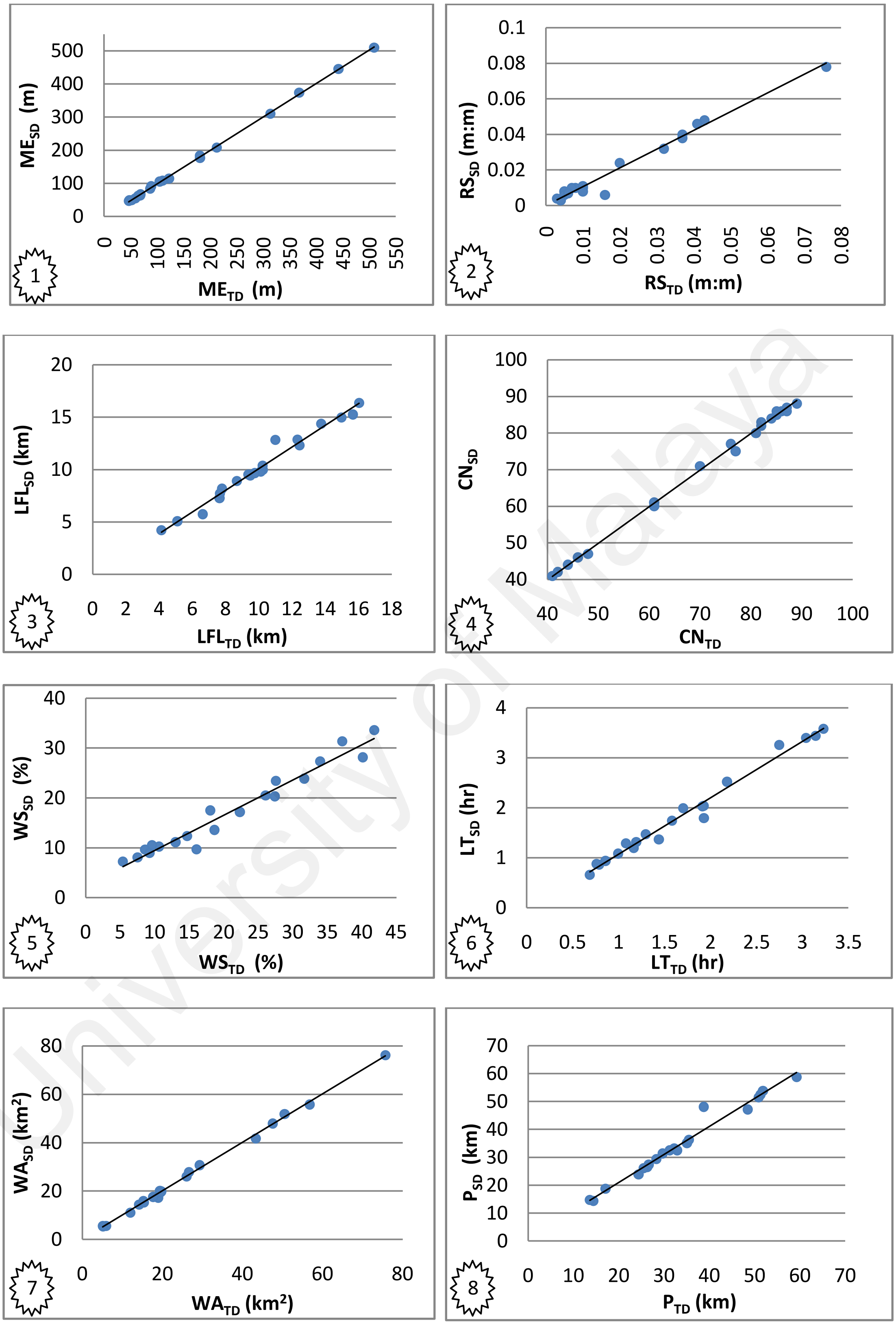

Figure 4.25: Scatter plots of Topo-derived parameters against SRTM-derived parameters in LF1; (1) Mean elevation, (2) river slope, (3) longest flow length, (4) curve number, (5) watershed slope and (6) lag time, (7) watershed area. (8) Perimeter.

Table 4.7: Results of statistical measures for evaluation of two DEM-derived parameters in LF1

DEM derivatives	RMSE	R^2	r	NSE	PBias
Perimeters	2302	0.987	0.974	0.967	-2.92
Mean elevation	3.55	0.993	0.986	0.984	0.81
River Slope	0.002	0.988	0.977	0.967	-6.00
Longest flow length	615	0.988	0.976	0.972	-1.05
SCS Curve Number	0.90	0.998	0.997	0.996	0.21
Lag time	0.19	0.991	0.983	0.923	-9.41
Watershed slope	4.30	0.979	0.958	0.781	17.97
Watershed area	0.72	0.998	0.997	0.998	-0.26
Overall agreement		0.99	0.98	0.95	

4.5.3 Comparison of DEM-derivatives for LF2

Scatter charts for DEM derivatives in LF2 are presented in Figure 4.26 and statistical measures are provided in Table 4.8. As it evident in scatter graphs, a weak agreement is found between two DEM-derivatives in LF2. Overall agreement between DEM-derivatives of Topo and SRTM DEMs is about 77, 53 and 33 percent based on R2, r and NSE respectively which demonstrate high level of discrepancy between Topo and SRTM DEM-derivatives.

Table 4.8: Results of statistical measures for evaluation of two DEM-derived parameters inFL2

DEM derivatives	RMSE	R^2	r	NSE	Bias
Perimeters	8802	0.466	0.217	0.620	-21.42
Mean elevation	8.35	0.666	0.444	0.974	-1.19
River Slope	0.006	0.763	0.582	-0.906	-54.55
Longest flow length	2455	0.625	0.391	0.009	-4.16
SCS Curve Number	1.88	0.908	0.825	0.776	0.73
Lag time	0.45	0.814	0.662	0.515	15.87
Watershed slope	3.511	0.716	0.512	0.251	-23.22
Watershed area	5.88	0.762	0.580	0.372	-5.05
Overall agreement		0.72	0.53	0.33	

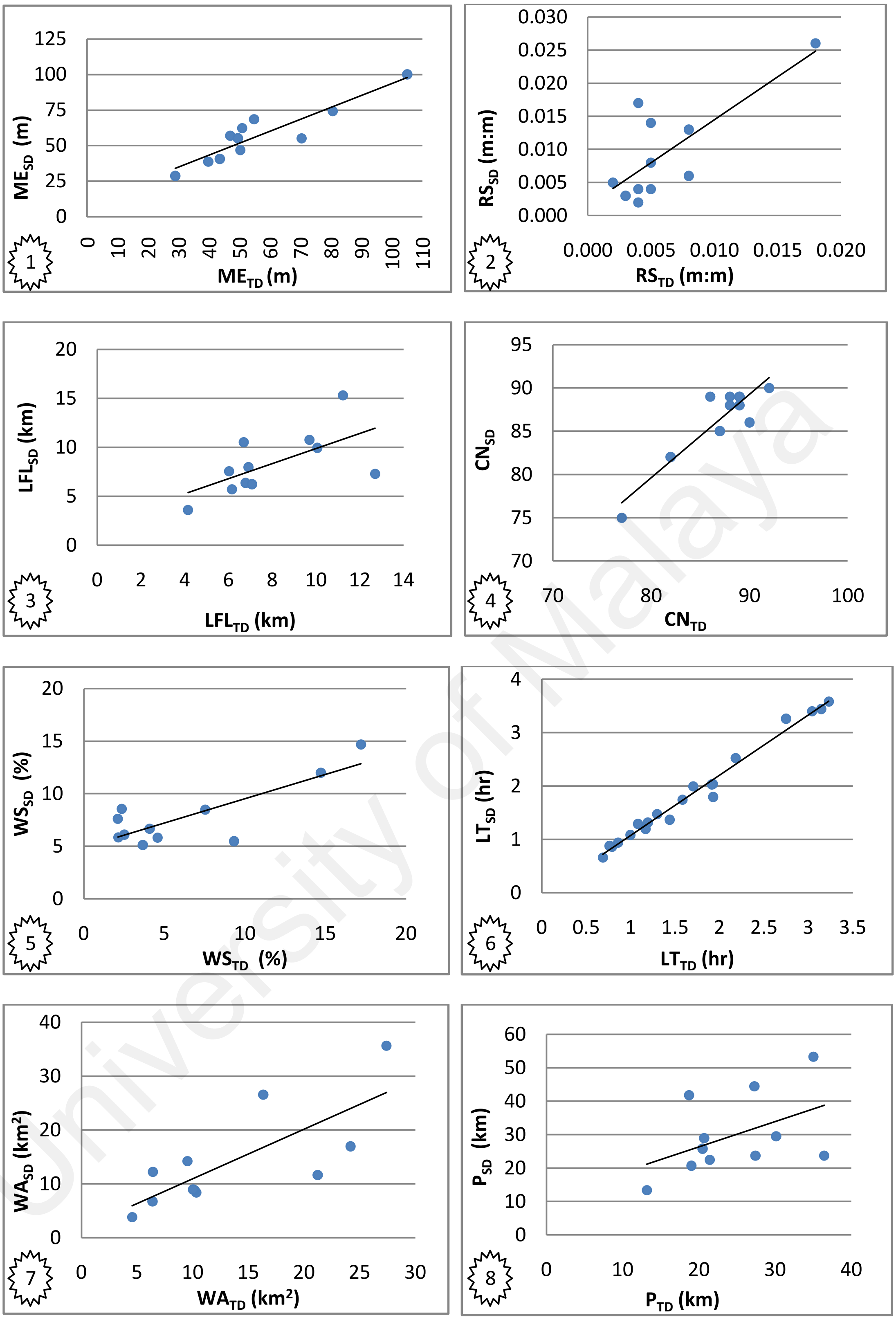

Figure 4.26: Scatter plots of Topo-derived parameters against SRTM-derived parameters in LF2; (1) Mean elevation, (2) river slope, (3) longest flow length, (4) curve number, (5) watershed slope and (6) lag time, (7) watershed area. (8) Perimeter.

4.6 General discussion

- Data collection: apart from the quality of data, it was experienced that purchasing process and licensing of digital topography at scale of 1:25000 is a tedious and time consuming step. While SRTM elevation data is free of charge and available at any time for 80 present of entire globe.
- Data pre-processing: To cover whole area with topo maps at scale of 1:25000, several sheets are needed for a medium to large watersheds that often miss matches are observed at junction edges. It is due to asynchronous cartographic data and non-uniformity of equipments that result in heterogeneous cartographic products. For instance, sheet number "3757a" generated from aerial photo taken in 1969 and sheet number "3858c" from aerial photo taken in 1982 (See Appendix A, Table A.4). Unlike, SRTM data produced in a short time (11-day mission in February of 2000) with a unique mechanism of technology which results in uniform and homogeneous data. SRTM data are accessible to the public via the internet. It is really cost effective and time saving for hydrologic modeling in a medium to large watersheds.
- The automated GIS-based hydrologic modeling toolkit (HEC-GeoHMS) has been enhanced with a variety of features to aid in SRTM assessment and analysis. It was shown the ability of free GIS tools for DEM processing and watershed parameterization. However there are still some difficulties in coupling GeoHMS with ArcGIS. In addition, GeoHMS is free but the framework (ArcGIS) is not free.
- Void filling technique: In addition to previous procedures that developed for SRTM void filling by others, ILWIS's undefined-majority filter (MAJUNDEF) was applied and found out that MAJUNDEF filter is suitable approach for filing void areas of SRTM elevation data if the void area is limited pixels.
- Watershed delineation: result of watershed boundary delineation proved that SRTM-DEM can depict 78 percent Klang watershed with no significant

discrepancy in visual interpretation. However 22 percent of watershed that fall in highly urbanized and gentle slope don't match with boundaries derived from Topo-DEM that generated from digital topo at scale of 1:25000 and 1:10000.

- Watershed parameterization: statistical measures for investigated parameters lead us to the following conclusions based on the three investigated alternatives.
- SRTM-derivatives of Klang watershed as one unit of consideration:

As shown in Table 4.5 close values of $\boldsymbol{r}$ and NSE to one is obtained for all investigated parameters which indicated that there is a reasonable level of performance for SRTM elevation data and its DEM-derivatives are significantly befitted to Topo-DEM. Relatively highest value of RMSE and lowest values of $\boldsymbol{r}$ and NSE (0.73, 0.64) are observed for subbasins perimeter that statistically enhance the observed discrepancies in Figure 4.19. Positive value of bias for watershed slope indicates that SRTM-DEM predict 12 percent underestimate. The reason may relate to resampling original SRTM elevation data from 30 m to 90m resolution that cause DEM smoothing and slope reduction. While, river slope is estimated about 12 percent over estimate compare to slope derived from Topo-DEM. comparatively high value of RMSE (1523 m) for longest flow length represents the weakness of SRTM-DEM to depict stream channels compare to mean elevation and watershed area. Negative bias (-2 %) indicate that SRTM-DEM over estimates the longest flow length by 2 percent. Watershed area and mean elevation are predicted with pretty close correlation to reference DEM-derivatives and low bias that implies on high level of performance of SRTM-DEM.

- SRTM-derivatives on low to non-urbanized areas of Klang watershed characterized by moderate to steep slope (LF1):

Statistical measures of r and NSE has became closer to one while RMSE and PBias has significantly decreased for all investigated parameters in low to none urbanized areas characterized by rugged topography. This indicate that there is a high level of performance for SRTM elevation data and DEM-derived parameters from SRTM are significantly befitted to Topo-DEM. comparatively low values of RMSE and PBias and high values of r and NSE statistically enhance the ability of SRTM-DEM in deriving watershed parameters. Meanwhile, no change is observed for RMSE of watershed slope and PBias has been increased from 12 to 18 percent that reasonably denote the underestimate approximation of watershed slope by SRTM-DEM in hilly areas. While, negative PBias of -6% for river slope convey the fact that SRTM-DEM estimates rive slope higher than actual value but with better estimation in hilly areas compare to urbanized and flat areas. Relatively high value of RMSE (615 m) for longest flow length still represents the weakness of SRTM-DEM to depict drainage network compare to mean elevation and watershed area. Low and negative bias (-1 %) indicate that SRTM-DEM over estimates the longest flow length by 1 percent in hilly areas. Watershed area and mean elevation are predicted with perfect correlation and low bias that implies a perfect level of performance for SRTM-DEM in non- urban areas characterized by hilly topography.

- SRTM-derivatives in urbanized areas of Klang watershed characterized by gentle to moderate slope (LF2):

Statistical measures of r and NSE has significantly decreased but RMSE and PBias has increased for all investigated parameters in urbanized areas characterized by gentle to moderate slopes. Mean values of NSE index (33%) indicate that there is a low level of suitability for SRTM elevation data and its DEM-derivatives that do not befitted to Topo-DEM derivatives. Comparatively high values of RMSE and PBias and low values of r and NSE statistically enhance the unsuitability of SRTM-DEM in deriving watershed parameters for hydrologic modeling specifically watershed slope and river slope.

As it evident in Table 4.5, Table 5.7 and Table 4.8, statistical measures for averaged-CN represent a good agreement between two DEM-derivatives. However closer correlation and minimum RMSE and PBias are observed in sub-watershed remarked as LF1. It can be due to the fact that secondary DEM-derivative of CN is less sensitive to the source of DEM. The reason is related to nearly uniform spatial distribution of CN in Klang watershed.

4.7 Spatio-temporal Analysis of Rainfall events measured by gauges and satellite sensor

Land use map representing the watershed conditions of year 2002, therefore, an attempt was mead to find some storm events in this year. Obviously, due to localized rainfall in study area, it is difficult to find the events that meet all criteria in all investigated rain gauges. However, considering the criteria listed in section 8 storms were identified suitable for further investigation as listed in Table 4.9.

Table 4.9: Investigated storms for selecting suitable rainfall-runoff event for modeling

2002	06-May		29-Apr		02-Jun		11-Jun		06-Sep		08-Oct		08-Nov		21-Dec	
Gauge ID	R mm	5DPR mm	R mm	5DPR mm	R mm	5DPR mm	R mm	5DPR mm	R mm	5DPR mm	R mm	5DPR mm	R mm	5DPR mm	R mm	5DPR mm
3015001	29.5	32.5	73	58	7	1	11	8	2	5	0.5	98.5	0	18	46	61.5
3016001	51	20.0	99	6	0	0	37	24	39	13	33	19	0	0	74	49
3016102	11.5	20.0	69.5	55	32.5	1	13.5	41.5	48	12	5.5	97.5	33.5	73.5	57.5	50
3016103	*	*	*	*	*	*	*	*	50	150.5	21.5	85.5	*	*	*	*
3116003	59.5	55.5	90	74	93.5	63	51.5	26	18	31	107	47.5	56	50.5	24.5	88.5
3116004	60.5	58.0	93	76	94	20	54	26	19	31	108	46	57	51	24	89
3116006	38.5	33.0	101.5	90	5.5	10.5	62.5	16	2	19	39.5	106	20.5	79	7.5	61.5
3116074	45.0	32.0	95	51	100	24	42	16	35	60	110	70	76	37	18	43
3117002	24.0	24.0	77	25	2	3	138	42	10	76	48	38	2	24	20	52
3117070	63.0	30.0	57	18	80	43	55	22	97	31	82	47	40	81	28	70
3117101	2.5	60.0	29	60	37.5	0.5	16.5	19	0	1	11	4.5	9	108	69.5	65
3117102	14.5	27.0	65.5	27	47.5	4	18.5	13	92	23.5	70	110.5	30.5	89.5	41.5	67.5
3117104	30.0	35.0	111	14	0	0	12	8	2	5	1	99	0	20	48	67
3216004	16.0	32.5	158	33	3.5	0	63	16	9.5	41	21	54.5	9.5	68	8.5	105.5
3216005	5.0	13.0	59	40	12	41	17	30	77	50	17	99	32	16	0	10
3217002	42.0	26.0	121	14	11	7.5	58.5	14.5	32.5	106.5	26	22	2	8.5	32.5	40
3217003	28.5	22.5	71	18	3	26.5	95.5	38.5	47	63	45	43	1	31	22.5	52
3217004	57.0	14.0	94.5	34.5	0	2.5	38	47.5	69	96.5	19	15.5	6	45	25	28
3217005	*	*	*	*	*	*	*	*	35	66	*	*	*	*	*	*
3317001	0.0	71.0	88	64.5	1.5	8	8.5	68.5	8	19	75	58.5	10.5	85.5	3	25.5
3317004	27.0	9.5	67.5	130.5	43	17.5	20	32.5	4	17	9.6	25	0	38.5	*	*
3217102	*	*	*	*	*	*	*	*	*	*	34	57	14	24	19	45
Mean	31.8	33.1	85.24	46.76	30.2	14.4	42.7	26.8	33.1	43.67	42.1	59.21	20	47.4	29.9	56.32
Std	20.5	17.3	27.87	31.53	36.2	18	33.1	15.4	30.4	38.7	36	33.23	22.7	30.8	21.2	23.19
C.V	0.64	0.52	0.32	0.67	1.2	1.25	0.78	0.58	0.92	0.88	0.86	0.561	1.14	0.65	0.71	0.41

R: Accumulated rainfall; 5DPR: 5-days prior rainfall

Accumulated rainfall and 5-days prior rainfall for investigated storms were plotted in bar chart showed in Figures 4.27-4.34. It is observed some events have not recorded in all investigated gauges. For example, rainfall event of 6-May 2002 was not caught in gauge 3016001. This can be due to technical problems in that gauge during the specific events. An attempt was made to recover missing records using nearby stations. But no significant correlation is found. Considering above mentioned criteria the coefficient of variation (C.V) was calculated to find the relatively uniform rainfall events. Four events with lower value of C.V ware identified suitable for further analysis. Those are storm event of 6-May, 29-Apr 11-Jun, and 21-Dec.

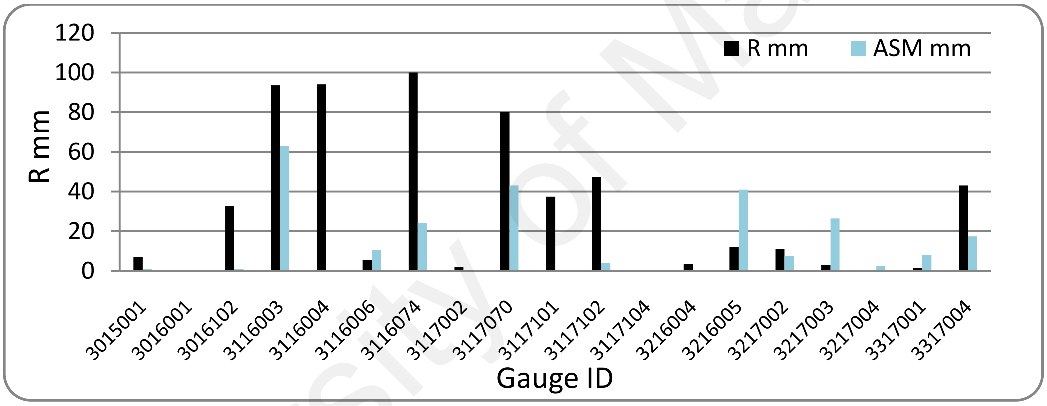

Figure 4.27: Distribution of total rainfall recorded at stations for storm Jun. 2, 2002

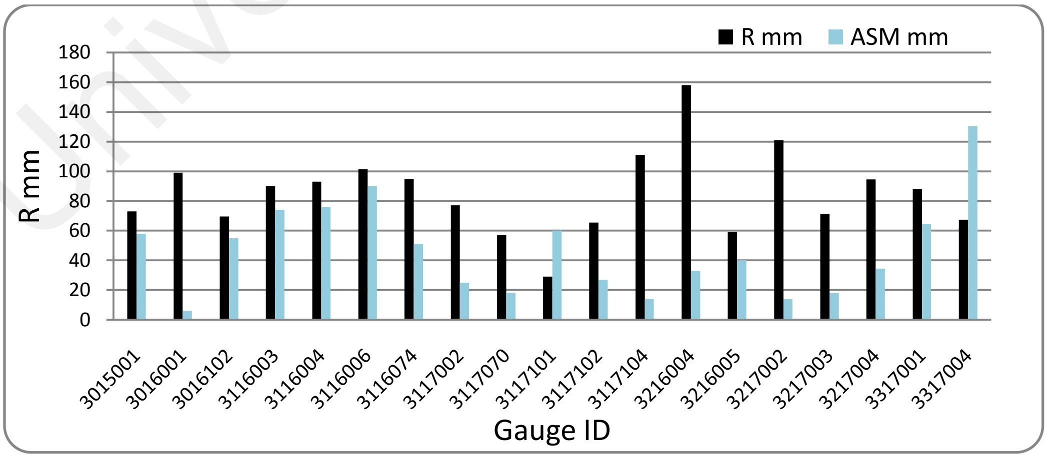

Figure 4.28: Distribution of total rainfall recorded at stations for storm Apr 29, 2002

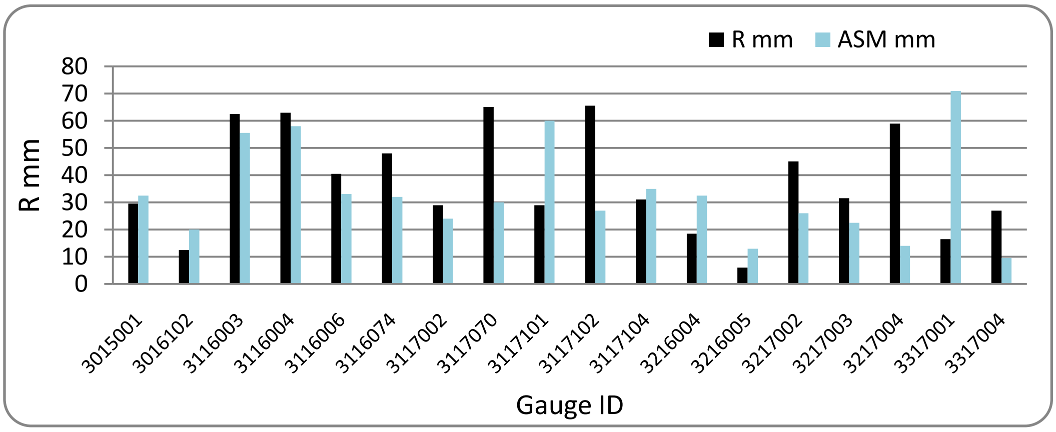

Figure 4.29: Distribution of total rainfall recorded at stations for storm May 6, 2002

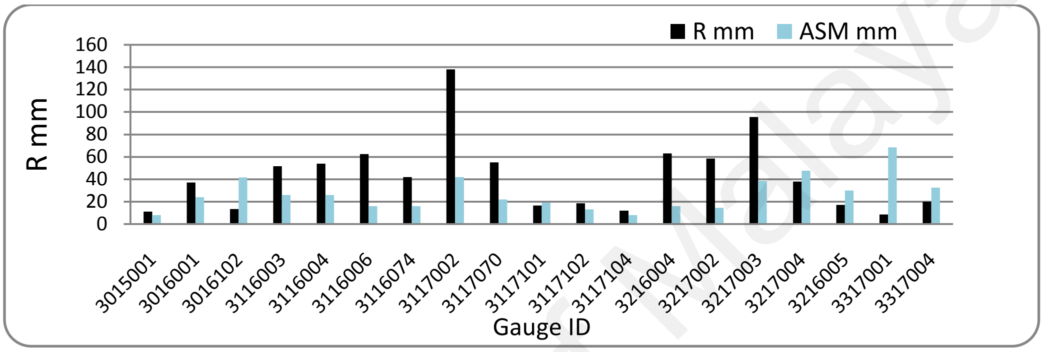

Figure 4.30: Distribution of total rainfall recorded at stations for storm Jun 11, 2002

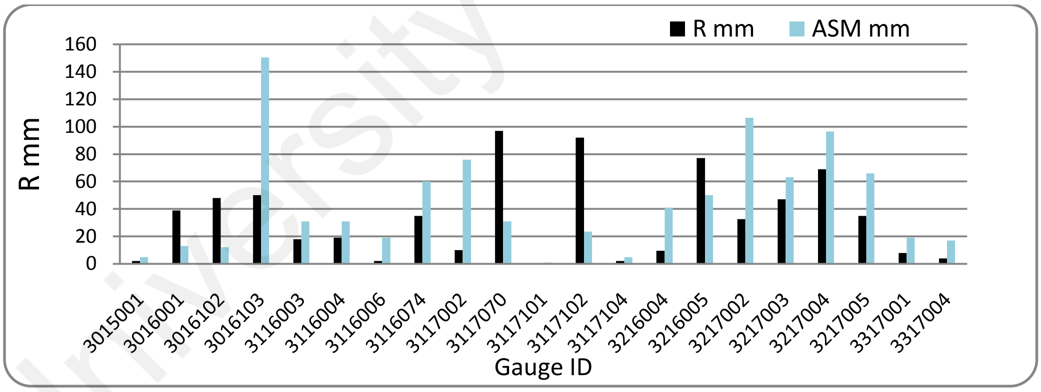

Figure 4.31: Distribution of total rainfall recorded at stations for storm Sep. 6, 2002

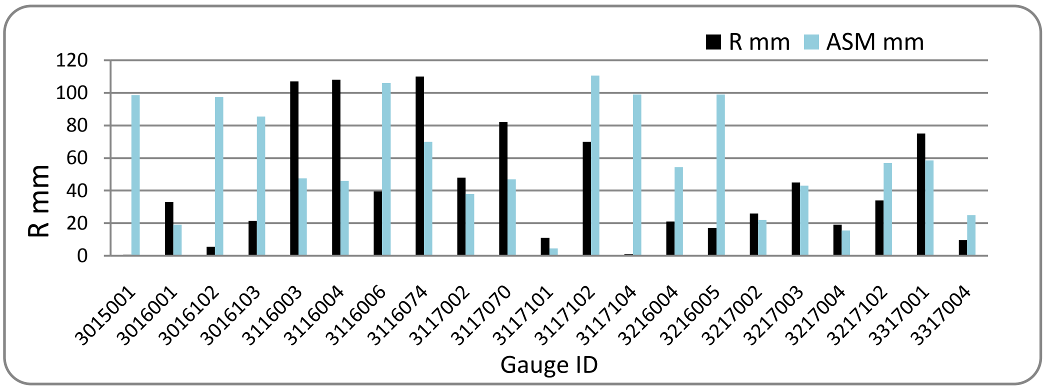

Figure 4.32: Distribution of total rainfall recorded at stations for storm Oct.8, 2002

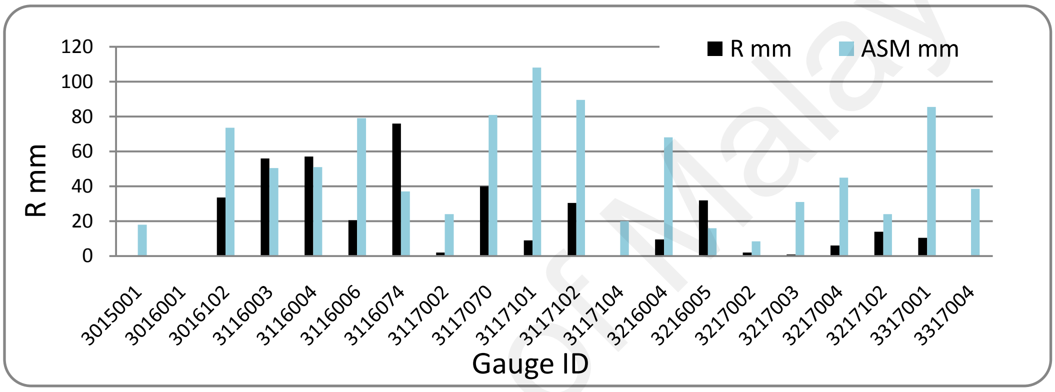

Figure 4.33: Distribution of total rainfall recorded at stations for storm Nov.8, 2002

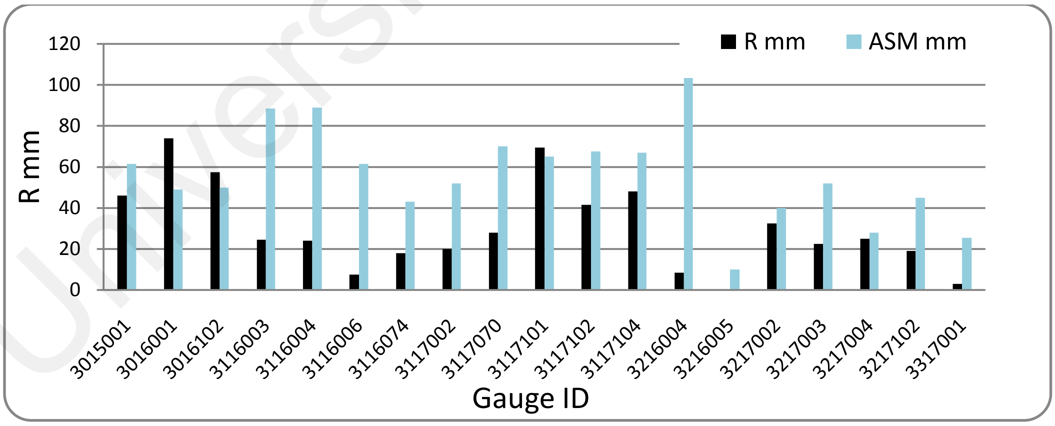

Figure 4.34: Distribution of total rainfall recorded at stations for storm Dec. 21, 2002

4.7.1 Implementing Kriging interpolation for selected storm

Kriging method with Gaussian Semi-variogram model was applied to define the areal storm patterns of to four storm events (See Figure 4.35). 18 recording rain-gauges contribute to interpolation for event 6-May and 19 recording rain-gauges for events 29-Apr, 11-Jun and 21-Dec. Then GIS tools were used to calculate the weighted average rainfall for sub-watersheds.

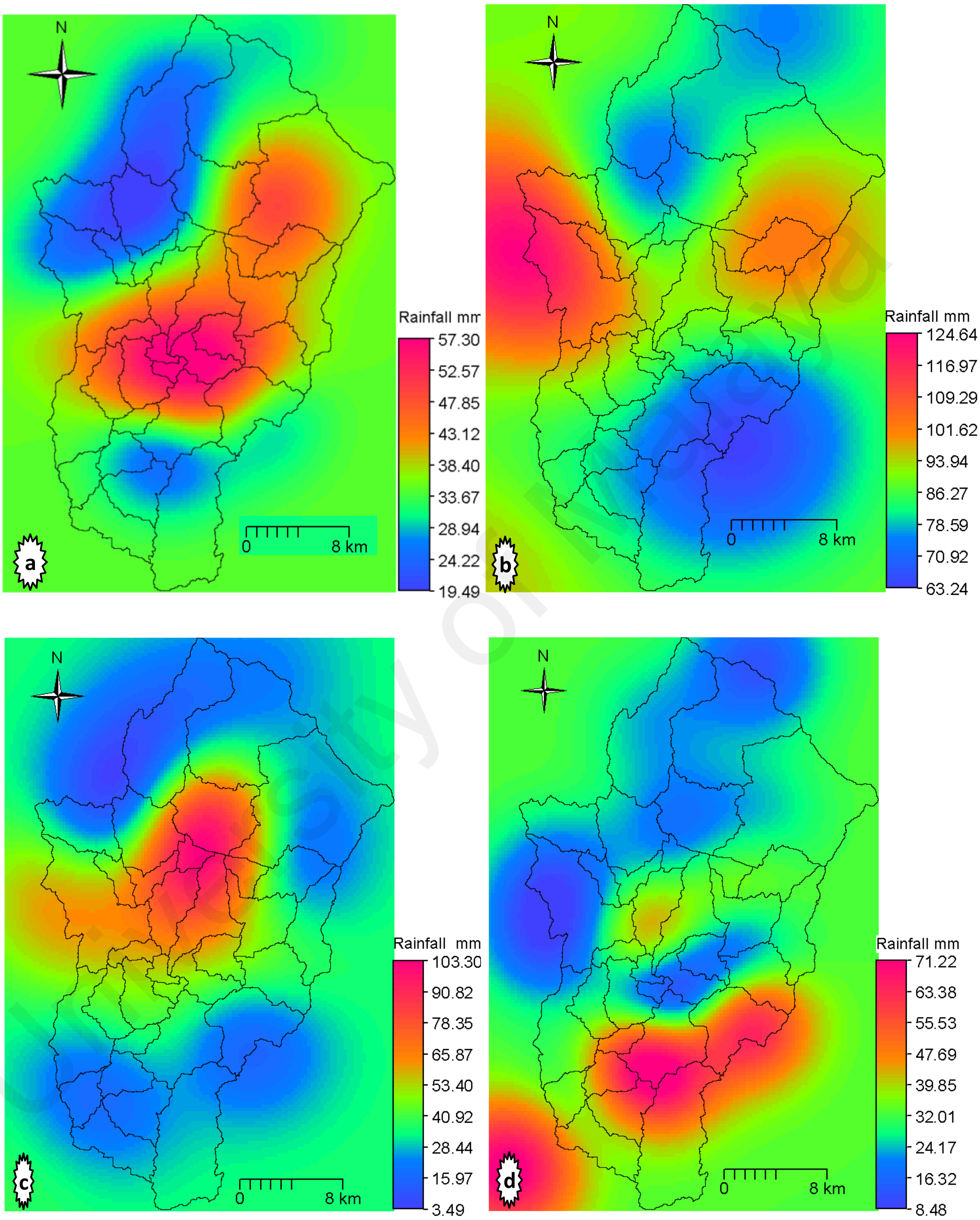

Figure 4.35: Spatial distribution of rainfall events over Klang watershed using Kriging interpolation with Gaussian Semi-variogram model; a) rainfall event 6-May2002, b) rainfall event 29-Apr2002, c) rainfall event 11-jun2002 d) rainfall event 21-Dec2002

Temporal pattern of storms in each sub-watershed is defined based on the nearest station to its center of gravity.

4.7.2 Temporal pattern of selected storms

Temporal pattern of selected storms were analyzed with 15 min time interval. It is observed that storm duration and temporal distribution of investigated storms are irregular and demonstrate high degree of variation in space and time that effect the time-to-peak of flood hydrograph. For example as demonstrated in Table 4.10 and Figure 4.36 and 4.37, peak discharge occurred on 17:45 PM at stream flow gauge 3116434 and 18:45 PM at gauge 3116430 with 1 hour delay for event 29-Apr. However, for the event of 21-Dec time-to-peak occur at 21:15 PM at gauge 3116434 and 20:00 PM at gauge 3116430 with 1 hour and 15 minutes earlier.

Table 4.10: Observed time-to-peak and peak runoff for selected flood events

Flood Event	$Q_{3116434}$	T_{peak}	$Q_{3116433}$	T_{peak}	$Q_{3116430}$	T_{peak}
	m^3/s		m^3/s		m^3/s	
06-May	83.37	14:45	32.50	14:45	361.29	15:30
29-Apr	40.48	17:45	61.22	16:45	154.55	18:45
11-Jun	168.28	20:45	147.55	20:45	448.96	21:00
21-Dec	23.33	21:15	47.27	21:30	121.46	20:00

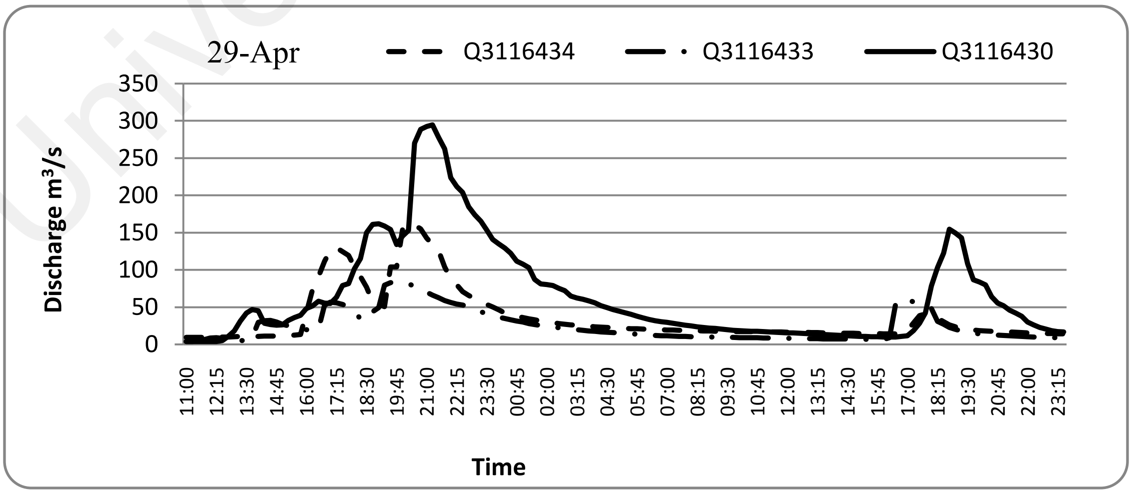

Figure 4.36: Observed flood hydrograph resultant from storm event of 29-Apr 2002

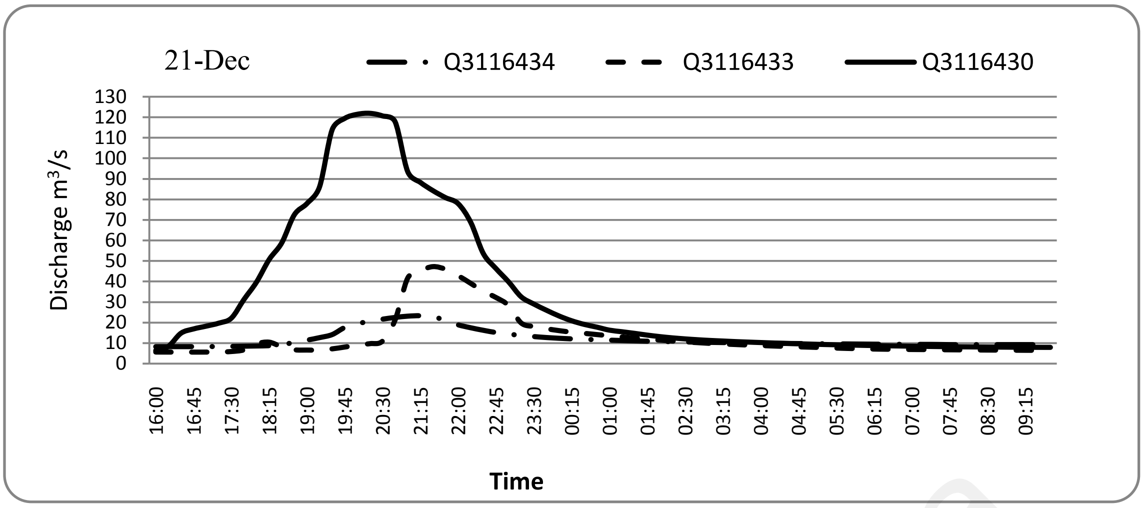

Figure 2.37: Observed flood hydrograph resultant from storm event of 21-Dec 2002

Coefficient of variation was used to explain the temporal variation of storm events over Klang watershed (see Table 11).

Table 4.11: Temporal variations of selected storm events

Flood event	Number of stations	Accu. mean rainfall mm	rainfall duration (hr)		
			Mean	Std	C.v
06-May	18	31.8	2.21	0.83	0.37
29-Apr	19	85.4	7.61	1.37	0.18
11-Jun	19	42.7	3.62	0.8	0.22
21-Dec	19	29.9	1.68	1	0.59

Rainfall event of 29-Apr represent relatively lower degree of variation in time so that it seems to be the first choice for rainfall-runoff modeling, but according to Figure 4.22 corresponding flood hydrograph has a complex shape. Refer to criteria that listed in section simple-storm structure, resulting in well-defined hydrographs with distinct peaks are more desirable for model calibration. Therefore; flood events on 6-May, 11-June and 21-Dec are respectively more desirable (see Figure 4.38 and 4.39).

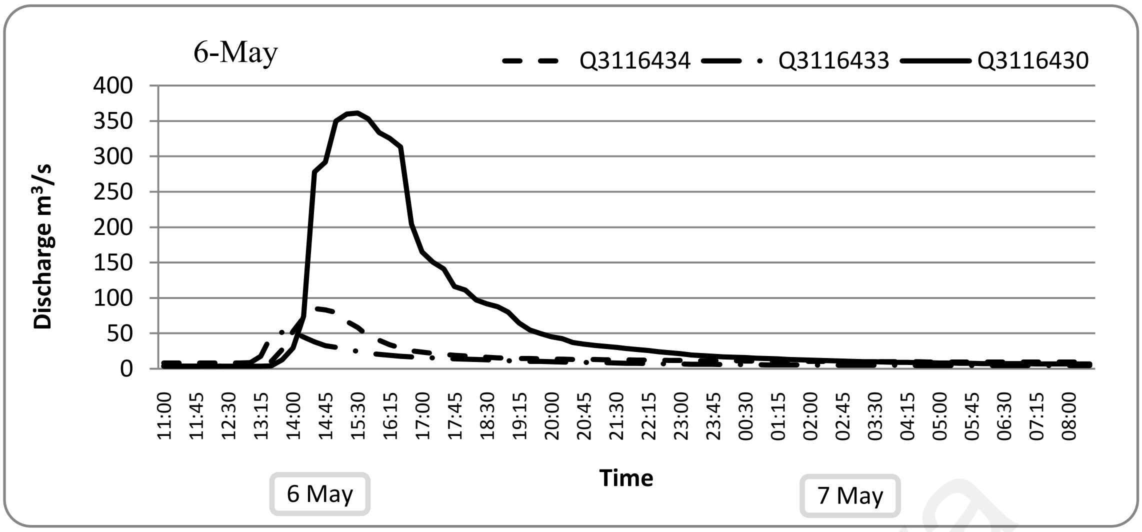

Figure 4.38: Observed flood hydrograph resultant from storm event of 6-May 2002

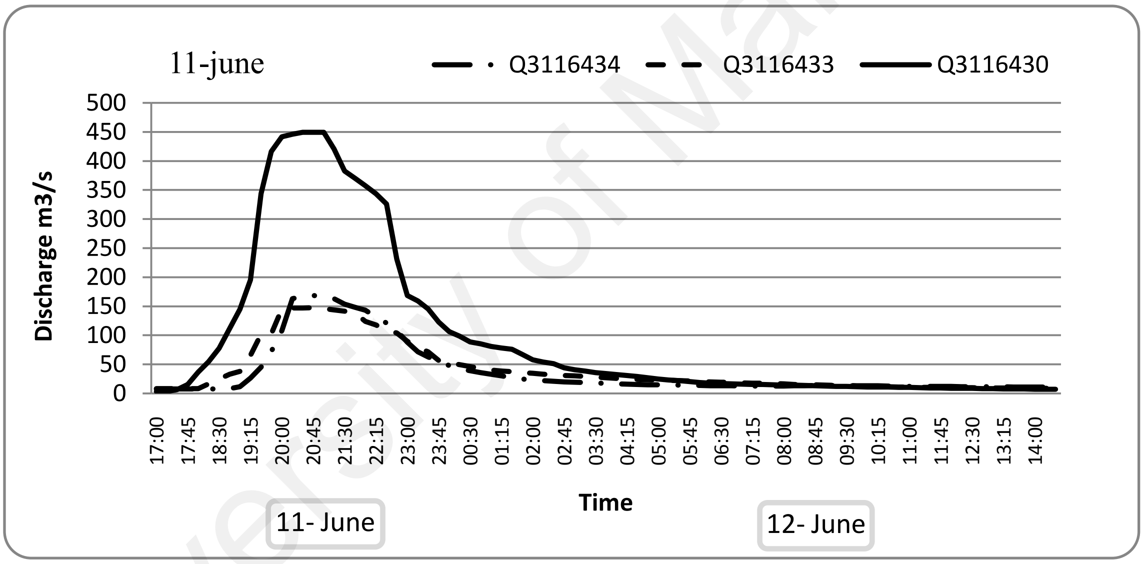

Figure 4.39: Observed flood hydrograph resultant from storm event of 11-Jun 2002

15-minutes time interval distributions of event 6-May catch in 18 recording rain gauges were plotted in Figure 4.40 and Table 4.12.

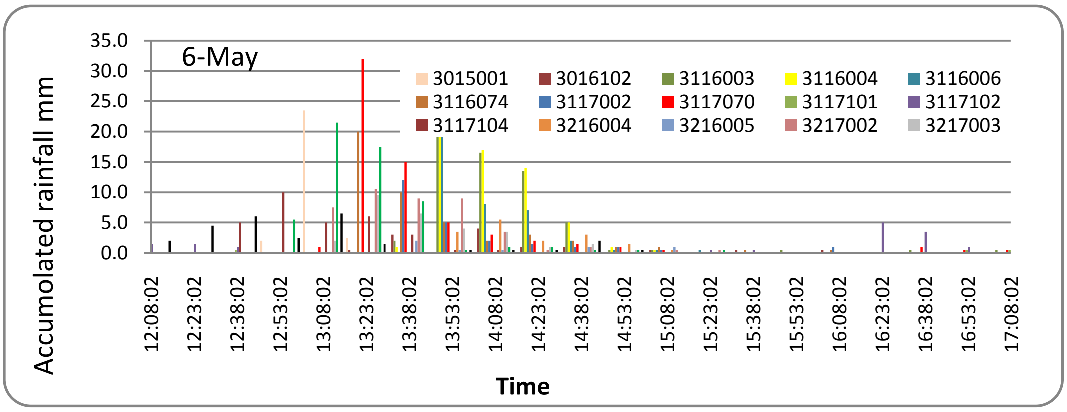

Figure 4.40: Graphical representation of storm pattern (6-May) at 18 rain gauges.

Table 4.12: Observed temporal pattern of storm event (6-May) at 18 rain gauges.

UTC Time	Gauge ID																	
	3015001	3016102	3116003	3116004	3116006	3116074	3117002	3117070	3217003	3217004	3217002	3216004	3216005	3117104	3317004	3117102	3117101	3317001
11:53:02	0.0	0.0	0.0	0.0	0.0	0.0	0.0	0.0	0.0	0.0	0.0	0.0	0.0	0.0	0.0	0.0	0.0	0.0
12:08:02	0.0	0.0	0.0	0.0	0.0	0.0	0.0	0.0	0.0	0.0	0.0	0.0	0.0	0.0	2.0	1.5	1.0	0.0
12:23:02	0.0	0.0	0.0	0.0	0.0	0.0	0.0	0.0	0.0	0.0	0.0	0.0	0.0	0.0	4.5	1.5	0.0	0.0
12:38:02	0.0	0.0	0.0	0.0	0.0	0.0	0.0	0.0	0.0	0.0	0.0	0.0	0.0	5.0	6.0	1.0	0.5	0.0
12:53:02	2.0	0.0	0.0	0.0	0.0	0.0	0.0	0.0	0.0	5.5	0.0	0.0	0.0	10.0	2.5	0.0	0.0	0.0
13:08:02	23.5	0.0	0.0	0.0	0.0	0.0	0.0	1.0	2.0	21.5	7.5	0.0	0.0	5.0	6.5	0.0	0.0	0.0
13:23:02	2.5	0.5	0.0	0.0	0.0	20.0	0.0	32.0	9.5	17.5	10.5	0.0	0.0	6.0	1.5	0.0	0.0	0.0
13:38:02	0.0	3.0	2.0	1.0	0.0	10.0	12.0	15.0	6.5	8.5	9.0	0.0	2.0	3.0	0.0	0.0	0.0	0.0
13:53:02	0.0	0.0	20.0	21.0	19.5	5.0	5.0	5.0	4.0	0.5	9.0	3.5	0.5	0.5	0.5	0.0	0.0	0.0
14:08:02	0.0	4.0	16.5	17.0	8.0	2.0	2.0	3.0	3.5	1.0	3.5	5.5	0.5	0.5	0.5	0.0	0.0	0.0
14:23:02	0.0	1.0	13.5	14.0	7.0	3.0	1.5	2.0	1.0	1.0	0.5	2.0	0.0	0.0	0.5	0.0	0.0	0.0
14:38:02	0.0	1.0	5.0	5.0	2.0	2.0	1.0	1.5	1.5	0.5	1.0	3.0	1.0	0.0	2.0	0.0	0.0	0.0
14:53:02	0.0	0.0	0.5	1.0	0.5	1.0	1.0	1.0	0.5	0.5	0.0	1.5	0.0	0.0	0.5	0.0	0.0	0.0
15:08:02	0.0	0.5	0.5	0.5	0.5	1.0	0.5	0.5	0.0	0.0	0.5	0.5	1.0	0.0	0.0	0.0	0.0	0.0
15:23:02	0.0	0.0	0.0	0.0	0.5	0.0	0.0	0.0	0.0	0.5	0.5	0.0	0.0	0.0	0.0	0.5	0.0	0.0
15:38:02	0.0	0.5	0.0	0.0	0.0	0.5	0.0	0.0	0.0	0.0	0.0	0.0	0.0	0.0	0.0	0.5	0.0	0.0
15:53:02	0.0	0.0	0.5	0.0	0.0	0.0	0.0	0.0	0.0	0.0	0.0	0.0	0.0	0.0	0.0	0.0	0.0	0.0
16:08:02	0.0	0.5	0.0	0.0	0.0	0.5	1.0	0.0	0.0	0.0	0.0	0.0	0.0	0.0	0.0	0.0	0.0	0.0
16:23:02	0.0	0.0	0.0	0.0	0.0	0.0	0.0	0.0	0.0	0.0	0.0	0.0	0.0	0.0	0.0	5.0	0.0	0.0
16:38:02	0.0	0.0	0.5	0.0	0.0	0.0	0.0	1.0	0.0	0.0	0.0	0.0	0.0	0.0	0.0	3.5	0.0	0.0
16:53:02	0.0	0.0	0.0	0.0	0.0	0.0	0.0	0.5	0.0	0.0	0.0	0.0	0.0	0.0	0.0	1.0	0.5	0.0
17:08:02	0.0	0.0	0.5	0.0	0.0	0.0	0.0	0.5	0.0	0.0	0.0	0.0	0.0	0.0	0.0	0.0	0.5	0.0
17:23:02	0.5	0.5	0.0	0.0	0.5	0.0	0.0	0.0	0.0	0.0	0.0	0.0	0.0	0.0	0.0	0.0	0.0	0.0
17:38:02	0.0	0.0	0.0	0.0	0.0	0.0	0.0	0.0	0.0	0.0	0.0	0.0	0.0	0.0	0.0	0.0	0.0	0.0
17:53:02	0.0	0.0	0.0	1.0	0.0	0.0	0.0	0.0	0.0	0.0	0.0	0.0	0.0	0.0	0.0	0.0	0.0	0.0

4.7.3 TRMM3B42 event

TRMM data downloaded in Netted format that can be read by ArcGIS 9.3. Horizontal resolution of TRMM data version 6 is 15′×15′ or ~27.8×27.8 km.

Considering Figure 4.41, Klang watershed fall in 5 TRMM grids identified with 1, 3, 4, 5 and 6.

TRMM V6 was downloaded from the following web page:

http://disc2.nascom.nasa.gov/Giovanni/tovas/TRMM_V6.3B42.2.shtml .

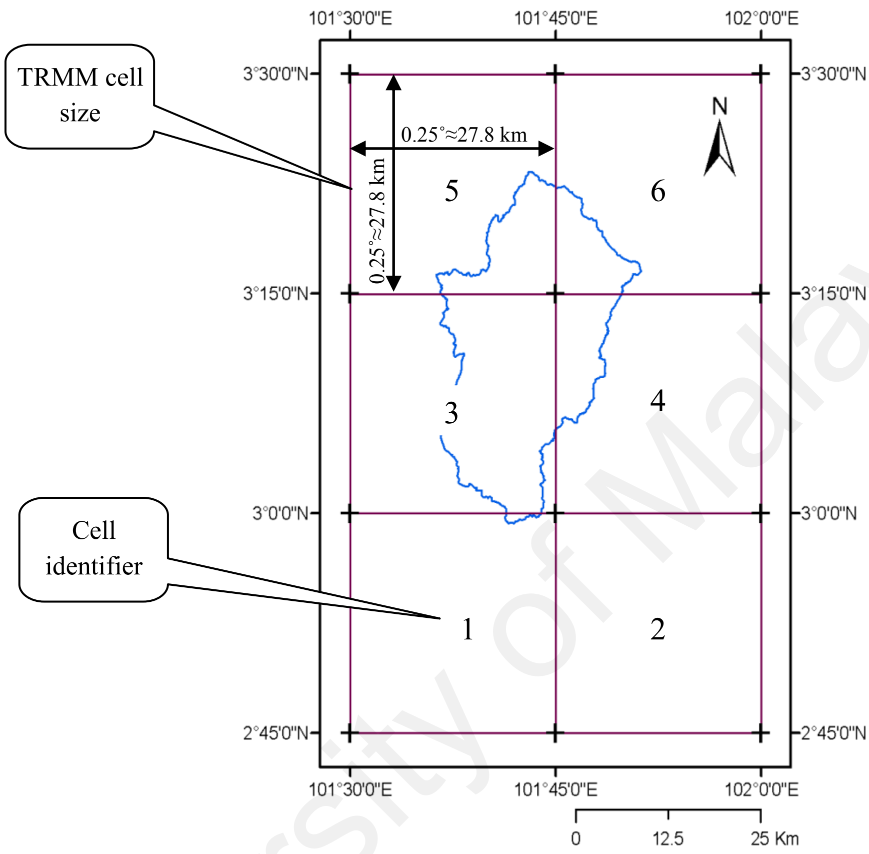

Figure 4.41: TRMM grid map overlaid on Klang watershed.

To evaluate the behavior of TRMM rainfall estimates with actual data, 3-hourly and total rainfall estimates of TRMM for the selected events were compared with gauge rainfall data in 6 cells. 3-hourly TRMM maps for the investigated events were plotted in Figure 4.42, 4.43, 4.44 and 4.45. The value in each cell represents the amount of rainfall acquired within 3 hours starting from 1.5 hour before and 1.5 hour after the specified time. To specify the hyetograph ordinates four pairs of digit is used. For example the first ordinate of TRMM hyetograph for event 6-May 2002 is shown with 06-06-05-02 which denotes the Time-Day-Month-Year respectively

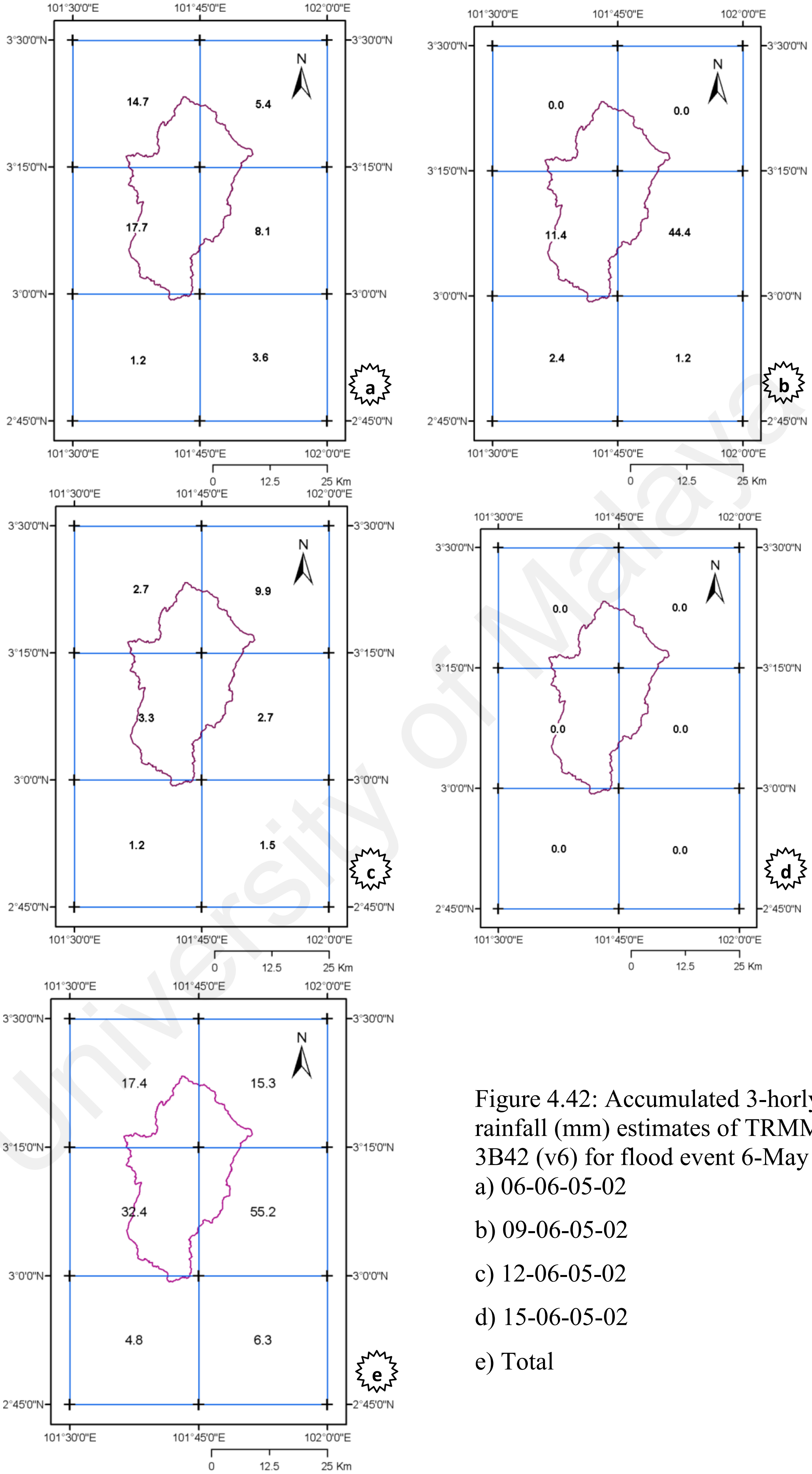

Figure 4.42: Accumulated 3-horly rainfall (mm) estimates of TRMM 3B42 (v6) for flood event 6-May 2002.

a) 06-06-05-02

b) 09-06-05-02

c) 12-06-05-02

d) 15-06-05-02

e) Total

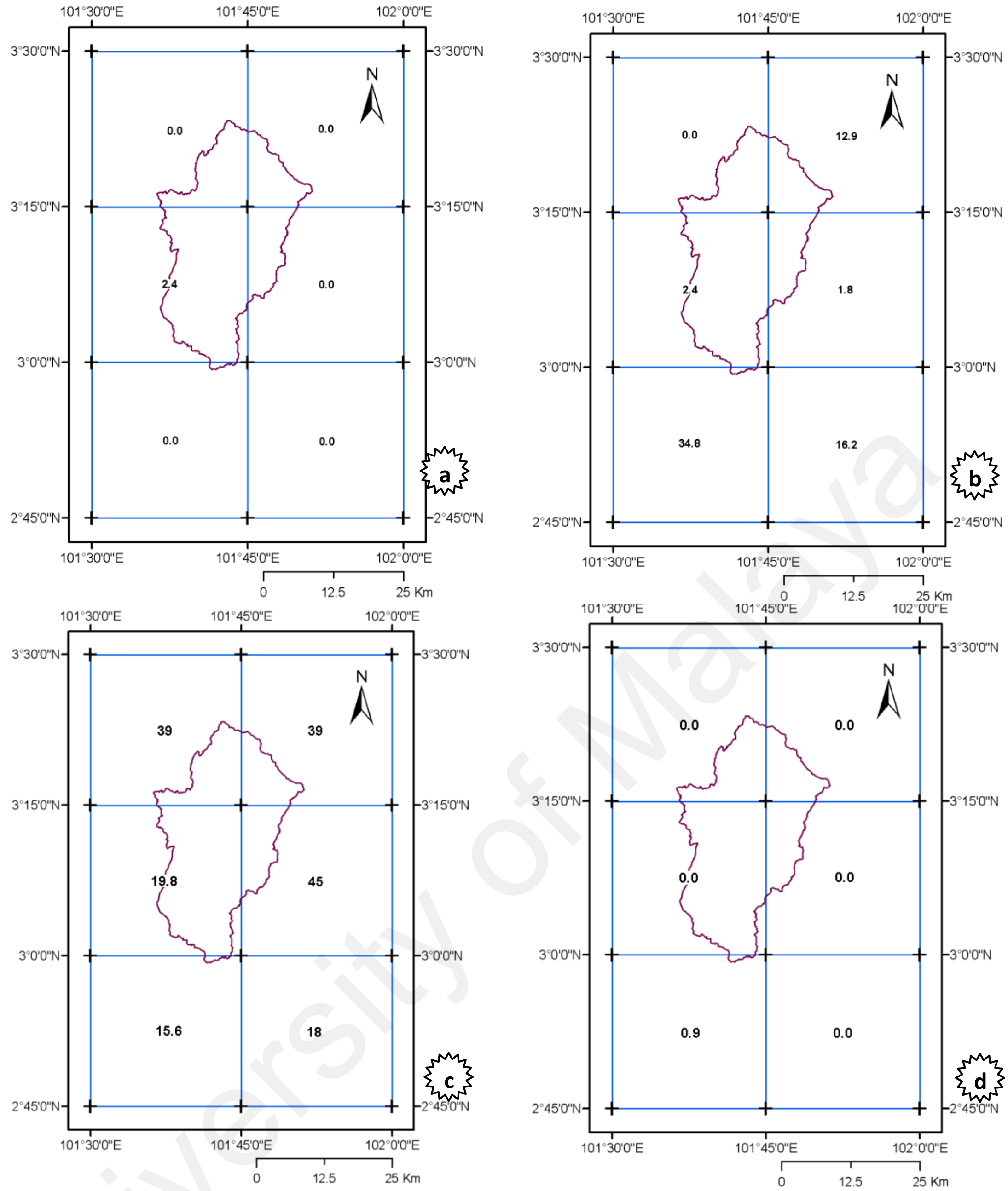

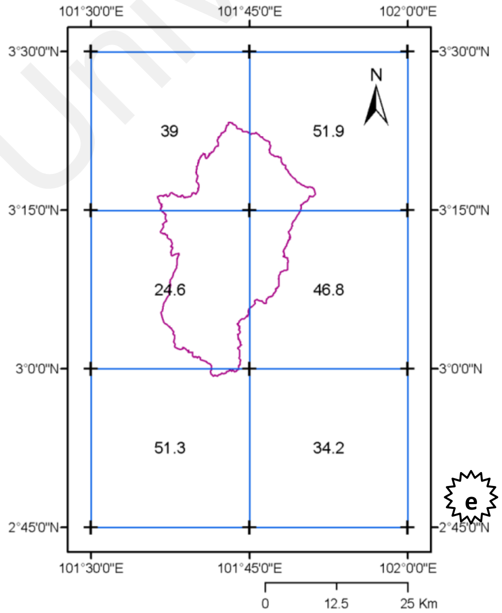

Figure 4.43: Accumulated 3-horly rainfall (mm) estimates of TRMM 3B42 (v6) for flood event 29-Apr 2002.

a) 06-29-04-02

b) 09-29-04-02

c) 12-29-04-02

d) 15-29-04-02

e) Total

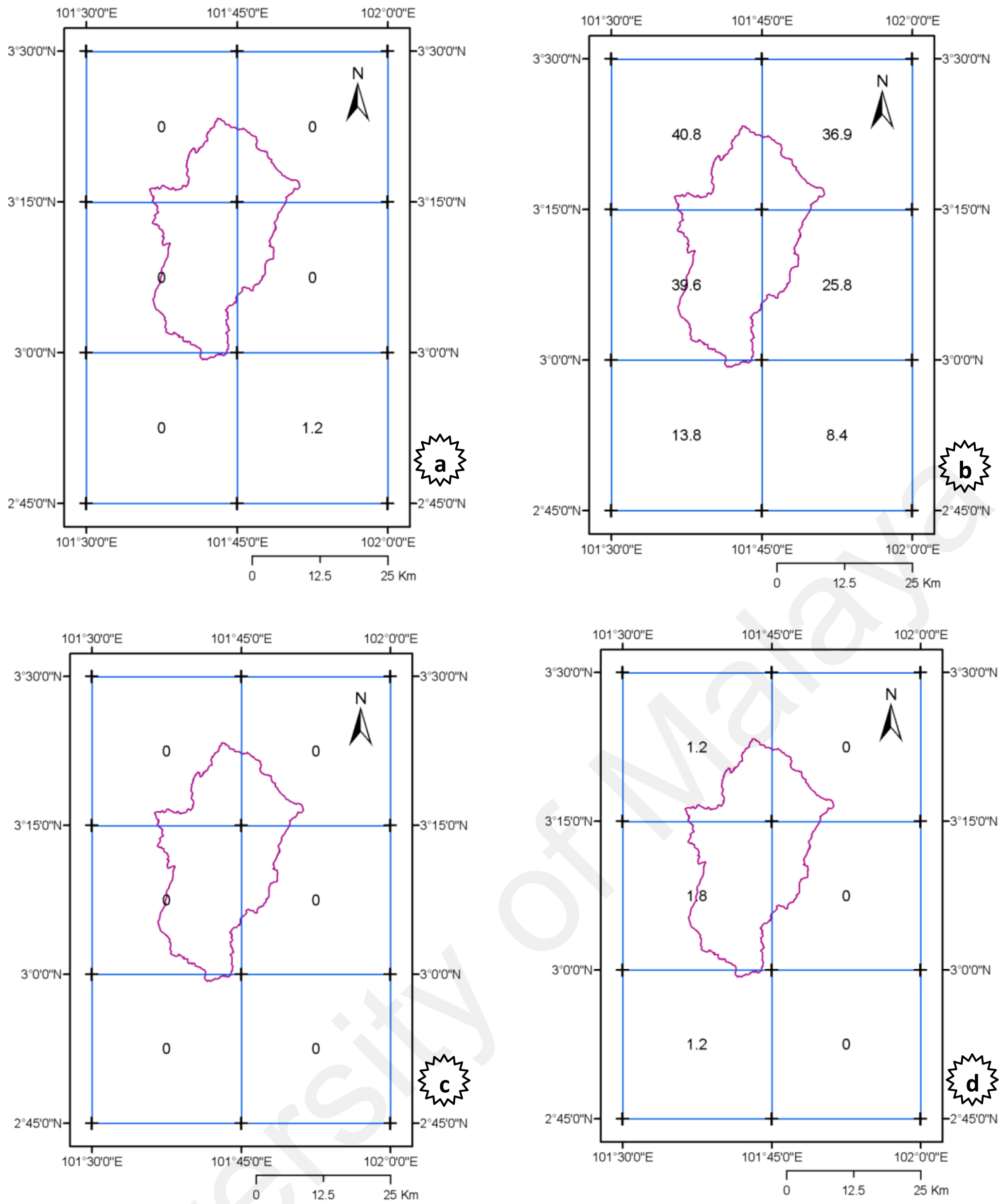

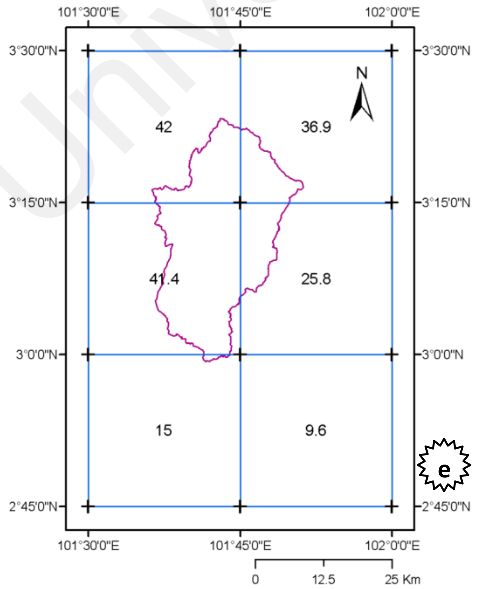

Figure 4.44: Accumulated 3-horly rainfall (mm) estimates of TRMM 3B42 (v6) for flood event 11-June 2002.

a) 09-11-04-02

b) 12-11-04-02

c) 15-11-04-02

d) 18-11-04-02

e) Total

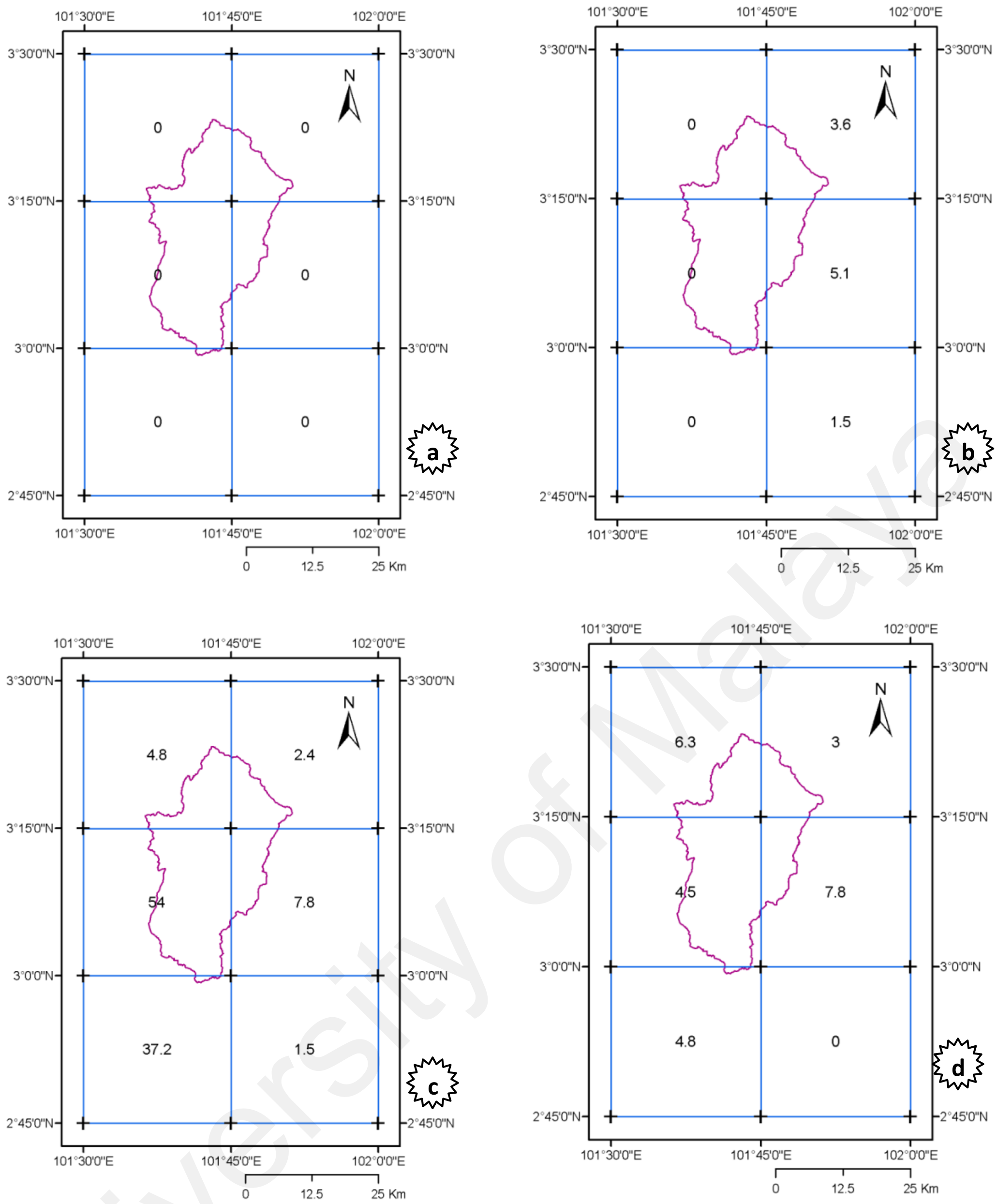

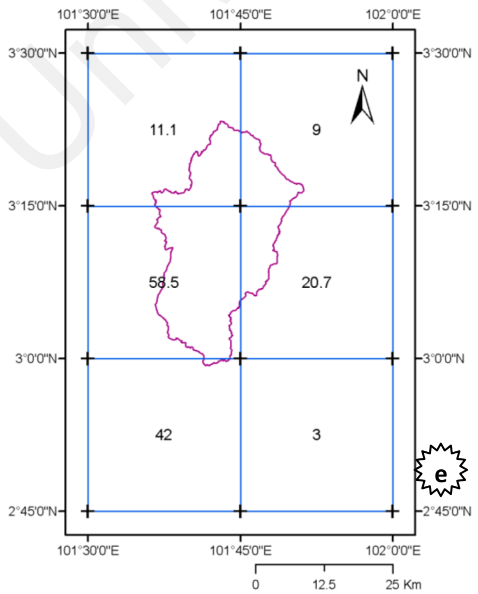

Figure 4.45: Accumulated 3-horly rainfall (mm) produced by TRMM 3B42 (v6) for rainfall event 21Dec2002.

a) 03-21-12-02

b) 06-21-12-02

c) 09-21-12-02

d) 12-21-12-02

e) Total

4.7.4 Cell-base comparison

Comparison is made between gauges rainfall (Gag.R) and TRMM rainfall (TRM.R) data. Accumulated rainfall was calculated from TRMM data for flood events observed in 6-May, 29-Apr, 11- Jun and 21-Dec in each cell. Then grid map resultants from interpolation of actual rainfall events showed in Figure 4.35 were crossed with the TRMM grid map showed in Figure 4.41. Weighted average rainfall for each cell was then calculated by using aggregation operation in ILWIS3.4. Percent of error (PE) for TRMM prediction were calculated for four investigated storms as demonstrated in Table 4.13. It is observed that rainfall estimates by TRMM algorithm are 37 % under estimate for four investigated events.

Table 4.13: Cell-base comparison of observed rainfall with TRMM estimates

Cell id	06-May			29-Apr			11-Jun			21-Dec		
	TRM.R	Gag.R	PE	TRM.R	Gag.R	PE	TRM.R	Gag.R	PE	TRM.R	Gag.R	PE
	mm	mm	%	mm	mm	%	mm	mm	%	mm	mm	%
1	4.8	34.8	-86	51.3	88.9	-42	15.0	35.1	-57	42.0	46.6	-10
2	6.3	34.9	-82	34.2	85.2	-60	9.6	35.1	-73	3.0	33.1	-91
3	32.4	42.0	-23	24.6	91.6	-73	41.4	47.5	-13	58.5	37.0	58
4	55.2	39.4	40	46.8	83.5	-44	25.8	32.5	-21	20.7	39.5	-48
5	17.4	29.5	-41	39.0	89.3	-56	42.0	31.9	31	11.1	25.1	-56
6	15.3	38.8	-61	51.9	86.5	-40	36.9	31.7	17	9.0	24.1	-63
Relative Bias			-42			-53			-19			-35

TRM.R: TRMM rainfall estimate,

Gag.R: Gauge Rainfall PE: Percent of Error

4.7.5 Comparison of total rainfall

Total amount of rainfall for specified storms was calculated from both gauge data and TRMM estimates. High correlation coefficients of 0.99 exist between the observed and TRMM estimates as shown in Table 4.14. However, negative bias indicates that TRMM rainfall data can estimate the total gauges rainfall by overall 35% less than actual data.

Table 4.14: Comparison of total rain depth estimated by TRMM and measured in rain gauges for investigated flood events

Even	Total TRM.R	Total Gag.R	PE
	mm	mm	%
06-May	21.9	31.3	-30
29-Apr	41.3	84.0	-51
11-Jun	27.7	42.7	-35
21-Dec	22.4	29.4	-24
Relative Bias			-35
Correlation coefficient			0.99

There is a close correlation (r=0.99) between observed and TRMM estimates for the total rainfall depth. In spite of that, there is no significant correlation for temporal pattern of storms. In other word, as shown in Figure 4.46 hyetograph ordinates derived from TRMM don't match with observed hyetographs of selected events.

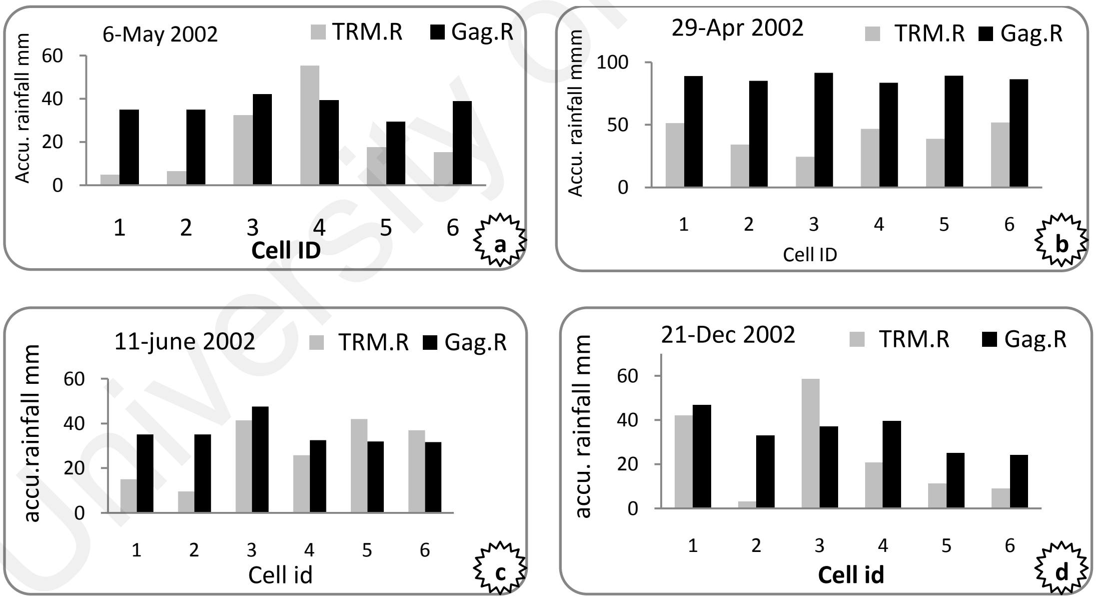

Figure 4.46: Spatial distribution of total rain depth over 6 TRMM cells.

a) Comparison of TRMM estimates with observed storm depth of 6-May 2002

b) Comparison of TRMM estimates with observed storm depth of 29-Apr 2002

c) Comparison of TRMM estimates with observed storm depth of 11-June 2002

c) Comparison of TRMM estimates with observed storm depth of 21-Dec 2002

4.7.6 Sub-watershed comparison

To calculate the amount of rain that falls in each sub-watershed, the accumulated rainfall map resultants from Kriging interpolation for investigated flood events were crossed with sub-watershed map. With the same way, accumulated TRMM estimates for the same events were crossed with sub-watershed map to calculate the amount of rain that falls in each sub-watershed resultants from TRMM estimates. Figure 4.47 demonstrates operation involved for calculating the rainfall in each sub-basin. The procedure was repeated for three other events.

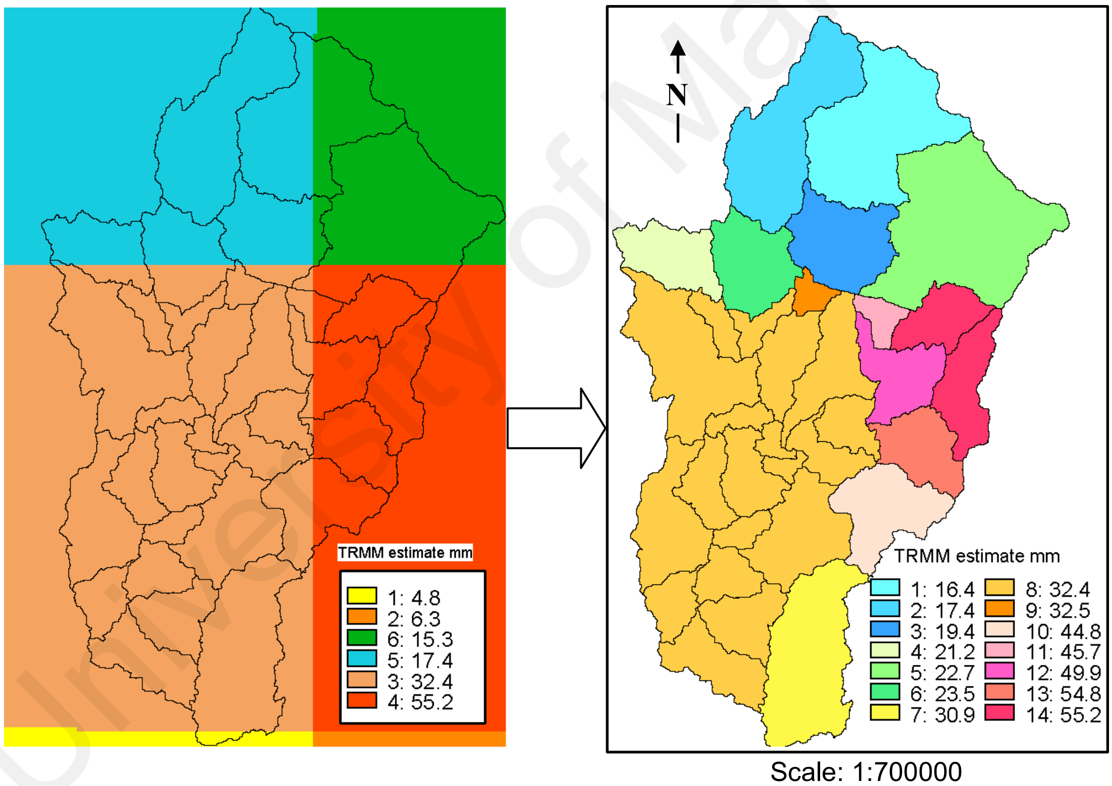

Figure 4.47: Sub-basins wiz estimation of accumulated TRMM rainfall (event 6-May) over Klang watershed. Crossing sub-watersheds with TRMM estimate result from event of 6-May 2002 (left). Groping the TRMM cell values based on sub-watersheds using ILWIS (right)

As it observed in Table 4.15 there is no significant correlation between two estimates. Moreover,

Table 4.15: Caparison the amount of rain that falling to the sub-watershed from gauge rainfall and TRMM rainfall estimates.

SW	6May		29Apr		11Jun		21Dec	
	Gag	TRM	Gag	TRM	Gag	TRM	Gag	TRM
	mm	mm	mm	mm	mm	mm	mm	mm
s1	24.8	17.4	79.3	39.0	19.3	42.0	22.8	11.1
s2	31.5	16.4	79.5	45.4	30.7	39.5	20.6	10.1
s3	35.3	19.4	82.8	38.6	79.0	41.3	20.7	17.1
s4	41.7	22.7	93.6	50.7	31.4	34.9	28.4	11.7
s5	38.3	55.2	93.9	46.8	33.0	25.8	31.4	20.7
s6	42.9	55.2	102.1	46.8	30.3	25.8	32.4	20.7
s7	43.5	45.7	97.4	37.6	65.4	32.3	33.1	35.6
s8	32.8	32.2	84.3	24.8	100.2	41.4	24.5	55.9
s9	21.1	23.5	82.4	33.1	51.9	41.8	22.7	29.6
s10	23.9	21.2	102.7	35.3	26.6	41.8	23.9	22.7
s11	41.9	32.4	91.6	24.6	79.9	41.4	37.7	56.5
s12	45.8	32.4	91.6	24.6	75.2	41.4	32.7	56.5
s13	44.0	49.9	95.1	41.7	49.3	29.4	27.4	29.0
s14	42.0	54.8	80.8	46.4	37.3	26.1	36.0	21.3
s15	31.1	32.4	91.2	24.6	77.3	41.4	28.6	56.5
s16	34.0	32.4	110.2	24.6	58.0	41.4	17.4	56.4
s17	51.2	32.4	97.2	24.6	58.7	41.4	31.5	56.5
s18	58.0	32.4	89.9	24.6	53.4	41.4	23.9	56.5
s19	57.4	32.4	81.9	24.6	44.4	41.4	19.8	56.5
s20	51.1	32.4	88.1	24.6	45.9	41.4	28.8	56.5
s21	38.7	32.4	73.8	24.6	29.0	41.4	54.6	56.5
s22	31.6	30.9	75.3	26.0	28.6	40.0	46.0	55.7
s23	43.9	32.4	90.7	24.6	42.1	41.4	31.3	56.5
s24	36.1	32.4	80.9	24.6	32.4	41.4	53.1	56.5
s25	36.9	32.4	88.3	24.6	30.9	41.4	31.5	56.5
s26	33.0	32.4	84.1	24.6	18.4	41.4	37.6	56.5
s27	28.7	32.4	79.5	24.6	21.8	41.4	54.9	56.5
s28	28.8	32.4	78.0	24.6	21.7	41.4	51.0	56.5
s29	33.4	32.4	83.6	24.6	24.0	41.4	39.3	56.5
s30	38.5	44.8	69.0	36.7	22.4	32.9	54.0	37.0
s31	54.3	32.5	86.1	24.7	52.5	41.3	20.8	56.3
s32	58.5	32.4	85.0	24.6	46.5	41.4	17.1	56.5
s33	27.3	32.4	101.1	24.6	56.7	41.4	22.0	56.5
Mean	38.8	33.5	87.6	30.8	44.7	38.8	32.0	44.0
STD	10.0	9.8	9.2	8.8	20.9	5.2	11.4	17.5
R	0.3		0.1		0.2		0.3	

4.8 Satellite-based Flood Modeling with HEC-HMS

The main objective of this research is achieved by calibrating a rainfall-runoff model for the selected flood event with DEM-derived databases from Topo-DEM and SRTM-DEM and TRMM. Several numerical processes are involved to estimate flood magnitude. The processes mainly include constructing HEC-HMS components which are calculation of loss rate, hydrograph transformation, base flow separation and flood routing.

4.9 Constructing HEC-HMS components

HEC-HMS utilizes three components for rainfall runoff simulation.

4.9.1 Watershed elements

Watershed elements including sub-watersheds, junctions, reaches and hydraulic structures were derived from both Topo-DEM and STRM-DEM by using Geo-HMS. The GeoHMS creates a file named "basin.hms". This file can directly be read with HEC-HMS. It shows the sub-basins and their internal connections.

Figure 4.48 demonstrates the watershed model derived from Topo-DEM. Each element contains the necessary information regarding the type of process. For instance, by clicking on s1, element name, downstream element, area, loss method, transform method and baseflow method used in that element are identified.

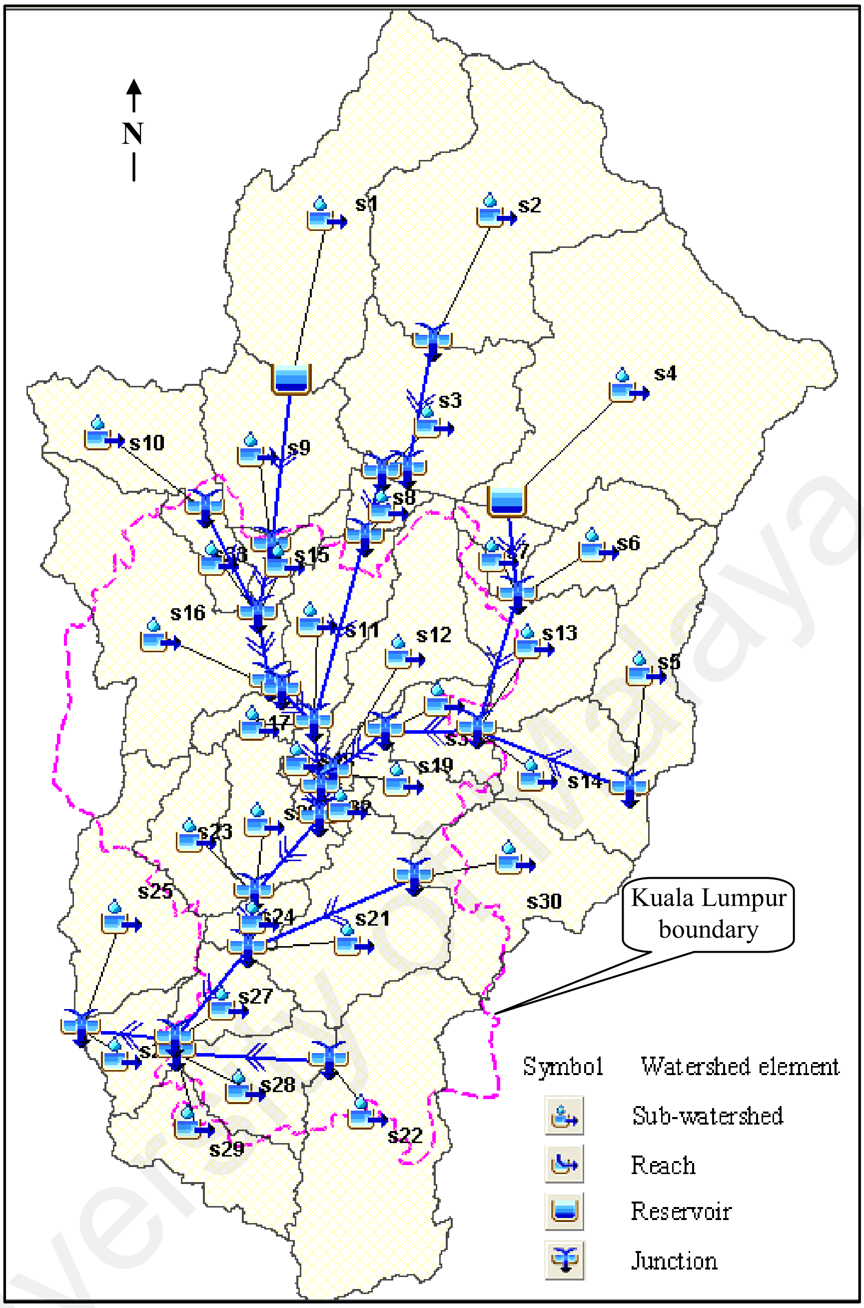

Figure 4.48: HEC-HMS model for Klang watershed

4.9.2 Loss method

The HEC-HMS provides several infiltration loss methods. However, SCS method is the possible method with available data. Default value for λ is 0.2 in HEC-HMS model. However, HEC-HMS offers the possibility to calculate I_a from any other acceptable value for λ. Value for λ=0.2 and λ=0.05 was used to calculate modified CN values as illustrated in Table 4.16.

Table 4.16: Loss estimation parameters based on SCS method

SW	WA	$CN_{0.2}$	IA		$S_{0.2}$	$I_{a0.2}$	$I_{a0.05}$	$S_{0.05}$	$CN_{0.05}$
	km^2		km^2	%	mm	mm	mm	mm	
sw1	50.47	44	0.01	0.03	323.2	64.65	16.16	1022.95	29
sw2	56.74	42	0.15	0.27	350.7	70.15	17.54	1123.61	27
sw3	29.26	61	0.88	3.02	162.3	32.48	8.12	463.45	47
sw4	75.65	46	0.00	0.00	298.1	59.63	14.91	932.16	31
sw5	19.46	41	0.00	0.00	365.5	73.10	18.28	1178.12	26
sw6	15.20	48	0.48	3.16	275.1	55.03	13.76	849.94	33
sw7	5.85	70	1.03	17.6	108.8	21.77	5.44	292.57	59
sw8	4.56	82	1.77	38.7	55.76	11.15	2.79	135.55	75
sw9	24.18	77	8.53	35.2	75.87	15.17	3.79	193.17	68
sw10	19.69	61	2.39	12.1	162.3	32.48	8.12	463.45	47
sw11	16.34	87	11.16	68.3	37.95	7.59	1.90	87.10	83
sw12	21.23	86	9.72	45.8	41.35	8.27	2.07	96.11	81
sw13	19.32	81	6.05	31.3	59.58	11.92	2.98	146.29	74
sw14	18.91	77	7.55	39.9	75.87	15.17	3.79	193.17	68
sw15	6.38	92	1.85	28.9	22.09	4.42	1.10	46.73	90
sw16	43.29	82	17.88	41.2	55.76	11.15	2.79	135.55	75
sw17	5.06	86	1.75	34.5	41.35	8.27	2.07	96.11	81
sw18	3.25	86	1.48	45.5	41.35	8.27	2.07	96.11	81
sw19	10.33	89	6.56	63.5	31.39	6.28	1.57	70.02	85
sw20	14.12	85	5.91	41.8	44.82	8.96	2.24	105.46	80
sw21	27.40	87	13.47	49.1	37.95	7.59	1.90	87.10	83
sw22	47.49	87	13.44	28.3	37.95	7.59	1.90	87.10	83
sw23	11.94	88	4.29	35.9	34.64	6.93	1.73	78.40	84
sw24	5.11	89	2.40	46.9	31.39	6.28	1.57	70.02	85
sw25	25.97	89	16.33	62.8	31.39	6.28	1.57	70.02	85
sw26	9.52	88	5.00	52.5	34.64	6.93	1.73	78.40	84
sw27	10.02	82	6.50	64.8	55.76	11.15	2.79	135.55	75
sw28	15.29	85	2.78	18.2	44.82	8.96	2.24	105.46	80
sw29	17.62	76	0.84	4.76	80.21	16.04	4.01	205.93	67
sw30	26.57	84	14.97	56.3	48.38	9.68	2.42	115.14	78
sw31	10.17	89	7.91	77.7	31.39	6.28	1.57	70.02	85
sw32	2.84	89	1.73	60.9	31.39	6.28	1.57	70.02	85
sw33	6.42	90	2.79	43.4	28.22	5.64	1.41	61.95	87
Min	2.84	41	0.00	0.00	22.09	4.42	1.10	46.73	18
Max	75.65	92	17.88	77.7	365.5	73.10	18.28	1178.12	84
Mea	20.47	77	5.38	34.9	95.69	19.14	4.78	271.60	61
Std	17.05	16	5.22	22.8	103.6	20.72	5.18	339.65	21
Sum	675.6		177.6						

SW: Sub- watershed

IA: Impervious area

CN: Curve number

$I_{a\,0.2}$: Initial abstraction (derived from Eq.2.4 with λ=0.2)

$I_{a\,0.05}$: Initial abstraction (derived from Eq.2.4 with λ=0.05)

$S_{0.2}$: The potential maximum storage derived from Eq.2.5

$S_{0.05}$: The potential maximum storage derived from Eq.2.6

4.9.3 Selected rainfall-runoff events

The flood event of May 6 2002 is a well-defined, storm-induced event that hit almost the entire watershed. The spatial coverage of this event indicates that the storm cell had to be centered at the watershed during the heavy outburst. Figure 4.24 depicts this event from 15 min observations at Suleiman bridged (gauge ID 3116430). Almost no rainfall has observed before this event, and the streamflow was clearly at its minimum base-flow level. The flood peak has a very simple, classical shape that makes this event excellent for the calibration. Furthermore, the magnitude of this event is noticeable. Flood events of 29-Apr, 11-June and 21-Dec are used for validation.

4.9.4 Unit hydrograph transformation

SCS transformation function in HEC-HMS provides two different graph types to define the shape of the unit hydrograph. According to Scharffenberg and Fleming (2008) the "Standard" shape is generally applicable across the United States. The "Delmarva" shape has been found to be applicable in coastal plain areas; therefore, Delmarva shape was employed in this study.

4.9.5 Kinematic wave routing method

The component of kinematic wave routing method is shown in Figure 4.49 for the reach RSW11. It employs channel geometries and Manning's *n* roughness coefficient. In urban areas of Klang watershed, natural drainage system is rarely observed. Most of channels have uniform geometric cross section made by concrete. Therefore no significant changes are expected for Manning's *n* along the reach elements. The total length of the reach element measured from maps of the watershed.

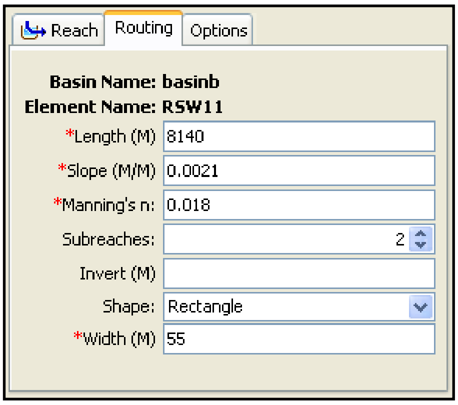

Figure 4.49: Component of kinematic wave routing method for the reach RSW11

Based on the field observations and using the available design reports and maps for the flood mitigation in Klang watershed such as DID (1994) and DID (2003b), routing parameters was determined for the reaches as listed in Table 4.17.

Table 4.17: Routing parameters based on kinematic wave method

Reach name	Length (m)	Bed slope (m:m)	Manning's n	Shape	wide (m)	Slop side xH:1V
RSW9	9500	0.0052	0.035	Rectangle	30	-
RSW15	3170	0.0025	0.035	Rectangle	40	-
RSW33	4250	0.0042	0.035	Rectangle	30	-
RSW16l	3650	0.0011	0.018	Rectangle	30	-
RSW17	1650	0.0006	0.018	Rectangle	50	-
RSW3l	6230	0.0064	0.018	Rectangle	40	-
RSW8	2850	0.0049	0.020	Rectangle	55	-
RSW11	8140	0.0021	0.018	Rectangle	55	-
RSW18	3155	0.0003	0.018	Rectangle	50	-
RSW7	4170	0.0079	0.020	Rectangle	40	-
RSW13	5890	0.0015	0.018	Trapezoid	50	2
RSW14	7280	0.0058	0.018	Rectangle	30	-
RSW31	2500	0.0016	0.018	Rectangle	50	-
RSW19	2500	0.0004	0.018	Rectangle	50	-
RSW18s	723	0.0028	0.018	Rectangle	55	-
RSW32	3400	0.0003	0.018	Rectangle	60	-
RSW20	3780	0.0024	0.018	Rectangle	60	-
RSW24	2000	0.0005	0.018	Trapezoid	70	2
RSW21	7740	0.0026	0.018	Rectangle	30	-
RSW27	4500	0.0007	0.018	Trapezoid	75	2
RSW28	5000	0.0044	0.018	Trapezoid	30	2
RSW26s	500	0.0020	0.018	Trapezoid	30	2
RSW26	3320	0.0003	0.018	Trapezoid	80	2

4.9.6 Reservoir Flood routing method

The HEC-HMS provides several storage-outflow relationships for reservoir routing. Those are elevation-storage-outflow or elevation-area-outflow relationship that is depending on the characteristics of the reservoir, the outlet, and the spillway. There are two major reservoirs in Klang watershed which are Batu dam and Klang gate dam. According to Figure 4.50 and Figure 4.51 and other complementary information collected from Dam division of DID at Jalan Sultan Salahuddin Kuala Lumpur a storage-Discharge relationship was established for Klang Gate dam and Batu dam (see Figure 4.52 and 4.53)

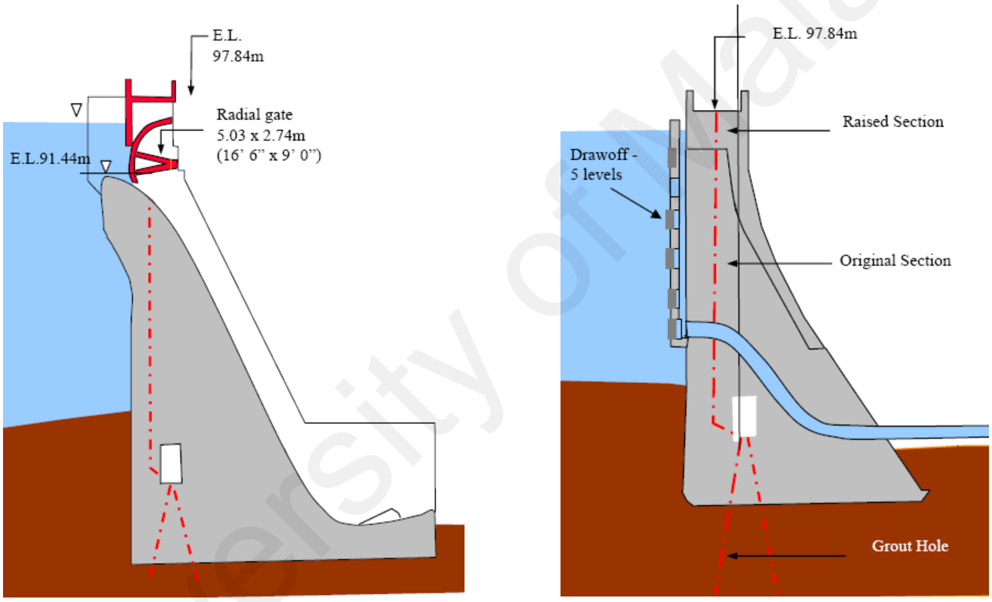

Figure 4.50: Cross section of Klang Gate Dam. Taken from Gibson and Dodge (1983)

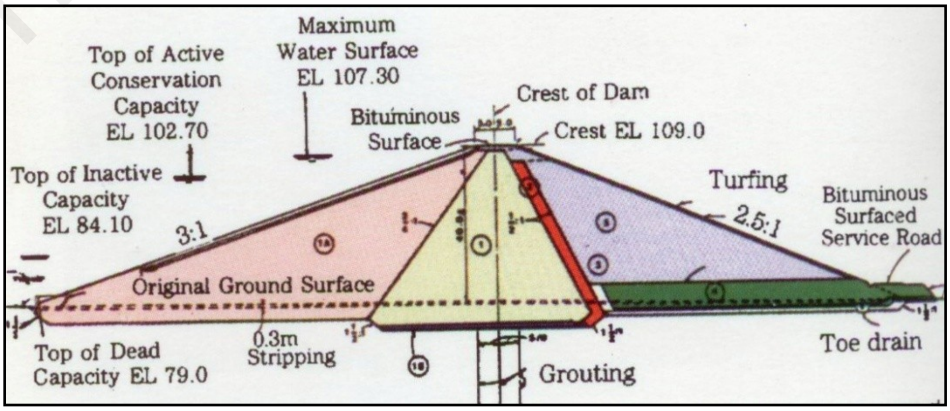

Figure 4.51: Cross section of Batu Dam. Taken from DID

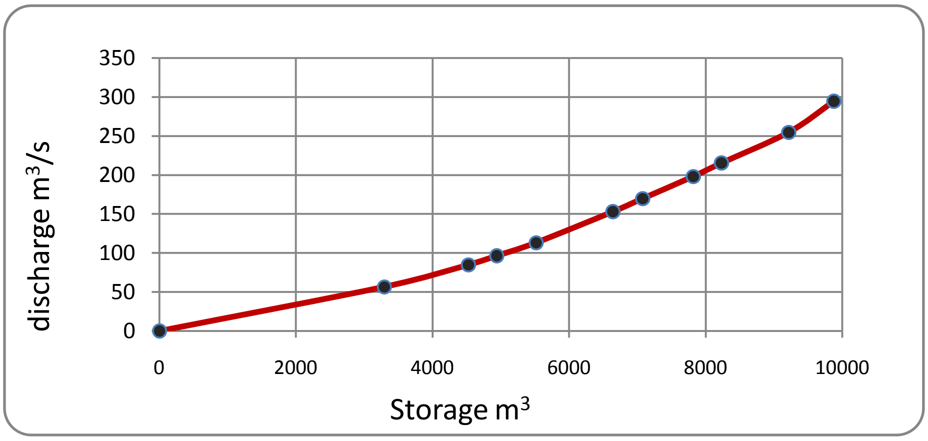

Figure 4.52: Storage-discharge relationship of Klang Gate dam

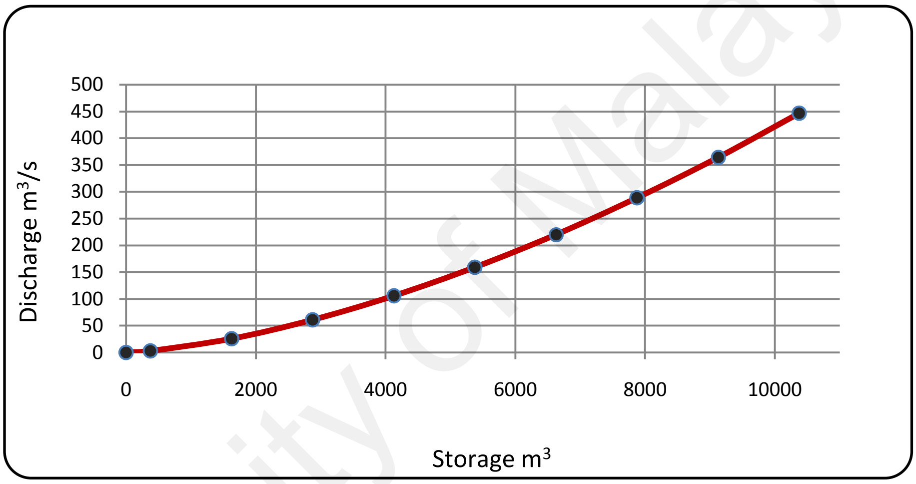

Figure 4.53: Storage-discharge relationship of Batu dam

4.10 Meteorological model

The first suitable rainfall event to calibrate the model is the event 6-May. Rainfall hydrograph with 15 minutes time interval for all precipitation gauges that contribute to this event were interred to the model. As an example Figure 4.54 showed storm hyetograph of rain gauge 3116003. Each precipitation gauge has its own hyetograph that define the temporal pattern of storm.

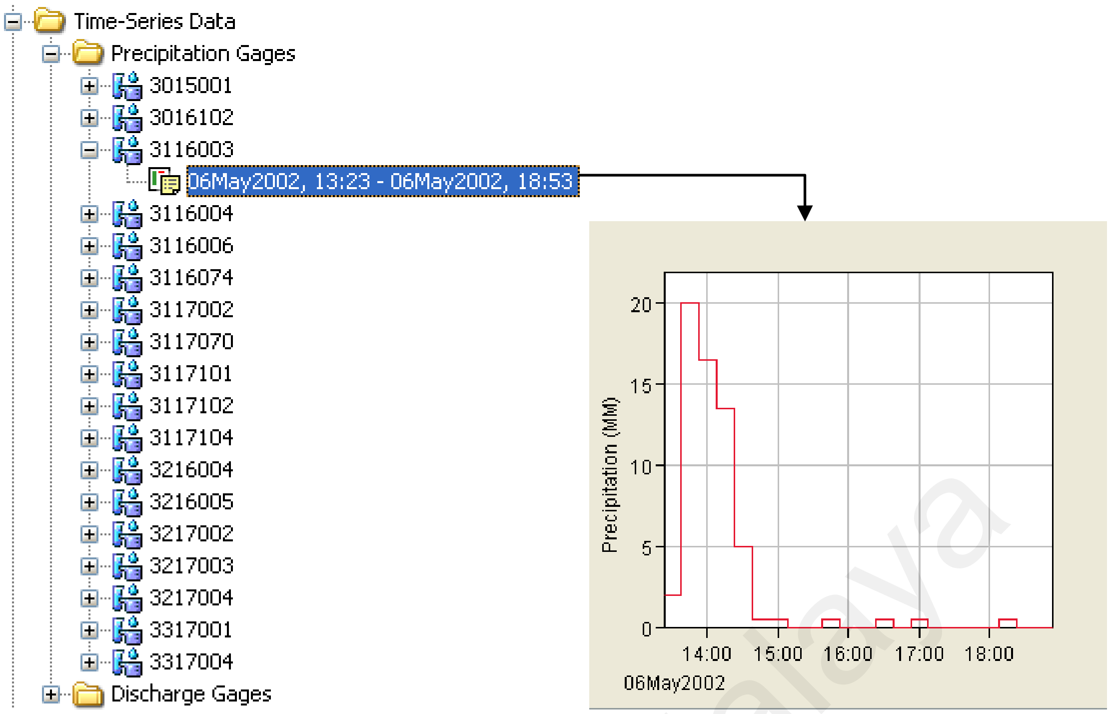

Figure 4.54: Illustration of rain gauge 3116003 and its hyetograph for event 6-May

4.11 HEC-HMS output for flood event 6-May

The model was set up for event 6-May and simulation run was created through run manager. To answer the research questions several possible conditions were examined.

4.11.1 Running for Topo-DEM derived parameters and rain gauges data (Run1)

The HEC-HMS model was setup with DEM-derivatives of Topo-DEM and observed rainfall hyetographs on 6 may 2002. Corresponding observed stream flow data were interred to the model. The model was set to SCS method for calculating the losses and required data were interred. In this stage traditional SCS equation with CN value from Table 4.2 (remarked in Table 4.15 with $\boldsymbol{CN_{0.2}}$) was used for estimation of losses. Kinematic wave routing method was used for flood routing and relevant parameters were used from Table 4.16. Meteorological model was set for flood event 6-May and corresponding rainfall hyetographs were specified for each gauging station. Starting and ending of rainfall-runoff process is set in control specification menu. Precipitation gauges were specified in the Time-Series Data menu and observed stream flow data were interred in the Discharge Gauges menu. Storage-Discharge function for Klang Gate and Batu dams were specified in Paired Data management menu. Time interval was set for 15 minutes for both rainfall and stream flow data. The base flow at stream flow stations were set to "no base flow" but the base flow have been subtracted from observed flow hydrographs at those stations. HMS provides the result in different forms graphically and tabular. Result can be viewed in Global Summary table, element graph, element Summary table and element time series table. To track the behavior of the model for different scenarios, the flood hydrograph for sub basin SW13, Sulaiman Bridge and outlet of the Klang watershed are discussed. Result for other elements is provided in a form of global Summary tables in Appendix C. The following are simulation results for the selected elements. Figure 4.55 shows the rainfall and corresponding hydrograph for sub-watershed SW13 and comparison of observed and simulated hydrograph are demonstrated in Figure 4.56.

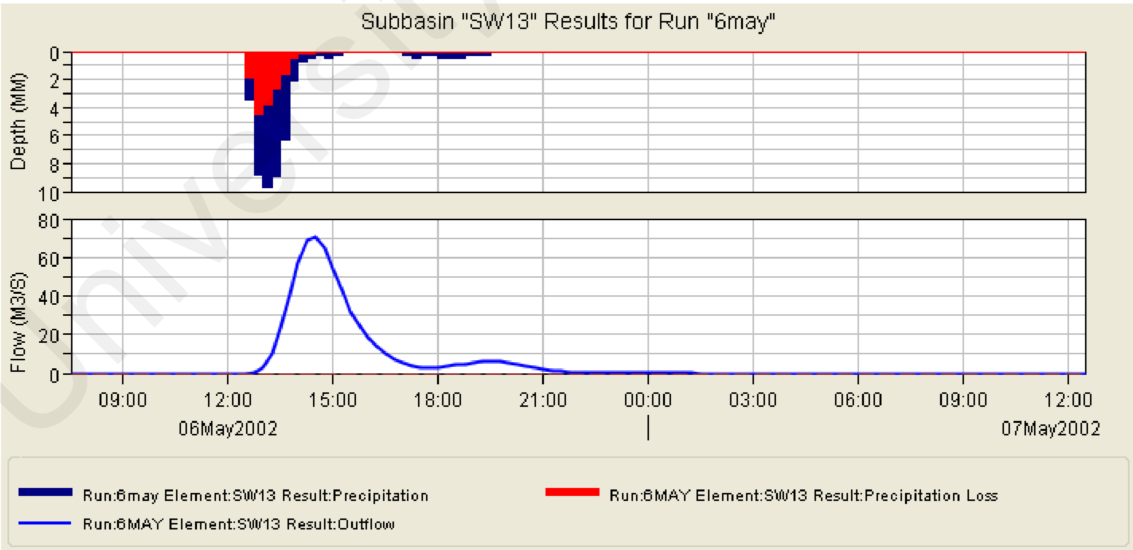

Figure 4.55: Flood hydrograph resultant from event 6-May in sub-watershed SW13

Primary flow simulation at Sentul (ID: 3116434) and Tun Razak (ID: 3116433) stations showed inconsistencies when comparing observed streamflow at Sentul and Tun Razak station and there is no good correlation between simulated and observed peak flow and time of peak at those stations. It may be due to constructing flood diversion from Gombak River to Batu impounding reservoir and from Keroh River to Jinjang reservoir (see Figure 4.56). There is no enough information available for their storage-discharge relationships and the magnitude of flow that divert to the reservoirs. Therefore many uncertainties associate with flood hydrograph at those stations. Consequently, calibration of the model is followed based on observed flow at Sulaiman Bridge station.

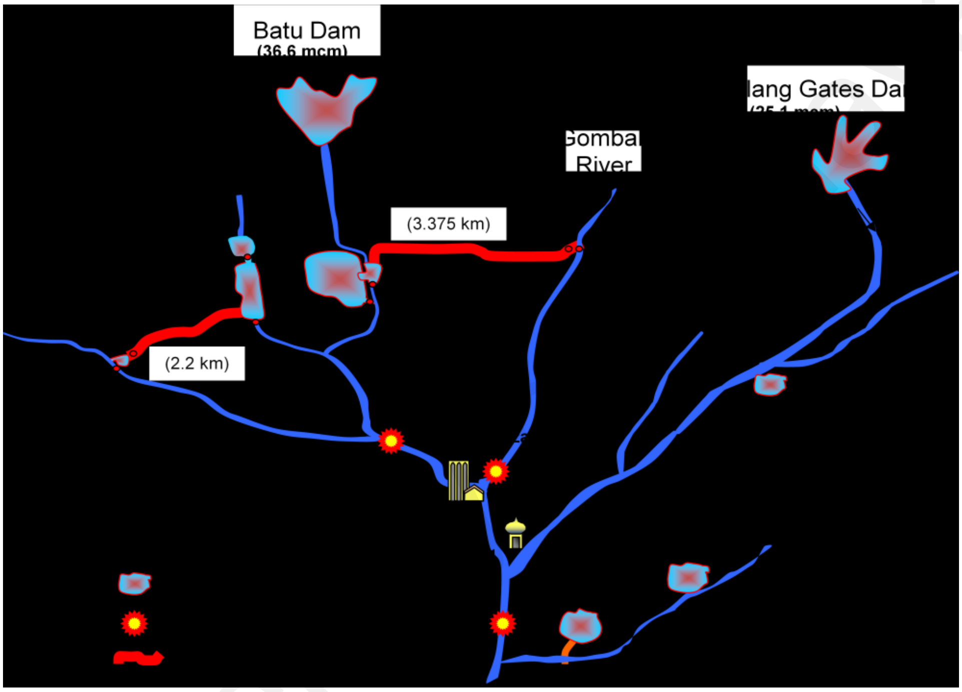

Figure 4.56: Schematic illustration flood diversion channels of Klang watershed

A significant correlation coefficient of 0.93 is existed between observed and calculated hydrograph (see Figure 4.57). Based on Nash-Sutcliffe efficiency simulated hydrograph can explain the shape of observed hydrograph by 86%. Surprisingly, time of peak for simulated flood event 6-May completely match with the observed time of peak at Sulaiman Bridge station.

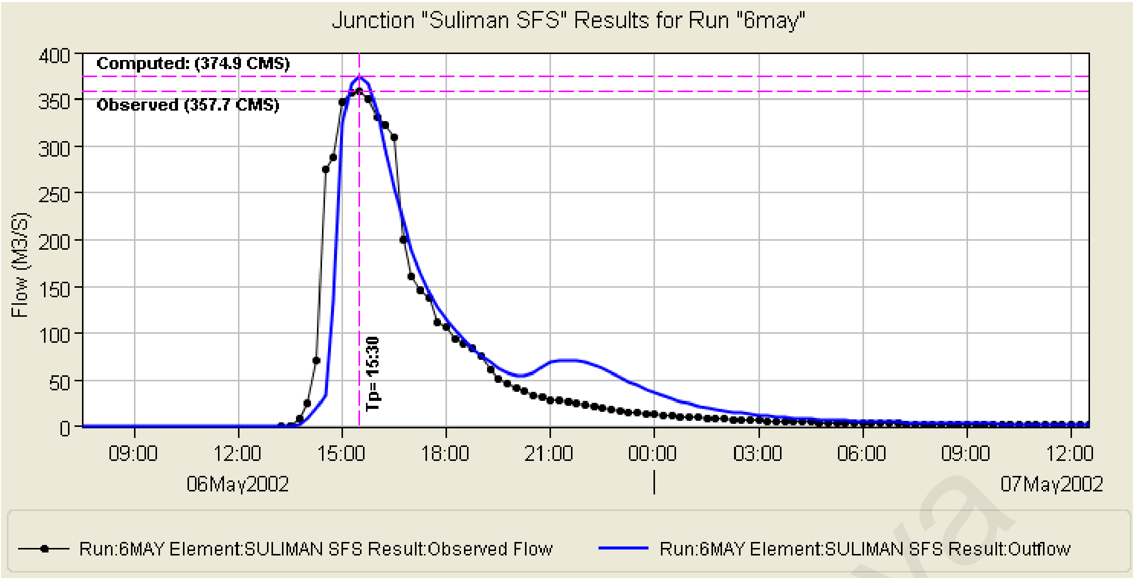

Figure 4.57: Observed and simulated flood hydrograph resultant from event 6-May at Sulaiman Bridge.

Predicted flood hydrograph at outlet of Klang watershed is shown in Figure 4.58. Computed peak flow at outlet occurs at 16:15 6-May with magnitude of 628.3 m^3/s

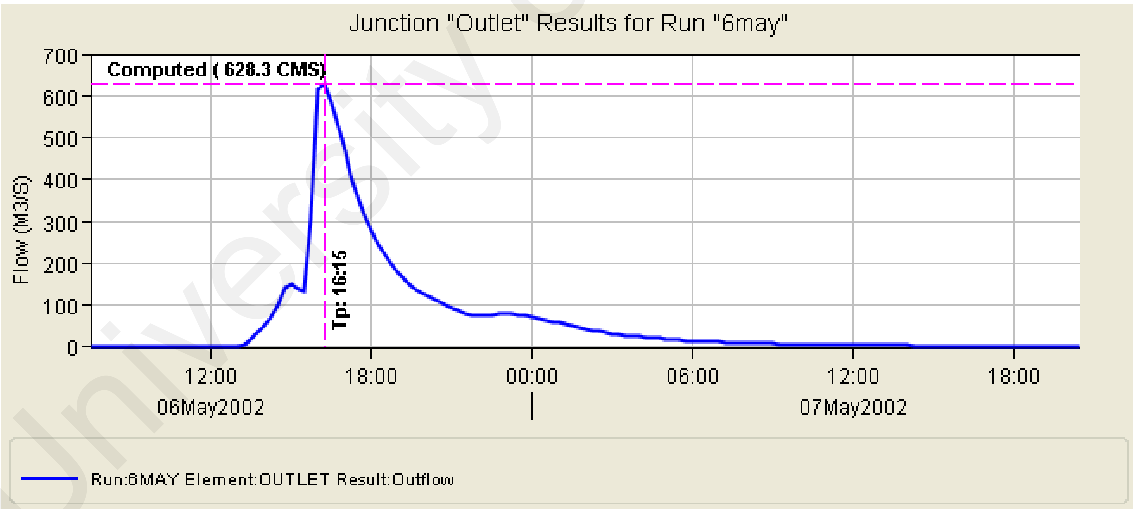

Figure 4.58: Computed flood hydrograph resultant from run1 at watershed outlet

4.11.2 Running for modified CN (Run2)

The Initial Abstraction ratio (I_a/S, orλ) in the SCS method was assumed in its original development to have a value of 0.20 (see Eq.2.3 and 2.4). Hawkins et al.(2002a) have investigated this assumption using event rainfall-runoff data from several hundred plots, and λ values determined by two different methods. Results indicated that λ value of about 0.05 gives a better fit to the data and gives more appropriate results for use in runoff calculations. The effects of this change are shown in terms of calculated runoff depth and hydrograph peaks, CN definition, and in soil moisture accounting. In this run, loss estimation parameters including CN and I_a was changed to new $CN_{0.5}$ and $I_{a\,(0.05)}$ in HMS model and the other components of the model was remained the same. As expected the flood simulation results was significantly improved. A perfect simulation for Peak flood, time to peak and volume were found for this event. Flood hydrograph at SW13, Sulaiman Bridge and outlet of the watershed are presented in Figure 4.59, 4.60 and 4.61. Summary results of flood simulation at Sulaiman Bridge station are listed in Table 4.18. The Nash-Sutcliffe efficiency is decreased from 86% to 85%.

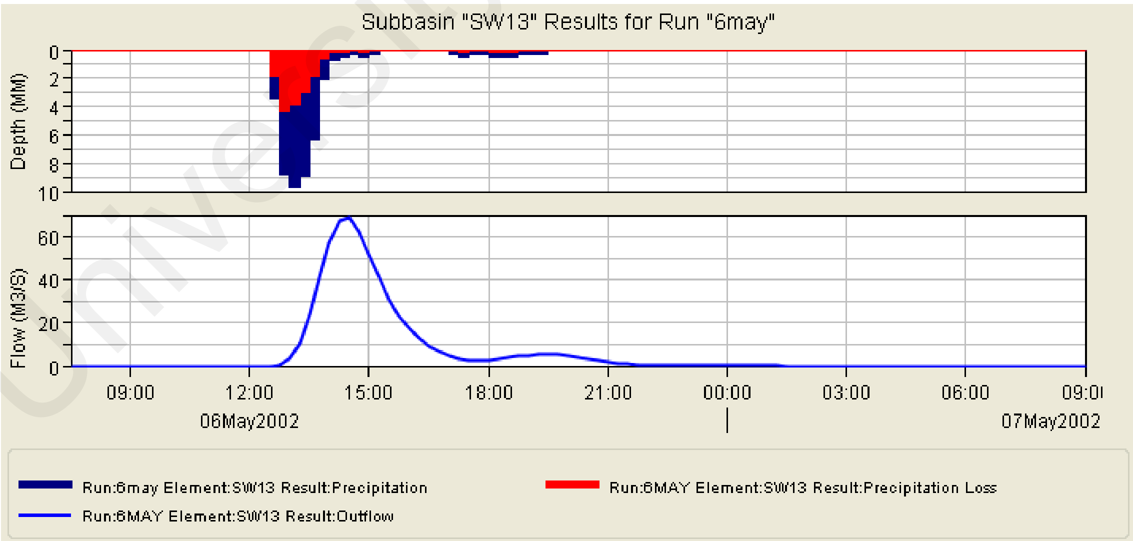

Figure 4.59: Flood hydrograph resultant from Modified CN in sub-watershed SW13

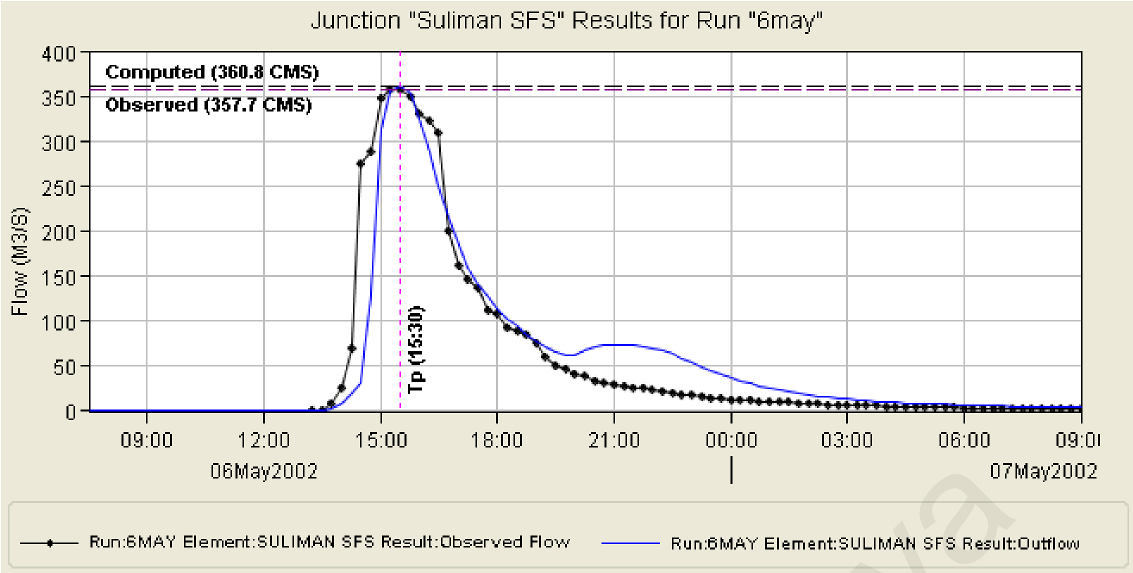

Figure 4.60: Observed and simulated flood hydrograph resultant from modified-CN for event 6-May at Sulaiman Bridge.

Table 4.18: Summary results of for flood event of 6 May 2002 at Sulaiman bridge station

Summary results	Computed	Observed
Peak outflow m^3/s	360.8	357.7
Total outflow mm	10.78	9.83
Date/time of peak outflow	6May2002,15:30	6May2002,15:30

Predicted flood hydrograph at outlet of Klang watershed for Run2 is shown in Figure 4.61. No change is observed for time of peak but peak discharge is decreased about 2%.

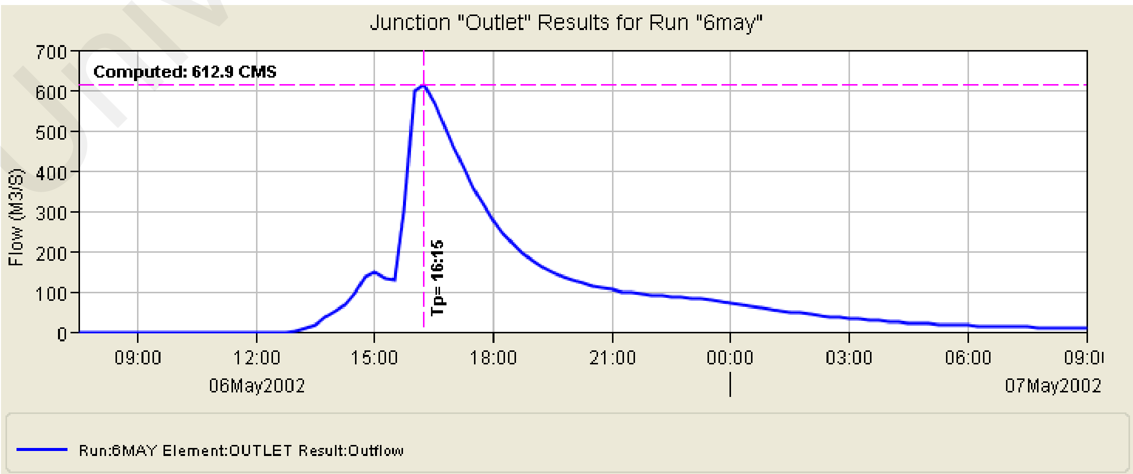

Figure 4.61: Computed flood hydrograph resultant from modified CN in sub-watershed SW13

4.11.3 Running for SRTM-derived sub-watershed area (Run3)

According to the result for Run2 it is considered that Run2 is the optimized flood simulation and therefore it can consider as reference for impact assessment of investigated parameters. To assess the performance of SRTM-derivatives, the sub-watershed area derived from SRTM-DEM were substituted with the sub-watershed areas derived from Topo-DEM in the HEC-HMS model. The other parameters were remained the same. Computed flow hydrograph for sub-watershed SW13 is shown in Figure 4.62. Total loss at SW13 is 17 mm and total direct runoff is about 27 mm. computed peak flow for this sub-basin is $71.3\ m^3/s$. Observed and computed flood hydrograph at Sulaiman Bridge is illustrated in Figure 4.63. As it evident time of peak does not change but the peak value is decreased from 360.8 (m^3/s) to 316.5 (m^3/s). The NSE is significantly decreased from 85% to 78% and gives 11% under estimate for peak discharge. The RMSE increased from 37 to 45 which indicate 17% growth in RMSE.

It is important to know that the total drainage area derived from Topo-DEM and SRTM-DEM at Sulaiman Bridge is 464.6 km^2 and 460.5 km^2 respectively. This means that Topo-DEM depict watershed area about 1% larger than SRTM-DEM at that particular point. Whereas computed peak flood is decreased about 11% when watershed areas derived from SRTM-DEM is served. It is may be due to existing discrepancies between two DEM-derived watershed boundaries which affect other input parameters such as rainfall, impervious area, watershed slope etc. Moreover the total volume of the outflow is well simulated when watershed area derived from SRTM-DEM is served by HEC-HMS. Figure 4.64 illiterates predicted flood hydrograph at the watershed outlet for Run3. Peak discharge is decreased from 612.9 m^3/s to 562 m^3/s which indicate about 8% reduction in peak discharge.

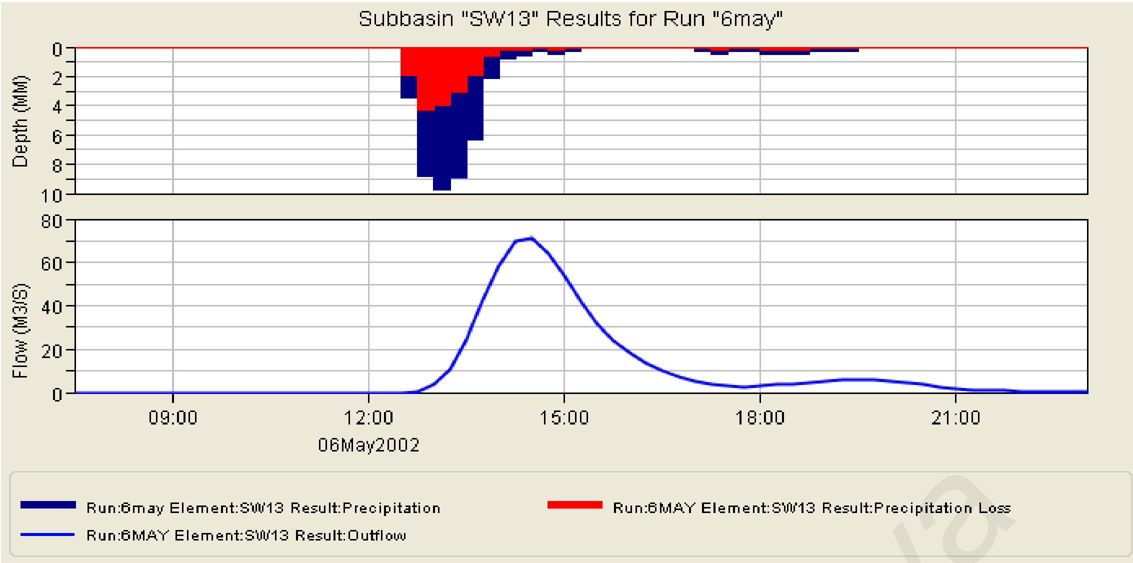

Figure 4.62: computed flow hydrograph at sub basin SW13

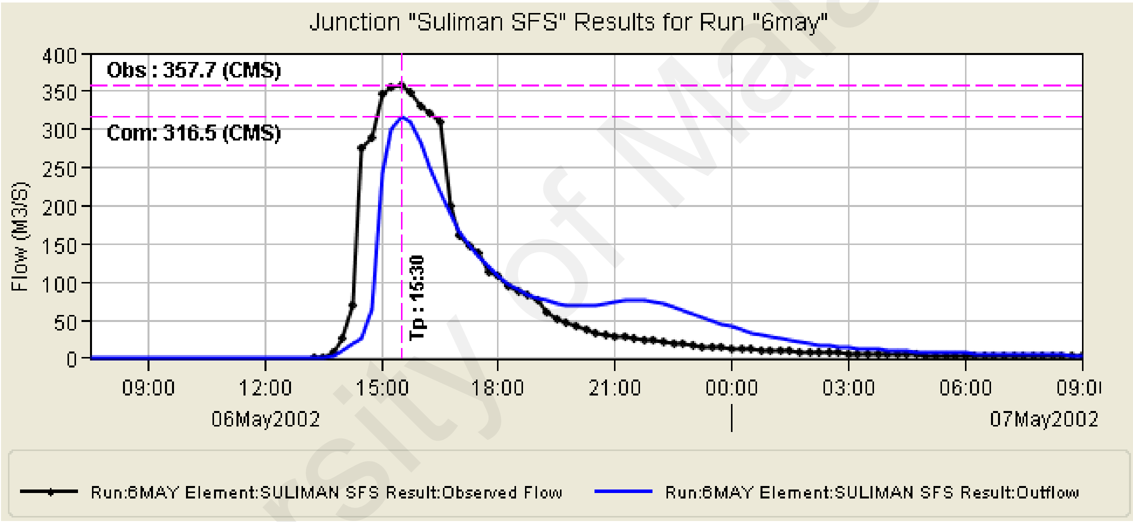

Figure 4.63: observed and computed flood hydrograph at Sulaiman Bridge based on SRTM-derived sub-watershed areas.

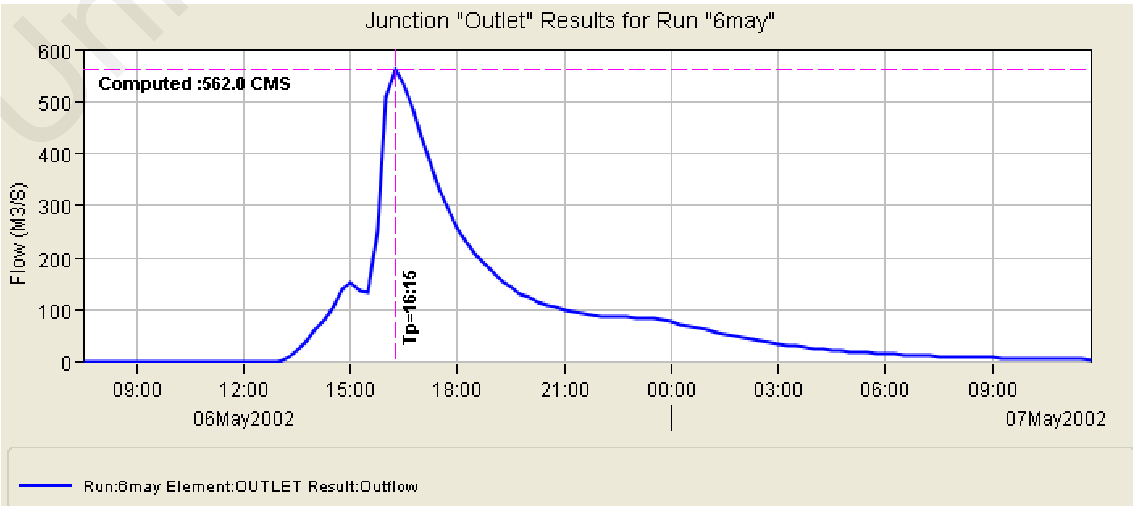

Figure 4.64: Computed flood hydrograph resultant from Run3 in sub-watershed SW13

4.11.4 Running for Topo-derived sub-watershed area and TRMM data (Run4)

Run4 has designed to assess the performance of TRMM estimates for flood event 6-may 2002. Klang watershed lies on six TRMM cells with uniform rainfall estimates in each cell. To account the temporal and spatial pattern of event of 6-May, TRMM cells was considered as regular rain gauge network containing six raingauges named Cell1, Cell2, Cell3, Cell4, Cell5 and Cell6 (see Figure 4.65). Temporal pattern was defined with 3-hour time interval for each gauge. With overlying the TRMM grid on DEM-derived sub-watershed boundaries, the raingauges that affect the sub-basins are specified.

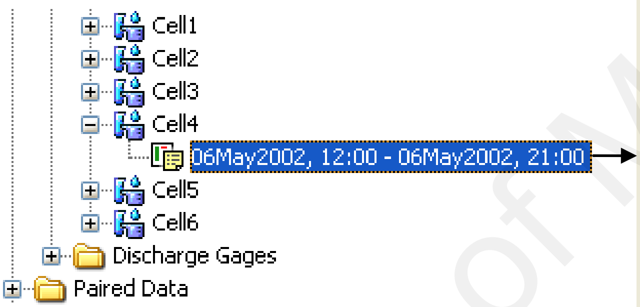

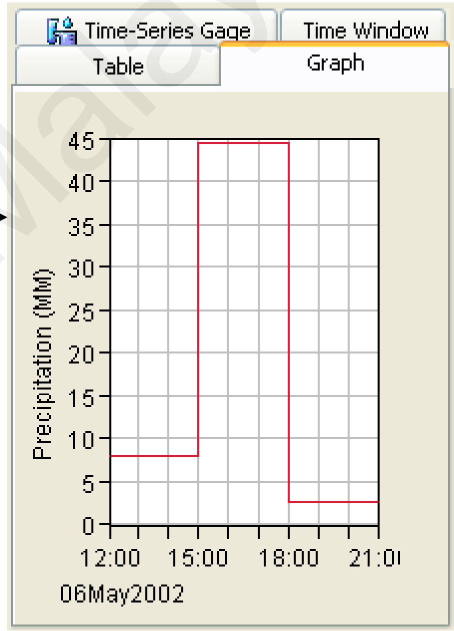

Figure 4.65: TRMM hyetograph at gauge Cell4 (Event 6-May 2002)

The other parameters was remained the same as Run2. As shown in Figure 4.66 the peak discharge for computed hydrograph in sub-basin SW13 is significantly decreased from 68.6 to 41 m^3/s. but total volume of flow is increased from 539.1 to 690.3 (1000 m^3). It is due to the fact that TRMM estimates a greater value of rainfall for SW13 with longer period which cause a much longer time base for computed flow hydrograph (see Figure 4.67). In addition, time of peak and shape of hydrograph have changed. Flood hydrograph for Run4 at Sulaiman Bridge and watershed outlet are presented in Figure

4.67 and 4.68 respectively. Percent of error in peak discharge gives 60% under estimate for simulated peak discharge at Sulaiman Bridge.

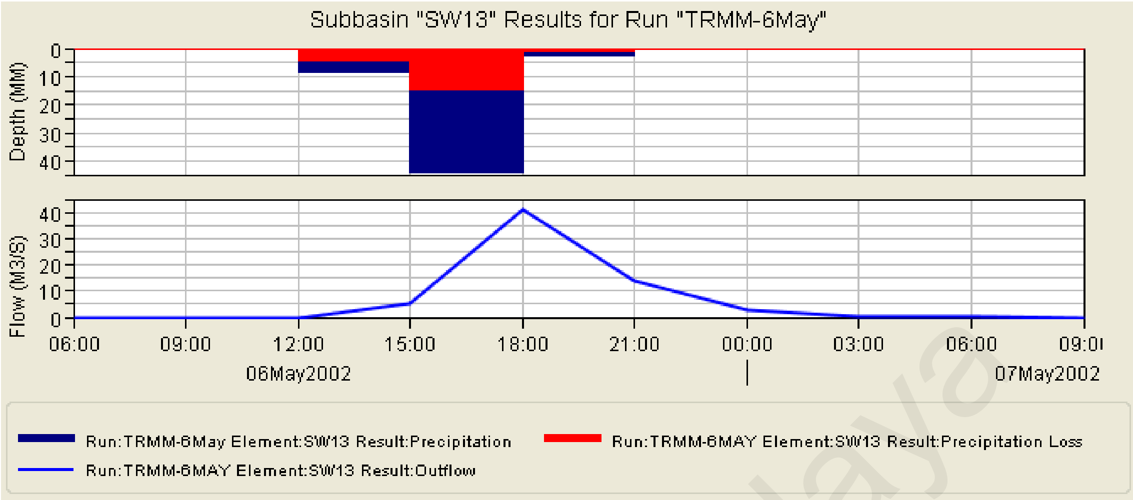

Figure 4.66: Computed flood hydrograph resultant from Run4 in sub-watershed SW13

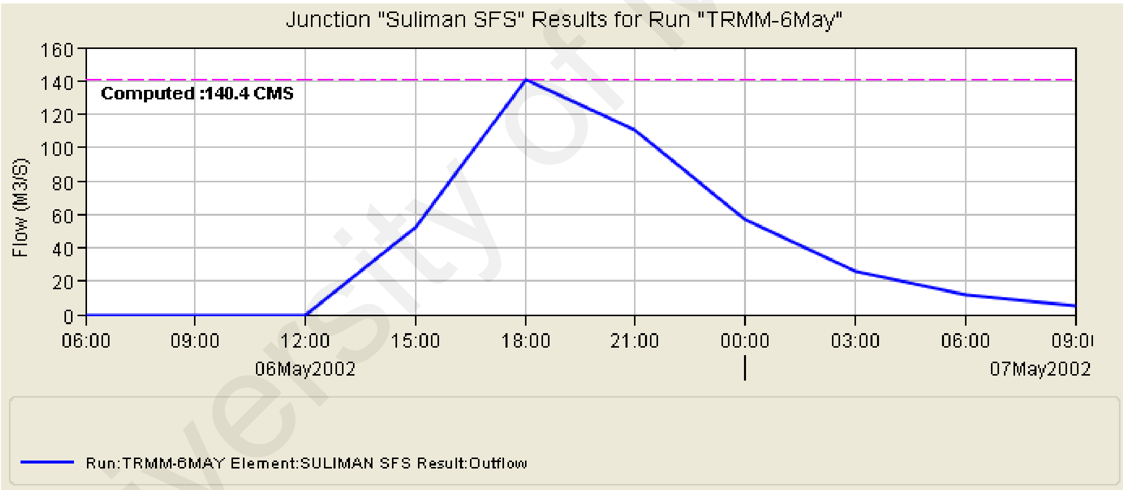

Figure 4.67: Computed flood hydrograph for Run4 at Sulaiman Bridge

In addition time of peak shifts from 15:30 (observed) to 18:00 with 2.5 hours delay which implies the weakness of TRMM estimate for reservoir operation and flood forecasting. However, the percent of error in total volume of outflow is about 12% underestimate. The same trend is observed for computed flow hydrograph at the outlet. Percent of error in peak discharge indicates 58% under estimate for simulated peak discharge at the outlet. Similarly, computed flood hydrograph at the outlet confirms that computed peak discharge resultant from TRMM estimate is lower than computed peak discharge in Run2. But, the percent of error in total volume of outflow is about 9% overestimate. Moreover, time of peak and shape of hydrograph do not match with the observed.

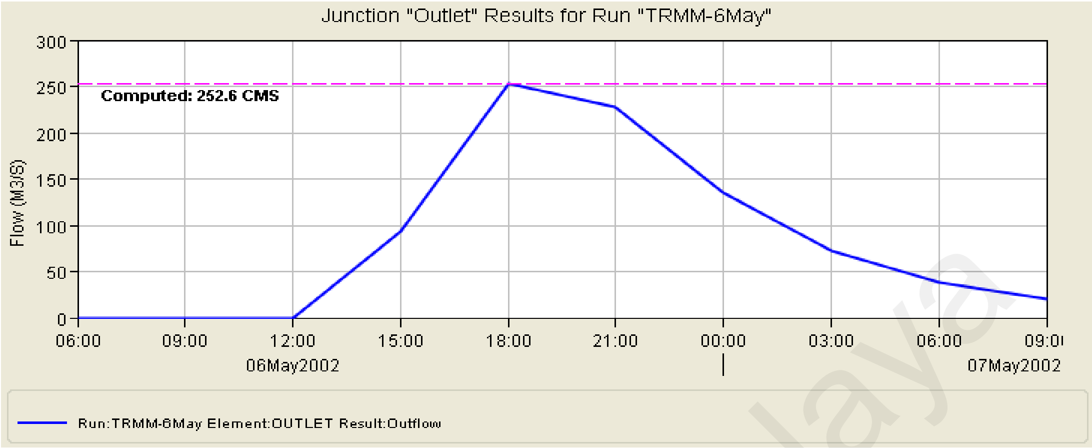

Figure 4.68: Computed flow hydrograph resultant from Run4 at the watershed outlet

4.11.5 Running for SRTM-derived sub-watershed area and TRMM data (Run5)

Simultaneous use of SRTM-derived areas and TRMM rain estimate are employed in Run5. Computed flow hydrograph for Run5 at SW13, Sulaiman Bridge and outlet are presented in Figure 4.69, 4.70 and 4.71. Computed peak discharge at SW13 is increased slightly for this scenario but it is still 38% underestimate compare to the computed peak flow in Run2. Percent of error in peak discharge indicates 60% under estimate for simulated peak discharge at Sulaiman Bridge.

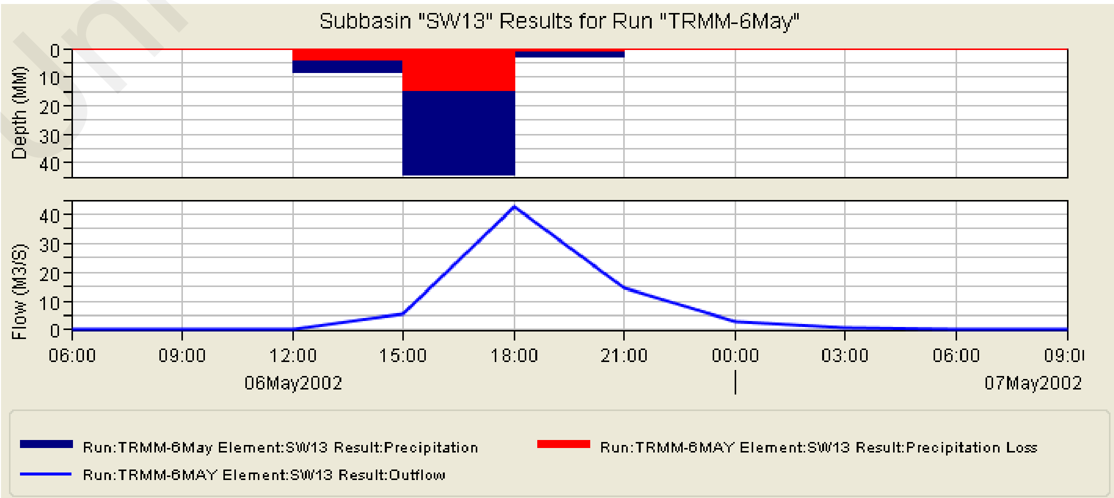

Figure 4.69: Computed flood hydrograph resultant from Run5 in sub-watershed SW13

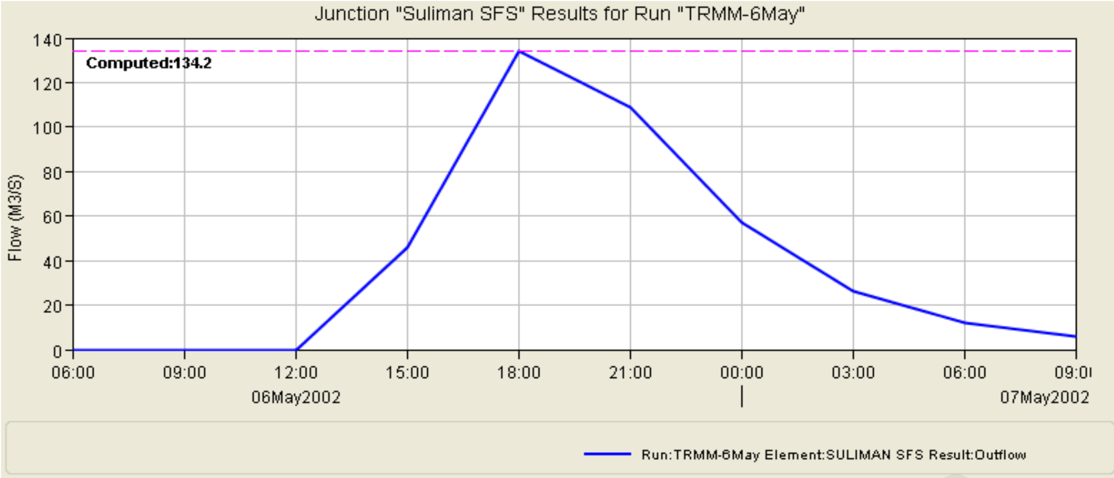

Figure 4.70: Observed and computed flood hydrograph for Run5 at Sulaiman Bridge

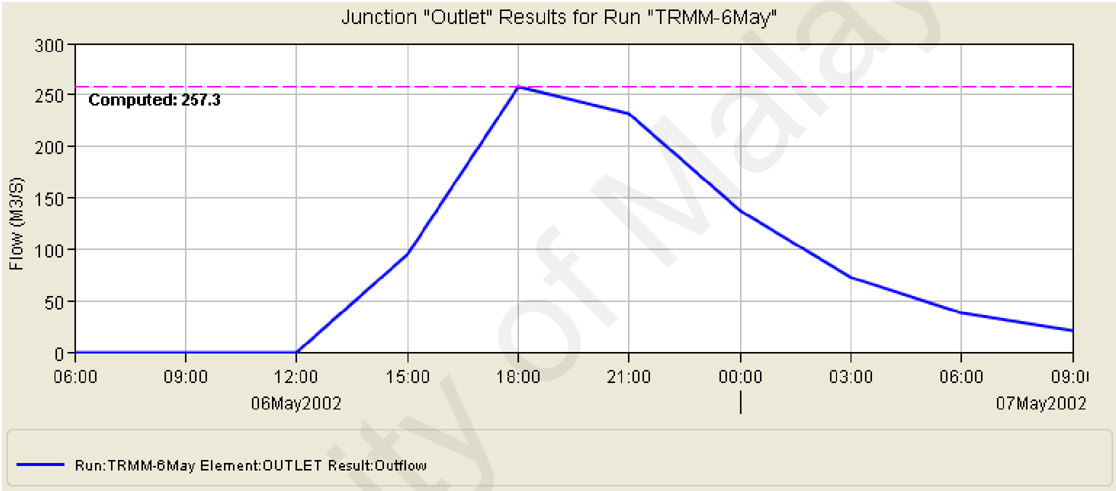

Figure 4.71: Computed flow hydrograph resultant from Run5 at the watershed outlet

Peak discharge at Sulaiman Bridge is reduced from 612.9 m^3/s to 134.2 m^3/s which denote high percent of error in estimation of peak flood. However, the percent of error in total volume of outflow is about 15% under estimate. Moreover, time of peak and shape of hydrograph do not match with the observed hydrograph.

Table 4.19: Statistical measures for different Runs at Sulaiman Bridge

Statistical measures	Run1	Run2	Run3	Run4	Run5
NSE	0.86	0.85	0.78	-	-
PE of Peak %	4.81	0.87	-11.52	-60	-78.3
r	0.93	0.93	0.89	-	-
RMSE	35.74	37.02	44.87	-	-

4.12 Overall assessment of the modeling results

It is observed that Run2 exhibit a reliable simulation for peak and time of Peak flood. Therefore it will be as reference for assessment of other scenarios. Peak discharge and volume for eighty hydrologic elements were investigated based on different conditions that considered in each Run and presented in Table 4.20. Summary results for each Run are providing in Appendix C. A clear message is perceived from Table 4.20 and Figure 4.71 which is TRMM estimates are not suitable for simulation of peak and time of peak specifically for flood event in Klang watershed that is frequently affected by flash floods. But reasonable estimation is obtained for total volume of outflow. However, flood simulation results for Run3 demonstrate a good agreement between observed and computed flood hydrograph when drainage area derived from SRTM-DEM is served by the model.

Table 4.20: Statistical measures different Runs for eighty hydrologic elements

Statistical measures	Peak discharge m^3/s			Volume $1000m^3$		
	Run2-Run3	Run2-Run4	Run2-Run5	Run2-Run3	Run2-Run4	Run2-Run5
NSE	0.98	0.45	0.44	0.99	0.97	0.96
r	1.00	0.97	0.96	1.00	0.98	0.98
RMSE	21.5	117.43	118.8	141.9	351.93	418.6

Chapter V:

Summary and Conclusion

5.1 Summary

This research involves with analyzing public domain spatial data for the purpose of flood simulation through the public domain hydrologic model. A huge amount of data were collected and processed based on analytical and statistical approaches. Valuable result at the technological and application levels has been found out of this research. At the technological level, GIS has proven to be a useful tool that has the ability to extract multiple parameters from a DEM and create a hydrological database from it. We showed that how effectively public domain GIS software can be used for hydrological analysis such as generating CN map; mapping the impervious areas; defining the spatial pattern of rainfall events, image processing and so on. We employed the contributions of internet technology and WebGIS in supporting hydrological modeling and distribution of satellite data which has significantly facilitated data collection and reduce administrative bureaucracy. The HEC-GeoHMS was found to be useful geospatial hydrology tool kit for engineers and hydrologists with limited GIS experience. Data management, terrain preprocessing, watershed processing, hydrologic parameter estimation and supporting HMS are the important features of GeoHMS that assisted this research. However there are some limitations to work with precipitation grids out of US. It is because the standard hydrologic grid has been defined based on the Albers equal-area conic map projection for the US.

We experienced that HEC-HMS program has comprehensive capabilities for conducting GIS-based hydrologic simulation. The program has well designed to define hydrologic elements and its internal relationship. High flexibilities were observed for defining the loss estimation, rainfall-turnoff transformation, flood routing methods. However, it only supports the hydrologic routing approach. In addition, there are some graphic limitations in viewing map documents and printing graphical results.

At the application level, we explored the strengths and weaknesses of two public domain satellite data for the purpose of watershed modeling and flood simulation. There are two major outcome results at the application level. First, we were able to prove the practical use of SRTM-DEM compared with cartographic digital elevation data sets derived from topographic map at scale of 1:25000. It was found out that SRTM-DEM provided competitive results for delineating watershed boundaries and deriving physical parameters including area, slope, lag time and mean elevation. The performance of SRTM-DEM was assessed in three scenarios. In the first scenario the whole Klang watershed was analyzed using GeoHMS and ILWIS. The results were assessed by means of several statistical measures including RMSE, Nash-Sutcliffe efficiency index, correlation coefficient and bias. The overall agreement of 87% was found based on the Nash-Sutcliffe efficiency index for all investigated parameters which imply investigated parameters can be derived from SRTM-DEM with 87% similarity to Topo-DEM derivatives. At the second scenario sub-basins located in the urban areas were ignored. It was proven that investigated parameters can be derived from SRTM-DEM with 95 percent similarity with data extracted from the Topo-DEM on the non-urbanized areas with rugged topography. The weakness of SRTM-DEM is distinguished in the third scenario where the lowest level of prediction (0.33) is exhibited for sub-basins located in the heart of Klang watershed which implies these data should be used with caution in flat and urbanized areas. Complementary results were obtained from flood simulation where we observed 11% under estimate for peak discharge compare to the observed peak just by substituting sub-basins area derived from SRTM-DEM. A significant difference in peak discharge is occurred by a minor change (about 1 percent) in total drainage area at that point and relatively lower value of NSE (78%) is obtained. Meanwhile, the total volume of the outflow is well simulated when watershed area derived from SRTM-DEM is served by HEC-HMS. Finally, it is concluded that SRTM elevation dataset has the ability to obviate the lack of terrain data for watershed modeling specifically in the regions that no appropriate data are available. In addition, drainage areas derived from SRTM-DEM can be used for flood modeling with a reasonable degree of accuracy for peak discharge and volume specifically in non-urban areas. More importantly, SRTM-DEM is cost effective and much time saving.

As second major outcome result at the application level is that we explored the weaknesses of TRMM estimates for explaining the behavior of rainfall events at a well instrumented watershed in a tropic region. It was observed for all investigated cases that TRMM estimates depict the rainfall depth about 35 percent less than the actual value measured at the rain gauges. It was also observed that the percentage of error is increased with increasing rainfall depth up to 52 percent. Close correlation between gauge data and TRMM estimates (0.99) indicate that our results can be extended to other rainfall events with acceptable level of confidence. Flood simulation with TRMM input data at Sulaiman Bridge demonstrate 60% underestimated for peak discharge with 2.5 hours delay in time of peak. The percent of error in peak reaches to 78% when TRMM and SRTM inputs are used simultaneously. A loose agreement (45%) was found based on the Nash-Sutcliffe efficiency index between computed and observed peak discharge which denotes that coarse spatio-temporal resolution of TRMM data do not provide enough detail information about the peak and time of peak discharge specifically for the flood events in Klang watershed that is frequently affected by flash floods. In contrast, it is seen that volume of outflow from a flood event 6-May is predicted using TRMM estimates with 97% similarity to the observed data. It may relate to the coarse temporal resolution of TRMM (3 hours) that cause unreal elongation of rainfall duration.

Notable results were found from spatial analysis of storm patterns over the study area. It was proven that the effective influence range of rain gauges located in Klang watershed is about 6273 m, from which it can be concluded that effective radius of gauges is about 3136 m. This result exhibits a non-uniform distribution and inadequate rain gauges in Klang watershed. For instance in the Ampang area there is only on station available at JPS Ampang and the closest to the north is at Klang Gates. Consequently there is a gap of approximately 11 km which is significant for the most common localized storm patterns. Therefore, it is proposed to add some rain gauges for having a better definition of the storm pattern.

Furthermore, it was shown that Gaussian Semi-variogram model demonstrate slightly better estimation compare to Spherical and Exponential Semi-variogram models and propagates much lesser standard error at the effective influence range. Furthermore, it was shown that the effect of pixel size on the areal storm pattern analysis using Kriging. We showed that the appropriate cell size for storm pattern analysis rage from 200 to 500 m. Moreover a novel approach was developed for the concurrent use of two indicators (Moran's I, Geary's C) using raster GIS to identify the effective spatial correlation extent which is an important criteria in Kriging interpolation method. According to the above findings and considering the TRMM cell dimension (27.5×27.5 km), it can be concluded that spatial resolution of TRMM estimates are much coarser (about 9 times) than needed. Consequently it is not possible to draw adequate information about the spatial variation of localized storms in tropic regions as it can be drawn from the dense rain gauges network of Klang watershed. However, TRMM estimates are a useful source of data for the area with sparse gauge density with distance longer than 30 km. Along with the above findings several other results were discovered. Validation of new initial abstraction ratio for Klang watershed is the most important secondary result. It was proven that HMS model is best calibrated for peak discharge with initial abstraction ratio of 0.05. Therefore it can be concluded that this ratio is advisable for other applications of SCS method in the tropic region of peninsular Malaysia and other similar regions.

5.2 Conclusion

1- At the technological level, GIS has proven to be a useful tool that has the ability to extract multiple parameters from a DEM and create a hydrological database from it. Public domain GIS software can be used effectively for mapping hydrological parameters such as CN map; mapping the impervious areas; defining the spatial pattern of rainfall events, image processing and so on. We experienced that contributions of internet technology and WebGIS in supporting hydrological modeling and distribution of satellite data which has significantly facilitated data collection and reduce administrative bureaucracy.

2- SRTM-DEM provided competitive results for watershed delineation, stream delineation and physical parameters such as area, slope, lag time and mean elevation specifically in non-urbanized areas with rugged topography. Moreover SRTM- DEM is very coast effective and time saving in hydrological researches. However SRTM-DEM should be used with cousin in flat urban areas.

3- TRMM estimates exhibit a rough estimation about spatial and temporal pattern of observed storms. Therefore it do not draw adequate information about the spatial variation of localized storms in tropic regions as it can be drawn from the dense rain gauges network of Klang watershed. However, TRMM estimates are a useful source of data for the area with sparse gauge density with distance longer than 30 km. TRMM estimates depict the rainfall depth under estimated (about 35%) than the actual value measured at the rain gauges. Moreover with coarse temporal resolution of TRMM cannot capture the actual pattern of rainfall hyetograph and therefore the values and time of peak discharge.

4- SRTM-DEM is a trustable source of data for flood simulation particularly in non-urbanized areas. But TRMM hyetograph provide underestimated result (about 60%) for peak discharge and cannot simulated the shape of hydrograph. Therefore TRMM estimates are not suitable source of data for flash flood study which mostly occurs in short time and characterized by localized storms. However integrating TRMM and SRTM data give a reasonable estimation for volume of the floods in midsize watersheds.

5- Flood hydrograph is best calibrated for peak discharge with the modified ratio of initial abstraction to maximum potential retention (λ) in SCS model. Therefore, it is recommended to use modified ratio for flood simulation and other applications of SCS method in the tropic region of peninsular Malaysia and similar regions.

5.3 Future plan

Among several SRTM-derivatives the area was utilized for flood modeling. Further research must be conducted to assess the other DEM-derivative and its impact on flood hydrograph. In addition, spatial resolution of public domain satellite-based DEM have significantly improved by Advanced Space borne Thermal Emission and Reflection Radiometer (ASTER) Global Digital Elevation Model (GDEM). The ASTER-GDEM has developed jointly by the Ministry of Economy, Trade, and Industry (METI) of Japan and the NASA. The ASTER-GDEM is available at no charge to the public since June 29, 2009 via the internet from the Earth Remote Sensing Data Analysis Center (ERSDAC) of Japan and NASA's Land Processes Distributed Active Archive Center (LP DAAC). It covers land surfaces between 83°N and 83°S with estimated accuracies of 20 meters at 95 % confidence for vertical data and 30 meters at 95 % confidence for horizontal data. It is thought with utilizing the new DEM our results can be significantly improved. In addition the weaknesses of TRMM will obviate by the Global Precipitation Measurement (GPM) mission which is the successor to TRMM. It is planning to include a core Satellite (proposed for launch in 2013) and data from several “constellation” satellites already in orbit that together will help better understanding the horizontal, vertical, and temporal structure of rainfall events which will improve hydrologic predictions through application of more accurate and frequent precipitation measurements. Feature research should be focus on the ability and performance of GDEM and GPM in supporting hydrological models. It is believed GPM data and ASTER-GDEM will significantly improve the GIS-based hydrological analysis such as flood simulation, flood plain mapping, erosion modeling etc.

List of References:

ABDULLAH, K. Year. Stormwater Management and Road Tunnel (SMART) An Underground Approach to Mitigating Flash Floods. *In:* SEPTEMBER, -. ed. International Workshop on Flash Floods in Urban Areas and Risk Management, 2006 KL, Malaysia.

ABRAHAMS, A. D., PARSONS, A. J. & LUK, S. H. 1988. Hydrologic and sediment responses to simulated rainfall on desert hillslopes in Southern Arizona, Catena. *15*, 103–107.

AGHAKOUCHAK, A., NASROLLAHI, N. & HABIB, E. 2009. Accounting for Uncertainties of the TRMM Satellite Estimates. *Remote Sensing. 2009, 1, 606 - 619; doi:10.3390/rs1030606,* vol.1, pp.606 - 619.

AHN, G.-C. 2007. *The Effect of Urbanization on The Hydrologic Regime of The Big Darby Creek Watershed, Ohio.* Degree Doctor of Philosophy, School of The Ohio State University.

AKBARI, A. 1998. *Coupled time-area overland and HEC-1 channel routing of Kardeh watershed.* M.S, ITC, The Netherlands.

AKBARI, A., OTHMAN, F. & SAMAH, A. A. 2008. Spatial Storm Pattern Analysis Using Kriging, Case Study; upper Klang River Basin. *Malaysian Science and technology Congress (MSTC2008).* KLCC,Kuala Lumpur,Malaysia.

AKBARI, A., SAMAH, A. A. & OTHMAN, F. 2009. Effect of Pixel Size on the Areal Storm Pattern Analysis using Kriging *Journal of Applied Science,* vol.9, pp.3707-3714.

ALARCON, V .J. & O'HARA, C. 2006. Using IFSAR and SRTM Elevation Data for Watershed Delineation of a Costal Watershed. *MAPPS/ASPRS 2006 Fall Conference.* San Antonio, Texas.

ALSDORF, D. E., RODRIGUEZ, E. & LETTENMAIER, D. P. 2007. Measuring surface water from space .*Reviews of Geophysics,* vol.45.

AMBROISE, B., PERRIN, J. L. & REUTENAUER, D. 1995. Multicriterion validation of a semidistributed conceptual model of the water cycle in Fecht catchment *Water Resources Research,* vol.31, pp.1467-1481.

AN, W. 2007. *The Study of GIS-Based Hydrological Model in Highway Environmental Assessment.* Doctor of Philosophy, University of Pittsburgh.

ANDERSON, M. G. 2005. Encyclopedia of Hydrological Sciences. *In:* AVISSAR, R., BEAR, J. & BEVEN, K. (eds.). West Sussex, England: John Wiley & Sons Ltd.

ARONOFF, S. 1989. *Geographic Information Systems: A Management Perspective,* Ottawa, WDL Publications.

ASCE. 1996. *Policy Statement 447 - Hydrologic Data Collection* [Online]. [Accessed August 4 2010.[

BACCHI, B. & KOTTEGODA, A. N. T. 1995 .Identification and calibration of spatial correlation patterns of rainfall. *Journal of Hydrology,* 165, 311-348.

BAHREMAND, A. & DE SMEDT, F. 2008. Distributed Hydrological Modeling and Sensitivity Analysis in Torysa Watershed, Slovakia. *Water Resour Manage,* 22, pp.393–408.

BALL, J. E. 1994. The influence of storm temporal patterns on catchment response. *Journal of Hydrology,* Vol.158, Pages 285-303

BALTAS, E. A., DERVOS, N. A. & MIMIKOU, M. A. 2007. Technical Note: Determination of the SCS initial abstraction ratio in an experimental watershed in Greece. *Hydrol. Earth Syst. Sci.,* vol.11**,** pp.1825–1829.

BEDIENT, P. B., HUBER, W. C. & VIEUX, B. E. 2008. *Hydrology and Floodplain Analysis,* New York, Prentice Hall.

BEKOE, E. O. 2005. *Application of a hydrological model in a data-poor tropical West African catchment: a case study of the Densu Basin of Ghana.* Doctor of Philosophy.

BELL, V. A. & MOORE, R. J. 2000. the sensitivity of catchment runoff models to rainfall data at different spatial scales. *Hydroloy & Earth System Sciences,* 4**,** 653-667.

BEVEN, K. J. 2001. *Rainfall-runoff modelling. The Primer,* New York, John Wiley & Sons.

BHASKAR, N. R., JAMES, W. P. & RAVIKUMAR S. DEVULAPALLI 1992. Hydrologic Parameter Estimation Using Geographic Information System. *Journal of Water Resources Planning and Management,* vol.118**,** pp. 492-512.

BITEW, M. & GEBREMICHAEL, M. 2010. Evaluation Through Independent Measurements: Complex Terrain and Humid Tropical Region in Ethiopia. *Satellite Rainfall Applications for Surface Hydrology***,** 205-214.

BRIMICOMBE, A. 2009. *GIS, Environmental Modeling and Engineering,* New York, US, CRC Press.

BUCKLEY, D. J. 1997. *The GIS Primer* [Online]. Pacific Meridian Resources, Inc. [Accessed July 24 2009.[

BURROUGH, P. A. & MCDONNELL, R. A. 1998. *Principles of Geographical Information Systems* Oxford University Press.

CAI, X. & YEH, T.-C. J. (eds.) 2008. *Quantitative Information Fusion for Hydrological Sciences,* Berlin: Springer.

CAU, P. & PANICONI, C. 2007. Assessment of alternative land management practices using hydrological simulation and a decision support tool: Arborea agricultural region, Sardinia. *Hydrology and Earth System Sciences,* vol.11**,** 12.

CHEBUD, Y. A. & MELESSE, A. M. Year. Ground Waters Flow Simulation Of the Lake Tana Basin, Ethiopia. *In:* ABTEW, W. & MELESSE, A. M., eds. Hydrology and Ecology of the Nile River Basin under Extreme Conditions, June 16-19 2008 Adis Ababa, Ethiopia.

CHEN, B., XIA, L. Z., YANG, Z. F. & CHEN, G. Q. 2001. Retrospect and prospect of watershed hydrological model *Communications in Nonlinear Science and Numerical Simulation,* 6**,** 172-177.

CHEN, J., LIN, G., YANG, Z. & CHEN, H. 2010 The relationship between DEM resolution, accumulation area threshold and drainage network indices. *18th International Conference on Geoinformatics.* Beijing, China IEEE.

CHOW, V. T., MAIDMENT, D. & MAYS, L. 1988. *Applied Hydrology,* New York, McGraw-Hill Science p-11.

CLARK, C. 1943. Storage and the unit hydrograph. *Proc. Am. Soc. Civ. Eng,* vol. 9**,** pp. 1333-1360.

COSTA-CABRAL, M. C. & BURGES, S. 1994. Digital elevation model networks (DEMON): A model of flow over hillslopes for computation of contributing and dispersal areas. *Journal of Water Resources Research,* vol.30**,** pp. 1681-1692.

CRAWFORD, N. H. & BURGES, S. J. 2004. HISTORY OF THE STANFORD WATERSHED MODEL. *Water Resources IMPACT,* 6**,** 3.

CUNDERLIK, J. M., MCBEAN, G., BURN, D. H., MORTSCH, L., GOLDT, R. & HELSTEN, M. 2003. Hydrologic model selection for CFCAS project:

Assessment of Water Resource Risk and Vulnerability to Changing Climatic Conditions. *Water Resources Research Report.* University of Western Ontario

CUNDERLIK, J. M. & SIMONOVIC, S. P. 2004. Calibration, verification, and sensitivity analysis of the HEC-HMS hydrologic model. *CFCAS project: Assessment of Water Resources Risk and Vulnerability to Changing Climatic Conditions.* Ontario University of Western Ontario and University of Waterloo

DAVIE, T. 2008. *Fundamentals of Hydrology,* New York, Taylor & Francis.

DEFRIES, R. & BELWARD, A. S. 2000. Global and regional land cover characterization from satellite data; an introduction to the Special Issue. *International Journal of remot sensingan; introduction to the Special Issue,* vol.21**,** 1083-1092.

DESA, M. N. & NIEMCZYNOWICZ, J. 1996a. Spatial variability of rainfall in Kuala Lumpur, Malaysia : long and short term characteristics. *Hydrological sciences journal,* vol. 41**,** pp.345-362.

DESA, M. N. & NIEMCZYNOWICZ, J. 1996b. Temporal and spatial characteristics of rainfall in Kuala Lumpur, Malaysia. *Atmospheric Research,* 42**,** 263-2.77

DESA, M. N. & NIEMCZYNOWICZ, J. 1997. Dynamics of short rainfall storms in a small scale urban area in Coly Limper, Malaysia. *Atmospheric Research,* 44**,** 293-315.

DID 1994. Klang River Basin Integrated Flood Mitigation projects, Malaysia. *In:* DRAINAGE ,D. O. I. A. (ed.). Kaula Lumpur: KINHILL.

DID 2003a. Klang River Basin Environmental Improvement and Flood Mitigation Project, final report. *In:* DRAINAGE, D. O. I. A. (ed.). Kuala Lumpur, Malaysia: Department of Irrigation and Drainage.

DID 2003b. Klang River Basin Environmental Improvement Final Report and Flood Mitigation Project. *In:* DRAINAGE, D. O. I. A. (ed.) Final Report ed. Kuala Lumpur: DR. NIK & ASSOCIATES SDN. BHD.

DID 2003c. Klang River Environmental Improvement and Flood Mitigation Project,Final Report 2003. *In:* DRAINAGE, D. O. I. A. (ed.). Kuala Lumpur.

DINGMAN, S. L. 2002. *Physical hydrology,* New Jersey, USA, Prentice Hall.

DIRKS, K. N. D., HAY, J. E., STOW, C. D. & HARRIS, D. 1998. High-resolution studies of rainfall on Norfolk Island Part II: Interpolation of rainfall data. *Journal of Hydrology,* 208**,** 187–193.

DISKIN, M. H. & SIMON, E. 1979. The relationship between the time bases of simulation models and their structure. *Water Resources Bulletin,* 15**,** 1716-1732.

DJOKIC, D. & YE, Z. Year. DEM Preprocessing for Efficient Watershed Delineation. *In:* Esri Users Conference, 1999 San Diego, CA.

DJOKIC, D. & YE, Z. 2000. DEM Pre-processing for efficient watershed delineation. *Hydrologic and Hydraulic Modelling Support with Geographic Information Systems***,** 65–84.

DOAN, J. H. 2003. Geospatial Hydrologic Modeling Extension HEC-GeoHMS-User's Manual. *Version 1.1.* Davis, California: US Army Corps of Engineers-HEC.

EARLS, J. & DIXON, B. Year. Spatial Interpolation of Rainfall Data Using ArcGIS: Comparative Study. *In:* ESRI User Conference 2007 San Diego,California, USA. ESRI

EFSTRATIADIS, A., NALBANTIS, I., KOUKOUVINOS, A., ROZOS, E. & KOUTSOYIANNIS, D. 2007. HYDROGEIOS: A semi-distributed GIS-based hydrological model for disturbed river basins. *Hydrology and Earth System Sciences Discussions,* 4 pp.51.

FAIRFIELD, J. & LEYMARIE, P. 1991. Drainage networks from grid digital elevation models. *Water Resources Research,* vol. 27**,** pp. 709-717.

FALORNI, G., TELES, V., VIVONI, E., BRAS, R. & AMARATUNGA, K. 2005 . Analysis and characterization of the vertical accuracy of digital elevation models from the Shuttle Radar Topography Mission. *Journal of Geophysical Research,* 110**,** F02005.

FARIA, D., POMEROY, J. & ESSERY, R. 2000a. Effect of covariance between ablation and snow water equivalent on depletion of snow-covered area in a forest. *Hydrological Processes,* 14**,** 2683-2695.

FARIA, D. A., POMEROY, J. W. & ESSERY, R. L. H. 2000b. Effect of covariance between ablation and snow water equivalent on depletion of snow covered area in a forest *Hydrological Processes,* vol.14**,** pp.2683-2695.

FAURES, J.-M., GOODRICH, D. C. & WOOLHISER, D. A. 2006. Impact of small-scale spatial rainfall variability on runoff modeling. *Nordic Hydrology* 37**,** 261–275

FEIDAS, H., KOKOLATOS, G., NEGRI ,A., MANYIN, M. & CHRYSOULAKIS, N. 2006a. A TRMM-Calibrated infrared technique for rainfall estimation: application on rain events over eastern Mediterranean. *Advances in Geosciences,* 7**,** 181-188.

FELDMAN, A. 2000. *Hydrologic Modeling System HEC-HMS: Technical Reference Manual*, US Army Corps of Engineers, Hydrologic Engineering Center.

FELDMAN, A. D., ELY, P. B. & GOLDMAN, D. M. 1981 .The New HEC-1 Flood Hydrograph Package. Davis, CA: US Army Corps of Engineers,Institute for Water Resources, Hydrologic Engineering Center (HEC(

FENG, C.-C. 2004. *Probing Barriers to the Integration of Geographic Information Systems and Hydrologic Models.* Doctor of Philosophy, the State University of New York.

FLEMING, M. J. & DOAN, J. H. 2009. HEC-GeoHMS Geospatial Hydrologic Modeling Extension. Version 4.2 ed. Davis, CA: US Army Corps of Engineers,Institute for Water Resources,Hydrologic Engineering Center.

FORD, D., PINGEL, N. & DEVRIES, J. J. 2008. Hydrologic Modeling System HEC-HMS ,Applications Guid. Davis, CA: U.S. Army Corps of Engineers, Hydrologic Engineering Center, HEC.

FREEMAN, T. G. 1991. Calculating catchment area with divergent flow based on a regular grid. *Computers and Geoscience,* vol. 17.

FRIED, J. J. 1991. Geographically Based Models for Surface and Estuarine Waters and River/Aquifer Interfaces. *In:* TARDIFF, R. G. & GOLDSTEIN, B. (eds.) *Methods for Assessing Exposure of Human and Non-Human Biota.* John Wiley & Sons

GARBRECHT, J. & CAMPBELL, J. 1997. TOPAZ: an automated digital landscape analysis tool for topographic evaluation, drainage identification, watershed segmentation and subcatchment parameterization. *In:* AGRIC.-ARS, U. S. D .O. (ed.). Oklahoma, USA.

GARBRECHT, J. & MARTZ, L. W. 2000. Digital Elevation Model Issues In Water Resources Modeling. *In:* MAIDMENT, D. R. & DJOKIC, D. (eds.) *Hydrologic and hydraulic modeling support:with geographic information systems.* New York: ESRI Press.

GESCH, D., WILLIAMS, J. & MILLER, W. Year. A Comparison of U.S. Geological Survey Seamless Elevation Models with Shuttle Radar Topography Mission Data. *In:* IEEE International Geoscience and Remote Sensing Symposium, July 9-13 2001 Sydney, NWS, Australia, . Institute of Electrical and Electronics Engineers, Inc., pp.754-756.

GIAJ. 1998. *GTOPO30 Documentation* [Online]. Geospatial Information Authority of Japan. Available: http://www1.gsi.go.jp/geowww/globalmap-gsi/gtopo30/README.html [Accessed June.[2009

GIBSON, K. & DODGE, R. A. 1983. Hydraulic Model Studies of Modification to Klang Gates Dam, Malaysia. *Engineering and Research Center.* Denver, Colorado: Hydraulics Branch, Division of Research Engineering and Research Center

GILES, P. T. & FRANKLIN, S. E. 1996. Comparison of derivative topographic surfaces of a DEM generated from stereoscopic SPOT images with field measurement. (10); . *Photogrammetric Engineering and Remote Sensing,* vol.62**,** 1165-1171.

GOMEZ, M. R. S. 2007. *Spatial and temporal RAinfall Gauge Data Analaysis and Validation with TRMM Microwave Radiometer surface Rainfall Retrievals.* Master, International Institue fro Geo-information Science and Earth Observation.

GOODCHILD, M. 2001. Metrics of scale in remote sensing and GIS. *International Journal of Applied Earth Observation and Geoinformation,* vol.3 114–120.

GOODCHILD, M. F. 2003. Geographic Information Science and Systems for Environmental Managment. *Annual Review of Environmental Resources,* n. 28**,** 493-519.

GOODCHILD, M. F., PARKS, B. O. & STEYAERT, L. T. (eds.) 1993. *Environmental Modeling with GIS,* New York: Oxford University Press, 31-43.

GOOVAERTS, P. 2000. Geostatistical approach for incorporating elevation into the spatial interpolation of rainfall. *Journal of Hydrology*.129-113 ,228 ,

GOSAIN, A. K. & RAO, S. 2004. GIS-based technologies for watershed management. *CURRENT SCIENCE,* VOL. 87**,** 6.

GRAY, D. M. 1961. Synthetic unit hydrographs for small watersheds. *Journal of the Hydraulics Division,* vol. 87**,** pp. 33-54.

GREEN, W .H. & AMPT, G. 1911. Studies of soil physics, Part 1-the flow of air and water through soils. *Journal of Agricultural Sciences,* vol.4**,** pp.1-24.

GROHMANN, C. H. & STEINER, S. S. 2008. SRTM resample with short distance-low nugget kriging. *International Journal of Geographical Information Science,* 22**,** 895 - 906

GRUNTFEST, E. & HUBER, C. J. 1991. Toward a comprehensive national assessment of flash flooding in the United States. *Episodes,* vol.14**,** pp.26-35.

GUPTA, H. V., SOROOSHIAN, S. & YAPO, P. O. 1999. Status of Automatic Calibration for Hydrologic Models: Comparison with Multilevel Expert Calibration. *Journal of Hydrologic Engineering,* Vol. 4**,** pp.135-143.

HAAN, C. T., JOHNSON, H. P. & BRAKENSIEK, D. L. (eds.) 1982. *Hydrologic modeling of small watersheds* ,Michigan,US: American Society of Agricultural Engineers.

HAASE, D. & FROTSCHER, K. 2005a. Topography data harmonisation and uncertainties applying SRTM, laser scanner and cartographic elevation models. *Advances in Geosciences,* 5**,** 65-73.

HABERLANDT, U. 2006. Geostatistical Interpolation of Hourly Precipitation from Rain Gauges and Radar or a large-Scale Extrem Rainfall event. *Journal of Hydrology*.

HANCOCK, G. R., MARTINEZ, C., EVANS, K. G. & MOLIERE, D. R. 2006. A comparison of SRTM and high-resolution digital elevation models and their use in catchment geomorphology and hydrology: Australian examples. *Earth Surface Processes and Landforms,* vol.31**,** pp.1394–1412.

HARRIS, A., RAHMAN, S., HOSSAIN, F., YARBOROUGH, L., C., A., BAGTZOGLOU & EASSON, G. 2007b. Satellite-based Flood Modeling Using TRMM-based Rainfall Products. *Sensors* vol.7**,** pp.3416-3427.

HAWKINS, R., JIANG, R., WOODWARD, D., HJELMFELT, A ,.VAN MULLEM, J. & QUAN, Q. Year. Runoff curve number method: examination of the initial abstraction ratio. *In*, 2002a.

HAWKINS, R. H. 1998. Local Sources For Runoff Curve Numbers. *11th Annual Symposium of the Arizona Hydrological Society.* Tucson,AZ.

HAWKINS, R. H. Thursday, April 23 2009. *RE: Developing new SCS-CN table (Email message).* Type to A.AKBARI.

HAWKINS, R. H., JIANG, R., WOODWARD, D. E., HJELMFELT, A. T., VAN MULLEM, J. A. & QUAN, Q. D. Year. Runoff Curve Number Method: Examination of the Initial Abstraction Ratio. *In:* Proceedings of the Second Federal Interagency Hydrologic Modeling Conference, 2002b Las Vegas, Nevada. ASCE Publications.

HELLWEGER, F. & MAIDMENT, D. 1997. *AGREE - DEM Surface Reconditioning System* [Online]. Available: http://www.crwr.utexas.edu/gis/gishyd98/quality/agree/agree.htm [Accessed 20 june 2008.[

HELLWEGER, F. L. & MAIDMENT, D. R. 1999. Definition and Connection of Hydrologic Elements Using Geographic Data. *Journal of Hydrologic Engineering,* Vol. 4**,** pp. 10-18.

HENDRICKS, G., ALSDORF, D., PAVELSKY, T. & SHENG, Y. Year. Channel Slope From SRTM Water Surface Elevations in the Amazon Basin. *In*, 2003a. 1016.

HENDRICKS, G. A., ALSDORF, D. E., PAVELSKY, T. M. & SHENG, Y. 2003b. Channel Slope From SRTM Water Surface Elevations in the Amazon Basin. *American Geophysical Union* December ed.: http://adsabs.harvard.edu/abs/2003AGUFM.H12D1016H.

HENGL, T. 2006. Finding the right pixel size. *Journal of Computer & Geosciences,* Vol. 32 pp.1283-1298.

HISCOCK, J. G. & HILBURN, R. T. Year .WAM - GIS WATERSHED ASSESSMENT MODEL. *In:* ESRI user conference, 1998 US. ESRI.

HOLTAN, H. N. 1932. A concept for infiltration estimates in watershed engineering. *Bulletin.* Washington, D.C.. USDA, ARS.,

HOONG, N. K. 2004. *Effects Of SMART ON FLOOD FLOW WITH MIKE 11 Application.* Bs, UTM.

HORTON, R. E. 1933. The role of infiltration in Hydrologic Cycle. *Transactions of American Geophysical Union,* vol.14**,** pp.446-460.

HORTON, R. E. 1940. An approach toward a physical interpretation of infiltration capacity. *Soil Science Society American Proceedings,* vol.5**,** pp.399-417.

HOSSAIN, F. 2004. *Investigating error propagation in flood prediction based on remotely-sensed rainfall.* University of Connecticut.

HUANG, G. & CHEN, Y. D. 2008. Low flow simulation for the Dongjiang basin using the Xinanjiang watershed hydrological model. *IAHS* 319**,** 7.

HUANG, M., GALLICHAND, J., WANG, Z. & GOULET, M. 2006. A modification to the Soil Conservation Service curve number method for steep slopes in the Loess Plateau of China. *Hydrological Processes,* vol.20**,** pp.579–589.

HUFFMAN, G. J. & BOLVIN, D. T. 2009. Real-Time TRMM Multi-Satellite Precipitation Analysis Data Set Documentation. Laboratory for Atmospheres, NASA Goddard Space Flight Center and Science Systems and Applications.

HUGGINS, L. F. 1982. Surface runoff, storage and routing. *In:* HAAN, C. T., P, J. H. & BRAKENSIEK, D. L. (eds.) *Hydrologic Modeling of Small Watersheds.* American Society of Agricultural Engineers.

HUGGINS, L. F. & MONKE, E. J. 1966. *The mathematical simulation of the hydrology of small watersheds.,* Lafayette, Purdue Water Resources Research Centre.

JACOBS, J., MYERS, D. & WHITFIELD, B. 2003. Improved rainfall/runoff estimates using remotely sensed soil moisture. *Journal of Am Water Resources Association,* vol.39 ,pp.313–324.

JAMALUDDIN, M. J. 1985. Flash flood problems and human responses to the flash flood hazard in Kuala Lumpur area, Peninsular Malaysia. *Akademika,* vol.26**,** pp.18.

JARVIS, A., RUBIANO, J., NELSON, A., FARROW, A. & MULLIGAN, M. 2004a. Practical use of SRTM data in the tropics – Comparisons with digital elevation models generated from cartographic data. *In:* (CIAT), I. C. F. T. A. (ed.). Cali, Colombia: CIAT.

JARVIS, A., RUBIANO, J., NELSON, A., FARROW, A. & MULLIGAN, M. 2004b. Practical use of SRTM data in the tropics: comparisons with digital elevation models generated from cartographic data. *Working document,* 198**,** 32.

JENSON, S. K. Year. Methods and applications in Surface depression analysis. *In:* OF, U. S. G. S. P., ed. Auto-Carto, 8, 1987 Baltimore, Maryland, US. pp.131-144.

JENSON, S. K. & DOMINGUE, J. O. 1988. Extracting Topographic Structure from Digital Elevation Data for Geographic Information System Analysis. *Photogrammetric Engineering and Remote Sensing,* Vol. 54**,** pp. 1593-1600.

JOHNSON ,L. E. 2009. *Geographic Information Systems in Water Resources Engineering*, CRC Press.

JONES, N. L., WRIGHT, S. G. & MAIDMENT, D. R. 1990. Watershed delineation with triangle-based terrain models. *Journal of Hydraulic Engineering,* vol. 116**,** pp. 1232-1251.

JONSDOTTIR, H. 2006. *Stochastic Modelling of Hydrologic Systems.* Informatics and Mathematical Modelling, Technical University of Denmark.

JOYCE, R. J., JANOWIAK, J. E. & P.A. ARKIN, P. X. 2004. CMORPH: A method that produces global precipitation estimates from passive microwave and infrared data at 8 km, hourly resolution. *J. Climate,* vol. 5**,** pp.487-503.

JPL/NASA. 2006. *The Shuttle Radar Topography Mission ,http://www2.jpl.nasa.gov/srtm/* [Online]. CA,USA. [Accessed 15 May 2009.[

JPS 2003. Klang River Environmental Improvement and Flood Mitigation Project,Final Report 2003. *In:* DRAINAGE, D. O. I. A. (ed.). Kuala Lumpur.

JUPEM 2006. Country Report 2006: Integration of Built and Natural Environmental Datasets within a National SDI. *In:* DEPARTMENT OF SURVEY AND MAPPING, M. (ed.). Kuala Lumpur,: online report: avalable at http://www.geom.unimelb.edu.au/research/SDI_research/Integrated/Int_Template_Malaysia.pdf.

JUTLA, A. S. 2006. *Simulation of the Hydrological Processes on Reconstructed Watersheds Using System Dynamics.* the Degree of Master of Science University of Saskatchewan,Canada.

KARAMOUZ, M. & ARAGHINEJAD, S. 2005. *Advanced hydrology*, Amirkabir University Press.

KIEL, B., ALSDORF, D. & LEFAVOUR, G. 2006. Capability of SRTM C- and X-band DEM Data to Measure Water Elevations in Ohio and the Amazon. *Photogrammetric Engineering & Remote Sensing,* Vol. 72**,** pp.1-8.

KIM, Y., ENGEL, B., LIM, K., LARSON, V. & DUNCAN, B. 2002. Runoff impacts of land use changes in Indian River Lagoon watershed. *J Hydrologic Engineering,* vol.7**,** pp.245–251.

KING, M. D., CLOSS, J., WHARTON, S. & MYERS, M. (eds.) 2004. *EOS Data Products Handbook*.

KISS, R. 2004. Determination of drainage network in digital elevation models, utilities and limitations. *Journal of Hungarian Geomathematics,* vol.2**,** pp.16-29.

KNEBLA, M. R., YANGA, Z.-L., HUTCHISONB, K. & MAIDMENT, D. R. 2005 Regional scale flood modeling using NEXRAD rainfall, GIS,and HEC-HMS/RAS: a case study for the San Antonio River Basin Summer 2002 storm event. *Journal of Environmental Management* 75 pp.11.

KOBOLD, M. 2007. Hydrological Modelling of Floods. *In:* ASHLEY, R., GARVIN, S., PASCHE, E., ANDREASVASSILOPOULOS & ZEVENBERGEN, C. (eds.) *Advances in Urban Flood Management.* Taylor & Francis.

KONECNY, G. 2003. *Geoinformation : Remote Sensing, Photogrammetry and Geographic Information Systems,* New York, Taylor & Francis Routledge.

KOOLHOVEN, W., HENDRIKSE, J., NIEUWENHUIS, W., RETSIOS, B., SCHOUWENBURG, M., WANG, L., BUDDE, P. & NIJMEIJER, R. 2007. The Integrated Land and Water Information System (ILWIS). 3.4 ed. Enschede, The Netherlands ITC.

KOUDMANI, M. 2004. Applications of Remote Sensing to Hydrology and Hydrogeology. *International Conf. on Water Resources & Arid Environment.* Bab Breed - Kallaseh, Damascus.

LAGACHERIE, P. & MCBRATNEY, A. Year. perspectives for digital soil mapping. *In:* LAGACHERIE, P., MCBRATNEY, A. & VOLTZ, M., eds. Global Workshop on Digital Soil Mapping 14–17 September 2004 2005 Montpellier, INRA. Elsevier, pp. 1–15.

LAI, S. H., AMIN, M. S. M., LAW, P. L & .SEN, Y. March 2008. APPLICATIONS OF GIS AND REMOTE SENSING IN THE HYDROLOGICAL STUDY OF THE UPPER BERNAM RIVER BASIN, MALAYSIA. *The Institution of Engineers, Malaysia (,,),* Vol. 69.

LEA, N. L. & , I., : , 1992. An aspect driven kinematic routing algorithm. *In:* PARSONS, A. J. & ABRAHAMS, A. D. (eds.) *Overland flow: hydraulics and erosion mechanics.* London.UK: Taylor and francis.

LEHNER, B., VERDIN, K. & JARVIS, A. 2006a. HydroSHEDS Technical Documentation Version 1.0 (available online at: http://gisdata.usgs.gov/webappcontent/HydroSHEDS/downloads/HydroSHEDS_TechDoc_v10.pdf). *In:* SURVEY, U. S. G. (ed.(.

LEHNER, B., VERDIN, K. & JARVIS, A. 2006b. HydroSHEDS,Technical Documentation. *In:* USGS (ed.). Washington, DC.

LI, Z., ZHU, Q. & GOLD, C. 2005a. *Digital Terrain Modeling Principles and Methodology,* Boca Raton,Florida, USA, CRC Press.

LIU, Y. B., YI, Y., BATELAAN, O. & DE SMEDT, F. Year. Assessing grid size effects on runoff and flow response using a GIS-based hydrologic model. *In:* LI, S. N. & TAO, V., eds. 13th International Conference on Geoinformatics, Sept. 17-19 2005 Toronto, Canada. pp1-8.

LOAGUE, K. & CORWIN, D. L. 2000. Regional-Scale Assessment of non-point source Groundwater Contamination. *In:* GURNELL, A. M. & MONTGOMERY, D. R. (eds.) *Hydrological Applications of GIS.* Wiley; 1 edition.

LONGLEY, P. 2005. *Geographic information systems and science*, John Wiley & Sons Inc.
LONGLEY, P. A., GOODCHILD, M. F., MAGUIRE, D. J. & RHIND, D. W. 2005. *Geographical Information Systems and Science,* Barcelona, Spain, John Wiley & Sons.
LOWREY, M. R. K. 2006. *Regional scale flood modeling and watershed investigation, using NEXRAD rainfall, GIS, and HEC-HMS/RAS: A case study for the San Antonio River Basin, Texas.* Doctor of Philosophy, The University of Texas at Austin.
LYON, J. G. (ed.) 2003 *GIS for Water Resources and Watershed Management,* New York: Taylor & Francis.
MACARTHUR, R. & DEVRIES, J. J. 1993. Introduction and Application of Kinematic Wave Routing Techniques Using HEC-1. Davis, CA: US Army Corps of Engineers, Institute for Water Resources, Hydrologic Engineering Center (HEC (
MAIDMENT, D. 1993a. GIS and hydrologic modeling. *Environmental modeling with GIS***,** 147-167.
MAIDMENT, D. 2002. *Arc Hydro: GIS for Water Resources,* New York, Esri Press.
MAIDMENT, D. R. 1993b. GIS and hydrologic modeling. *In:* GOODCHILD, M. F. (ed.) *Environmental modeling with GIS.* New York: Oxford University Press, Inc.
MAIDMENT, D. R. 1996 .GIS and Hydrologic Modeling - an Assessment of Progress. *The Third International Conference on GIS and Environmental Modeling.* Santa Fe, New Mexico.
MAIDMENT, D. R. 1998. *Introduction to Spatial Hydrology* ESRI press.
MAIDMENT, D. R. & DJOKIC, D. 2000. *Hydrologic and hydraulic modeling support:with geographic information systems,* New York, ESRI Press.
MARTIN, P., LEBOEUF, E., DOBBINS, J., DANIEL, E. & ABKOWITZ, M. 2005a. INTERFACING GIS WITH WATER RESOURCE MODELS: A STATE OF THE ART REVIEW1. *JAWRA Journal of the American Water Resources Association,* 41**,** 1471-1487.
MARTIN, P. H., LEBOEUF, E. J., DOBBINS, J. P., DANIEL, E. B. & ABKOWITZ, M. D. 2005b. INTERFACING GIS WITH WATER RESOURCE MODELS: A STATE-OF-THE-ART REVIEW1. *Journal of the American Water Resources Association (JAWRA),* 41**,** 17.
MARTıNEZ-MENA, M., ALBALADEJO, J. & CASTILLO, V. 1998. Factors influencing surface runoff generation in a Mediterranean semiarid nvironment: Chicamo watershed8. *SE Spain, Hydrological Processes,* 12**,** 741–754.
MARTINUZZI, S ,.GOULD, W. A., GONZALEZ, O. M. R., ROBLES, A. M., MALDONADO, P. C. & CABAN, N. P.-B. J. F. 2008. Mapping tropical dry forest habitats integrating Landsat NDVI, Ikonos imagery, and topographic information in the Caribbean Island of Mona. *Rev. Biol. Trop*) *.Int. J. Trop. Biol. 2008,* Vol. 56**,** pp.16.
MCCUEN, R. 1982. *A Guide to hydrologic Analysis Using SCS Methods*, Prentice Hall.
MCCUEN, R. H. 1998. *Hydrologic analysis and design*, Prentice-Hall International.
MEIJERINK, A. M. J. 1996. Remote Sensing Applications to Hydrology:Groundwater. *Hydrological Sciences Journal,* vol.41**,** pp.459-561.
MELESSE, A. M. 2004. DEM-RS-GIS BASED STORM RUNOFF HYDROGRAPH ESTIMATION FOR THE HEART RIVER SUB-ASIN, MISSOURI RIVER BASIN. *Journal of Environmental Hydrology,* Vol.12**,** 24.
MEYER, W. J. 1985. *Concepts of Mathematical Modeling,* New York, McGraw-Hill Book Company.

MILIARESIS, G. C. 2008. Quantification of Terrain Processes. *In:* ZHOU, Q., LEES, B. & TANG, G.-A. (eds.) *Advances in Digital Terrain Analysis.* Berlin: Springer-Verlag Heidelberg.

MILLER, C. & LAFLAMME, R. 1958. The digital terrain model : theory and applications. *Photogrammetric Engineering,* 24**,** 433–442.

MILLER, S. N., SEMMENS, D. J., GOODRICH, D. C., HERNANDEZ, M., MILLER, R. C., KEPNER, W. G. & GUERTIN, D. P. 2007 .The Automated Geospatial Watershed Assessment Tool. *Environmental Modelling & Software,* 22**,** 365-377.

MISHRA, S. K., PANDEY, R. P., JAIN, M. K. & SINGH, V. P. 2008. A Rain Duration and Modified AMC-dependent SCS-CN Procedure for Long Duration Rainfall-runoff Events. *Water Resour Manage* vol.22**,** pp.861–876.

MISHRA, S. K. & SINGH, V. P. 1999. Another Look at SCS-CN Method. *Journalof Hydrologic Engineering,* Vol. 4**,** pp.257-264.

MLMIKOU, M. & GORDIOS, J. 1989. Predicting the mean annual flood and flood quantiles for ungauged catchments in Greece. *Hydrological Sciences Journal,* vol.34**,** pp.169-184.

MOCKUS, V. 1965. Estimation of Direct Runoff From Storm Rainfall. *SCS National Engineering Handbook, Section 4.* Washington, DC.: Hydrology, Soil Conservation Service.

MOORE, I. D. & GRAYSON, R. B. 1991. Terrain-based catchment partitioning and runoff prediction using vector elevation data. *Water Resources Research,* vol. 27**,** pp. 1177-1191.

MOREDA, F., KOREN, V., ZHANG, Z., REED, S. & SMITH, M. 2006. Parameterization of distributed hydrological models: learning from the experiences of lumped modeling *Journal of Hydrology,* vol.320**,** P. 218-237

MORIASI, D. Thursday, May 21 2009 *RE: Application of Nash-Sutcliffe efficiency* Type to LABORATORY, R. H. U.-A. G. R.

MORIASI, D .N., ARNOLD, J. G., VAN LIEW, M. W., BINGNER, R. L., HARMEL, R. D. & VEITH, T. L. 2007. Model evaluation guidelines for systematic quantification of accuracy in watershed simulations. *Transactions of the ASABE* 50**,** 885-900

NAS 2008. Earth Observations from Space: The First 50 Years of Scientific Achievements. *In:* COMMITTEE ON SCIENTIFIC ACCOMPLISHMENTS OF EARTH OBSERVATIONS FROM SPACE, B. O. A. S. A. C., DIVISION ON EARTH AND LIFE STUDIES (ed.). Washington: the National Academy of Sciences.

NASA (ed.) 2006 .*Earth Science Reference Handbook, A Guide to NASA's Earth Science Program and Earth Observing Satellite Missions,* Washington, D.C.: National Aeronautics and Space Administration.

NASA 2009. Readme for TRMM Product 3B42 (V6) http://disc.sci.gsfc.nasa.gov/precipitation/documentation/TRMM_README/TRMM_3B42_readme.shtml.

NASH, J. E. & SUTCLIFFE, J. V. 1970. River flow forecasting through conceptual models. Part I– a discussion of principles. *Journal of Hydrology,* 10**,** 282-290.

NELSON, E. J., JONES, N. L. & MILLER, A. W. 1994. Algorithm for precise drainage-basin delineation. *Journal of Hydraulic Engineering,* vol. 120**,** pp. 298-312.

NIEMCZYNOWICZ, J. 1984. Investigation of the Influence of Rainfall Movement on Runoff Hydrograph. *Nordic Hydrology,* Vol 15**,** 71-84.

NIEMCZYNOWICZ, J. 1987. Storm tracking using rain gauge data. *Journal of Hydrology,* Vol.93**,** 135-152.

NIJMEIJER, R. 2001. Image Processing. *In:* SCHARRENBORG, H. (ed.) *ILWIS 3.0 Academic, User's Guide.* ITC. the Netherlands.
O'CALLAGHAN, J. F. & MARK, D. M .1984 .The extraction of drainage networks from digital elevation data. *Computer Vision, Graphics, and Image Processing,* vol. 28**,** pp. 328-344.
OBLED, C., WENDLING, J. & BEVEN, K. 1994. The sensitivity of hydrological models to spatial rainfall patterns: an evaluation using observed data. *Journal of Hydrology,* Vol. 159**,** 305-333.
OGDEN, F .L., GARBRECHT, J., DEBARRY, P. A. & JOHNSON, L. E. 2001. GIS and Distributed Watershed Models II. *Journal of Hydrologic Engineering,* Vol. 6**,** 9.
OSBORN, H. B. & LANE, L. J. 1982. Precipitation. *In:* JOHNSON, H. P. & BRAKENSIEK, D. L. (eds.) *Hydrologic Modeling of Small Watersheds.* American Society of Agricultural Engineers Monograph.
OSORIO, J., WOLFE, M., HEATWOLE, C., BENHAM, B. & CARDENAS, A. Year. Comparison of watershed boundaries derived from SRTM and ASTER digital elevation datasets and from a digitized topographic map. *In:* 2007 ASABE Annual International Meeting, 17 - 20 June 2007 Minneapolis Convention Center, Minneapolis, Minnesota
OXFORD 2005. Oxford Dictionary. *A Dictionary of Science.* FIFTH EDITION ed. New York: Oxford University Press.
PACIOREK, C. & SCHERVISH, M. 2006. Spatial modelling using a new class of nonstationary covariance functions. *Environmetrics,* 17**,** 483-506.
PANDA, S. S. 2006. Lecturer (power point presentation) entiteled : Advanced GIS, accessible in giscenter.isu.edu/training/ppt/AdvGIS/Lecture13.ppt. Idaho State University web page.
PATRICK, N. A. & STEPHENSON, D. 1990. Spatial variation of rainfall intensities for short duration storms. *Hydrological Sciences,* 35**,** 667.
PETERS-LIDARD, C. D. & WOOD, E. 1994. Estimating storm areal average rainfall intensity in field experiments. *Water Resources Research* 30.
PEUCKER, T. K. & DOUGLAS, D. H. 1975. Detection of surface-specific points by parallel processing of discrete terrain elevation data. *Computer Graphics and Image Processing,* vol.4**,** pp. 375-387.
PHILIP, J. R. 1957. The theory of infiltration1.The infiltration equation and its solution. *journal of Soil Science,* vol.83**,** pp.345-347.
PHILLIPS, D. L., DOLPH, J. & MARKS, D. 1992. A comparision of Geostatistical Procedures fro spatial analysis of Precipitation in Mountainous terrain. *Joricultural of Agricultural and forest Meteorology,* Vol.58**,** pp.119-141.
PONCE, V. M. & HAWKINS, R. H. 1996. Runoff Curve Number: Has It Reached Maturity? *Journal of Hydrologic Engineering,* Vol. 1**,** pp. 11-19.
PRYDE, J. K., OSORIO, J., WOLFE, M. L., HEATWOLE, C., BENHAM, B. & CARDENAS, A. 2007. Comparison of watershed boundaries derived from SRTM and ASTER digital elevation datasets and from a digitized topographic map. *2007 ASABE Annual International Meeting.* Minneapolis Convention Center, Minneapolis, Minnesota, US: American Society of Agricultural and Biological Engineers (ASABE.(
QUATTROCHI, D. & GOODCHILD, M. (eds.) 1997. *Scale in Remote Sensing and GIS, ,* Boca Raton, FL: Lewis Publishers.
RAGHUNATH, H. 2006a. *Hydrology: principles, analysis and design*, New Age International.
RAGHUNATH, H. M. 2006b. *Hydrology: Principles, Analysis and Design,* New Delhi, New Age International.

RASEMANN, S., SCHMIDT, J., SCHROTT, L. & DIKAU, R. 2004. Geomorphometry in mountain terrain. *Geographic information science and mountain geomorphology*, 101.

REDDY, J. R. 2005. A Text Book of Hydrology. 2 ed. India: Firewall Media.

REDFEARN, H. D. 2005. *Rainfall-runoff changes due to urbanization: a comparison of different spatial resolutions for lumped surface water hydrology models using HEC-HMS.* Master of Science (Environmental Science), University of North Texas.

REUTER, H., NELSON, A. & JARVIS, A. 2007. An evaluation of void-filling interpolation methods for SRTM data. *International Journal of Geographical Information Science,* 21**,** 983-1008.

RICHARD, L. A. 1931. Capillary conduction through porous mediums. *Journal of Physics,* vol.1**,** pp.318-333.

ROBAYO, O. 2005. *Map to Map: Converting a NEXRAD Rainfall Map into a Flood Inundation Map.* Doctor of Philosophy applied research, University of Texas.

ROBERTS, D. M. & ROBERTS, F. H. 1998. *Correlation Coefficient* [Online]. New York 13069 (USA) MathBits.com - Frederick and Donna Roberts [Accessed April 14, 2009.[

RODRIGUEZ, E., MORRIS, C. S., BELZ, J. E., CHAPIN, E. C., MARTIN, J. M., DAFFER, W. & HENSLEY, S. 2005. An Assessment of the SRTM Topographic Products. *Technical Report JPL.* Pasadena,CA,USA.

ROSSITER, D. G. 2003. *Methodology for Soil Resource Inventories, ITC Lecture Notes SOL.27*

The Netherlands, 110pp., Enschede,The Netherlands, ITC.

ROUSE, J. W., HAAS, R. H., SCHELL, J. A. & DEERING., D. W. Year. Monitoring Vegetation Systems in the Great Plains with ERTS. *In:* Proceedings of the Third Earth Resources Technology Satellite 1-Symposium, 1974 Greenbelt: NASA. NASA, 3010-317.

SAATY, T. L. & ALEXANDER, J. M. 1981. *Thinking With Models* New York, Press in Oxford.

SANYAL, J. & LU, X. 2004. Application of remote sensing in flood management with special reference to monsoon Asia: a review. *Natural Hazards,* 33**,** 283-301.

SCHARFFENBERG, W. A. & FLEMING, M. J. 2008. Hydrologic Modeling System HEC-HMS; User's Manual. Davis, California: US Army Corps of Engineers, Institute for Water Resources, Hydrologic Engineering Center.

SCS 1972a. Hydrology, sec. 4. *National Engineering Handbook.* Washington: Soil Conservation Service, U. S. Department of Agriculture. ,

SCS 1972b. SCS National Engineering Handbook, Section 4. *SCS National Engineering Handbook.* Washington, DC.: Hydrology, Soil Conservation Service.

SERAFIN, R. J., ALEXANDER, M. J., ANDERSON, F. R., BENDER, M. L., BIERBAUM, R. M., CARROLL, M. A., CLAYSON, C. A., DABBERDT, W. F., EMANUEL, K. A., HARTMANN, D. L., LEAVITT, P. R., LOGAN, J. A., MORRIS, V. R., ROWLAND, F. S. & HAAR, T. H. V .2007 .NOAA's role in space-based global precipitation estimation and application. *In:* DICKINSON, R. (ed.) 1 ed. Washington, DC,USA: National Academices Press.

SEYBERT, T. A. 1996. *Effective Partitioning of Spatial Data for Use in a Distributed Runoff Model , .* Doctor of Philosophy The Pennsylvania State University.

SHAABAN, A. J., FENG, H. Y. & NASIR, K. A. M. 2008. Potential and Effectiveness of Rainwater Harvesting in Enhancing the Effectiveness of On-Site Detention (ROSD) Facilities in Controlling Surface Runoff at Taman Wangsa Melawati, Kuala Lumpur (available online

:http://www.nahrim.gov.my/download/pksa/rainwater/Paper%207.pdf).
NAHRIM.

SHAMSI, U. M. 2002. *GIS Tools for Water, Wastewater, and Stormwater Systems*, ASCE Press

SHAMSI, U. M. 2005. *GIS Applications for Water, Wastewater, and Stormwater Systems*, CRC Press.

SHERMAN, L. K. 1932. Streamflow from rainfall by the unit-graph method. *Engineering News Record,* vol.108**,** pp.501-505.

SHRESTHA, M. N. 2003. Spatially Distributed Hydrological Modelling considering Land-use changes using Remote Sensing and GIS. *Map Asia 2003.* PWTC, kuala lumpur, Malaysia: GISdevelopment.net.

SINGH, G., SASTRAJ, G. & JOSHI, B. P. 1996a. *Manual of Soil and water Conservation Practice in India*, Central Soil & Water Conservation Research & Training Institute.

SINGH, J., KNAPP, H. V. & DEMISSIE, M. 2004. Hydrologic modeling of the Iroquois River watershed using HSPF and SWAT. *Illinois State Water Survey Contract Report.* Illinois: Illinois Department of Natural Resources and the Illinois State Geological Survey.

SINGH, V., SINGH, V. P. & FIORENTINO, M. 1996b. *Geographical Information Systems in Hydrology* Springer

SINGH, V. P. 1988. *Hydrological Systems,* NJ,USA, Prentice Hall.

SINGH, V. P. (ed.) 1995. *Computer Models of Watershed Hydrology,* Highland Ranch, Colorado, USA: Water Resources Publications.

SINGH, V. P. & FREVERT, D. K. (eds.) 2006. *Watershed Models,* Boca Raton,USA: CRC Press.

SINGH, V. P. & WOOLHISER, D. A. 2002. Mathematical Modeling of Watershed Hydrology. *Journal of Hydrologic Engineering,* Vol. 7**,** 23.

SKIDMORE, A. K. 1990. Terrain position as mapped from a gridded digital elevation model. *International Journal of Geographical Information Systems,* vol.4**,** pp.33-49.

SMITH, A. A. 2004. MIDUSS Version 2 Reference Manual. Dundas, Ontario, Canada: Alan A. Smith Inc.

SMITH, J. A., BAECK, M. L., MORRISON, J. E., STURDEVANT-REES, P., TURNER-GILLESPIE, D. F. & BATES, P. D. 2002. The regional hydrology of extreme floods in an urbanizing drainage basin. *Journal of Hydrometeorology,* vol.3**,** pp.267-282.

SMITH, R. E. 1972. The infiltration envelop: Results from a theoretical infiltrometer. *Journal of Hydrology,* vol.17**,** pp.1-21.

SMITH, R. E. Year. Rational models for infiltration hydrodynamics. *In:* International Symposium on Rainfall-Runoff Modeling, May 18-21 1981 Mississippi State. Mississippi State University.

SNYDER, F. F. 1938. Synthetic unit-graphs. *Trans. Am. Geophys. Union,* vol. 19**,** pp. 447-454.

SOROOSHIAN, S. 1983. Surface water hydrology: online estimation. *Reviews of Geophysics and Space Physics,* vol.21**,** pp.706-721.

SOROOSHIAN, S., HSU, K.-L., COPPOLA, E., TOMASSETTI, B., VERDECCHIA, M. & VISCONTI, G. (eds.) 2008. *Hydrological Modelling and the Water Cycle: Coupling of the Atmosphere and Hydrological Models*: Springer.

SOROOSHIAN, S., HSU, K.-L., GAO, X., GUPTA, H. V., IMAM, B. & BRAITHWAITE, D. 2000a. Evaluation of PERSIANN system satellite-based estimates of tropical rainfall. *American Meteorological Society,* vol.81**,** pp.2035-2046.

SOROOSHIAN, S., HSU, K., XIAOGANG ,G., GUPTA, H., IMAM, B. & BRAITHWAITE, D. 2000b. Evaluation of PERSIANN system satellite-based estimates of tropical rainfall. *Bulletin of the American Meteorological Society,* 81**,** 2035-2046.

STRAUB, T. D., MELCHING, C. S. & KOCHER, K. E. 2000. Equations for Estimating Clark Unit-Hydrograph Parameters for Small Rural Watersheds in Illinois. Urbana,Illinois USGS,Illinois Department of Natural Resources, Office of Water Resources.

SU, F., HHONG, Y. & LETTENMAIER, D. P. 2007. Evaluation of TRMM Multisatellite Precipitation Analysis (TMPA) and Its Utility in Hydrologic Prediction in the La Plata Basin. *Journal of Hdyrometeorology,* vol.9**,** pp.622-640.

SUI, D. Z. & MAGGIO, R. C. 1999. Integrating GIS with hydrological modeling: practices, problems, and prospects *Computers, Environment and Urban Systems,(Publisher: Elsevier),* 23**,** pp,33-51.

SYED, K. H. 1999. *The Impacts of Digital Elevation Model Data Type and Resolution on hydrologic Modeling.* Doctor of Phlosophy University of Arizona.

TARBOTON, D. G. 1997. A new method for the determination of flow directions and upslope areas in grid digital elevation models. *Water Resources Research,* vol. 33**,** pp. 309-319.

THAVORNTAM, W., WATTANAKIJ, N. & MONGKOLSAWAT, C. Year. Estimation of rainfall spatial interpolation methods in North-East Thailand. *In:* Asian Conference on Remote Sensing (ACRS 2007) 12 to 16 November 2007 (PWTC), Kuala Lumpur, Malaysia.

TICK, L. J. & SAMAH, A. A. 2004. *Weather and climate of Malaysia,* Kuala Lumpur, University Malaya Perss.

TULU, M. D. 20 .05*SRTM-DEM Suitability in Runoff Studies.* Master ITC.

USACE 1994. Engineering and Design - Flood-Runoff Analysis *In:* ARMY, D. O. T. (ed.). US Army Corps of Engineers

USACE 1996. Hydrologic Aspects of Flood Warning – Preparedness Programs. *In:* ENGINEERS ,U. S. A. C. O. (ed.) *Technical Letter* Washington, DC.: U.S. Army Corps of Engineers.

USDA 1986. Urban Hydrology for Small Watersheds (TR-55). *In:* UNITED STATES DEPARTMENT OF AGRICULTURE, N. R. C. S., CONSERVATION ENGINEERING DIVISION (ed.) Second Ed ed .Washington, DC: United States Department of Agriculture.

USGS. 2008. *HydroSHEDS (Hydrological data and maps based on SHuttle Elevation Derivatives at multiple Scales)* [Online]. U.S. Geological Survey Available: http://hydrosheds.cr.usgs.gov/datasource.php [Accessed May 15 2009.[

UTTS, J. M. 2004. *Seeing Through Statistics,* Canada, Duxbury Press.

VALENZUELA, C. & BAUMGARDNER, M. 1990. Selection of appropriate cell sizes for thematic maps. *ITC Journal* 3**,** 219–224.

VARLEY, I. & MARR, A. Year. Urbanisation and its effect on infiltration and flood detention in Kuala Lumpur. *In:* JAMES, R., DANIELL, T. & TAKARA, K., eds. intl conf. Water sensitive urban design, 22-23 November 2004 Adelaid, Australia. IHP-VI, Techn. Doc. in Hydrol. 3, , 130-136.

VERDI, R. J. 2007 .*Implications of Spatial Resolution on Hydrological Network Modeling : A Case Study in the Chipola river basin, Florida.* Master of Science, The Florida State University.

VIESSMAN, W. & LEWIS, G. L. 2003a. Hydrologic Simulation and streamflow analysis .*Introduction to Hydrology.* NJ, USA: Prentice Hall, Pearson Education In.

VIESSMAN, W. & LEWIS, G. L. 2003b. ***Introduction to hydrology,*** New Jersey, USA, Prentice Hall.
VIESSMAN, W. J., LEWIS, G. L. & KNAPP, J. W. 1989. *Introduction of hydrology,* New York ,Harper and Row Publishers.
VIEUX, B. 2004a. *Distributed hydrologic modeling using GIS*, Kluwer Academic Publishers.
VINK, A. 1975. *Land Use in Advancing Agriculture* ,New York, NY, Springer.
WALE, A., T.H.M., R., R.J.J., D. & A., G. Year. Hydrological Balance of LakeTana, Upper BlueNile Basin, Ethiopia. *In:* ABTEW, W. & MELESSE, A. M., eds. Hydrology and Ecology of the Nile River Basin under Extreme Conditions, June 1 2008 19-6Adis Ababa, Ethiopia.
WATTS, L. G. & CALVER, A. 1991. Effects of Spatially-Distributed Rainfall on Runoff for a Conceptual Catchment. *Nordic Hydrology,* 22**,** 1-14.
WONG, T. H., MANSOR, S. B., MISPAN, M. R., SULAIMAN, W. N. A. & AHMAD, N. 2001. An application of remote sensing in hydrology - a case study in Malaysia. *Geoscience and Remote Sensing Symposium, 2001. IGARSS '01. IEEE 2001 International* Sydney, NSW IEEE Xplore Digital Library.
WOODWARD, D., HAWKINS, R., JIANG, R., HJELMFELT JR, A., VAN MULLEM, J. & QUAN, Q. Year. Runoff curve number method: examination of the initial abstraction ratio. *In*, 2004. ASCE.
WOODWARD, D. E., HAWKINS, R. H., JR., A. T. H., MULLEM, J. A. V. & QUAN, Q. D. 2002. Curve Number Method: Origins,Applications and Limitations. Available at:www.wsi.nrcs.usda.gov/products/W2Q/H&H/tech_info/topics/CNarchive.html.
WOOLHISER, D. A. & BRAKENSIEK, D. L. 1982. *Hydrologic system synthesis;Hydrologic modeling of small watersheds,* St. Joseph, American Society of Agricultural Engineers.
WURBS, R. A. 1998. Dissemination of generalized water resources models in the United States. *Water International,* vol.23**,** 190–198.
YANG, C. R. & TSAI, C. T. 2000. Development of a GIS-based flood information system for floodplain modeling and damage calculation. *Journal of the American Water Resources Association,* 36**,** pp.567-557(12.(
YE, W., BATES, B. C., VINEY, N. R., SIVAPALAN, M. & JAKEMAN, A. J. 1997. Performance of conceptual rainfall-runoff models in low-yielding ephemeral catchments. *Water Resources Research,* vol.33**,** pp.153-166.
YEGANE, R. & PAYVANDI, A. A. 2005. Applications of maps at scale of 1:25000 in crisis managment. *Geomatic 84.* Tehran,Iran: National Cartographic organization (available in: http://www.civilica.com/Paper-GEO84-GEO84_90.html.(
YONGBO, L. 2004. *Development and application of a GIS-based hydrological model for flood prediction and watershed management.* PhD, Vrije Universiteit Brussels.
YOUNG, R., ONSTAD, C., BOSCH, D. & ANDERSON, W. 1987. AGNPS:an Agricultural Non-Point Source Pollution Model:a large water analysis model. *In:* AGRI., U. S. D. O. (ed.). U.S. Dept. of Agri.
YU, Z. 1997. Grid-spacing Effect on WatershedHydrological Simulations. *Journal of Hydrologcal Science & Technology,* v.13**,** p.75-85.
ZERGER, A. 1999. Digital Elevation Modelling for natural hazard risk assessment. *Australian Journal of Emergency Management,* Vol.13 pp.61-65.
ZHOU, Q., LEES, B. & TANG, G.-A. (eds.) 2008. *Advances in Digital Terrain Analysis,* Berlin Springer.

List of Appendices

Appendix A: Status of world mapping and List of used digital topo sheets

Table A.1 Status of world mapping in1990 (Source: Konecny, 2003)

Scale range	1:25,000	1:50,000	1:100,000	1:200,000
Africa	2.9%	41.4%	21.7 %	89.1%
Asia	15.2%	84%	56.4%	100 %
Australia and Oceania	18.3%	24.3%	54.4%	100%
Europe	86.9%	96.2%	87.5%	90.9%
Former USSR	100 %	100%	100%	100%
North America	54.1%	77.7%	37.35	99.2%
South America	7%	33%	57.9%	84.4%
World	33.5%	65.6%	55.7%	95.1%

Table A.2: Update rates of world mapping (Source: Konecny, 2003)

Scale range	1:25,000	1:50,000	1:100,000	1:200,000
Africa	1.7%	2.2 %	3.6 %	1.4%
Asia	4.0 %	2.7 %	0.0 %	1.9 %
Australia and Oceania	0 %	0.8 %	0 %	0.3 %
Europe	6.6 %	5.7 %	7.0 %	7.5 %
Former USSR	0 %	0 %	0 %	0%
North America	4.0%	2.7%	0.0 %	6.5 %
South America	0 %	0.1 %	0 %	0.3 %
World	5.0 %	2.3 %	0.7 %	3.4 %

Table A.3: List of used digital topo sheets at scale of 1:10000

No.	File name	Sheet name	Date of Aerial Photo
1	6A.dxf	Jinjang	1992
2	6D.dxf	Jinjang	1992
3	6F.dxf	Jinjang	1992
4	7A.dxf	Gombak Setia	1989&1992
5	7B.dxf	Gombak Setia	1989&1993
6	7C.dxf	Gombak Setia	1989&1994
7	7D.dxf	Gombak Setia	1989&1995
8	7E.dxf	Gombak Setia	1989&1996
9	7F.dxf	Gombak Setia	1989&1997
10	8A.dxf	Kg. Klang Gates Baharu	1986&1992
11	8C.dxf	Kg. Klang Gates Baharu	1986&1993
12	8E.dxf	Kg. Klang Gates Baharu	1986&1994
13	15B.dxf	Damansar	1992
14	15D.dxf	Damansar	1992
15	15F.dxf	Damansar	1992
16	16A.dxf	Kuala Lumpur	1992
17	16B.dxf	Kuala Lumpur	1992
18	16C.dxf	Kuala Lumpur	1992

Table A.3, continued

No.	File name	Sheet name	Date of Aerial Photo
19	16D.dxf	Kuala Lumpur	1992
20	16E.dxf	Kuala Lumpur	1992
21	16F.dxf	Kuala Lumpur	1992
22	17A.dxf	Ampang	1995
23	17C.dxf	Ampang	1995
24	17E.dxf	Ampang	1995

Table A.4: List of used digital topo sheets at scale of 1:25000

No.	File Name	Sheet Name	Date of Arial photo
1	3757a	Damansara	1969
2	3757b	Kuala Lumpur	1982
3	3757c	Shah Alam	1997
4	3757d	Petaling Jaya	1982
5	3758c	Rawang	1982
6	3758d	Selayang Baru Utara	1982
7	3857a	Ampang	1983
8	3857c	Kajang	1983
9	3858c	Kampong Janda Baik	1982

Appendix B: Types of Known Hydrological models

Table B.1: Popular hydrological models

Model	Location of development	Time Scale	type of process and Spatial scale
Hydrologic Engineering Centre-Hydrologic Modeling System (HEC-HMS)	USA	Event based And Continuous	Physically based, semi-distributed
National Weather Service (NWS)	USA	Continuous	Process based, lumped parameter
Hydrologic Simulation Package-Fortran (HSPF)	USA	Continuous	Physically based, semi-distributed
University of British Columbia Model (UBC)	Canada	Continuous	Process based lumped parameter
Waterloo Flood System (WATFLOOD)	Canada	Continuous	Process based semi-distributed
Simple Lumped Reservoir Parametric (SLURP)	Canada	Continuous	Process based, semi-distributed
Runoff Routing Model (ROBR)	Australia	Event based	Lumped
Watershed Bounded Network Model (WBN)	Australia	Event based	Geomorphology based, lumped
Physically Based Runoff Production Model (TOPMODEL)	Europe	Continuous	Physically based, distributed
System Hydrologic European (SHE)	Europe	Continuous	Physically based, distributed
Xinanjiang Model	China	Continuous	Lumped, process based

Table B.2: Known Hydrological model, types of data mode and their interface level (Source : (Martin et al., 2005a)

No	Model	GIS platform	Focus	Interface level	Data model	References
1	GLEAMS	ArcGIS	Hydrology,	1	V	Stallings et al. (1992)
2	CMLS	ArcGIS	Hydrology	1	V	Zhang et al. (1990)
3	MODFLOW	ArcGIS	Ground water	1	R	Hinaman (1993)
4	ANSWERS	GRASS	Watershed erosion	1	R	Srinivasan and Engel (1991)
5	SPUR	ERDAS	Watershed hydrology	1	R	Sasowsky and Gardner (1991)
6	AGNPS	ArcGIS	Hydrology	1	R	SathyaKumar and Farell-Poe (1995)
7	QUAL2E	ERDAS	Water quality	1	R	Yang et al. (1999)
8	MATLAB	ArcGIS	Surface water quality	1	V	Masrili-Libelli et al. (2001)
9	MIKE 11	ArcGIS	Stormwater hydrology	1	V,R	Thompson et al. (2004)
10	MIKE SHE	ArcGIS	Watershed hydrology	1	V,R	Borah and Bera (2004)
11	HEC-HMS	ArcGIS	Flood modeling	1	R	Chang et al. (2000)
12	SWMM	ArcGIS	Stormwater hydrology	1	R	Huber and Dickinson (1988)
13	MIKE Basins	ArcGIS	Watershed hydrology	2	V,R	Jha and Das Gupta (2003)
14	AGNPS	ArcGIS	Water quality	2	V	Tim and Jolly (1994)
15	AGNPS	GRASS	Watershed erosion	2	R	Engel et al. (1993)
16	AGNPS	ERDAS	Hydrology	2	R	Olivieri et al. (1991)
17	AGNPS	GRASS	Hydrology	2	R	Park et al. (1995)
18	SWAT	GRASS	Watershed hydrology	2	R	Srinivasan and Arnold (1994)
19	SMoRMOD	GRASS	Rainfall-runoff	2	R	Zollweg et al. (1996)
20	HSPF, QUAL2E	ArcGIS	modeling system	2	R,V	Whittemore and Beebe (2000)
21	Runoff Model	ArcGIS	Urban runoff	2	R	Wong et al. (1997)
22	HAZUS-MH	ArcGIS	Natural Hazard	2	R	USFEMA (2005)
23	SMR	GRASS	Hydrology	2	R	Frankenberger et al. (1999)
24	WEPP	GRASS	Watershed hydrology	2	R	Savibi et al. (1995)
25	PSRM	ArcGIS	Watershed runoff	2	R,V	Shamsi (1996)
26	WHPA	ArcGIS	Ground water	2	V	Vieux et al. (1998)
27	AgriFlux	IDRISI	Ground water	2	V	Lasserre et al. (1999)
28	MODLFOW	ArcGIS	Ground water	2	V	Tsou and Whittemore (2001)
29	MATLAB	ArcGIS	Ground water	2	V	Raterman et al. (2001)
30	GLEAMS	Arc/CAD	Ground water	2	V	de Paz and Ramos (2002)
31	SCS Runoff Model	MapInfo	Pesticide runof	3	R	Li et al. (2002)
32	AGNPS	ArcGIS	NPS pollution	3	R	Liao and Tim (1997)
33	IDOR2D	ArcGIS	Water quality	3	R,V	Tsanis and Boyle (2001)
34	USLE	IDRISI	Soil erosion	3	R	Fistikoglu and Harmancioglu (2002)
35	PDTank	ArcGIS	Watershed management	3	V	Xu et al. (2001)

Interface Level: 1 = linked, loose coupling, 2 = combined, tightly coupled, particle integration; 3 = integrated, embedded coupling, modeling within.

Data Format: R = Raster; V = vector

Appendix C: Time-series results of flood simulation by HEC-HMS

Table C.1: Time-series results flood simulation at Sulaiman Bridge for event 6-May2002 (Run1)

Date	Time	Computed outflow	Observed outflow
		m^3/s	m^3/s
06May2002	13:15	0	0
06May2002	13:30	0.2	0.2
06May2002	13:45	2.5	8.8
06May2002	14:00	9.6	25.7
06May2002	14:15	20.1	70.4
06May2002	14:30	33.1	274.5
06May2002	14:45	135.5	288.6
06May2002	15:00	324.5	346.6
06May2002	15:15	367.1	356.2
06May2002	15:30	374.9	357.7
06May2002	15:45	365.7	349.5
06May2002	16:00	334.7	329.9
06May2002	16:15	295.5	321.9
06May2002	16:30	255.6	309.8
06May2002	16:45	219.6	200.8
06May2002	17:00	188.9	161.2
06May2002	17:15	163.5	146.8
06May2002	17:30	143.4	137.6
06May2002	17:45	127.7	112.4
06May2002	18:00	114.6	107.7
06May2002	18:15	103.1	93.8
06May2002	18:30	93.2	88.2
06May2002	18:45	84.5	84.2
06May2002	19:00	76.4	76.2
06May2002	19:15	69	60.8
06May2002	19:30	62.9	51.2
06May2002	19:45	58.1	46
06May2002	20:00	54.9	41.6
06May2002	20:15	54.1	38.6
06May2002	20:30	57.7	33.4
06May2002	20:45	64.8	31.2
06May2002	21:00	68.9	29.4
06May2002	21:15	70.2	27.9
06May2002	21:30	70.4	26.6
06May2002	21:45	70.2	25
06May2002	22:00	69.1	23.4
06May2002	22:15	66.3	21.9
06May2002	22:30	62.5	20.4
06May2002	22:45	57.9	19
06May2002	23:00	53.3	17.5
06May2002	23:15	48.9	15.9
06May2002	23:30	44.7	15
06May2002	23:45	40.7	14
07May2002	00:00	37	13.2

Table C.1, continued

Date	Time	Computed outflow	Observed outflow
		m^3/s	m^3/s
07May2002	00:15	33.5	12.6
07May2002	00:30	30.3	12
07May2002	00:45	27.5	11.4
07May2002	01:00	25	10.8
07May2002	01:15	22.7	10.2
07May2002	01:30	20.7	9.6
07May2002	01:45	19	9.1
07May2002	02:00	17.4	8.5
07May2002	02:15	16	8.1
07May2002	02:30	14.8	7.6
07May2002	02:45	13.7	7.2
07May2002	03:00	12.7	6.8
07May2002	03:15	11.8	6.4
07May2002	03:30	11	6.1
07May2002	03:45	10.3	5.8
07May2002	04:00	9.6	5.5
07May2002	04:15	9	5.2
07May2002	04:30	8.5	5
07May2002	04:45	8	4.7
07May2002	05:00	7.5	4.5
07May2002	05:15	7.1	4.3
07May2002	05:30	6.7	4
07May2002	05:45	6.4	3.9
07May2002	06:00	6.1	3.7
07May2002	06:15	5.8	3.6
07May2002	06:30	5.5	3.5
07May2002	06:45	5.3	3.4
07May2002	07:00	5	3.3
07May2002	07:15	4.8	3.2
07May2002	07:30	4.6	3.2
07May2002	07:45	4.4	3.1
07May2002	08:00	4.3	3.1
07May2002	08:15	4.1	3
07May2002	08:30	3.9	3
07May2002	08:45	3.8	2.9
07May2002	09:00	3.7	2.9
07May2002	09:15	3.6	2.8
07May2002	09:30	3.4	2.8
07May2002	09:45	3.3	2.8
07May2002	10:00	3.2	2.8
07May2002	10:15	3.1	2.7
07May2002	10:30	3	2.7
07May2002	10:45	3	2.7
07May2002	11:00	2.9	2.7
07May2002	11:15	2.8	2.6
07May2002	11:30	2.7	2.6
07May2002	11:45	2.6	2.6

Table C.2: Time-series results flood simulation at Sulaiman Bridge for event 6-May2002 (Run2)

Date	Time	Computed outflow	Observed outflow
		m^3/s	m^3/s
6-May-02	13:15	0	0
6-May-02	13:30	0.2	0.2
6-May-02	13:45	2.5	8.8
6-May-02	14:00	9.5	25.7
6-May-02	14:15	19.7	70.4
6-May-02	14:30	32	274.5
6-May-02	14:45	128.9	288.6
6-May-02	15:00	313.6	346.6
6-May-02	15:15	354.5	356.2
6-May-02	15:30	360.8	357.7
6-May-02	15:45	353.7	349.5
6-May-02	16:00	324.3	329.9
6-May-02	16:15	287.1	321.9
6-May-02	16:30	249.1	309.8
6-May-02	16:45	214.5	200.8
6-May-02	17:00	185	161.2
6-May-02	17:15	160.7	146.8
6-May-02	17:30	141.4	137.6
6-May-02	17:45	126.4	112.4
6-May-02	18:00	114.1	107.7
6-May-02	18:15	103.3	93.8
6-May-02	18:30	94	88.2
6-May-02	18:45	85.9	84.2
6-May-02	19:00	78.3	76.2
6-May-02	19:15	71	60.8
6-May-02	19:30	65.2	51.2
6-May-02	19:45	62.1	46
6-May-02	20:00	62.9	41.6
6-May-02	20:15	68	38.6
6-May-02	20:30	72.1	33.4
6-May-02	20:45	73.5	31.2
6-May-02	21:00	74	29.4
6-May-02	21:15	74.1	27.9
6-May-02	21:30	73.6	26.6
6-May-02	21:45	72.7	25
6-May-02	22:00	70.8	23.4
6-May-02	22:15	67.5	21.9
6-May-02	22:30	63.4	20.4
6-May-02	22:45	58.7	19
6-May-02	23:00	54.1	17.5
6-May-02	23:15	49.6	15.9
6-May-02	23:30	45.5	15
6-May-02	23:45	41.5	14
7-May-02	0:00	37.8	13.2

Table C.2, continued

Date	Time	Computed outflow m^3/s	Observed outflow m^3/s
7-May-02	0:15	34.4	12.6
7-May-02	0:30	31.3	12
7-May-02	0:45	28.5	11.4
7-May-02	1:00	26	10.8
7-May-02	1:15	23.8	10.2
7-May-02	1:30	21.8	9.6
7-May-02	1:45	20.1	9.1
7-May-02	2:00	18.5	8.5
7-May-02	2:15	17.1	8.1
7-May-02	2:30	15.9	7.6
7-May-02	2:45	14.8	7.2
7-May-02	3:00	13.8	6.8
7-May-02	3:15	12.9	6.4
7-May-02	3:30	12.1	6.1
7-May-02	3:45	11.3	5.8
7-May-02	4:00	10.6	5.5
7-May-02	4:15	10	5.2
7-May-02	4:30	9.5	5
7-May-02	4:45	9	4.7
7-May-02	5:00	8.5	4.5
7-May-02	5:15	8.1	4.3
7-May-02	5:30	7.7	4
7-May-02	5:45	7.3	3.9
7-May-02	6:00	7	3.7
7-May-02	6:15	6.7	3.6
7-May-02	6:30	6.4	3.5
7-May-02	6:45	6.1	3.4
7-May-02	7:00	5.9	3.3
7-May-02	7:15	5.6	3.2
7-May-02	7:30	5.4	3.2
7-May-02	7:45	5.2	3.1
7-May-02	8:00	5.1	3.1
7-May-02	8:15	4.9	3
7-May-02	8:30	4.7	3
7-May-02	8:45	4.6	2.9
7-May-02	9:00	4.4	2.9
7-May-02	9:15	4.3	2.8
7-May-02	9:30	4.2	2.8
7-May-02	9:45	4.1	2.8
7-May-02	10:00	3.9	2.8
7-May-02	10:15	3.8	2.7
7-May-02	10:30	3.7	2.7
7-May-02	11:15	3.5	2.6

Table C.3: Summary results of flow simulation for eighty hydrologic elements resultant from rainfall event 6-May 2002 over Klang watershed (Run1).

Hydrologic element	Date/time	Run1		
		Area	Q_{peak}	Volume
		km^2	m^3/s	$1000\ m^3$
Ampang	06May2002, 16:30	19.5	1.6	30.6
Batu Dam	06May2002, 16:00	50.5	0	0
Gombak1	06May2002, 16:00	56.7	4.4	72.6
Gombak2	06May2002, 16:30	86.0	6.3	116.9
Gombak Diversion	06May2002, 18:15	90.6	14	193.4
Gombak outlet Divers	06May2002, 15:45	74.7	2.8	51.2
Jinjjan SFS	06May2002, 15:45	19.7	12.5	128.5
JR160	06May2002, 14:15	96.7	13.3	239.1
JR180	06May2002, 16:15	107.1	19	391
JR210	06May2002, 16:45	262.4	49.9	1346.3
JR240	06May2002, 15:00	196.1	333.5	3386.6
JR280	06May2002, 15:30	490.6	513.9	6108.5
JR300	06May2002, 15:45	549.7	594.1	6971.6
JR320	06May2002, 16:15	640.2	598.7	7618.2
JR330	06May2002, 14:15	80.4	40.8	475.2
JR350	06May2002, 16:15	47.5	7.9	190.3
JR470	06May2002, 14:30	154.4	157.6	1513
JR500	06May2002, 15:00	461.7	364.4	4866.9
Kerayung	06May2002, 15:00	26.6	55.9	539.7
Klang Gates Dam	06May2002, 22:45	75.7	1.9	128.2
Kwang seng WL	06May2002, 14:45	164.6	235.4	2105.3
Outlet	06May2002, 16:30	675.6	628.3	8364.6
RSW11	06May2002, 19:30	90.6	13.7	204.1
RSW13	06May2002, 15:30	96.7	12.8	227.3
RSW14	06May2002, 18:00	19.5	1.6	29.8
RSW15	06May2002, 16:30	74.7	2.8	51.1
RSW16l	06May2002, 16:45	107.1	18.7	386.6
RSW17	06May2002, 16:45	150.4	37.6	684.7
RSW18	06May2002, 17:15	262.4	49.6	1334
RSW18s	06May2002, 15:00	196.1	331.2	3389.6
RSW19	06May2002, 15:00	164.6	233.8	2083.7
RSW20	06May2002, 15:45	464.6	371.8	4935.1
RSW21	06May2002, 15:30	26.6	55.7	528.3
RSW24	06May2002, 15:45	490.6	513.3	6072
RSW26	06May2002, 16:30	640.2	592	7568.1
RSW26s	06May2002, 14:15	80.4	40	475.6
RSW27	06May2002, 16:15	549.7	578.8	6912.3
RSW28	06May2002, 16:45	47.5	7.8	188.4
RSW31	06May2002, 14:45	154.4	157.3	1499.1
RSW32	06May2002, 15:30	461.7	362.5	4819
RSW33	06May2002, 16:30	19.7	12.2	125.1
RSW3l	06May2002, 18:45	56.7	4.4	71
RSW7	07May2002, 01:45	75.7	1.9	122.9

Table C.3, continued

Hydrologic element	Date/time	Run1		
		Area	Q_{peak}	Volume
		km^2	m^3/s	$1000\ m^3$
RSW8	06May2002, 17:15	86.0	6.2	115.7
RSW9	06May2002, 07:30	50.5	0	0
Sentul SFS	06May2002, 16:30	150.4	37.9	687.7
Suliman SFS	06May2002, 15:30	464.6	374.9	4971.1
SW1	06May2002, 12:00	50.5	0	0
SW10	06May2002, 15:45	19.7	12.5	128.5
SW11	06May2002, 21:15	16.3	15.1	226.6
SW12	06May2002, 15:00	21.2	74.5	787.3
SW13	06May2002, 14:30	19.3	70.7	556.1
SW14	06May2002, 14:45	18.9	93	699.7
SW15	06May2002, 20:00	6.4	12.9	143.5
SW16	06May2002, 16:15	43.3	24.1	301.1
SW17	06May2002, 15:00	5.1	40.4	231
SW18	06May2002, 14:30	3.2	29.1	143.3
SW19	06May2002, 16:00	10.3	46.5	515.5
SW2	06May2002, 16:00	56.7	4.4	72.6
SW20	06May2002, 15:00	14.1	94.5	635.1
SW21	06May2002, 16:15	27.4	13.3	192.6
SW22	06May2002, 16:15	47.5	7.9	190.3
SW23	06May2002, 15:00	11.9	89.7	538.3
SW24	06May2002, 14:45	5.1	34.2	178.8
SW25	06May2002, 15:00	26.0	57.4	595.7
SW26	06May2002, 14:15	9.5	26.7	200.9
SW27	06May2002, 14:15	10.0	36.3	230.3
SW28	06May2002, 14:15	15.3	28.4	190.9
SW29	06May2002, 14:30	17.6	12.7	95.9
SW3	06May2002, 16:30	29.3	2.8	45.9
SW30	06May2002, 15:00	26.6	55.9	539.7
SW31	06May2002, 14:45	10.2	78.1	606.2
SW32	06May2002, 14:45	2.8	28.2	152.1
SW33	06May2002, 15:45	6.4	6.4	71.3
SW4	06May2002, 17:00	75.7	8.9	160.1
SW5	06May2002, 16:30	19.5	1.6	30.6
SW6	06May2002, 15:45	15.2	2.1	32.6
SW7	06May2002, 14:15	5.9	12.3	83.6
SW8	06May2002, 19:30	4.6	9.1	77.8
SW9	06May2002, 15:45	24.2	2.8	51.2

Table C.4: Summary results of flow simulation for eighty hydrologic elements resultant from rainfall event 6-May 2002 over Klang watershed (Run2).

Hydrologic element	Date/time	Run2		
		Area	Q_{peak}	Volume
		km^2	m^3/s	$1000\ m^3$
Ampang	06May2002, 16:30	19.5	3.3	55.2
Batu Dam	06May2002, 16:00	50.5	0	0
Gombak1	06May2002, 16:00	56.7	8.5	142.6
Gombak2	06May2002, 16:30	86.0	12.9	206.5
Gombak Diversion	06May2002, 18:15	90.6	19	279.8
Gombak outlet Divers	06May2002, 15:45	74.7	2.8	51.8
Jinjjan SFS	06May2002, 15:45	19.7	12.8	133.1
JR160	06May2002, 14:15	96.7	13.5	265.1
JR180	06May2002, 16:15	107.1	19.3	391.4
JR210	06May2002, 16:45	262.4	48.7	1395.4
JR240	06May2002, 15:00	196.1	323.1	3308.4
JR280	06May2002, 15:30	490.6	495.4	5995
JR300	06May2002, 15:45	549.7	578.2	6864.9
JR320	06May2002, 16:15	640.2	580.8	7495.6
JR330	06May2002, 14:15	80.4	40.3	505.8
JR350	06May2002, 16:15	47.5	9.5	228.6
JR470	06May2002, 14:30	154.4	150.2	1488.1
JR500	06May2002, 15:00	461.7	350.7	4822.4
Kerayung	06May2002, 15:00	26.6	58	558.6
Klang Gates Dam	06May2002, 22:45	75.7	2.9	145.8
Kwang seng WL	06May2002, 14:45	164.6	227.1	2067.6
Outlet	06May2002, 16:30	675.6	612.9	8188.2
RSW11	06May2002, 19:30	90.6	18.7	270.2
RSW13	06May2002, 15:30	96.7	12.9	241.4
RSW14	06May2002, 18:00	19.5	3.3	53.2
RSW15	06May2002, 16:30	74.7	2.8	50.7
RSW16l	06May2002, 16:45	107.1	18.9	384.8
RSW17	06May2002, 16:45	150.4	38.6	687.8
RSW18	06May2002, 17:15	262.4	48.4	1376.5
RSW18s	06May2002, 15:00	196.1	320.5	3309.9
RSW19	06May2002, 15:00	164.6	225.5	2038.7
RSW20	06May2002, 15:45	464.6	358.5	4857.9
RSW21	06May2002, 15:30	26.6	57.8	546.7
RSW24	06May2002, 15:45	490.6	495.1	5945.7
RSW26	06May2002, 16:30	640.2	577.4	7409.8
RSW26s	06May2002, 14:15	80.4	39.6	505.8
RSW27	06May2002, 16:15	549.7	560.7	6775.4
RSW28	06May2002, 16:45	47.5	9.5	224.1
RSW31	06May2002, 14:45	154.4	150	1469.6
RSW32	06May2002, 15:30	461.7	348.8	4757.2
RSW33	06May2002, 16:30	19.7	12.6	129.2
RSW3l	06May2002, 18:45	56.7	8.5	140.6

Table C.4, continued

Hydrologic element	Date/time	Run2		
		Area	Q_{peak}	Volume
		km^2	m^3/s	1000 m^3
RSW7	07May2002, 01:45	75.7	2.9	135.8
RSW8	06May2002, 17:15	86.0	12.9	203.9
RSW9	06May2002, 07:30	50.5	0	0
Sentul SFS	06May2002, 16:30	150.4	38.8	692.4
Suliman SFS	06May2002, 15:30	464.6	360.8	4905.5
SW1	06May2002, 12:00	50.5	0	0
SW10	06May2002, 15:45	19.7	12.8	133.1
SW11	06May2002, 21:15	16.3	14.4	216.5
SW12	06May2002, 15:00	21.2	73.3	773.7
SW13	06May2002, 14:30	19.3	68.6	539.1
SW14	06May2002, 14:45	18.9	87.2	654.4
SW15	06May2002, 20:00	6.4	12.6	140.6
SW16	06May2002, 16:15	43.3	24.9	307.6
SW17	06May2002, 15:00	5.1	38.5	220.9
SW18	06May2002, 14:30	3.2	27.5	136
SW19	06May2002, 16:00	10.3	44.7	496
SW2	06May2002, 16:00	56.7	8.5	142.6
SW20	06May2002, 15:00	14.1	90.8	610.3
SW21	06May2002, 16:15	27.4	13.5	193.4
SW22	06May2002, 16:15	47.5	9.5	228.6
SW23	06May2002, 15:00	11.9	87.6	526.8
SW24	06May2002, 14:45	5.1	34.2	179.1
SW25	06May2002, 15:00	26.0	56.4	585.1
SW26	06May2002, 14:15	9.5	25.7	193.3
SW27	06May2002, 14:15	10.0	33.8	214.3
SW28	06May2002, 14:15	15.3	27.5	184.5
SW29	06May2002, 14:30	17.6	12.9	97.2
SW3	06May2002, 16:30	29.3	4.7	65.9
SW30	06May2002, 15:00	26.6	58	558.6
SW31	06May2002, 14:45	10.2	77.1	598.1
SW32	06May2002, 14:45	2.8	27.4	148.3
SW33	06May2002, 15:45	6.4	6.4	70.8
SW4	06May2002, 17:00	75.7	14	241.3
SW5	06May2002, 16:30	19.5	3.3	55.2
SW6	06May2002, 15:45	15.2	3.4	47.9
SW7	06May2002, 14:15	5.9	12.2	81.4
SW8	06May2002, 19:30	4.6	8.6	75.9
SW9	06May2002, 15:45	24.2	2.8	51.8

Table C.5: Summary results of flow simulation for eighty hydrologic elements resultant from rainfall event 6-May 2002 over Klang watershed (Run3).

Hydrologic element	Date/time	Run3		
		Area	Q_{peak}	Volume
		km^2	m^3/s	$1000\ m^3$
Ampang	06May2002, 16:30	19.46	3.3	55.2
Batu Dam	06May2002, 16:00	51.82	0	0
Gombak1	06May2002, 16:00	55.74	8.4	140.1
Gombak2	06May2002, 16:30	86.39	13	207.3
Gombak Diversion	06May2002, 18:15	90.22	17.8	268.9
Gombak outlet Divers	06May2002, 15:45	68.79	2	36.4
Jinjjan SFS	06May2002, 15:45	19.77	12.8	133.6
JR160	06May2002, 14:15	97.52	12.8	279.3
JR180	06May2002, 16:15	107.5	23.6	449.6
JR210	06May2002, 16:45	271.49	57.2	1589.3
JR240	06May2002, 15:00	183.06	270.7	2765.9
JR280	06May2002, 15:30	485.992	441.1	5649.6
JR300	06May2002, 15:45	554.752	514.8	6617.6
JR320	06May2002, 16:15	644.302	531.1	7238.2
JR330	06May2002, 14:15	80.6	40.1	507.8
JR350	06May2002, 16:15	47.88	9.6	230.9
JR470	06May2002, 14:30	154.21	145.3	1465.3
JR500	06May2002, 15:00	457.795	308.5	4485.5
Kerayung	06May2002, 15:00	27.8	60.6	584.4
Klang Gates Dam	06May2002, 22:45	76.13	2.9	161.8
Kwang seng WL	06May2002, 14:45	163.03	211.7	1966.7
Outlet	06May2002, 16:30	684.472	562	8037.8
RSW11	06May2002, 19:30	90.22	17.5	260.5
RSW13	06May2002, 15:30	97.52	12.5	258
RSW14	06May2002, 18:00	19.46	3.3	53.6
RSW15	06May2002, 16:30	68.79	1.9	36.6
RSW16l	06May2002, 16:45	107.5	23.2	443.8
RSW17	06May2002, 16:45	149.19	43.8	736.4
RSW18	06May2002, 17:15	271.49	57	1581.8
RSW18s	06May2002, 15:00	183.06	267.7	2767.7
RSW19	06May2002, 15:00	163.03	210.8	1938.8
RSW20	06May2002, 15:45	460.632	314.6	4543.4
RSW21	06May2002, 15:30	27.8	60.1	572.5
RSW24	06May2002, 15:45	485.992	430.9	5607
RSW26	06May2002, 16:30	644.302	524.2	7164.6
RSW26s	06May2002, 14:15	80.6	39.3	507.9
RSW27	06May2002, 16:15	554.752	513.3	6538.9
RSW28	06May2002, 16:45	47.88	9.5	227.7
RSW31	06May2002, 14:45	154.21	144.8	1448
RSW32	06May2002, 15:30	457.795	304.5	4429.1
RSW33	06May2002, 16:30	19.77	12.6	130

Table C.5, continued

Hydrologic element	Date/time	Run3		
		Area	Q_{peak}	Volume
		km^2	m^3/s	$1000\ m^3$
RSW3l	06May2002, 18:45	55.74	8.3	138.3
RSW7	07May2002, 01:45	76.13	2.9	152.6
RSW8	06May2002, 17:15	86.39	13	205.1
RSW9	06May2002, 07:30	51.82	0	0
Sentul SFS	06May2002, 16:30	149.19	43.9	740.1
Suliman SFS	06May2002, 15:30	460.632	316.5	4577.3
SW1	06May2002, 12:00	51.82	0	0
SW10	06May2002, 15:45	19.77	12.8	133.6
SW11	06May2002, 21:15	26.58	23.4	352.2
SW12	06May2002, 15:00	11.65	40.2	424.6
SW13	06May2002, 14:30	20.06	71.3	559.7
SW14	06May2002, 14:45	17.17	79.2	594.1
SW15	06May2002, 20:00	6.72	13.3	148.2
SW16	06May2002, 16:15	41.69	24	296.2
SW17	06May2002, 15:00	5.5	41.9	240.2
SW18	06May2002, 14:30	3.245	27.5	136
SW19	06May2002, 16:00	8.38	36.3	402.5
SW2	06May2002, 16:00	55.74	8.4	140.1
SW20	06May2002, 15:00	14.37	92.5	621.1
SW21	06May2002, 16:15	35.64	17.6	251.5
SW22	06May2002, 16:15	47.88	9.6	230.9
SW23	06May2002, 15:00	10.99	80.6	485
SW24	06May2002, 14:45	5.32	35.7	186.6
SW25	06May2002, 15:00	25.96	56.3	584.8
SW26	06May2002, 14:15	14.21	38.4	288.5
SW27	06May2002, 14:15	8.95	30.1	191.4
SW28	06May2002, 14:15	15.21	27.3	183.5
SW29	06May2002, 14:30	17.51	12.8	96.5
SW3	06May2002, 16:30	30.65	4.9	69
SW30	06May2002, 15:00	27.8	60.6	584.4
SW31	06May2002, 14:45	8.82	66.8	518.7
SW32	06May2002, 14:45	2.837	27.4	148.3
SW33	06May2002, 15:45	12.22	12.3	134.8
SW4	06May2002, 17:00	76.13	14	242.8
SW5	06May2002, 16:30	19.46	3.3	55.2
SW6	06May2002, 15:45	15.88	3.5	50
SW7	06May2002, 14:15	5.51	11.5	76.7
SW8	06May2002, 19:30	3.83	7.2	63.8
SW9	06May2002, 15:45	16.97	2	36.4

Table C.6: Summary results of flow simulation for eighty hydrologic elements resultant from rainfall event 6-May 2002 over Klang watershed (Run4).

Hydrologic Element	Date/Time	Run4		
		Area	Q_{peak}	Volume
		km^2	m^3/s	$1000\ m^3$
Ampang	06May2002, 21:00	19.458	1.3	34.8
Batu Dam	07May2002, 03:00	50.469	0	0.1
Gombak1	06May2002, 21:00	56.744	0.1	2.3
Gombak2	06May2002, 15:00	86	1.1	25.3
Gombak Diversion	06May2002, 18:00	90.557	3.5	101.2
Gombak outlet Divers	06May2002, 15:00	74.651	5.6	166.3
Jinjjan SFS	06May2002, 15:00	19.689	6.9	124.5
JR160	06May2002, 18:00	96.701	6.7	117.2
JR180	06May2002, 18:00	107.137	18.4	564.4
JR210	06May2002, 18:00	262.381	54	1650
JR240	06May2002, 18:00	196.119	98.7	2467
JR280	06May2002, 18:00	490.638	151.5	4860.9
JR300	06May2002, 18:00	549.721	223.7	6685.5
JR320	06May2002, 18:00	640.153	242.8	8070.7
JR330	06May2002, 18:00	80.409	31.6	1102.5
JR350	06May2002, 18:00	47.494	20.2	778.7
JR470	06May2002, 18:00	154.393	73.6	1349
JR500	06May2002, 18:00	461.745	150	4206.2
Kerayung	06May2002, 18:00	26.573	64.3	1086.1
Klang Gates Dam	07May2002, 03:00	75.651	0	0
Kwang seng WL	06May2002, 18:00	164.563	78.7	1667.6
Outlet	06May2002, 18:00	675.649	252.6	8955.1
RSW11	06May2002, 18:00	90.557	3.2	94.4
RSW13	06May2002, 21:00	96.701	4.8	98.6
RSW14	06May2002, 21:00	19.458	1.2	32.1
RSW15	06May2002, 18:00	74.651	4.1	155.6
RSW16l	06May2002, 18:00	107.137	17.8	573.8
RSW17	06May2002, 18:00	150.431	39.9	1232.2
RSW18	06May2002, 18:00	262.381	50.2	1670.1
RSW18s	06May2002, 18:00	196.119	97.7	2478
RSW19	06May2002, 18:00	164.563	71.7	1705.3
RSW20	06May2002, 18:00	464.582	133.1	4359.7
RSW21	06May2002, 18:00	26.573	54	1093.1
RSW24	06May2002, 18:00	490.638	144.6	4887.4
RSW26	06May2002, 18:00	640.153	221.8	8089.2
RSW26s	06May2002, 18:00	80.409	31.4	1103.4
RSW27	06May2002, 18:00	549.721	203	6729.6
RSW28	06May2002, 18:00	47.494	18.8	775.5
RSW31	06May2002, 18:00	154.393	68.7	1383
RSW32	06May2002, 18:00	461.745	137.9	4259.1
RSW33	06May2002, 18:00	19.689	3.9	122.4

Table C.6, continued

Hydrologic Element	Date/Time	Run4		
		Area	Q_{peak}	Volume
		km^2	m^3/s	$1000\ m^3$
RSW3l	07May2002, 03:00	56.744	0.1	1.7
RSW7	06May2002, 06:00	75.651	0	0
RSW8	06May2002, 18:00	86	0.7	22.6
RSW9	06May2002, 06:00	50.469	0	0
Sentul SFS	06May2002, 18:00	150.431	40.9	1215.9
Suliman SFS	06May2002, 18:00	464.582	140.4	4329
SW1	07May2002, 00:00	50.469	0	0.1
SW10	06May2002, 15:00	19.689	6.9	124.5
SW11	06May2002, 18:00	16.335	7.3	225.4
SW12	06May2002, 18:00	21.23	19.1	538.7
SW13	06May2002, 18:00	19.321	41	690.3
SW14	06May2002, 18:00	18.913	31.5	527.9
SW15	06May2002, 18:00	6.378	5.3	145.6
SW16	06May2002, 18:00	43.294	23.1	642.1
SW17	06May2002, 18:00	5.058	3.6	98
SW18	06May2002, 18:00	3.245	2.2	58
SW19	06May2002, 18:00	10.326	8	223
SW2	06May2002, 21:00	56.744	0.1	2.3
SW20	06May2002, 18:00	14.119	9.9	271.2
SW21	06May2002, 18:00	27.402	21	593.3
SW22	06May2002, 18:00	47.494	20.2	778.7
SW23	06May2002, 18:00	11.937	8.5	230
SW24	06May2002, 18:00	5.108	4.1	111.8
SW25	06May2002, 18:00	25.974	22.9	650.1
SW26	06May2002, 18:00	9.522	7.8	215.8
SW27	06May2002, 15:00	10.023	8.5	237.7
SW28	06May2002, 18:00	15.292	8.1	211.7
SW29	06May2002, 18:00	17.623	4.7	115.3
SW3	06May2002, 15:00	29.256	1.1	23.6
SW30	06May2002, 18:00	26.573	64.3	1086.1
SW31	06May2002, 15:00	10.17	10.3	284.6
SW32	06May2002, 18:00	2.837	2.5	69.9
SW33	06May2002, 18:00	6.419	5.1	140.9
SW4	07May2002, 00:00	75.651	0	0
SW5	06May2002, 21:00	19.458	1.3	34.8
SW6	06May2002, 21:00	15.197	0.3	7.4
SW7	06May2002, 18:00	5.853	6.6	109.8
SW8	06May2002, 18:00	4.557	2.9	78.6
SW9	06May2002, 15:00	24.182	5.6	166.3

Table C.7: Summary results of flow simulation for eighty hydrologic elements resultant from rainfall event 6-May 2002 over Klang watershed (Run5).

Hydrologic element	Date/Time	Run5		
		Area	Q_{peak}	Volume
		km^2	m^3/s	$1000\ m^3$
Ampang	06May2002, 21:00	19.46	1.3	34.8
Batu Dam	07May2002, 03:00	51.82	0	0.1
Gombak1	06May2002, 21:00	55.74	0.1	2.3
Gombak2	06May2002, 15:00	86.39	1.2	26.4
Gombak Diversion	06May2002, 18:00	90.22	3.1	89.9
Gombak outlet Divers	06May2002, 15:00	68.79	3.9	116.7
Jinjjan SFS	06May2002, 15:00	19.77	7	125
JR160	06May2002, 18:00	97.52	6.3	111.1
JR180	06May2002, 18:00	107.5	22.2	647.6
JR210	06May2002, 18:00	271.49	61.3	1855.5
JR240	06May2002, 18:00	183.06	85.9	2114.6
JR280	06May2002, 18:00	485.992	144.6	4697.4
JR300	06May2002, 18:00	554.752	225.9	6754.1
JR320	06May2002, 18:00	644.302	243.9	8118.5
JR330	06May2002, 18:00	80.6	31.7	1107
JR350	06May2002, 18:00	47.88	20.3	785
JR470	06May2002, 18:00	154.21	72.1	1321.4
JR500	06May2002, 18:00	457.795	144.1	4064
Kerayung	06May2002, 18:00	27.8	67.2	1136.2
Klang Gates Dam	07May2002, 03:00	76.13	0	0
Kwang seng WL	06May2002, 18:00	163.03	75.9	1601.5
Outlet	06May2002, 18:00	684.472	257.3	9108.2
RSW11	06May2002, 18:00	90.22	2.8	84.8
RSW13	06May2002, 21:00	97.52	4.5	93.2
RSW14	06May2002, 21:00	19.46	1.2	32.1
RSW15	06May2002, 18:00	68.79	2.9	103
RSW16l	06May2002, 18:00	107.5	21.4	660.8
RSW17	06May2002, 18:00	149.19	42.6	1297.5
RSW18	06May2002, 18:00	271.49	57.1	1881.7
RSW18s	06May2002, 18:00	183.06	84.9	2124.3
RSW19	06May2002, 18:00	163.03	69	1638.1
RSW20	06May2002, 18:00	460.632	126.7	4209.6
RSW21	06May2002, 18:00	27.8	56.7	1144.9
RSW24	06May2002, 18:00	485.992	137.7	4721.2
RSW26	06May2002, 18:00	644.302	222.7	8136.4
RSW26s	06May2002, 18:00	80.6	31.5	1107.9
RSW27	06May2002, 18:00	554.752	204.9	6798.5
RSW28	06May2002, 18:00	47.88	19	781.9
RSW31	06May2002, 18:00	154.21	67.2	1354.7
RSW32	06May2002, 18:00	457.795	131.7	4111.8
RSW33	06May2002, 18:00	19.77	3.9	123.1
RSW3l	07May2002, 03:00	55.74	0.1	1.6

Table C.7, continued

Hydrologic element	Date/Time	Run5		
		Area	Q_{peak}	Volume
		km^2	m^3/s	$1000\ m^3$
RSW7	06May2002, 06:00	76.13	0	0
RSW8	06May2002, 18:00	86.39	0.7	23.8
RSW9	06May2002, 06:00	51.82	0	0
Sentul SFS	06May2002, 18:00	149.19	43.7	1279.2
Suliman SFS	06May2002, 18:00	460.632	134.2	4181.7
SW1	07May2002, 00:00	51.82	0	0.1
SW10	06May2002, 15:00	19.77	7	125
SW11	06May2002, 18:00	26.58	12	366.7
SW12	06May2002, 18:00	11.65	10.5	295.6
SW13	06May2002, 18:00	20.06	42.6	716.7
SW14	06May2002, 18:00	17.17	28.6	479.2
SW15	06May2002, 18:00	6.72	5.6	153.4
SW16	06May2002, 18:00	41.69	22.3	618.3
SW17	06May2002, 18:00	5.5	3.9	106.6
SW18	06May2002, 18:00	3.245	2.2	58
SW19	06May2002, 18:00	8.38	6.5	180.9
SW2	06May2002, 21:00	55.74	0.1	2.3
SW20	06May2002, 18:00	14.37	10.1	276.1
SW21	06May2002, 18:00	35.64	27.3	771.6
SW22	06May2002, 18:00	47.88	20.3	785
SW23	06May2002, 18:00	10.99	7.9	211.7
SW24	06May2002, 18:00	5.32	4.2	116.4
SW25	06May2002, 18:00	25.96	22.9	649.7
SW26	06May2002, 18:00	14.21	11.7	322.1
SW27	06May2002, 15:00	8.95	7.6	212.2
SW28	06May2002, 18:00	15.21	8.1	210.5
SW29	06May2002, 18:00	17.51	4.6	114.6
SW3	06May2002, 15:00	30.65	1.2	24.8
SW30	06May2002, 18:00	27.8	67.2	1136.2
SW31	06May2002, 15:00	8.82	8.9	246.8
SW32	06May2002, 18:00	2.837	2.5	69.9
SW33	06May2002, 18:00	12.22	9.8	268.2
SW4	07May2002, 00:00	76.13	0	0
SW5	06May2002, 21:00	19.46	1.3	34.8
SW6	06May2002, 21:00	15.88	0.3	7.7
SW7	06May2002, 18:00	5.51	6.2	103.4
SW8	06May2002, 18:00	3.83	2.4	66.1
SW9	06May2002, 15:00	16.97	3.9	116.7

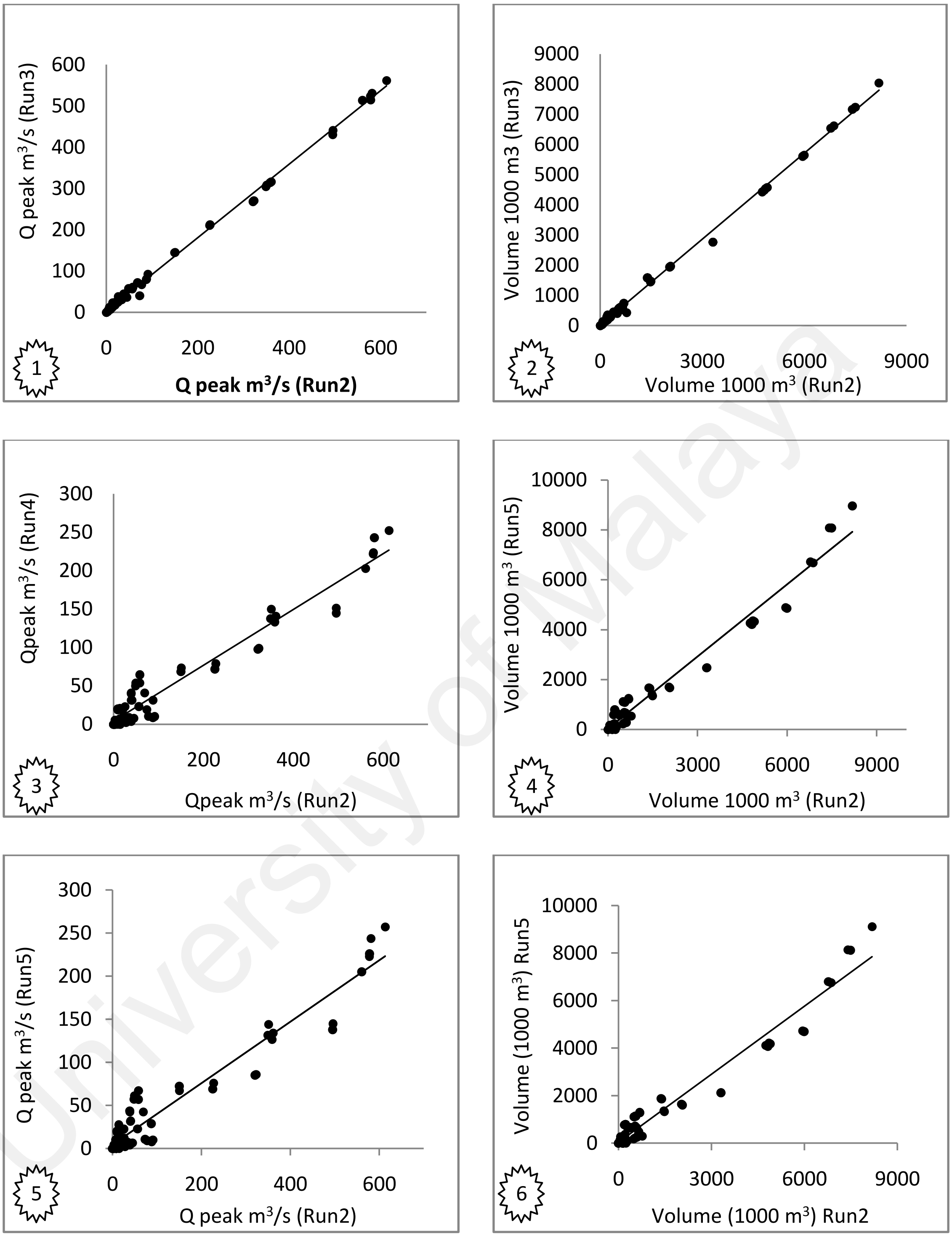

Figure C.1: Scatter plots for Summary results of investigated scenarios in all hydrologic elements:

(1) Computed peak discharge for Run2 vs. Run3, (2) Computed volume of flood for Run2 vs. Run3, (3) Computed peak discharge for Run2 vs. Run4, (4) Computed volume of flood for Run2 vs. Run4, (5) Computed peak discharge for Run2 vs. Run5, (6) Computed volume of flood for Run2 vs. Run5.

Appendix D:List of Publications from the Thesis

Journals:

1- **Abolghasem Akbari**, A.A.Samah, F. Othman (2009). Effect of Pixel Size on the Areal Storm Pattern Analysis using Kriging. *Journal of Applied Sciences*, Vol. 9, Issue: 20, pp.3707-3714. (ISI-Cited Publication)

2- **Abolghasem Akbari**, A.A.Samah, F. Othman (2010). Practical use of SRTM digital elevation dataset in the urban-watershed modeling. *Journal of Spatial Hydrology*. Vol.10, No.2, pp.13-26. (SCOPUS-Cited Publication)

3- Faridah Othman, **A. Akbari**, A. A. Samah. Spatial Rainfall Analysis for an Urbanized Tropical River Basin. *International Journal of the Physical Sciences*. Vol.6(20), pp.4861-4868. (ISI-Cited Publication)

4- **Abolghasem Akbari**, F. Othman, A. A. Samah (2011). Probing on Suitability of TRMM Data to Explain Spatio-temporal Pattern of Severe Storm in Tropic Region. *Journal of Hydrology and Earth System Sciences*. Vol.8, pp.1–34. (ISI-Cited Publication)

5- **Abolghasem Akbari**, F. Othman, A. A. Samah (2012). Integration of SRTM and TRMM date into the GIS-based hydrological model for the purpose of flood modeling. *Journal of Hydrology and Earth System Sciences*. (submitted) (ISI-Cited Publication)

Conferences:

1- Ramani Bai, **A. Akbari**, A. A. Samah, (2007), Flood Modeling & prediction Using GIS, exhibition PECIPTA 2007, 10 -12 August, KLCC, Kuala Lumpur, Malaysia (**Award : Bronze Medal**)

2- **Abolghasem Akbari**, Ramani Bai, A. A. Samah (2007), Developing Spatial Water Resource Database for a River Basin, international conference of MAP ASIA2007,14-16 August, Kuala Lumpur Malaysia. (Poster paper).

3- **Abolghasem Akbari**, Ramani Bai (2007), The Use of HEC-GeoHMS and HEC-HMS to Perform GIS-based Flood Analysis of a Watershed, Joint International Symposium & Exhibition on Geoinformation and GPS/GNSS, 5-7 November, Johor Bahru, Johor, Malaysia.

4- **Abolghasem Akbari**, Ramani Bai(2007), Application of GIS and RS in water supply systems,28th Asian conference on Remote Sensing (ACRS 2007), 12– 16 November 2007, PWTC, KL, Malaysia.

5- **Abolghasem Akbari**, Ramani Bai, A. A. Samah (2008), Estimating Spatial Curve Number (CN) for Flood Analysis of Urbanized watershed, international conference on Civil Engineering (ICCE08), 12-14 May, Hyatt Regency Hotel, Kuantan, Malaysia.

6- **Abolghasem Akbari**, A. A. Samah, Ramani Bai (2008), Spatial Data Updating Using Enhanced Satellite image, International Conference on Environmental Research and Technology (ICERT'08), Park Royal Hotel, 28-30 May, Penag, Malaysia.

7- Ramani Bai, Ramadas. G, A. A. Samah, **A. Akbari**, Desa.M.N.M (2008), Flood Risk Assessment and Real Time Warning System by GIS, 19th International Innovation and Technology Exhibition (ITEX'08). 9-11 May, KLCC, KL, Malaysia. (**Award : Silver Medal**)

8- **Abolghasem Akbari**, A. A. Samah, F. Othman (2009). Probing on the effectiveness of SRTM Digital Elevation Datasets in Urban Watershed Modeling. 10th APRU Doctoral Student Conference. 5-10 July 2009, Kyoto University, Kyoto, Japan.

9- **Abolghasem Akbari**, A. A. Samah, F. Othman (2009), Characteristics of SRTM Digital Elevation Data set in the Tropic Region, International conference for technical postgraduates (TECHPOS 2009). 14-15 Dec, The Legend Hotel, Kuala Lumpur, Malaysia,

Workshops:

1- Zaslavsky, I, Whitenack, T, A. A. Samah, A. Akbari (2009), International Workshop on Hydrologic Data Management and Modeling in South East Asia University of Malaya jointly with University of California (San Diego), City Campus Jalan Tun Ismail, 20 - 24 July Kuala Lumpur, Malaysia.